MARTIN MARIETTA CORPORATION

GPO PRICE	$ ______
CFSTI PRICE(S)	$ ______
Hard copy (HC)	3.00
Microfiche (MF)	.65

ff 653 July 65

FACILITY FORM 602

N68-25886 (ACCESSION NUMBER)	(THRU)
175 (PAGES)	1 (CODE)
NASA-CR-82004 (NASA CR OR TMX OR AD NUMBER)	02 (CATEGORY)

NASA CR-82004

FULL SCALE FLIGHT TEST REPORT

X-15A-2 ABLATIVE THERMAL PROTECTION SYSTEM

By A. B. Price

December 1967

Prepared under Contract No. NAS 4-1212

The Martin Marietta Corporation
Denver, Colorado

for

Flight Research Center
NATIONAL AERONAUTICS AND SPACE ADMINISTRATION

FULL SCALE FLIGHT TEST REPORT

X-15A-2 Ablative Thermal Protection System

MCR-68-15

December, 1967

REPRINTED 05-23-68

Prepared by: A. B. Price

A. B. Price

Approved by: D. V. Sallis

D. V. Sallis

Revision 1 - May 1968

THE MARTIN MARIETTA CORPORATION

Denver, Colorado

FOREWORD

This report is prepared as a part of NASA Contract 4-1212 and defines the program conducted to flight qualify the Martin Marietta ablative thermal protection system for the X-15A-2 aircraft. It is forwarded to the NASA Flight Research Center in accordance with contractual requirements.

REVISION I

CHANGE	PAGE
7	Figure reference
14	Clarify repair material
20	Clarify paragraph 3
43	Add title
62	Delete table reference
67	Figure references
68	Delete table reference
73	Spelling error
120	Table reference
121	Delete table reference
122	Add two dimensional analysis
123	Table reference
126	Add two dimensional analysis
127	Table reference
129	Table number
130	Table number
131	Table number
149	Add two dimensional analysis

ABSTRACT

The ablative thermal protection system designed for the X-15A-2 aircraft by the Martin Marietta Corporation was qualified through flight test and performance analysis. The procedures formulated for applying, partially refurbishing, and removing the ablation system were validated and an overall evaluation of the ablator's condition - after flight test exposures of Mach 5.0 and 6.7 are presented. An analytical correlation of the observed ablator performance was conducted to verify predictability and gain confidence in the ablator system's capabilities as the environmental envelope is expanded to the operational limits of the flight vehicle.

Potential problem areas are identified and their methods of resolution are presented.

TABLE OF CONTENTS

Table of Contents (Continued)

LIST OF TABLES

Tables IV-1 thru IV-12 reflect measured flight data and are omitted from this report to avoid classification of this document. These data are available from the NASA flight test records and are also compiled in Martin-Marietta report IR-68-1, "Flight Data for Ablator Protected X-15 Flights 2-52 and 2-53 (U)," Confidential

LIST OF FIGURES

List of Figures (continued)

List of Figures (Continued)

List of Figures (Continued)

List of Figures (Continued)

LIST OF SYMBOLS

Symbol	Description	Units
$\dot{q}_A$	heating rate to ablator surface	BTU/ft^{2}sec
$\dot{q}_F$	cold wall heating rate at 0°Fahrenheit	BTU/ft^{2}sec
$\dot{q}_l$	local heating rate	BTU/ft^{2}sec
$\dot{q}_M$	heating rate to aircraft skin	BTU/ft^{2}sec
$\dot{q}_R$	cold wall heating rate at 0°Rankine	BTU/ft^{2}sec
$\dot{q}_S$	stagnation heating rate	BTU/ft^{2}sec
H_R	recovery enthalpy	BTU/lb
H_{0^oF}	enthalpy of air at 0°Fahrenheit	BTU/lb
R_M	nose radius of aircraft structure	inches
R_A	nose radius of ablator detail	inches

I. INTRODUCTION

An ablative thermal protection system was designed for the X-15A-2 aircraft by the Martin Marietta Corporation under contract NAS4-1009. The system was intended to provide thermal protection for the existing aircraft's structure to flight regimes of up to Mach 7.4.

The Martin Marietta-developed MA-25s sprayable ablator was the primary material utilized in the system design. It is a room temperature curing elastomeric silicone base ablator suitable for spray application over complex vehicle configurations like the X-15. It was supplemented in the system design by pre-molded densified ablator details and structural ablator inserts as required over the vehicle to accommodate areas whose environmental conditions exceeded the capabilities of the MA-25s material.

The general arrangement of the ablation system is shown in Fig. I-1, and a complete description is contained in the X-15A-2 Thermal Protection System Design Report, ER-14535. This report serves to document the first application, partial refurbishment, and removal of the complete ablation system on the X-15A-2 aircraft; and its performance qualification by dual flight test exposure to Mach 5.0 and Mach 6.7 respectively.

In addition to the visual and mechanical evaluation of the thermal protection system's condition following the flight exposures, an analytical correlation of the ablator's performance was conducted. This served to verify the predictability of the ablator and gain confidence in extrapolation of the system's abilities to provide adequate thermal protection to the full operational capabilities of the aircraft.

FOLDOUT FRAME 1

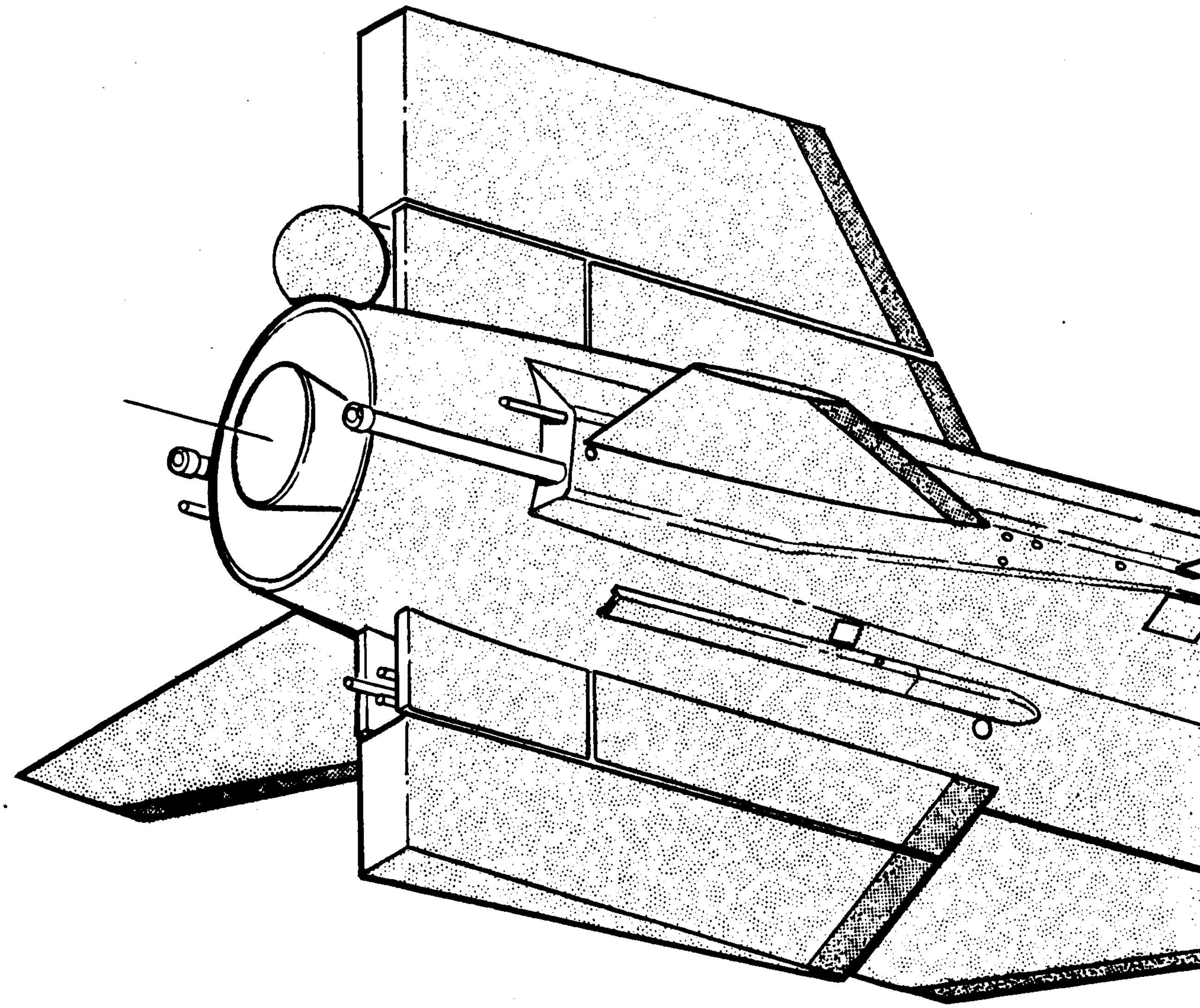

BARE

MA 25S ABLATOR

LEADING EDGE MATERIA

HARD POINT MATERIAL

FOLDOUT FRAME 2

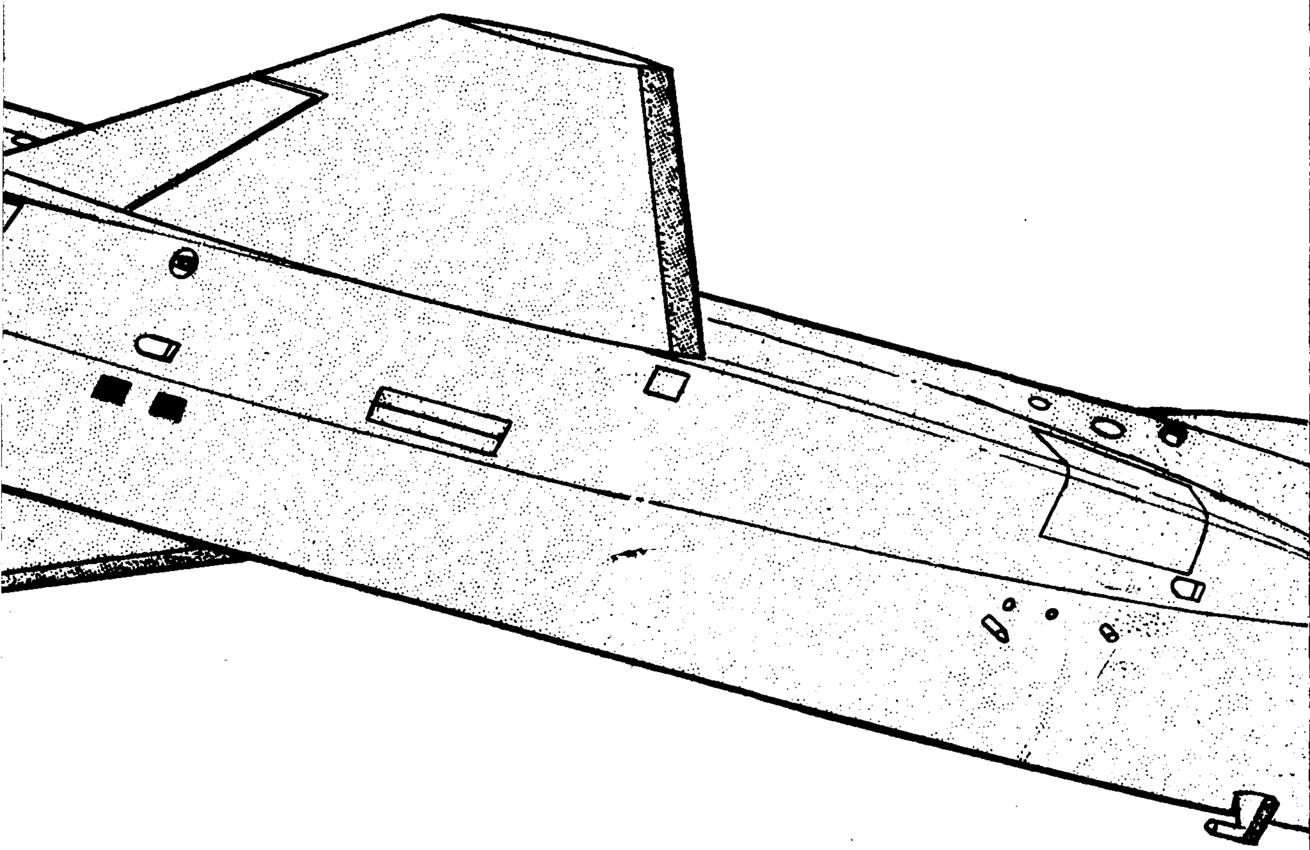

L

FOLDOUT FRAME 3

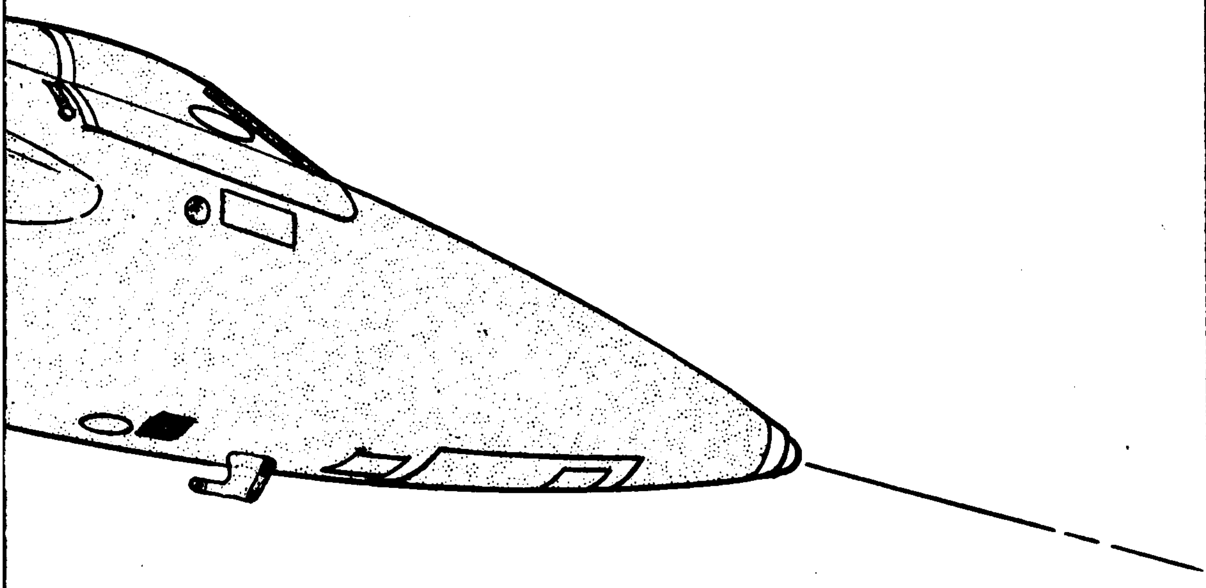

GENERAL ARRANGEMENT
X-15-2 THERMAL PROTECTION SYSTEM
FIGURE I-1

II. ABLATOR OPERATIONS

This program provided the first complete performance of the ablator application and refurbishment procedures as defined in the Application and Refurbishment Manual, ER-14539, dated March, 1967, and prepared under predecessor contract NAS4-1009. The ablator operations defined herein served to verify the accuracy and adequacy of the procedures defined in the manual for their accomplishment.

At least partial exercises for the four principle ablator operations (i.e., application, partial refurbishment, complete refurbishment, and removal) were conducted, and the full application and removal procedures were accomplished. In addition, a "touch-up" activity was initiated to permit reflight of the ablation system without restoring its full thermal protection capability.

The actual operations conducted during this program are defined in the remainder of this report section along with the acceptability of specified procedures, or recommended revisions thereto.

A. Full Scale Application

The first complete application of the ablative thermal protection was accomplished in good agreement with the schedule and procedure specified in the Application and Refurbishment Manual, ER-14539. Only a few conditions arose that could be modified to improve the overall operation. A brief description of each of the major phases of the application process is presented in the following paragraphs.

1. Cleaning - The preparatory cleaning of the aircraft for this first application was somewhat overdone. The surface condition of the vehicle, with its accumulation of contamination and overabundance of lacquer, necessitated extensive use of solvent during the rough cleaning operation. Because of this, all joints, gaps and openings were masked before initiation of cleaning operations to prevent the possibility of getting solvent into the aircraft's compartments.

Final cleaning was accomplished with powdered cleanser and water using the "water break" free test to ascertain cleaning adequacy. Excessive cleaning was performed in the areas of external aircraft markings in an attempt to remove all traces of the markings. Repeated cleaning failed to eliminate the visual evidence of the lettering, but the areas proved satisfactorily clean from a "water break" free criterion. Figure II-1 shows the cleaning operation in progress.

Other areas of the aircraft, especially around some of the fastener heads and skin joints, never did achieve a complete "water-break" free condition. Apparently, these areas continually bleed hydraulic fluid or other contamination, and final acceptance of area cleanliness was made without the full "water break" free condition. Because these conditions are apparent characteristics of the aircraft, cleaning and acceptance procedures should be revised to allow for them on future applications.

2. Masking - Contamination Control - The established masking procedures appeared adequate to protect the aircraft from internal ablator contamination, with one exception. This was protecting the gap between

the fixed and movable vertical tail sections. No protection method had been defined in the manual, but the need for one became apparent early in the masking operation. For this initial application, the gap was masked internally by inserting the tape into the gap and securing it to the upper and lower surfaces of the respective parts. This method appeared adequate during the ablator application, but the mask became dislodged during finishing operations when shop air was employed to remove the sanded ablator dust from the aircraft surface. Some of the ablator dust was carried into the gap and dropped through the torque tube opening into the compartment below. When discovered, the compartment was thoroughly vacuumed to remove all traces of the ablator dust. To eliminate similar occurrence of future applications, a procedure to externally mask across the gap has been developed and will be made a part of the protection procedure.

The remainder of the masking operation went without incident, and the polyethylene tape proved exceptionally good for this application. Figure II-2 shows the polyethylene tape being applied around the service panels of the ventral fin.

As a means of checking the adequacy of the masking during all phases of ablator operation, airborne contamination collectors, petri dishes with millipore filters, were placed in nine (9) of the aircraft compartments before starting any phase of the application process. They were removed after completion of the ablator application and the particle levels and counts were independently determined by NASA and

Martin Marietta Quality Control personnel. The levels of contamination determined from the collectors are presented in Table II-1 and acceptability is based on the contamination limits specified in MSFC Spec. 164. It is signficant to note the close agreement between NASA and Martin Marietta observed levels of contamination. Also of interest is the extremely low level of suspect ablator contamination determined by either agency.

The close agreement between readings is indicative of a good understanding of ablator identification characteristics by NASA Quality and would indicate no significant problems of contamination identification and classification on future ablator applications.

3. Molded Ablator Detail Installation - Installation procedures for the molded ablator details on the aircraft were satisfactory. The installation tools provided for the wing and horizontal stabilizer details functioned well, but a few minor tool modifications would make them more durable and somewhat easier to use. These modifications are delineated in section II-E of this report. Installation of the wing leading edge details using the bonding tools is depicted in Figures II-3 and II-4.

Leading edge details, other than those for the wing and horizontal stabilizer, were secured with tape until adhesive cure, and all installations proved satisfactory. The installed canopy leading edge detail is shown in Fig. II-5 before final finishing.

A special ablator detail was made for the leading edge of the dummy ramjet nose instrumentation rake. It was made from a spare piece of the vertical tail leading edge detail, and can be seen installed in Figure II-30.

4. Primary Ablator Application - The sprayed application of MA-25s ablator was made in accordance with the thickness requirements defined in the Application and Refurbishment Manual, ER-14539. The application was accomplished sequentially by aircraft areas as reflected in Figure II-6. The aircraft was completely covered with polyethylene sheeting to protect cleaned areas from overspray contamination during the sequential ablator applications. The covering is shown in Figure II-7, and was sectioned to permit exposing local areas of the aircraft as ablator application progressed.

Before the application of ablator to an area of the aircraft, trim marker strips were installed over the contamination control masking and a layer of DC93-027 was applied over the fastener heads and peripheral gaps of the seldom removed panels. Installed trim markers are shown in Figure II-8 for the ventral fin of the aircraft, and the DC-93-027 layer over one of the nose panels and the wing BCS panel can be seen in Figure II-1 and II-9, respectively.

Thickness control during the early stages of the application was the most significant difficulty encountered. This improved significantly as operations progressed and application personnel became more familiar with the deposition characteristics of the ablator material and the thickness requirements over the aircraft. Some areas of the aircraft proved to be beyond the optimum limits of reach for the sprayers.

This occurred on the wing upper surface near the root mid chord, and along the crown centerline of the fuselage. This condition resulted in a somewhat "cheezy" ablator application in these areas, but the layer was deemed adequate to protect the substrate during the flight test exposures. In future operations the ablator application sequence could be modified to provide greater use of cured coated surfaces for walkways when making the ablator application to these areas. There is no indication, however, that the ablator layer achieved in these areas during this application were inadequate from a performance standpoint.

When trimming of the cured ablator application commenced, it became apparent that the vinyl foam tape utilized for trim line identification was too thick and possessed too high an adhesive tack. Their thickness resulted in a very porous ablator layer adjacent to them, and their adhesive necessitated very careful removal to avoid dislodging the contamination control masks under them. These situations could be minimized by use of thinner strips in the future and specifying a lower tack strength for their adhesive.

Various portions of the "as sprayed" ablator application are shown in Figures II-10, 11 and 12. In Figure II-12, the trim markers are still in place under the ablator layer. The effects of overspray on the vertical tail due to the later spraying of the fuselage can also be seen. This is a very porous surface deposit, and is readily removed during finishing operation.

5. Finishing the Ablator Layer - Finishing the ablator application entails sanding the surface to remove overspray and irregularities, and to bring the ablator layer down to the design thickness requirements. A thickness tolerance of $\pm$ .020 inches was selected for sizing the ablator, however, a few local thickness variations in excess of this amount were experienced. Finishing operations on the vehicle are shown in Figure II-13 and II-14.

For this operation, as with the limited applications of the predecessor contract, marking pens were used to identify the grid points and the penetrating needle dial gage was employed to monitor the ablator thicknesses. On an extensive operation like this full ablator application, the repetitive sequence of marking the grid point, measuring the ablator thickness, and sanding the ablator layer, was extremely time consuming. The condition was further aggravated by the fact that only two (2) dial thickness gages were available among seven (7) persons sanding the ablator. It was evident that some method of retaining the grid point locations on the sanded surface was required. In addition, a means of identifying when the ablator layer was at the design thickness was desirable.

Finishing operations were improved by locally sanding the grid point locations down to final thickness. This then permitted complete areas to be sanded until all evidence of the local depressions were eliminated. On future applicatinns, consideration should be given to fabrication of tools to locally size the ablator at the grid point locations more quickly and with more accuracy than was possible during this application.

An integral part of the finishing operation was trimming the ablator layer and removing the vinyl foam trim marker tape. This operation is shown in Figure II-15, and the resultant porous edge of the ablator is visible in Figure II-16. It should be noted that the contamination control masks are still in place in Figure II-16, and a considerable amount of sanded ablator dust is present on the ablator surface and along the edges of the ablator layer.

Final thickness determinations of the ablator layer are obtained through use of a penetrating needle dial deflection gage as shown in Figure II-17. Final ablator thicknesses for this initial full ablator application are presented in Tables II-2 through II-6 for the various areas of the aircraft. Grid points referred to by the tables are those defined for ablator thickness control in the Application and Refurbishment Manual, ER-14539. The completed ablator application is shown in Figure II-18 for the horizontal stabilizer and in Figure II-19 for the complete aircraft.

Acceptance of the ablator application is based on final material durometer and on bond line and intermaterial strengths as determined by proof test loading plugs bonded to the surface of the vehicle. Durometer checks were conducted randomly over the aircraft, and all readings were greater than 40 on the shore "A" scale. The acceptable lower limit for the fully cured material is 30 on the shore "A" scale. Ten test plugs were bonded to the ablator surface and the ablator layer cut through their periphery. Acceptability of the application requires a proof loading of 40 psi. The test plugs are .5 square inches and, therefore, the acceptable test loading is 20 lbs. The location of the test plugs over the aircraft, the test loadings, and the failure modes are presented in Table II-7.

6. Hard Point Inserts and Miscellany - Inserts of Modified DC 93-027 material were applied to the aircraft in the areas of the drop tank inboard sway braces and the forward jacking point. MA-25s-1 inserts were bonded to the vehicle skin at active pressure port and handling and alignment fixture attachment points to provide the sharp geometric definition and operational durability required in these areas. Inserts of the MA-25s-1 material were also applied over the ram air door in the fuselage nose, and the engine compartment fire doors at the aft end of the fuselage.

7. Wear Layer Application - The sized ablator application was completely encapsulated with a layer of the DC90-090 material. This was brush applied to all the edges and voids in the ablator layer (Figure II-20), and spray applied over the remainder of the vehicle (Figure II-21).

The primary purpose of the wear layer coating is to seal the ablator surface. However, extra applications were made to provide the aircraft with a uniform white exterior for appearance purposes at NASA's request. External markings for the aircraft were applied directly over the wear layer with the standard high temperature aircraft lacquer.

8. Panel Edge Strips - The thermal protection system employs strips of MA-25s-1 material around the periphery of all service panels to provide the additional durability required in these areas during panel removal and replacement. To permit access to the attachment screws, local cutouts are provided in the strips. Two methods of securing the strips to the panels were evaluated during this first application. The majority of the edge strips were permanently bonded using DC93-027 adhesive. Eight (8) panels were arbitrarily selected near the aft end of the fuselage, and their peripheral strips were secured with a contact adhesive. Were this method to prove satisfactory, the local coring of the strips to provide fastener access could be eliminated since the strips could be applied after final installation of the panels. The experiment was intended to determine if the contact adhesive was adequate to hold the strips in place during the high speed flight environment.

Figures II-22 through II-28 show the complete ablative thermal protection system and some of the local details thereof.

B. Pre-Flight Support and Repairs

Between the completion of the ablative thermal protection system and the actual flight test, ablator operations were limited to monitoring the ablation system and making whatever repairs became necessary. Handling damage was minimal, and repairs to the ablator layer could be accomplished through the local addition of the MA-25s repair mix and restoration of the white wear layer. The primary task during this period was the installation of ablator buttons in the fastener access cutouts. The buttons were secured in the strip cutouts with contact adhesive whenever a panel was installed for the final time. Figure II-24 shows some of the fuselage crown panels with the ablator buttons in place. Other panels in the figure still required removal, and consequently their fastener access cutouts are unplugged. Final preflight support during servicing consisted almost exclusively of button installation.

C. Touch-Up Operation

Following the first flight test to Mach 5.0, the ablative thermal protection system was restored to a flight worthy condition in preparation for further testing. The condition of the ablator following the flight and an evaluation of its performance are presented in Section III-A of this report. Defined below are the ablator activities required to prepare the ablator system for another test flight.

1. Molded Ablator Details - With the exception of the leading edge ablator details for the modified ventral fin and the forward vane antenna, refurbishment was minimal. Only the wings and horizontal stabilizers had experienced any degree of charring and they were refurbished by merely sanding away the friable char layer. No attempt was made to remove all of the thermally affected material, and sanding of the parts was continued only until resilient material was encountered.

The canopy leading edge detail required no refurbishment, but its surface was lightly sanded to remove the wear layer in an attempt to minimize deposition on the windshield during the subsequent flight.

The forward antenna detail had suffered local erosion due to shock wave impingement during the flight. The heavily charred material was removed from this area, and the detail contour restored through use of an insert of 14-II repair material, which is a trowelable version of the 3560-IIA leading edge material.

The lower portion of the ventral fin detail was degraded beyond reuse. This area of the detail was removed from the aircraft and a replacement part was made by modifying a spare portion of a vertical tail leading edge segment. This was bonded in place on the ventral and faired into the adjacent detail to complete the installation. Refurbishment of the remaining portion of the original detail was accomplished by lightly sanding away the friable char layer. The refurbished area of the ventral fin is shown in Figure II-30.

2. Primary Ablator Layer - Two methods of restoring the MA-25s ablator layer were employed in this refurbishment. For small localized areas of damage, troweled repair mix was utilized. Where the area of refurbishment was significant, a spray application of material was required.

The troweled repair mix was used for the local gouges in the ablator layer and in the areas where surface blistering was encountered. For these cases, the damaged area was trimmed to eliminate all loose ablator particles before addition of the repair mix. The patches were troweled smooth by using spatulas dampened with appropriate solvent. This eliminated most of the sanding normally required after use of the repair material. In addition to the normal MA-25s repair mix, a thixotropic blend of filled DC90-090 was used to make repairs along panel edges and at gaps. This eliminated the need for subsequent white coating the repairs in these areas.

The only thermally degraded areas of ablator occurred along the leading edges of the wings and stabilizers, the upper and lower speed brakes, and the sides of the ventral fin. These areas were refurbished by sanding away the fully charred surface layer. Only on the lower speed brakes was the amount removed sufficient to warrant reapplication of material. For these, the partial refurbishment procedure of the Application and Refurbishment Manual, ER-14539, was utilized. The speed brakes were sanded down to apparent virgin material and the surfaces thoroughly vacuumed to remove all trace of sanding dust. A new, wet, application of ablator was made directly over the surfaces without further preparation, and the areas sprayed up to original design thicknesses. After an overnight cure period, it was discovered that the new application had not achieved a satisfactory bond to the existing ablator layer. Inspection of samples taken from speed brakes revealed that a complete cure had not yet been achieved at the application interface. Additional samples were taken, and after artificially accelerated curing, indicated that a satisfactory bond would be achieved after full cure of the material at the interface. Aircraft flight scheduling, however, precluded allocation of this additional curing period, so the ablator was completely stripped from the lower speed brakes. Removal was accomplished to the residual "fuzz", and a new ablator application was made, continuously, up to design thickness.

The only area of questionable ablator performance during the Mach 5.0 test flight had been the left side of the upper vertical tail. This area had exhibited delamination of the ablator at the spray layer interface. Complete refurbishment of this area was required, and the existing ablator was removed to the residual "fuzz". Reapplication of the ablator was accomplished in two stages up to the design thickness. To avoid the contamination problem encountered in this area during the initial application, an external mask was used across the fixed to movable vertical tail section gap. This necessitated removal of a strip of ablator from the upper edge of the fixed section, and local cleaning of the section edges to provide good tape adhesion. This protection method also resulted in strips along both tail sections that were devoid of ablator after the refurbishment application. These areas were filled with the modified DC90-090 material after finishing of the refurbished ablator area.

The refurbished ablator thicknesses for the speed brakes and the vertical tail section are shown in Table II-5.

Although no significant thermal degradation had been experienced by the ablator layer on the nose of the aircraft, a malfunction of the ball nose attitude control system necessitated replacement of this assembly. This required reapplication of the ablator to the forward end of the fuselage in the area of the ball nose assembly.

The existing quantity of ablator had been depleted in making the aforementioned system refurbishments. A batch of ablator material left over from a previous application was used to coat the ball nose assembly after tests indicated its usability. The refurbished area of the forward nose is shown in Figure II-31.

A new dummy ramjet was supplied for the forthcoming Mach 6.5 test flight. This assembly contained an Inconel nose cone to eliminate the need for ablator over this highly instrumented section of the ramjet. An application of the MA-25s ablator was made over the remainder of the assembly in accordance with the design requirements of the Application and Refurbishment Manual. Material availability required use of the "outdated" ablator for this application also. The completed ramjet assembly is shown in Figure II-32 while the final ablator thicknesses for this second application are presented in Table II-6.

3. <u>Wear Layer Application</u> - The only refurbishment for the wear layer was its restoration over the vehicle. The DC90-090 layer had suffered localized handling damage and abrasions, and varying degrees of thermal degradation. The condition of the material ranged from complete erosion at the leading edges, a powdered residue in adjacent areas, superficial blistering farther back, to no sign of thermal exposure. Repair encompassed light sanding to remove the powdered residue and break the blisters, followed by a brush application of new material.

4. <u>Panel Edge Strips</u> - Some of the MA-25s-1 strips had been secured

with contact adhesive during the first application. Performance during the flight prompted replacement of all these strips with permanently bonded ones. Only one small area of the permanently bonded strips had become dislodged during the first flight. This strip was removed, and the void filled with the thixotropic mix of DC90-090. This was done to evaluate the thermal performance of this material in a relatively large area.

D. Complete Ablator Removal

Original program intent was to "touch-up" the ablator system twice to allow a total of three flights with the initial application. The damage sustained by the aircraft's ventral fin prevented a rapid re-flight, and made the utility of a second "touch-up" activity questionable. Consequently, the program was redirected to substitute the complete removal of the ablator system from the aircraft. The actual removal operation was accomplished by NASA personnel in accordance with the procedures defined in ER-14539. Martin Marietta provided the technical support to insure adherence to approved procedures and certify when an adequate degree of external vehicle cleanliness had been achieved. The operation initially required the careful removal of the MA-25s-1 strips from the service panel peripheries and local cleaning of the panel edges. This was followed by reapplication of the contamination control masking to protect the aircraft interior from the contamination generated during the ablator removal. Rough stripping of the basic ablator layer followed completion of the masking activity. Stripping was accomplished with plexiglass scrapers, and was followed by scrubbing of the surface to remove all residual ablator material. Final cleaning was performed with aluminum wool and nylon pads with powdered cleanser. Wooden toothpicks proved useful in dislodging the ablator material from skin gaps and the heads of permanent structural fasteners. The procedure resulted in an aircraft devoid of ablator, and exhibiting at least a 75% "water break" free surface.

E. Conclusions and Recommendations

The first full scale ablator operations were performed in good agreement with the specified procedures. A few areas, however, could be modified to improve the accomplishment of future operations.

This report section defines the recommended changes to the application and refurbishment procedures, and to the installation aids provided. Some revisions were also required to the basic design of the ablation system, however, they are delineated in Section III-C of this report.

1. Application Equipment and Materials - Performance of the bonding tool for the wing leading edge details could be improved if the locking lip on the inboard end were lengthened to make positive contact with the wing structure, and links were added between tool sections. These modifications would prevent the tool from sliding outboard as tension is applied to the straps.

The description of the spray apparatus will be changed to eliminate reference to the "Evenflo" regulator. This piece of equipment was intended to prevent line surge and the resultant compacting of the ablator fillers in the delivery line to the spray gun. It was never used in any ablator application, and no compacting problems were encountered. Use of the "Evenflo" regulator would prevent using multiple guns with the spray apparatus.

The masking materials specified in the manual will be revised to reflect current thinking. The use of "Aclar" and aluminized glass tapes shall be removed, and the trim marker vinyl tape will be specified. Descriptions of the masking materials will be added to the material specifications to better identify the specific items.

The list of cleaning materials defined for the ablator removal will be expanded to include the nylon scouring pads, the type cleaning brushes, and the wooden toothpicks that proved useful during ablator removal. The nylon pads were effective for large area rough cleaning, and the brushes and toothpicks were necessary for indented locations such as bolt heads and seams.

2. Application and Refurbishment Procedures - From a procedural standpoint, the Quality acceptance requirements will be enumerated for the bonded leading edge sections, hard point inserts, surface cleaning and basic ablator application. Acceptance tests will be defined and acceptable limits established. Proof test plug quantities and locations over the vehicle will be specified, and interpretations of ablator failure modes will be discussed.

The basic application procedure will be revised to reflect the use of self adhering trim markers, and priming of the panel edges prior to peripheral strip attachment. The repair procedures will be rewritten to more adequately define the degree to which various repair techniques can be safely employed.

A new section will be added to identify the external markings necessary on the ablator protected aircraft and the materials to be used in their application.

TABLE II-1

X-15A-2 ABLATOR APPLICATION

CONTAMINATION CONTROL RECORD

COLLECTOR NO.	COLLECTOR LOCATION ON AIRCRAFT	READING BY	PARTICLE COUNT BY SIZE RANGE *								
			ABLATOR			METALLIC			OTHER		
			A	B	C	A	B	C	A	B	C
1	PANEL F-24	NASA	2			1			4	1	
		MARTIN							3		
2	PANEL F-16	NASA	1			18			17	4	
		MARTIN	1			30			11	5	
3	LOX FILL	NASA							7		
		MARTIN				2			1		
4	PANEL F-15	NASA	2						2	2	
		MARTIN				7			4	1	
5	PANEL F-203	NASA	1						4	1	
		MARTIN							8	3	
6	PANEL F-59	NASA				54			9		
		MARTIN **				14			3		
7	PANEL F-209	NASA				32	3		5	2	1
		MARTIN				25	3		2		
8	PANEL F-60	NASA				26			5		
		MARTIN				20			13	1	
9	PANEL F-48	NASA	13			29			91		
		MARTIN	5	1		92			27	2	

* MSFC SPEC 164 ALLOWABLE PARTICLE SIZES AND QUANTITIES
A - 175 to 700 Quantity 5
B - 700 to 2500 Quantity 1
C - 2500 Quantity 0

** Collector glass for No. 6 was broken in transit. Readings taken where feasible.

TABLE II-2

ABLATOR THICKNESS RECORD

FUSELAGE

DATA PLANE	X DIM	1 REQD	1 ACT	2 REQD	2 ACTUAL LEFT	2 ACTUAL RIGHT	3 REQD	3 ACTUAL LEFT	3 ACTUAL RIGHT	4 REQD	4 ACTUAL LEFT	4 ACTUAL RIGHT	5 REQD	5 ACT
A	1 ft	.130	.130	.125	.134	.120	.120	.098	.120	.135	.146	.152	.150	.141
B	3 ft	.155	.169	.140	.135	.137	.120	.119	.130	.135	.135	.130	.150	.134
C	5 ft	.175	.157	.160	.116	.165	.145	.151	.143	.145	.168	.153	.150	.149
D	7 ft	.205	.211	.190	.118	.164	.170	.168	.164	.160	.166	.172	.150	.146
E	9 ft	.203	.223	.195	.145	.146	.165	.156	.165	.155	.165	.150	.140	.150
F	11 ft	.210	.225	.180	.139	.140	.155	.156	.164	.145	.139	.140	.130	.135
G	13 ft	.185	.170	.165	.188	.174	.150	.151	.153	.135	.130	.148	.120	.143
H	15 ft	.165	.181	.155	.138	.155	.140	.144	.160	.125	.120	.139	.110	.130
I	17 ft	.145	.157	.140	.122	.138	.135	.132	.140	.110	.142	.110	.090	.100
J	19 ft	.125	.102	.125	.120	.133	.130	.128	.128	.100	.120	.102	.070	.096
K	21 ft	.100	.095	.110	.094	.123	.125	.130	.132	.090	.090	.114	.050	.060
L	23 ft	.080	.083	.100	.091	.122	.120	.124	.123	.075	.084	.100	.030	.056
M	25 ft	.080	.080	.100	.116	.095	.120	.131	.111	.075	.082	.103	.030	.046
N	27 ft	.080	.095	.100	.115	.100	.120	.111	.099	.075	.096	.064	.030	.051
O	29 ft	.115	.101	.115	.131	.116	.120	.083	.091	.090	.076	.092	.060	.069
P	31 ft	.115	.118	.115	.123	.105	.120	.101	.087	.090	.105	.133	.060	.065
Q	33 ft	.115	.116	.115	.116	.123	.120	.074	.100	.090	.093	.060	.060	.073
R	35 ft	/115	.125	.115	1125	.117	.120	.100	.120	.090	.102	.083	.060	.068
S	37 ft	.115	.111	.115	.117	.121	.120	.078	.093	.090	.109	.103	.060	.080
T	39 ft	.115	.127	.115	.112	.112	.120	.089	.110	.090	.081	.074	.065	.062
U	41 ft	.115	.108	.115	.108	.121	.120	.118	.112	.090	.104	.093	.065	.085L .080R
V	43 ft	.140	.096	.130	.138	.144	.120	.119	.118	.095	.114	.087	.075	.090L .096R
W	45 ft	.140	.122L .115R	.130	.102	.106	.120	.108	.093	.100	.111	.113	.085	.080L .097R
X	47 ft	.140	.149L .142R	.130	.142	.132	.120	.126	.088	.100	.110	.077	.085	.100L .092R
Y	49 ft	.140	.123L .114R	.130	.104	.103	.120	.089	.078	.100	.112	.094	.085	.092L .075R
Z	51 ft	.140	.129	.130	.118	.114	.120	.110	.136	.100	.099	.104	.085	.102

TABLE II-3

ABLATOR THICKNESS RECORD
WING & FLAP

LOC	X DIM	Y DIM	UPPER SURFACE REQD	UPPER SURFACE ACTUAL LEFT	UPPER SURFACE ACTUAL RIGHT	LOWER SURFACE REQD	LOWER SURFACE ACTUAL LEFT	LOWER SURFACE ACTUAL RIGHT
1	12	12	.140	.120	.140	.200	.221	.209
2	24	12	.140	.118	.156	.210	.220	.190
3	24	24	.100	.108	.095	.180	.160	.190
4	36	12	.135	.139	.160	.220	.210	.220
5	36	24	.080	.083	.075	.205	.156	.186
6	36	36	.040	.048	.058	.180	.143	.190
7	36	48	.020	.050	.025	.155	.139	.166
8	48	12	.120	.135	.122	.220	.206	.228
9	48	24	.060	.071	.068	.205	.136	.194
10	48	36	.040	.055	.045	.175	.146	.193
11	48	48	.015	.020	.022	.160	.148	.167
12	48	60	.015	.025	.027	.145	.166	.153
13	60	12	.120	.126	.120	.220	.210	.240
14	60	24	.060	.069	.060	.205	.152	.210
15	60	36	.020	.040	.024	.185	.156	.200
16	60	48	.015	.030	.026	.160	.170	.177
17	60	60	.015	.022	.023	.145	.156	.163
18	60	72	.015	.037	.019	.135	.154	.121
19	72	12	.120	.133	.116	.225	.225	.232
20	72	24	.060	.071	.070	.210	.167	.200
21	72	36	.020	.078	.024	.185	.167	.200
22	72	48	.015	.028	.016	.160	.158	.166
23	72	60	.015	.027	.019	.175	.150	.191
24	72	72	.030	.024	.051	.200	.192	.195
25	72	84	.025	.029	.023	.195	.168	.194

LOC	X DIM	Y DIM	UPPER SURFACE REQD	UPPER SURFACE ACTUAL LEFT	UPPER SURFACE ACTUAL RIGHT	LOWER SURFACE REQD	LOWER SURFACE ACTUAL LEFT	LOWER SURFACE ACTUAL RIGHT
26	72	96	.025	.025	.040	.190	.155	.200
27	84	12	.120	.123	.119	.230	.256	.234
28	84	24	.060	.068	.056	.210	.206	.200
29	84	36	.020	.035	.032	.190	.183	.200
30	84	48	.015	.035	.026	.170	.169	.193
31	84	60	.030	.020	.025	.200	.191	.225
32	84	72	.040	.028	.041	.205	.182	.224
33	84	84	.025	.022	.031	.195	.156	.200
34	84	96	.025	.031	.034	.190	.139	.191
35	96	12	.135	.122	.130	.265	.230	.263
36	96	24	.085	.068	.073	.230	.192	.220
37	96	36	.020	.029	.026	.190	.200	.208
38	96	48	.015	.033	.020	.175	.206	.201
39	96	60	.040	.032	.042	.205	.213	.219
40	96	72	.040	.025	.036	.200	.185	.218
41	108	12	.140	.115	.140	.265	.261	.266
42	108	24	.085	.079	.058	.230	.213	.218
43	108	36	.050	.025	.053	.215	.190	.230
44	108	48	.040	.026	.041	.205	.186	.216
45	108	60	.040	.040	.044	.200	.210	.234
46	120	12	.140	.134	.152	.265	.220	.261
47	120	24	.085	.053	.090	.230	.215	.250
48	120	36	.070	.044	.068	.220	.191	.221
49	120	48	.065	.022	.038	.215	.172	.221
50	132	30	.065	.040	.064	.215	.209	.218

TABLE II-4

ABLATOR THICKNESS RECORD
HORIZONTAL STABILIZER

LOC	X DIM	Y DIM	UPPER SURFACE			LOWER SURFACE		
			REQD	ACTUAL		REQD	ACTUAL	
				LEFT	RIGHT		LEFT	RIGHT
1	12	9	.210	.155	.205	.210	.193	.200
2	24	9	.210	.160	.210	.210	.185	.200
3	24	18	.175	.143	.166	.175	.158	.150
4	36	9	.205	.162	.216	.205	.168	.190
5	36	18	.170	.149	.163	.170	.138	.170
6	36	27	.150	.161	.137	.150	.154	.160
7	48	9	.200	.176	.202	.200	.172	.190
8	48	18	.165	.149	.160	.165	.141	.160
9	48	27	.145	.165	.147	.145	.156	.150
10	48	36	.130	.157	.138	.130	.136	.130
11	60	9	.195	.175	.188	.195	.174	.165
12	60	18	.160	.142	.135	.160	.145	.150
13	60	27	.140	.158	.144	.140	.150	.143
14	60	36	.130	.146	.130	.130	.140	.143
15	60	45	.125	.137	.135	.125	.132	.125
16	72	9	.190	.155	.175	.190	.178	.178
17	72	18	.150	.138	.146	.150	.160	.157
18	72	27	.135	.146	.143	.135	.148	.139
19	72	36	.125	.129	.123	.125	.133	.120
20	72	45	.120	.157	.105	.120	.152	.115
21	84	9	.180	.173	.188	.180	.175	.190
22	84	18	.145	.136	.139	.145	.138	.151
23	84	27	.130	.115	.136	.130	.135	.128
24	84	36	.120	.132	.127	.120	.131	.125
25	96	9	.170	.171	.152	.170	.178	.178
26	96	18	.140	.133	.127	.140	.122	.130
27	96	27	.125	.124	.123	.125	.132	.113
28	108	9	.160	.167	.157	.160	.184	.154
29	108	18	.130	.134	.136	.130	.112	.142
30	120	18	.120	.125	.122	.120	.127	.127

TABLE II-5

ABLATOR THICKNESS RECORD

VERTICAL TAIL

LOC	X DIM	Y DIM	REQD THKNS	ACTUAL THICKNESS LEFT SIDE ORIG	ACTUAL THICKNESS LEFT SIDE REFURB	ACTUAL THICKNESS RIGHT SIDE ORIG	ACTUAL THICKNESS RIGHT SIDE REFURB
1	9	12	.260	.286		.257	
2	21	12	.255	.286		.250	
3	33	12	.205	.260		.212	
4	45	12	.200	.240		.210	
5	57	12	.195	.200		.200	
6	69	12	.190	.213		.196	
7	81	12	.200	.214	.210	.197	.190
8	93	12	.200	.201	.184	.178	.155
9	105	12	.200	.207	.175	.180	.166
10	107	12	.200	.217	.187	.196	.180
11	9	3	.260	.267		.250	
12	21	3	.255	.247		.263	
13	33	3	.205	.217		.210	
14	45	3	.200	.220		.190	
15	57	3	.195	.210		.155	
16	69	3	.190	.201		.206	
17	81	3	.200	.199	.181	.187	.181
18	93	3	.200	.214	.167	.195	.203
19	105	3	.200	.217	.155	.206	.179
20	9	-6	.260	.256	.265	.246	
21	21	-6	.255	.238	.260	.257	
22	33	-6	.250	.238	.230	.263	
23	45	-6	.260	.250	.242	.240	
24	57	-6	.260	.275	.229	.266	
25	69	-6	.260	.232	.237	.256	
26	81	-6	.255	.248	.255	.251	
27	93	-6	.250	.237	.225	.256	
28	105	-6	.250	.238	.225	.257	
29	9	-15	.260	.260	.251	.265	
30	21	-15	.255	.240	.272	.252	
31	33	-15	.250	.264	.255	.260	
32	45	-15	.260	.276	.245	.269	
33	57	-15	.260	.250	.255	.258	
34	69	-15	.260	.232	.240	.268	
35	81	-15	.255	.248	.245	.250	
36	93	-15	.250	.254	.230	.247	
37	9	-24	.260	.266	.290	.256	
38	21	-24	.255	.257	.264	.245	
39	33	-24	.250	.256	.264	.232	
40	45	-24	.260	.259	.265	.252	
41	57	-24	.260	.259	.260	.249	
42	69	-24	.255	.228	.240	.220	
43	81	-24	.250	.255	.265	.234	
44	93	-24	.250	.230	.240	.263	

TABLE II-6

ABLATOR THICKNESS RECORD

MODIFIED VENTRAL FIN & DUMMY RAM-JET

LOC	X DIM	Y DIM	REQD THKNS	ACTUAL THICKNESS LEFT SIDE ORIG	ACTUAL THICKNESS LEFT SIDE REFURB	ACTUAL THICKNESS RIGHT SIDE ORIG	ACTUAL THICKNESS RIGHT SIDE REFURB
1	6	15	.185	.178		.183	
2	18	15	.205	.180		.168	
3	30	15	.195	.178		.196	
4	42	15	.190	.208		.208	
5	54	15	.200	.213	.210	.177	.183
6	66	15	.200	.175	.209	.159	.192
7	78	15	.200	.165	.198	.149	.191
8	6	6	.185	.152		.159	
9	18	6	.205	.172		.153	
10	30	6	.195	.168		.166	
11	42	6	.190	.202		.192	
12	54	6	.200	.202	.204	.174	.193
13	66	6	.200	.175	.204	.157	.199
14	78	6	.200	.172	.190	.168	.193

LOC	REQD THKNS	ACTUAL THICKNESS LEFT SIDE FIRST	ACTUAL THICKNESS LEFT SIDE SECOND	ACTUAL THICKNESS RIGHT SIDE FIRST	ACTUAL THICKNESS RIGHT SIDE SECOND
A-1	.310	.302	-	-	-
A-2	.250	.285	-	.296	-
A-3	.250	.260	-	-	-
B-1	.420	.388	.373	-	-
B-2	.390	.375	.387	.360	.353
B-3	.390	.326	.392	-	-
C-1	.310	.335	.336	-	-
C-2	.290	.282	.330	.278	.345
C-3	.290	.267	.340	-	-
D-1	.220	.212	.223	-	-
D-2	.180	.172	.202	.170	.195
D-3	.180	.150	.187	-	.189
E-1	.150	.135	.164	-	-
E-2	.090	.094	.127	.096	.131
E-3	.090	.088	.108	.088	.110

ABLATOR APPLICATION PROOF TEST RESULTS

TABLE II-7

TIME OF TEST	TEST PLUG LOCATION	LOAD	REMARKS
AFTER APPLICATION	TOP OF LEFT HOR. STAB.	22 lb.	SEPARATION IN ABLATOR
	BOTTOM LEFT HOR. STAB.	24 lb.	NO FAILURE
	TOP OF RIGHT HOR. STAB.	21 lb.	NO FAILURE
	BOTTOM RIGHT HOR. STAB.	-	PLUG ACCIDENTALLY REMOVED
	TOP OF LEFT WING	20 lb.	NO FAILURE
	BOTTOM OF LEFT WING	21 lb.	NO FAILURE
	TOP OF RIGHT WING	20 lb.	NO FAILURE
	BOTTOM OF RIGHT WING	20 lb.	NO FAILURE
	LEFT SIDE VERT. TAIL	19.5 lb.	SEPARATION AT SPRAY PLANE INTERFACE
	RIGHT SIDE VERT. TAIL	-	PLUG ACCIDENTALLY REMOVED
AFTER REFURBISHMENT	LEFT SIDE VERT. TAIL	>20 lb.	SEPARATION IN ABLATOR
	LEFT LOWER SPEED BRAKE	>20 lb.	SEPARATION IN ABLATOR
	RIGHT LOWER SPEED BRAKE	>20 lb.	SEPARATION IN ABLATOR
AFTER MACH 6.7 FLT.	FUSE. CROWN @ STA 46	20 lb.	SEPARATION IN PYROLYSIS ZONE OF ABLATOR
	FUSE. BOTTOM @ STA 117	34 lb.	SEPARATION IN ABLATOR
	FUSE. CROWN @ STA 225	30 lb.	SEPARATION IN ABLATOR
	FUSE. BOTTOM @ STA 335	46 lb.	SEPARATION IN ABLATOR
	FUSE. CROWN @ STA 450	12 lb.	SEPARATION AT ABLATOR SURFACE
	FUSE. BOTTOM @ STA 518	29 lb.	SEPARATION IN ABLATOR
	TOP OF LEFT WING	38 lb.	SEPARATION IN ABLATOR
	BOTTOM OF LEFT WING	20 lb.	SEPARATION IN PYROLYSIS ZONE OF ABLATOR
	TOP OF RIGHT WING	43 lb.	SEPARATION IN ABLATOR
	BOTTOM OF RIGHT WING	22 lb.	SEPARATION IN PYROLYSIS ZONE OF ABLATOR
	LEFT SIDE VERT. TAIL	-	TEST PLUG BOND FAILURE
	RIGHT SIDE VERT. TAIL	-	TEST PLUG BOND FAILURE

Figure II-1 Cleaning the Aircraft in Preparation for the Ablator Application

NASA Flight Research Center
Edwards, California

Figure II-2 Application of Tape Masks Around Panel Edges

NASA Flight Research Center
Edwards, California

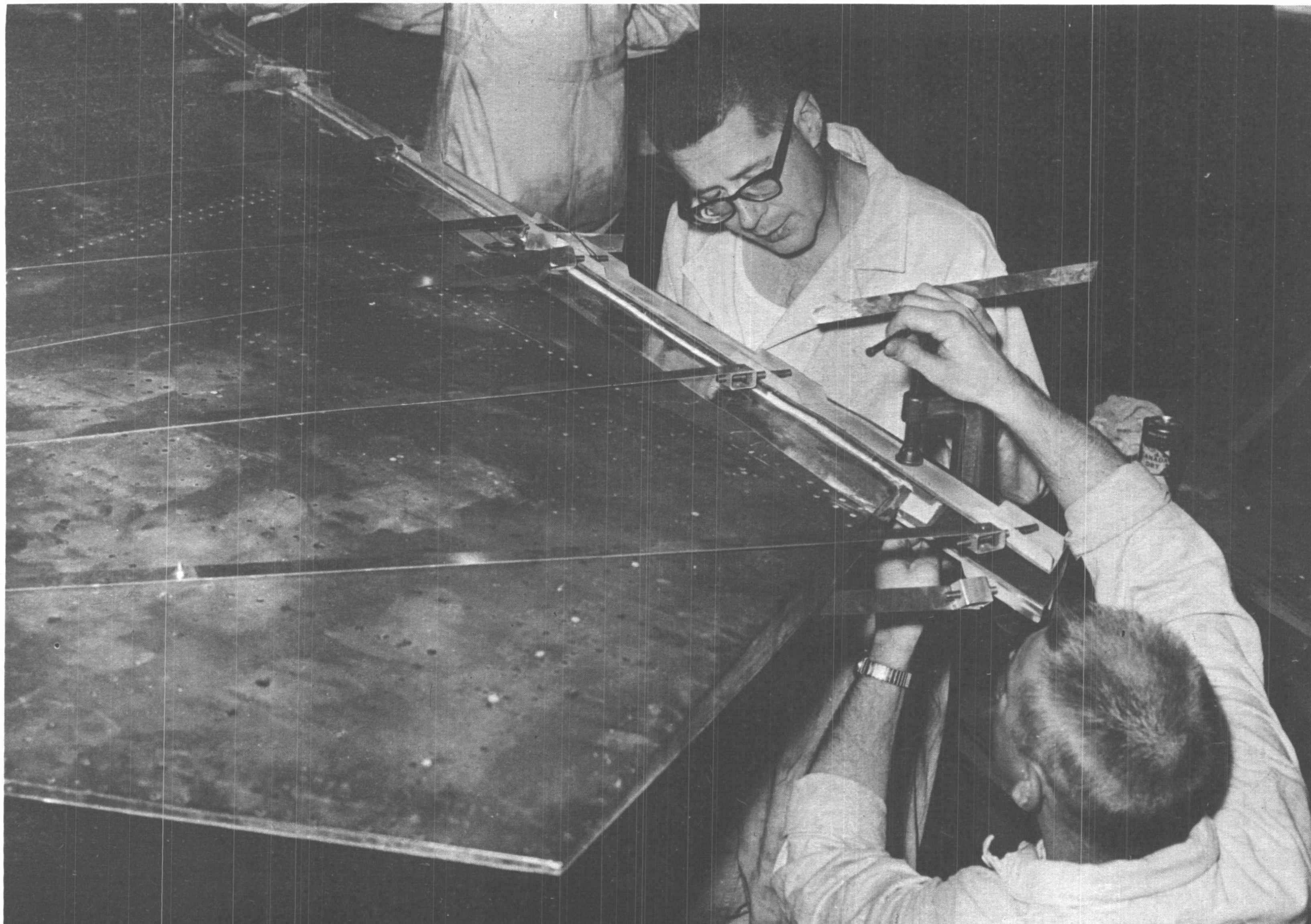

Figure II-3 Installing the Wing Leading Edge Ablator Details

Flight Research Center
Edwards, California

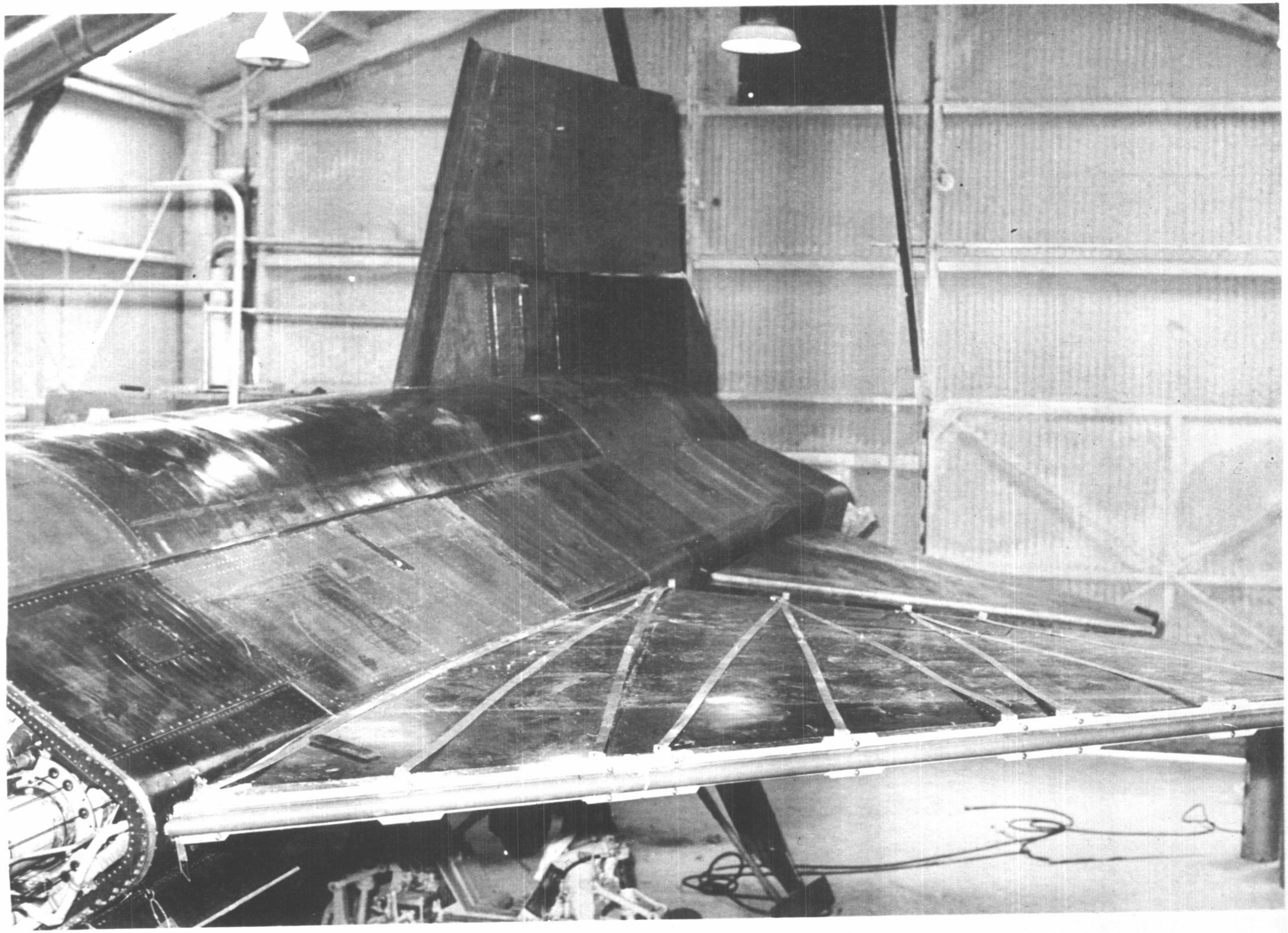

Figure II-4 Complete Installation of Wing Leading Edge with Bonding Tool in Plan

NASA Flight Research Center
Edwards, California

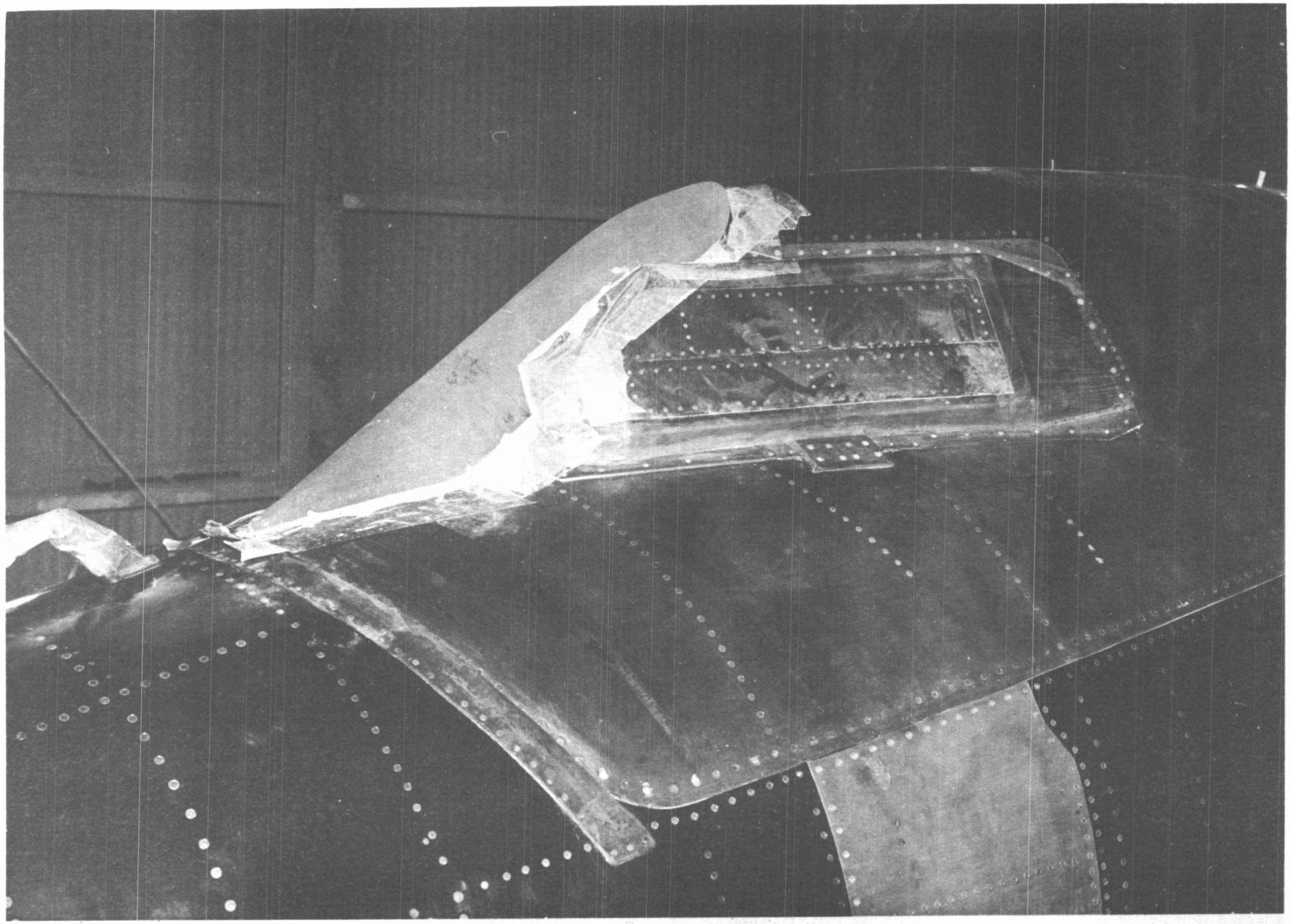

Figure II-5 Canopy Leading Edge Ablator Detail

Flight Research Center
Edwards, California

ABLATOR APPLICATION SEQUENCE

X-15A-2 T.P.S.

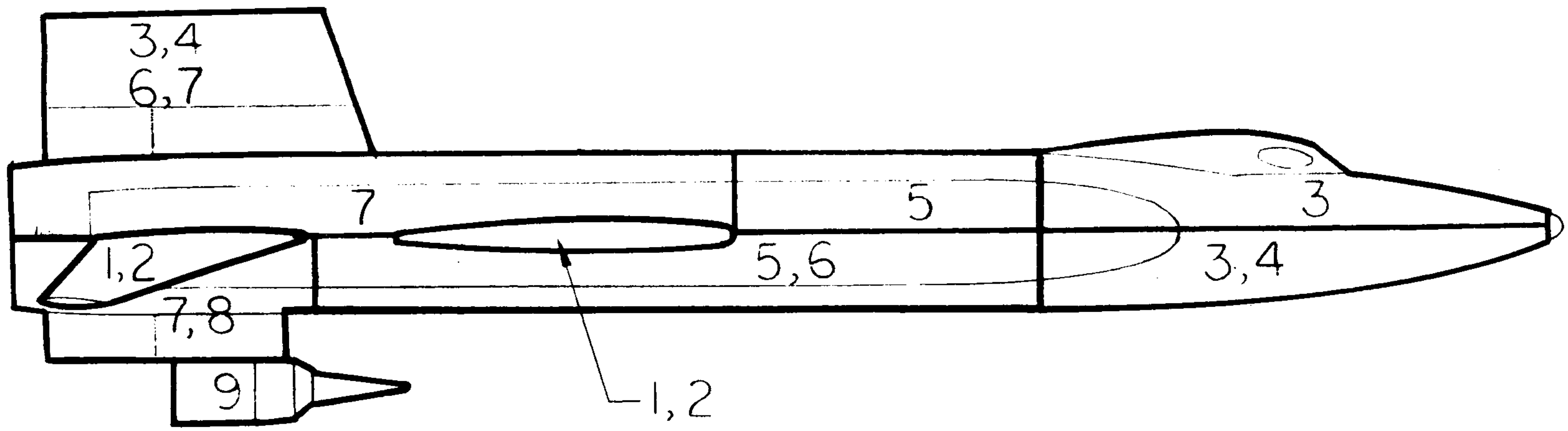

HEAVY LINES DEFINE AREAS OF CONTINUOUS ABLATOR APPLICATION

NUMBERS INDICATE SEQUENCE OF APPLICATION BY AREA

Figure II-6 **Sequence of Primary Ablator Applicator**

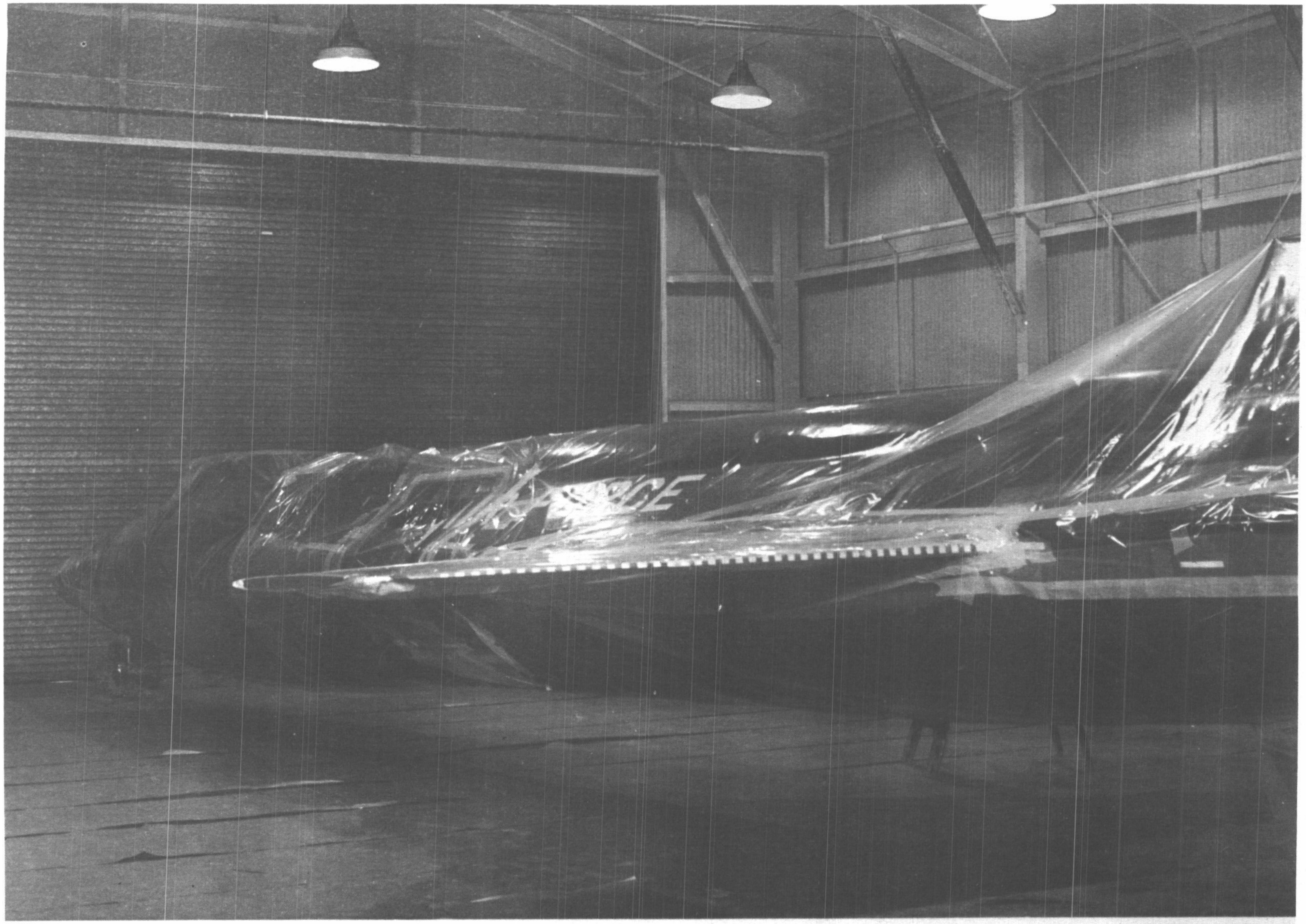

Figure II-7 Polyethylene Covered Aircraft Prior to Ablator Application

NASA Flight Research Center
Edwards, California

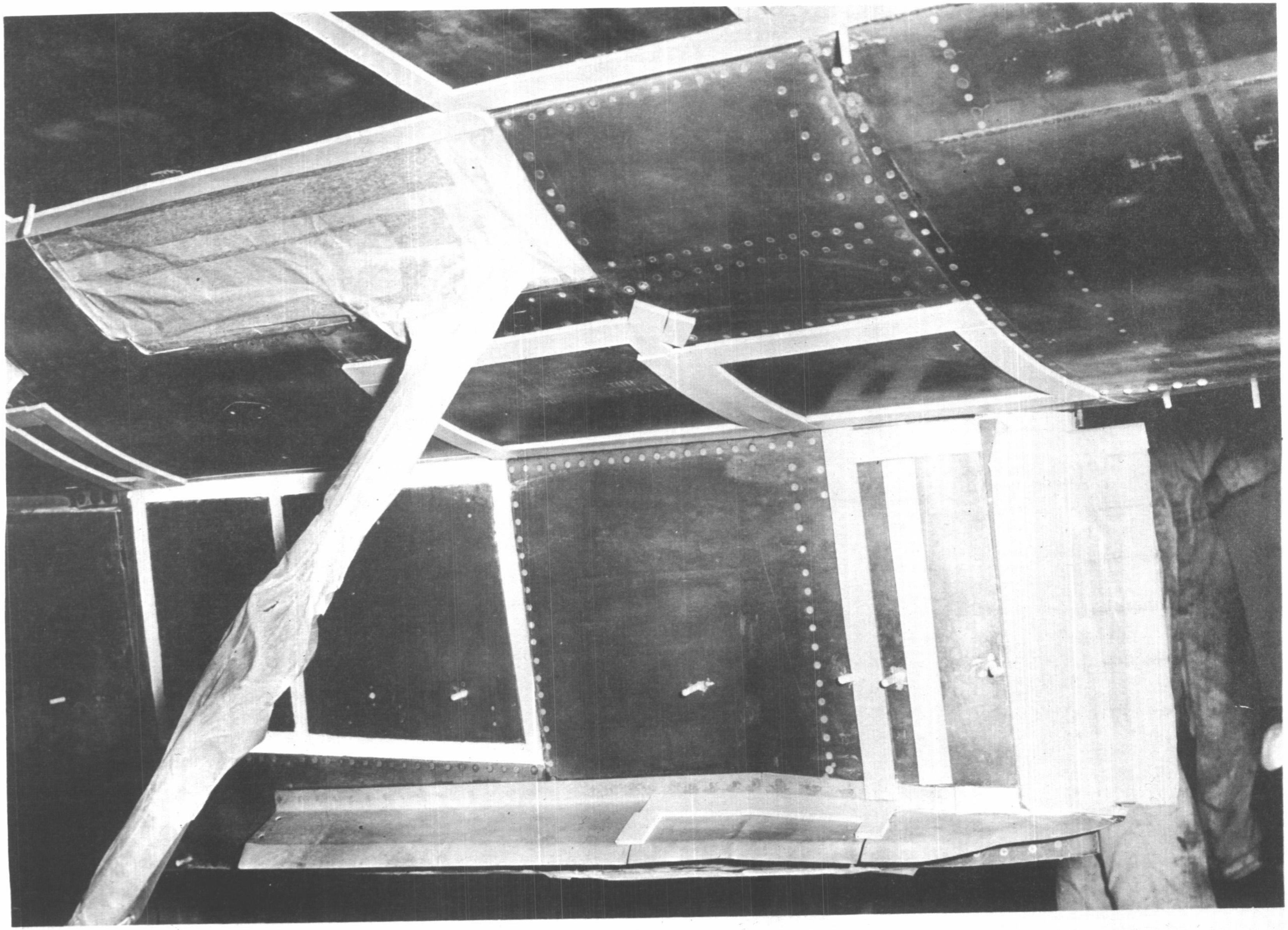

Figure II-8 Trim Marker Installation, Ventral Fin

Flight Research Center
Edwards, California

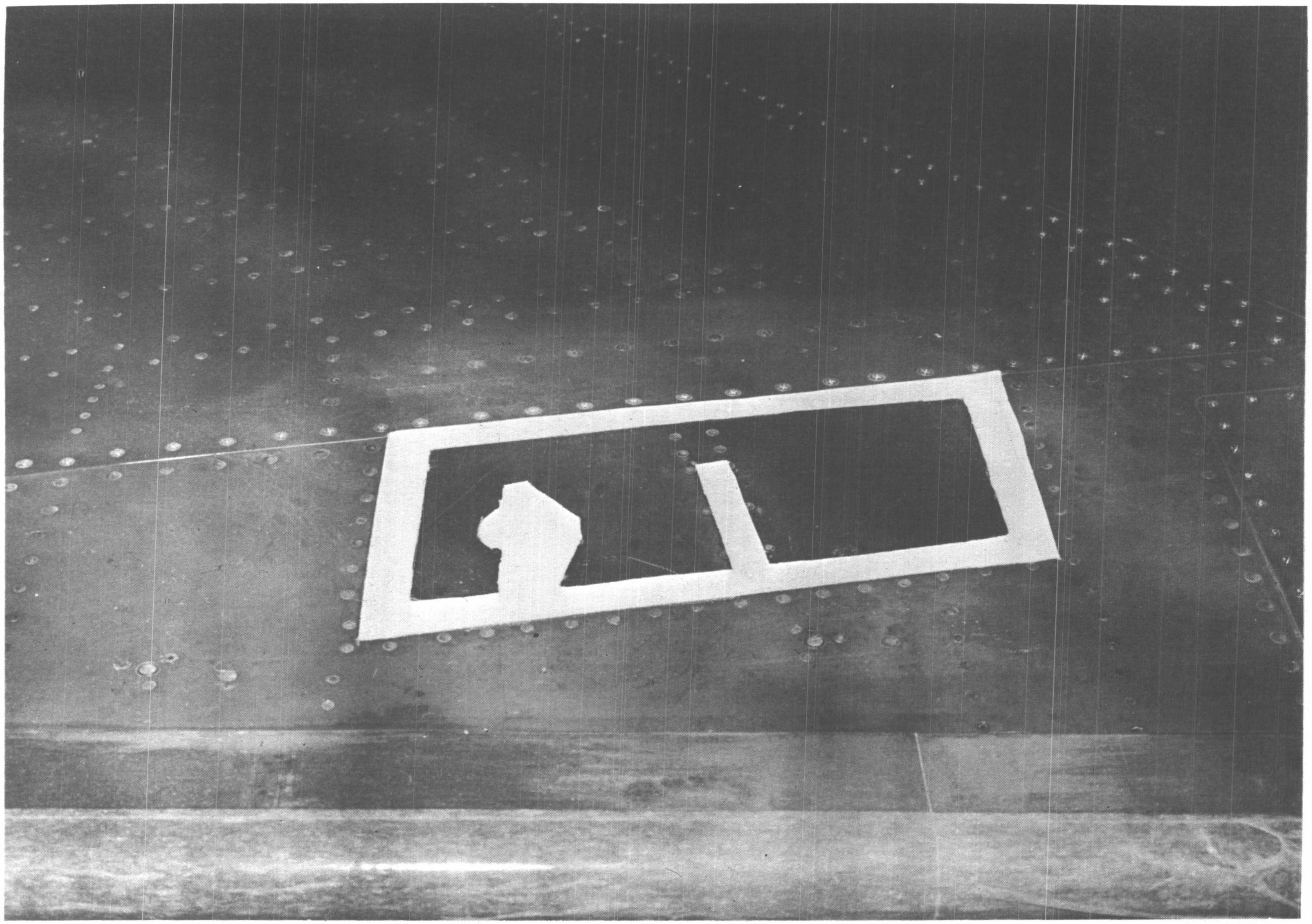

Figure II-9 . DC93-027 Over Periphery of Wing BCS Panel

Flight Research Center
Edwards, California

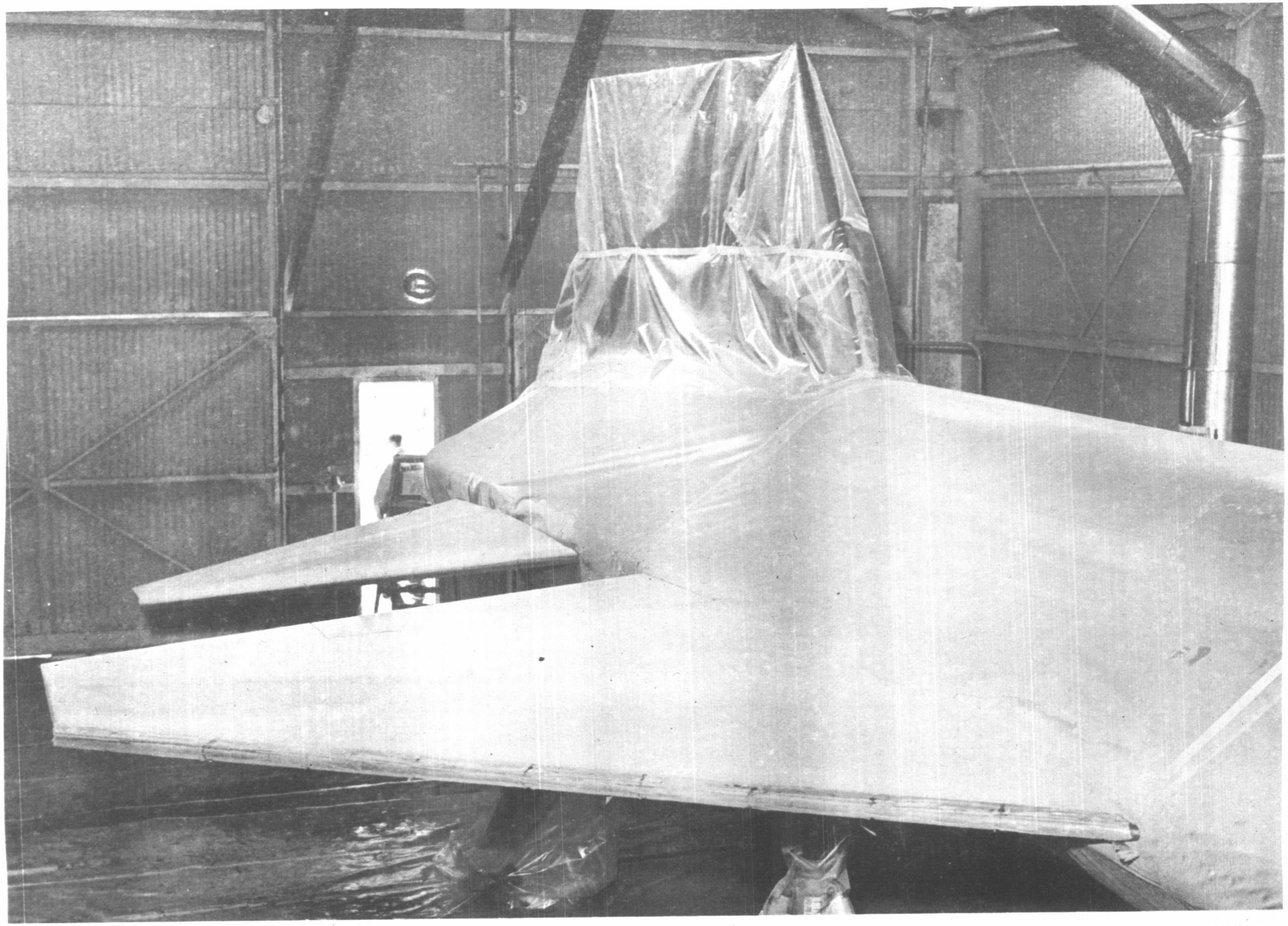

Figure II-10   Ablator Application, Wing and Stabilizer

NASA Flight Research Center
Edwards, California

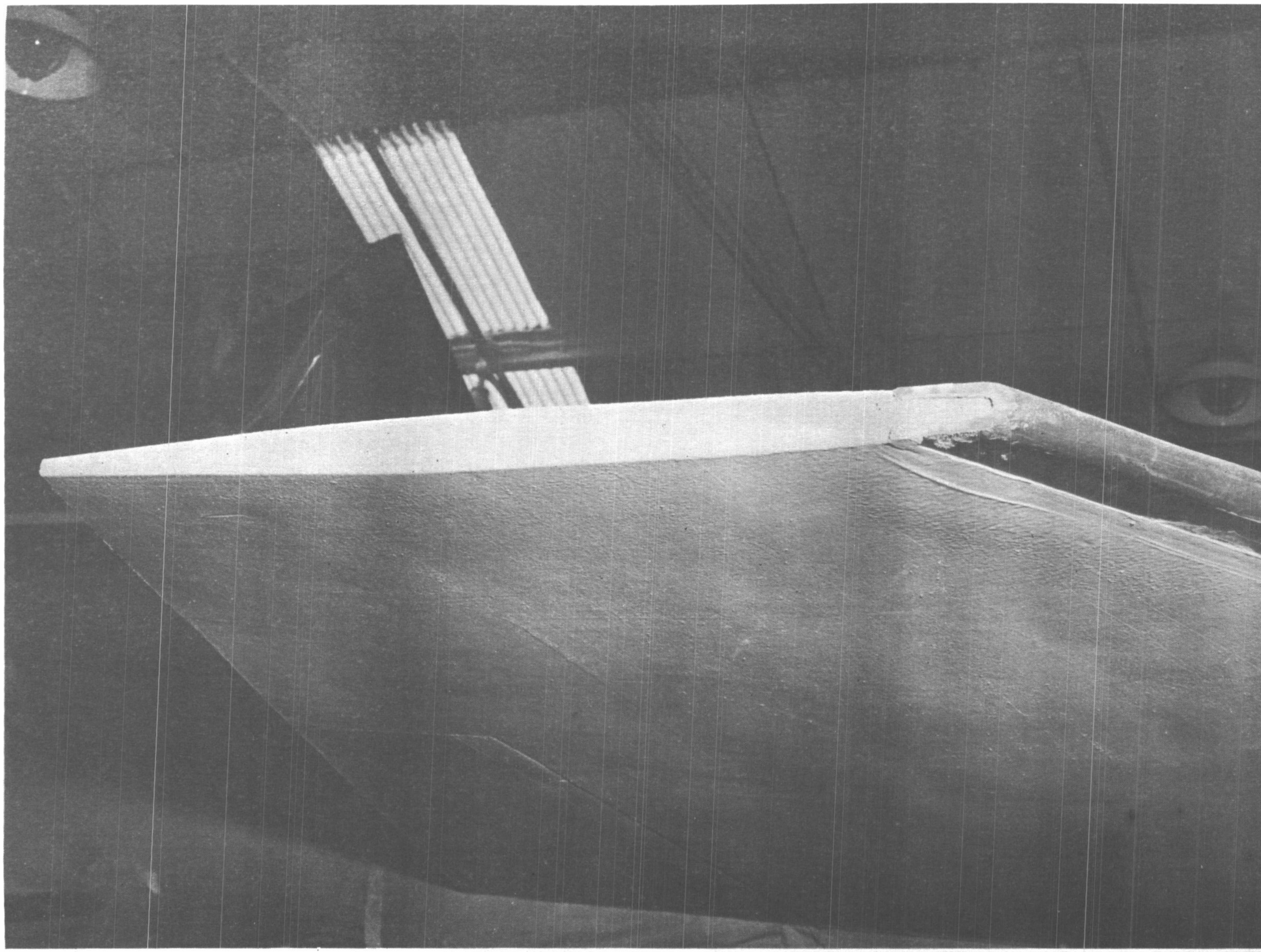

Figure II-11 Ablator Application, Wing Tip Lower Surface

NASA Flight Research Center
Edwards, California

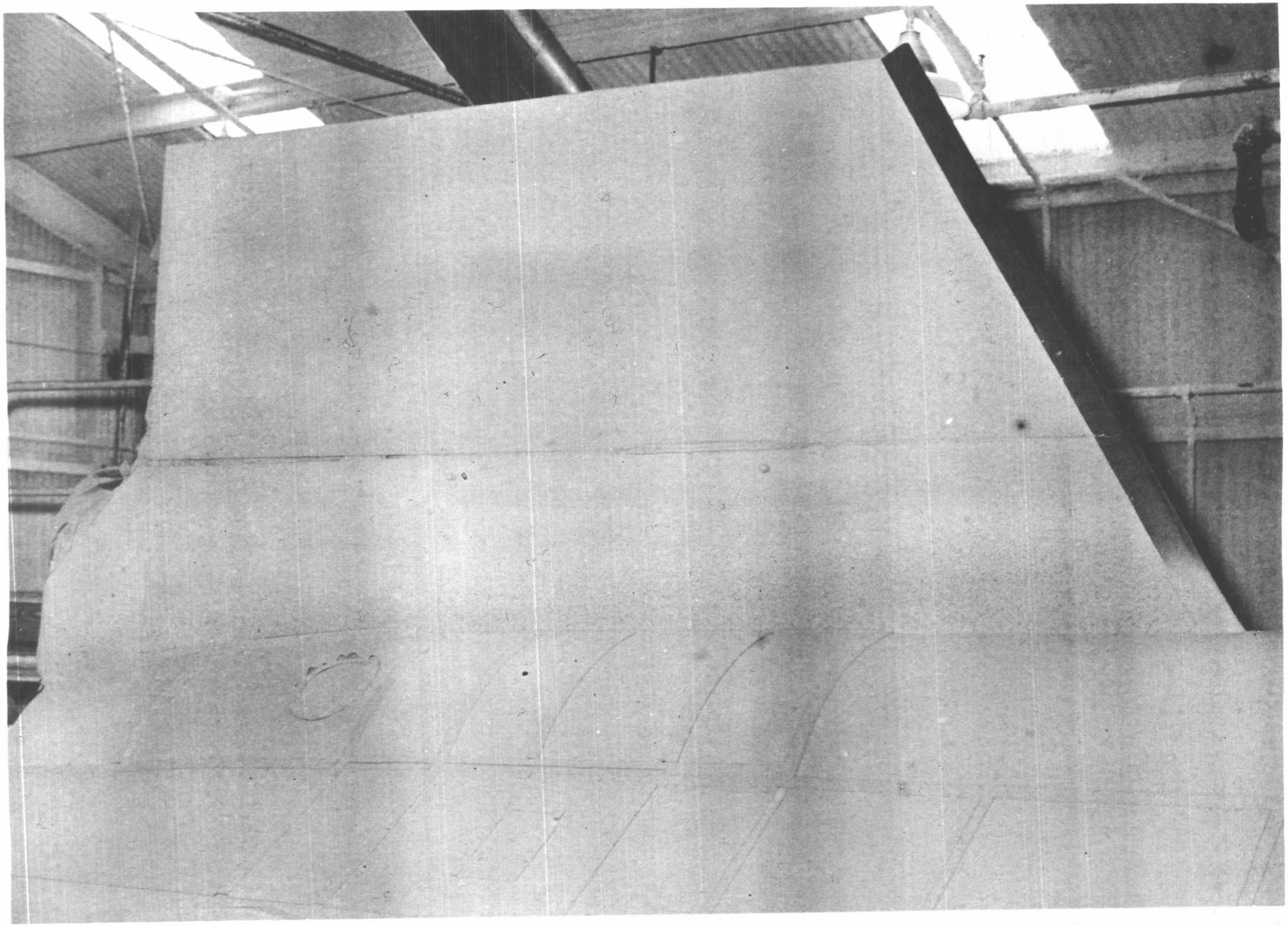

Figure II-12 Ablator Application, Aft Fuselage and Vertical Tail

NASA Flight Research Center
Edwards, California

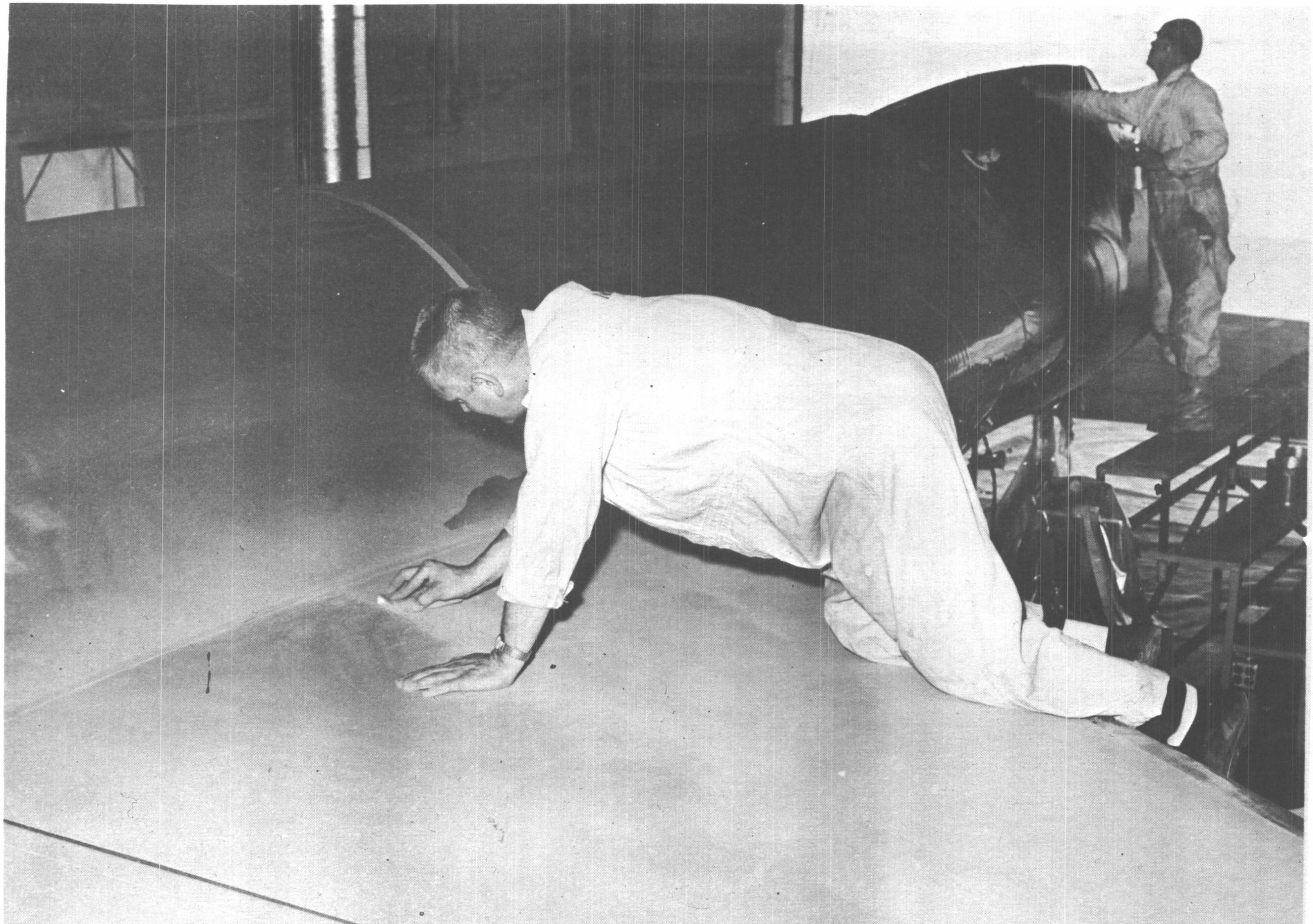

Figure II-13 Finishing the Wing Ablator Layer

Flight Research Center
Edwards, California

Figure II-14 Finishing the Fuselage Ablator Layer

Flight Research Center
Edwards, California

Figure II-15 Removing the Trim Markers from the Ablator Application

NASA Flight Research Center
Edwards, California

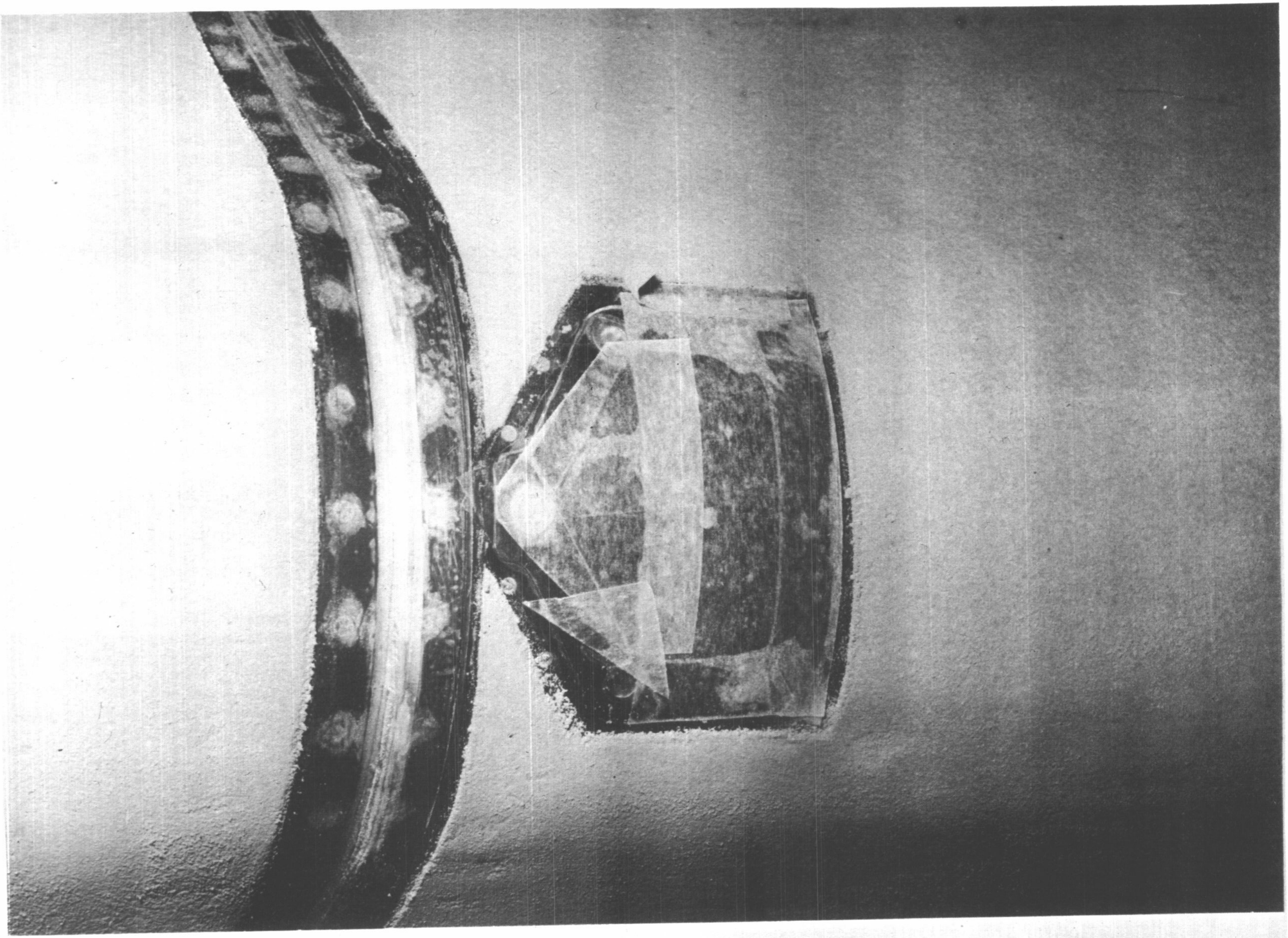

Figure II-16 Close-up of Ablator Layer with Trim Marker Removed

NASA Flight Research Center
Edwards, California

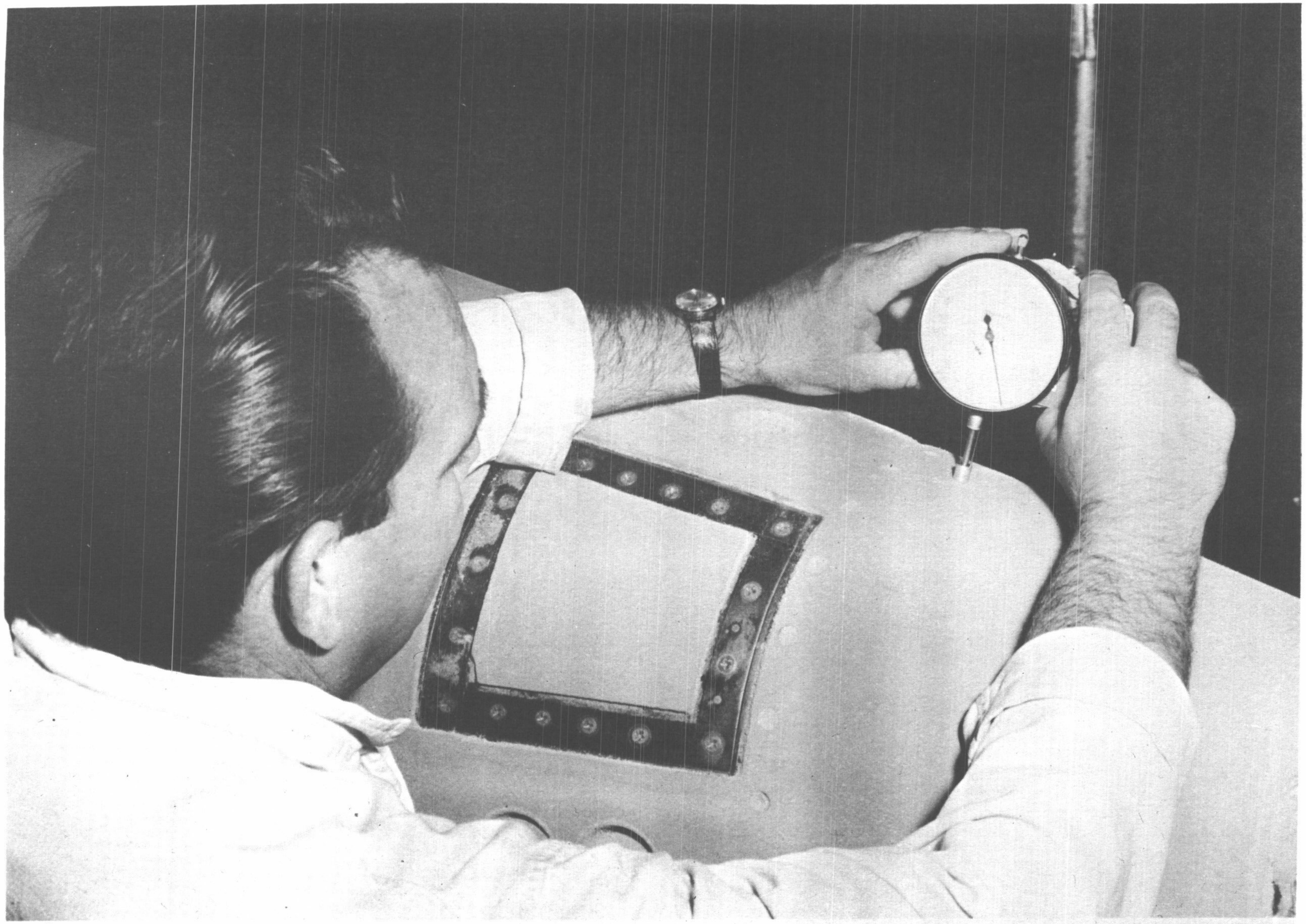

Figure II-17 Obtaining Final Ablator Thickness

NASA Flight Research Center
Edwards, California

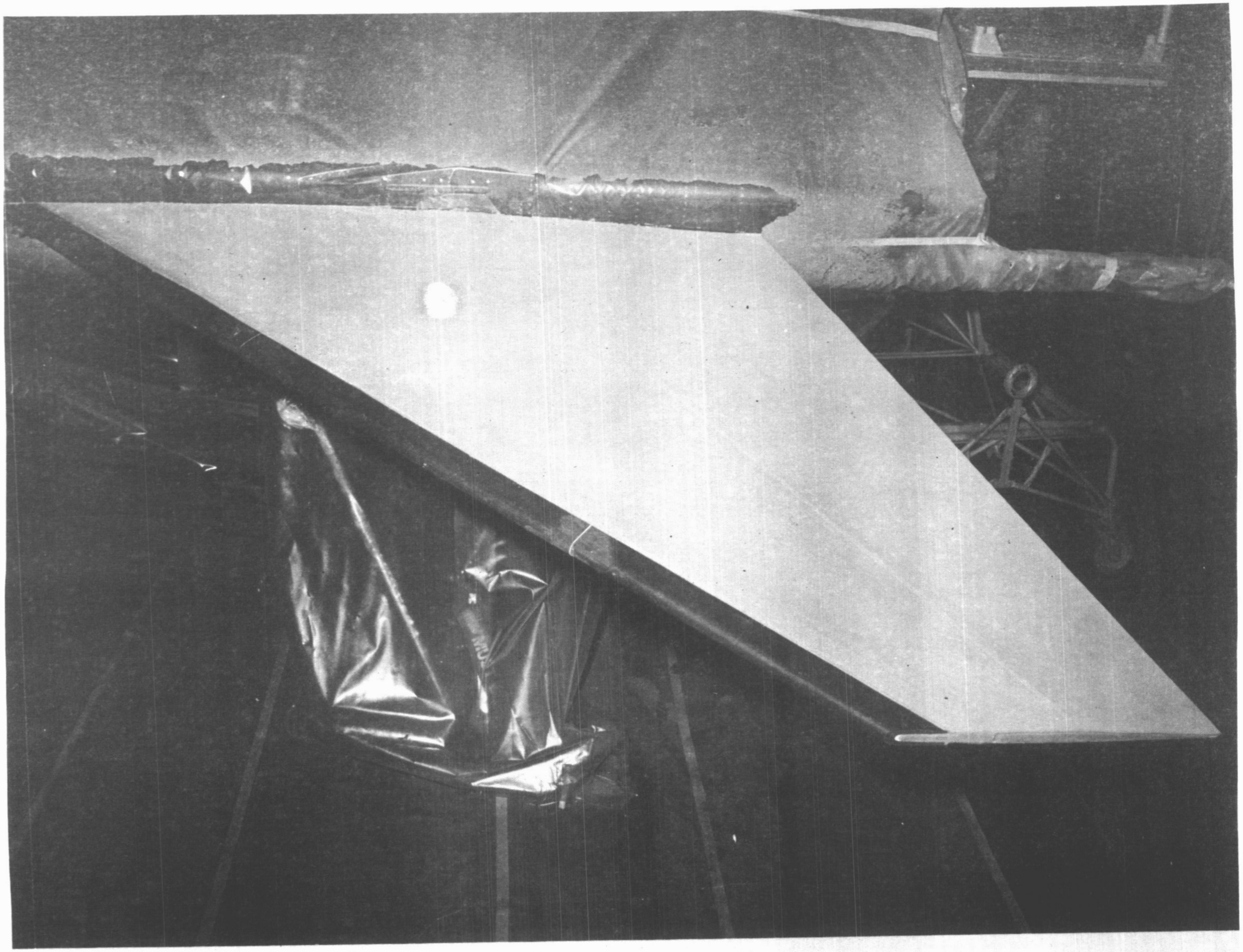

Figure II-18   Finished Stabilizer Ablator Application

Flight Research Center
Edwards, California

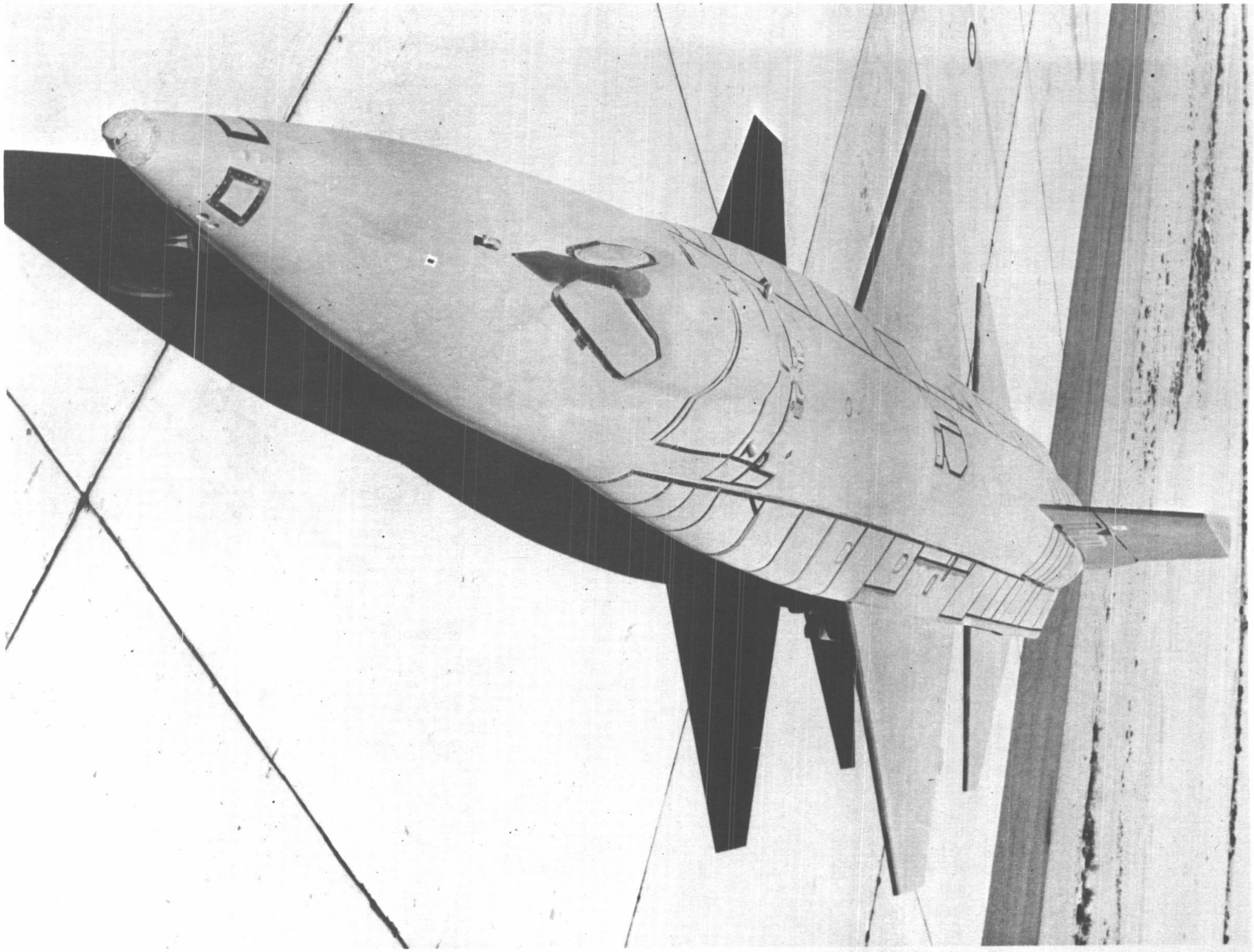

Figure II-19   Overall View of Basic Ablator Application

Figure II-20 Wear Layer Brushed on Ablator Edges

NASA Flight Research Center Edwards, California

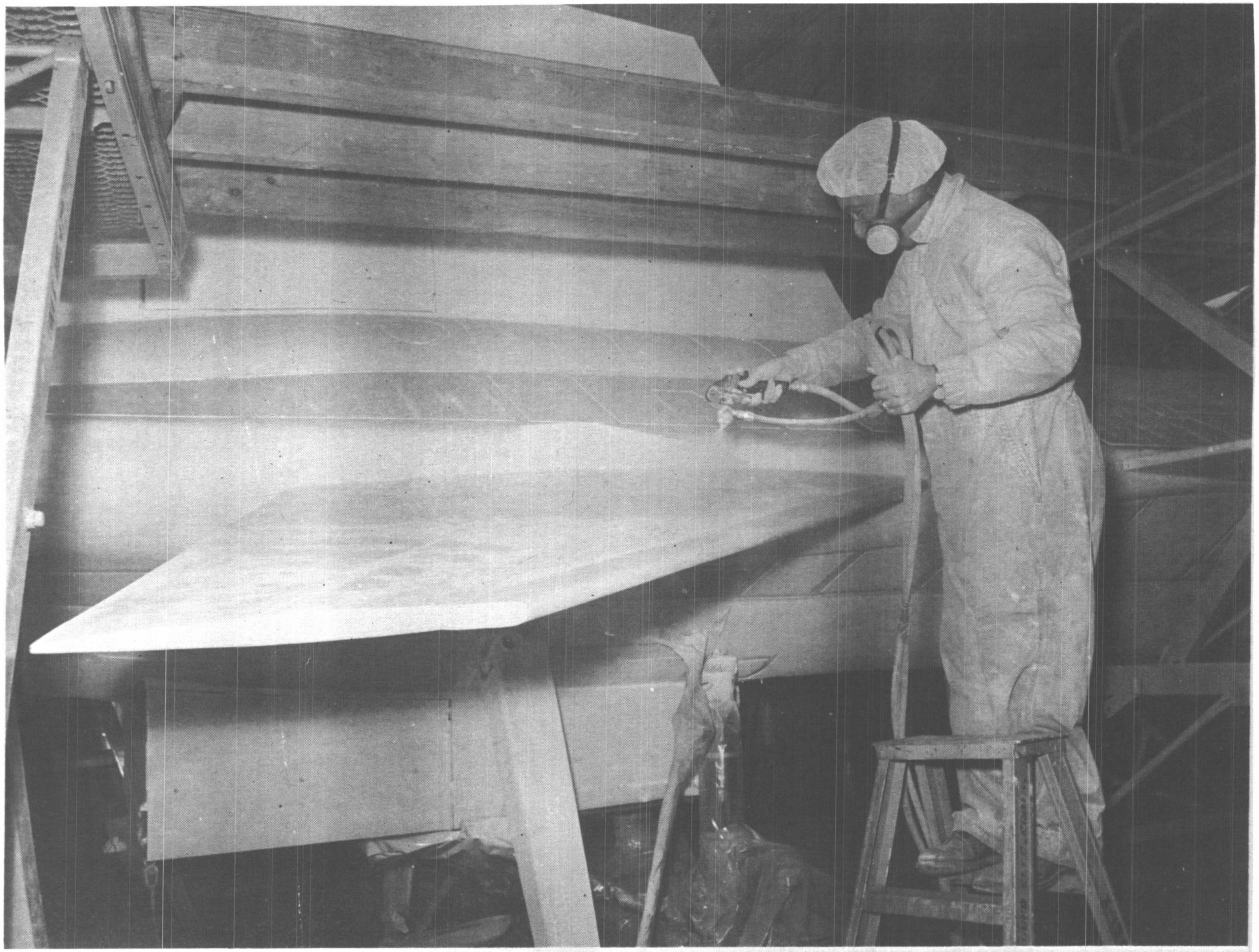

Figure II-21 Wear Layer Spray Application

Flight Research Center
Edwards, California

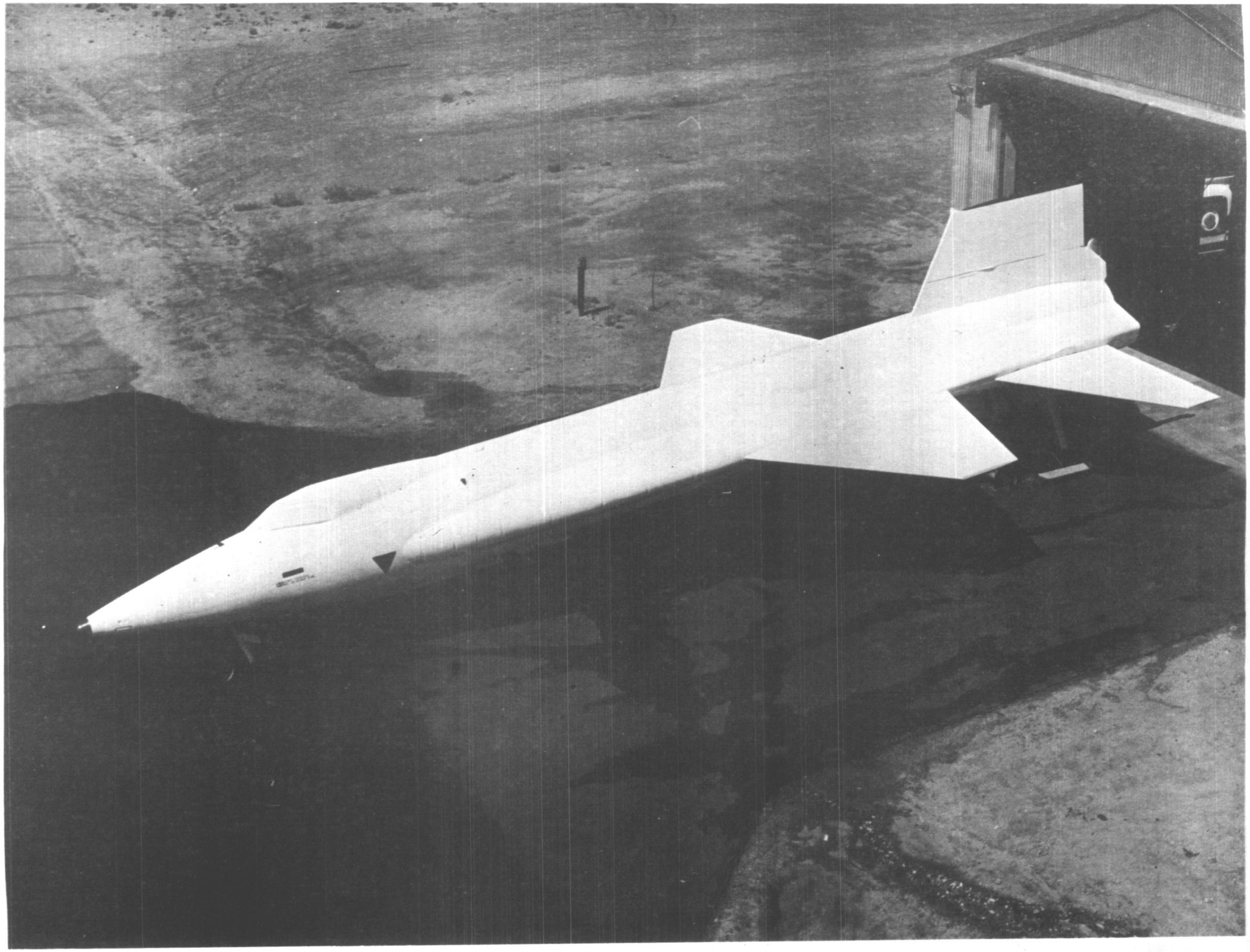

Figure II-22 Complete Ablator Application

Flight Research Center
Edwards, California

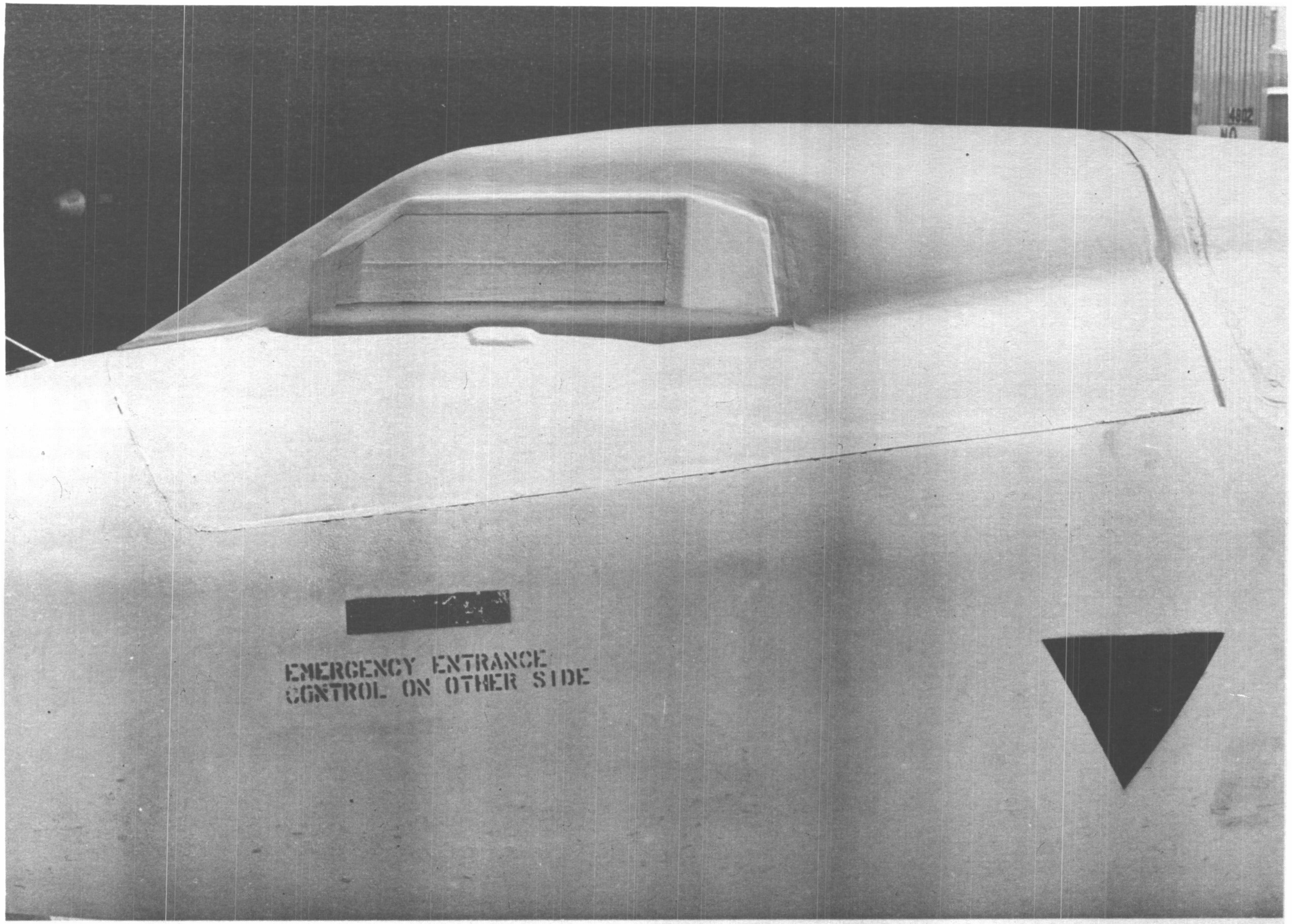

Figure II-23 Ablator Application on Canopy Eyelid Assembly

Flight Research Center
Edwards, California

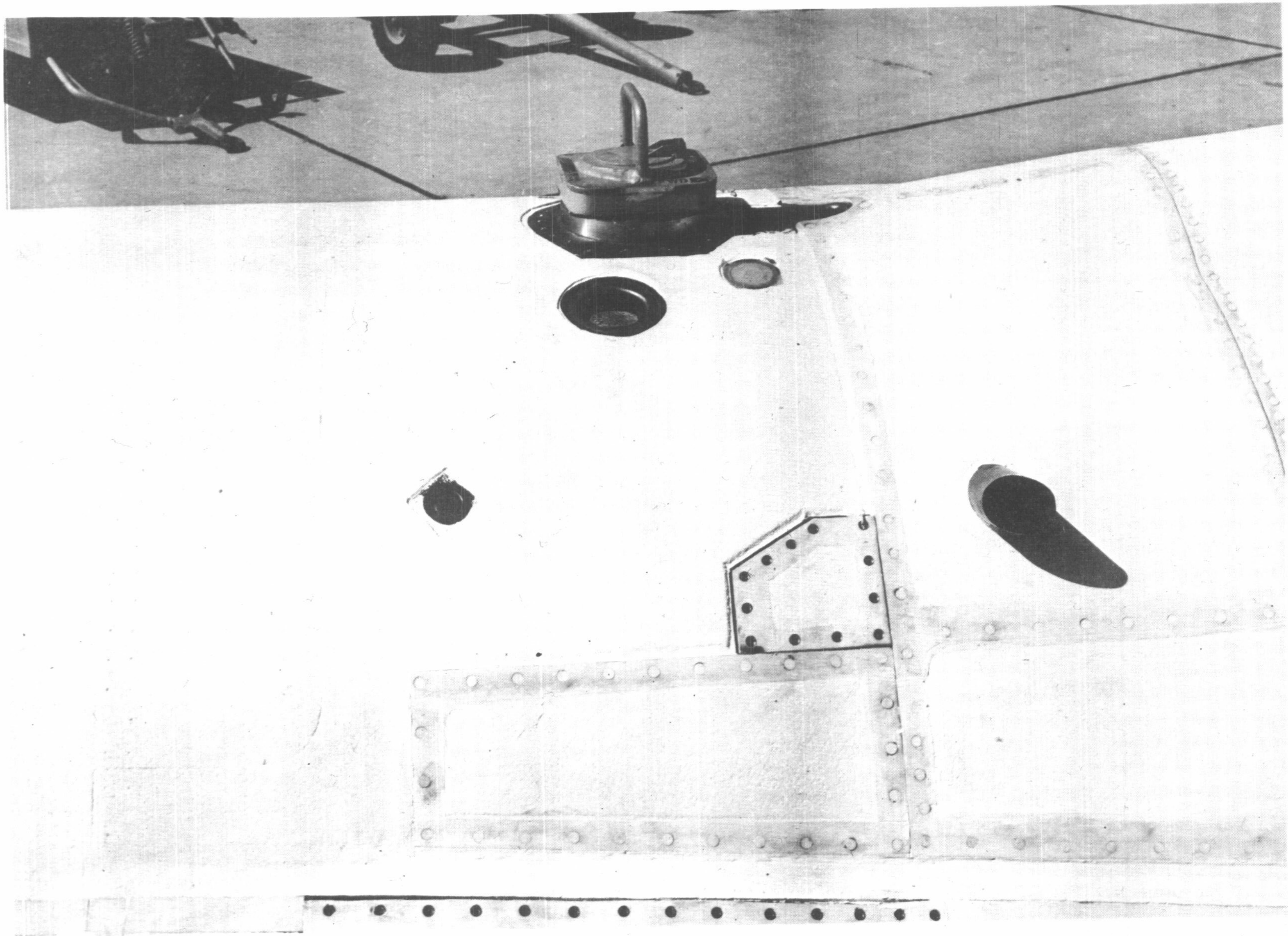

Figure II-24 Complete Ablator Application on Fuselage Crown

NASA Flight Research Center
Edwards, California

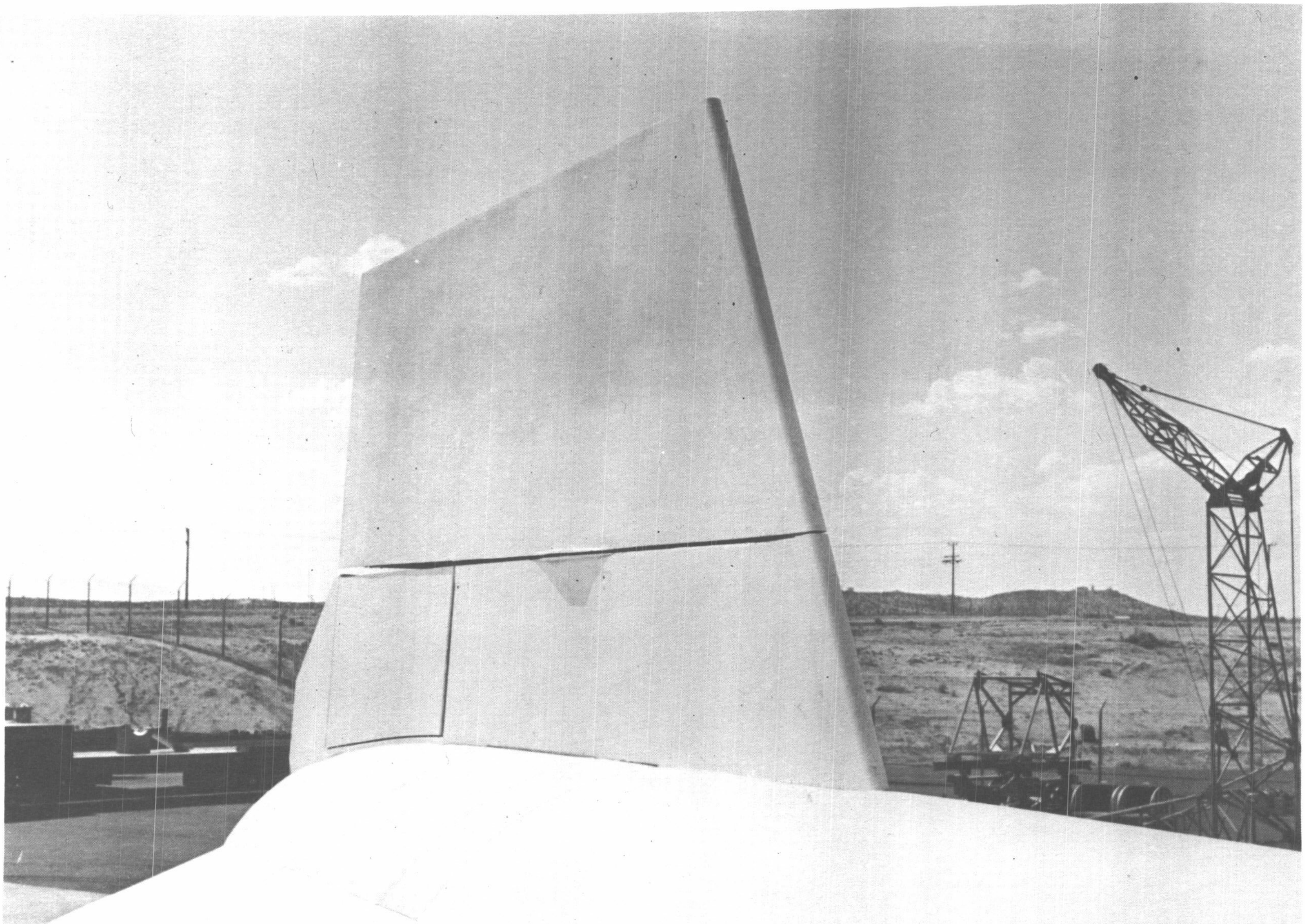

Figure II-25 Complete Ablator Application on Vertical Tail

NASA Flight Research Center
Edwards, California

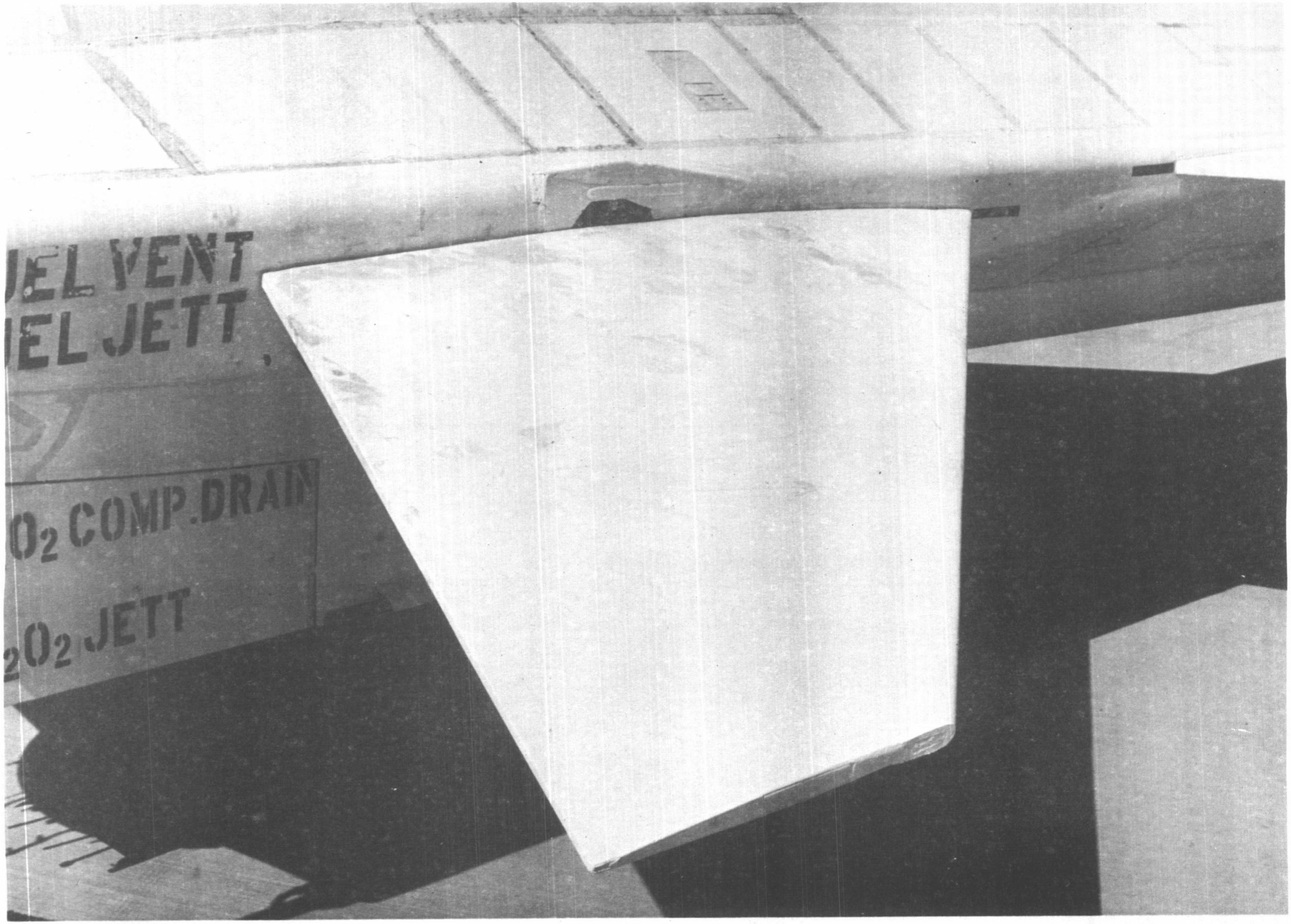

Figure II-26 Complete Ablator Application on Horizontal Stabilizer

NASA Flight Research Center
Edwards, California

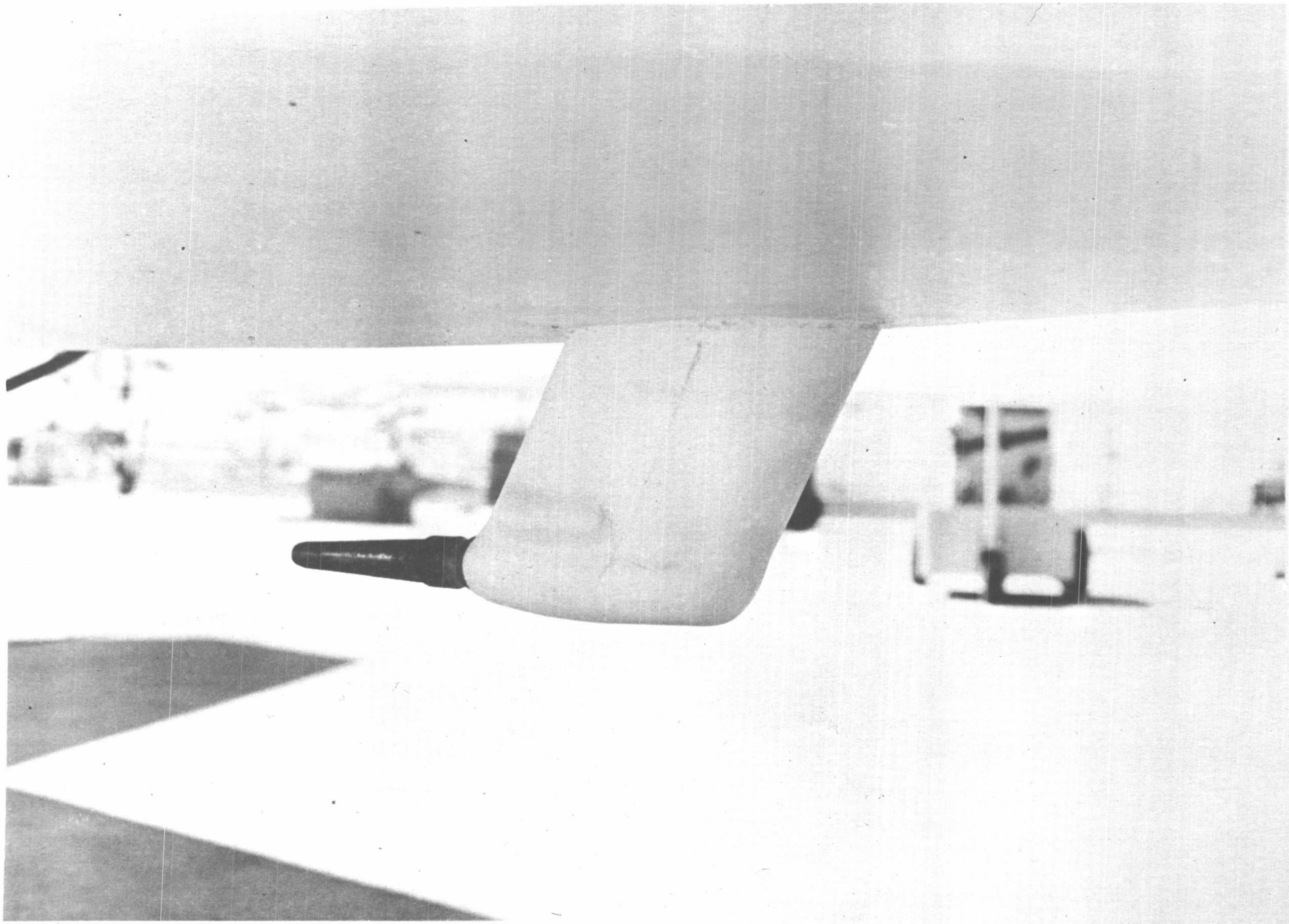

Figure II-27 Complete Ablator Application on Vane Antenna

Flight Research Center
Edwards, California

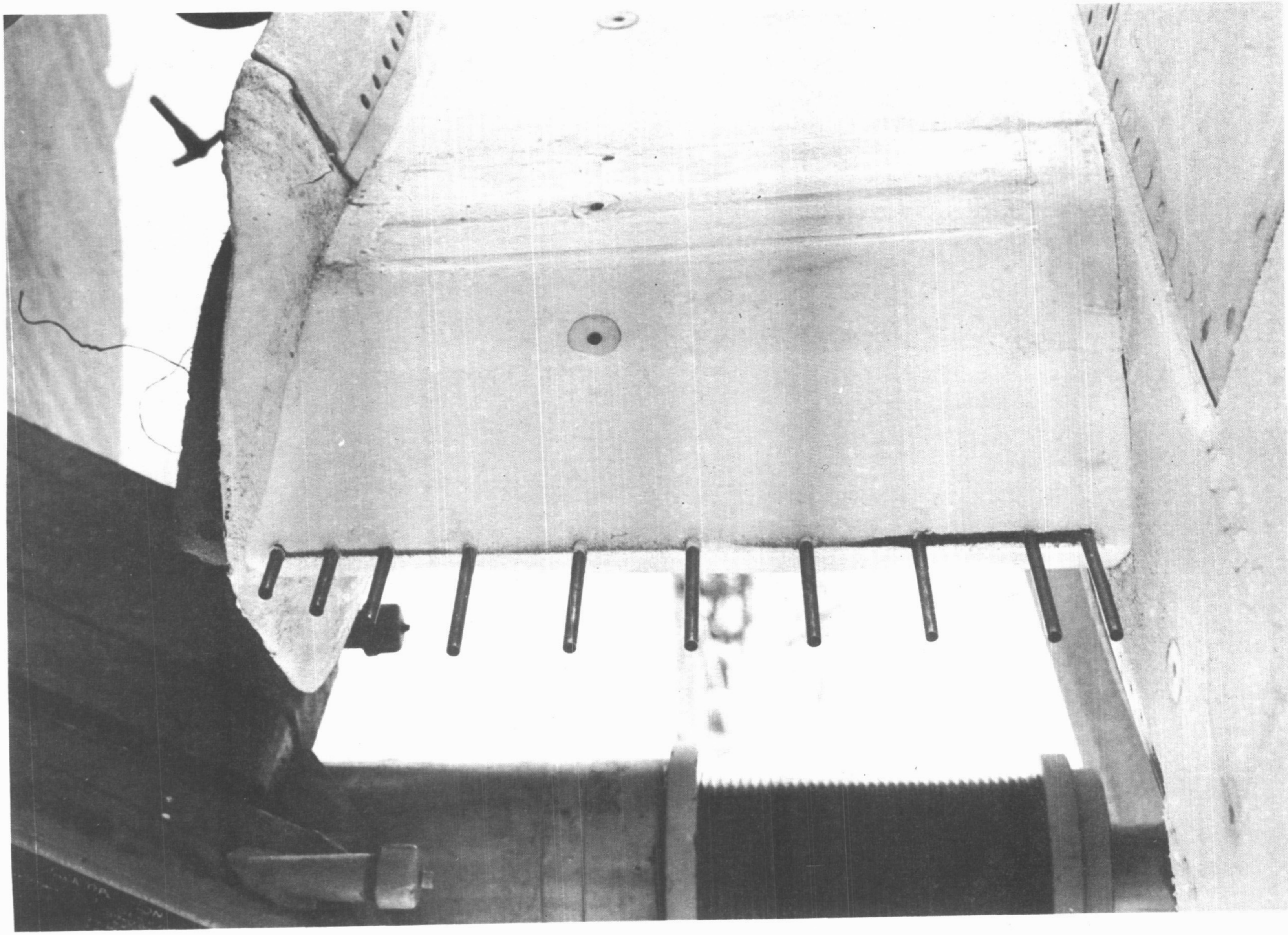

Figure II-28 Complete Ablator Application on Ventral Fin

Flight Research Center
Edwards, California

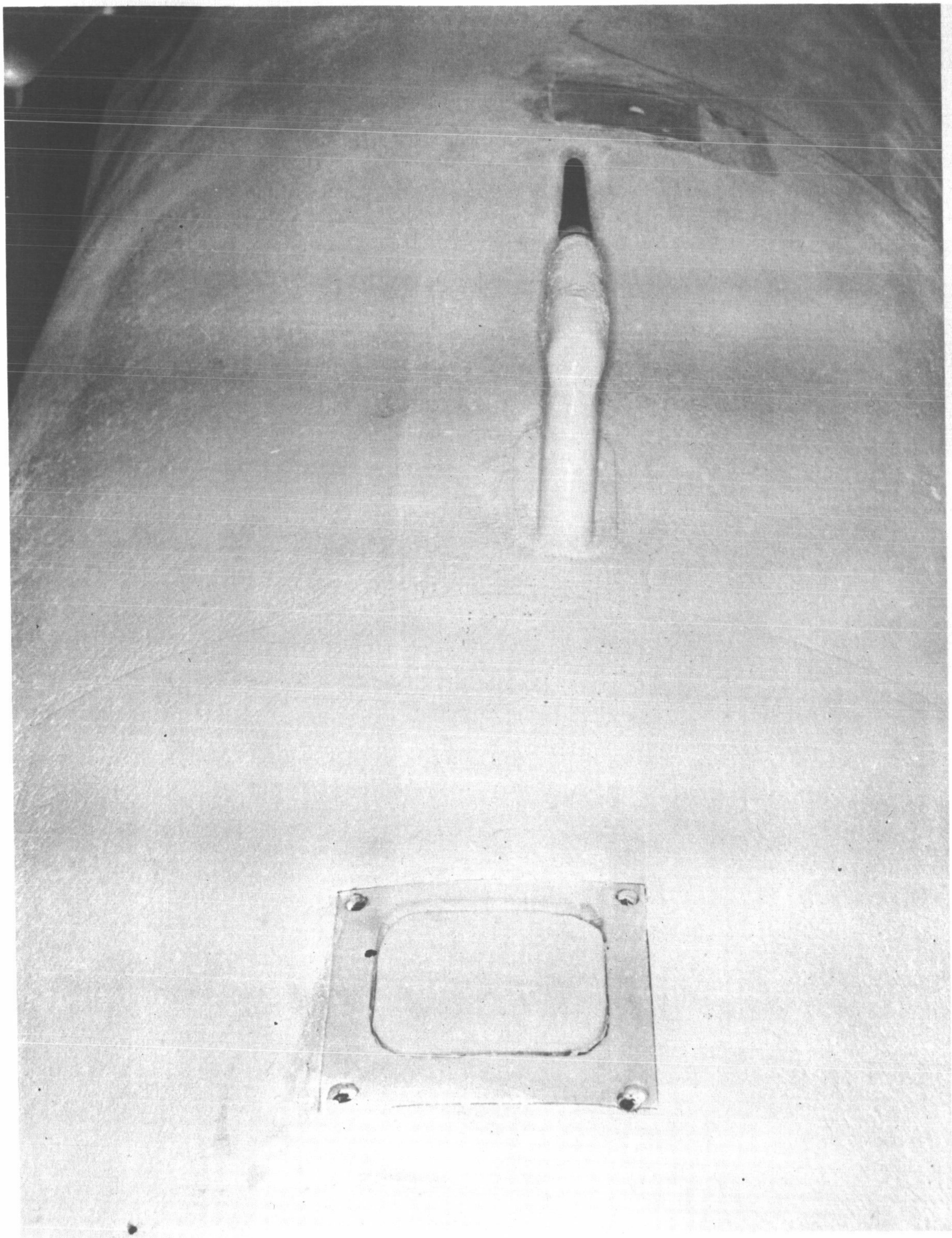

Figure II-29 Refurbished Ablator on Fuselage Belly

Flight Research Center
Edwards, California

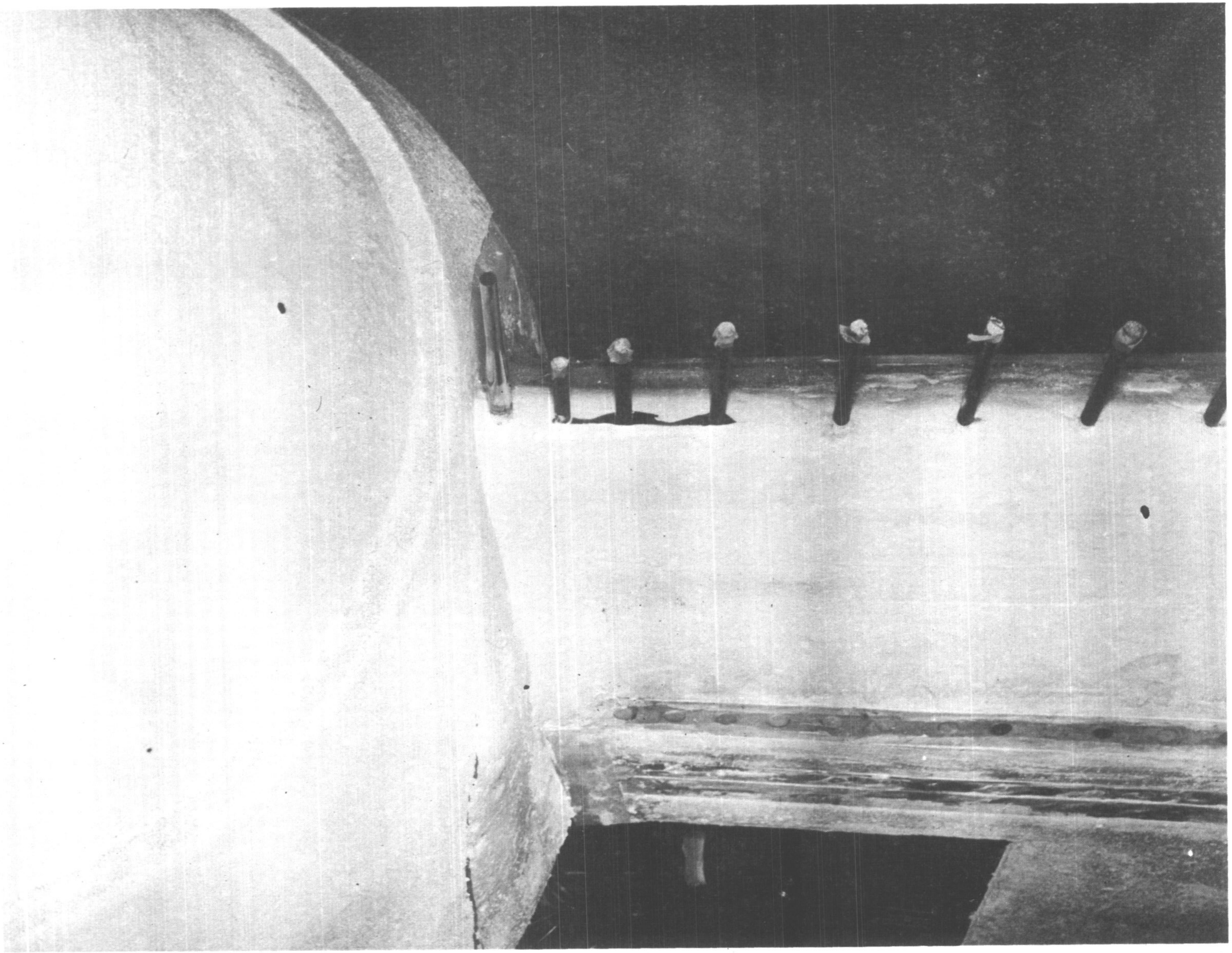

Figure II-30 Refurbished Ventral Fin Leading Edge

Flight Research Center
Edwards, California

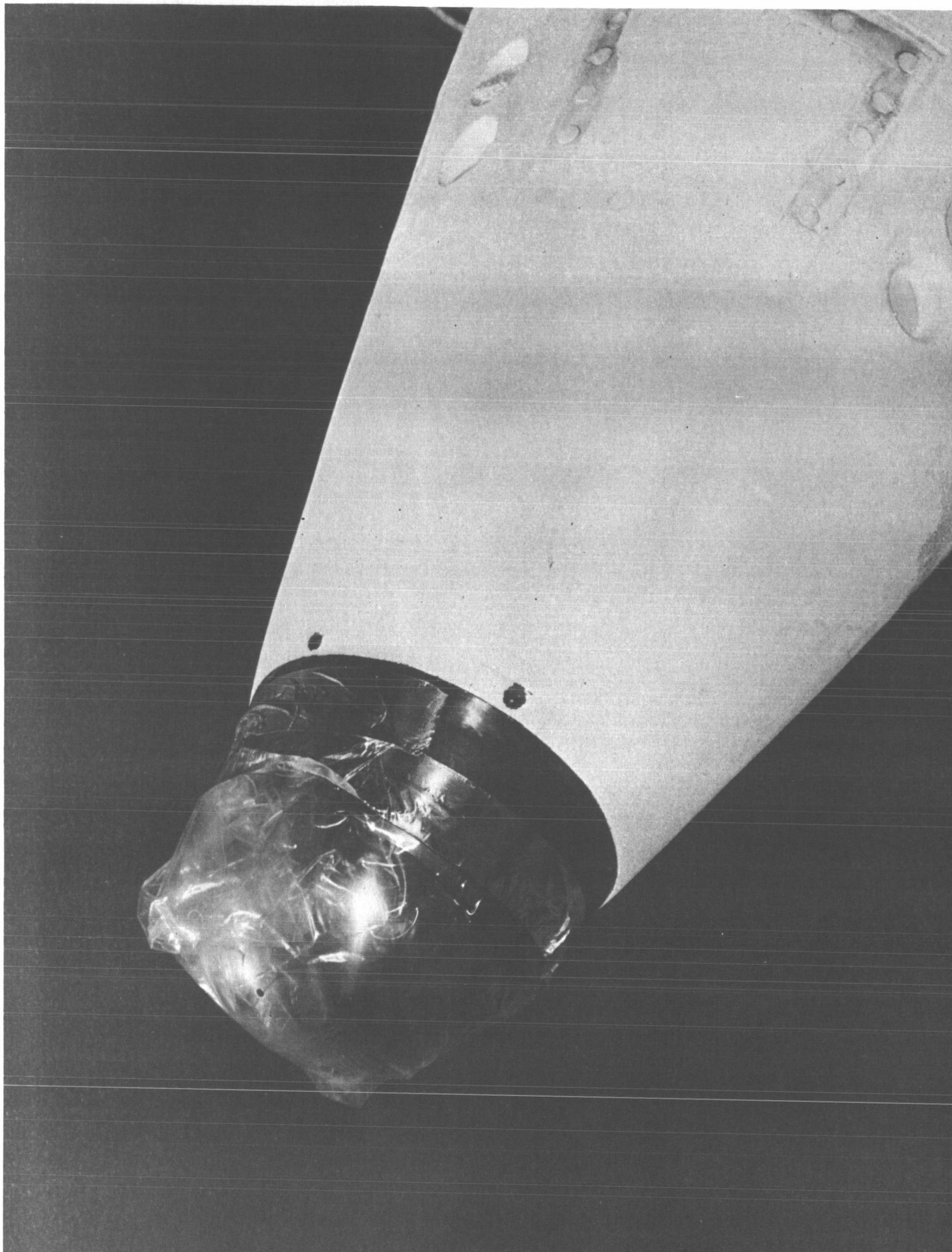

Figure II-31 Refurbished Ablator, Fuselage Nose

NASA Flight Research Center
Edwards, California

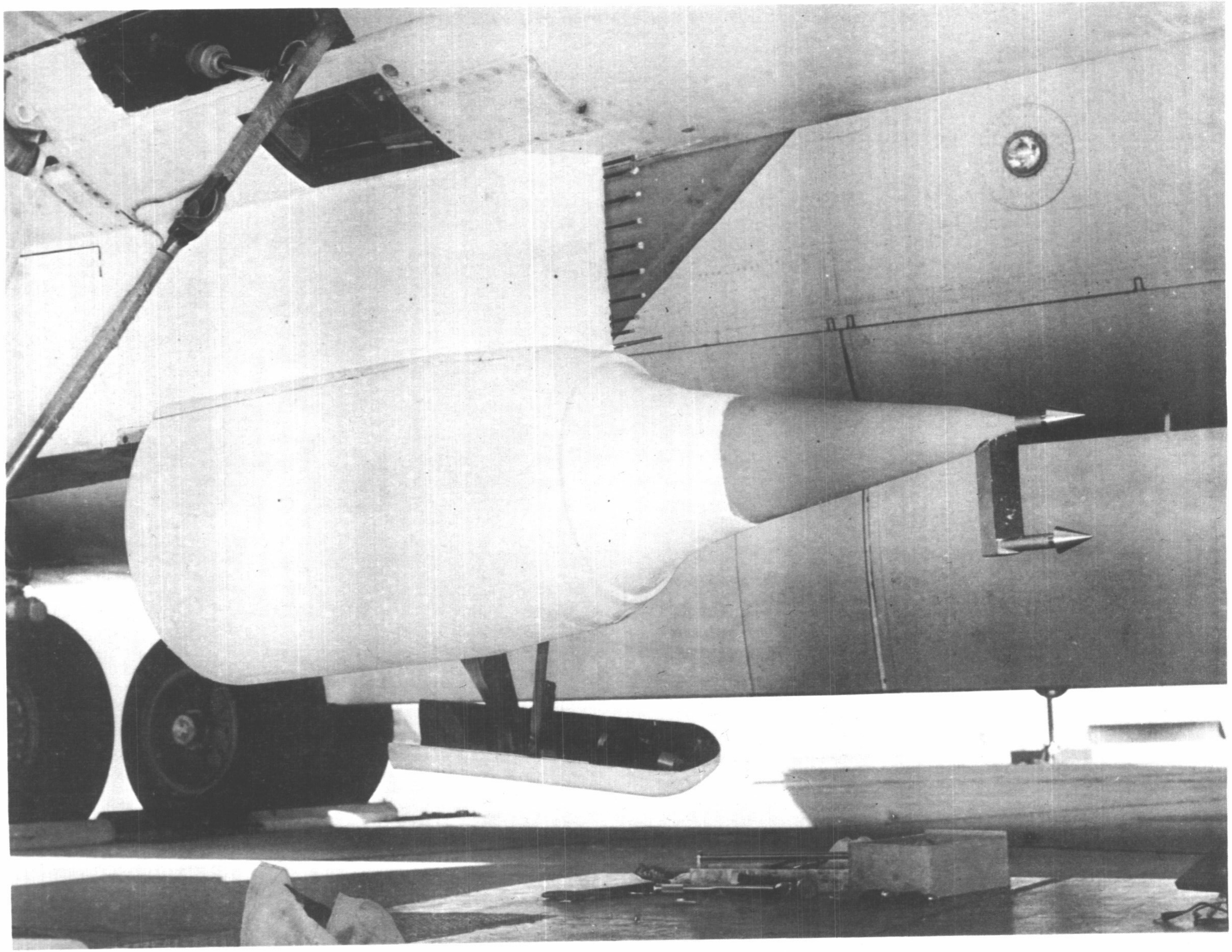

Figure II-32 Refurbished Ablator, Dummy Ramjet

NASA Flight Research Center
Edwards, California

III. FLIGHT TEST QUALIFICATION

Flight qualification of the ablation system will be accomplished by the sequential expansion of the flight test envelope up to full vehicle capability. The purpose of this program was to evaluate the ablator performance through the first stages of the envelope expansion.

Original program plans called for testing the first full ablator application to a flight regime of Mach 6.7. To accomplish this required use of the external drop tanks with the ablator protected aircraft. This would have exposed the mission to the uncertainties of using the drop tanks with the altered aircraft configuration (i.e.: modified ventral fin and dummy ramjet installation) for the first time. This was in addition to the undetermined performance of the modified vehicle at these speeds, and the effects of the full ablator application on handling and aerodynamic characteristics. Consideration of these factors led to a re-evaluation of the degree to which the environmental envelope should be expanded during the first test flight. It was decided, therefore, to limit the initial flight to Mach 5.0 and thereby eliminate the factors associated with use of the external drop tanks.

Although the ablative thermal protection system was designed and intended for single flight exposure, it was decided, based on previous multiple flights of the ablator on the ventral, that the thermal degradation of the Mach 5.0 mission should be minimal and would permit reflight with only minor touch-up to the ablator. The originally planned Mach 6.5 flight actually became the second test exposure of the ablation system. The program, therefore, served to qualify the ablator application through two discrete steps of environmental envelope expansion.

The condition of the ablator and an evaluation of its performance following the two test flights are defined in the remainder of this report section.

A. Mach 5.0 Flight

The first flight evaluation of the complete ablation system was accomplished without the use of external drop tanks. The aircraft configuration included the full ablative thermal protection system, the modified ventral fin and the dummy ramjet assembly. The mission achieved a maximum velocity of 4840 fps at an altitude of approximately 90,000 ft.

The condition of the ablation system following the flight are presented below for each of the major design features of the thermal protection system.

1. Molded Leading Edge Details - The ablator leading edge details showed very little thermal degradation as a result of the flight except in the area of the modified ventral fin.

The details along the wings and horizontal stabilizers had uniform and minor charring throughout their lengths. Sections of the charred wing leading edge are shown in Figure III-1 and III-2. Examination of the area revealed only minor surface fissuring with all char intact and good shape retention of the details. Measurements along the wings and stabilizers reflected fully charred layers .050 and .055 inches deep, respectively.

The ablator details for the canopy and vertical tail leading edges experienced almost no thermal degradation. Local erosion and blistering of the wear layer was the only evidence of thermal exposure.

These areas are shown in Figures III-3, -4, -7, and -8.

The leading edge of the forward vane antenna suffered local erosion to a depth of .100 inches. This is apparent in Figure III-5, and was precipitated by shock wave impingement set up by an excessively thick ablator insert over the ram air door just forward of the antenna. The remainder of the detail and the leading edge detail on the aft vane antenna showed minor, if not insignificant degradation.

The most severe damage after the Mach 5.0 flight was experienced by the molded ablator detail on the leading edge of the modified ventral fin. This part, shown in Figure III-6, was heavily charred along its length. The increased amount of thermal degradation was directly attributable to the shock wave interactions from the pressure probes and the dummy ramjet assembly. Very little char remained intact on the detail, and the lower portion had been eroded completely away. It was difficult to ascertain how much of the erosion had taken place during the flight since sand impact at landing had caused similar, though less significant, erosion of ablator on earlier ventral fin flight test experiments. Except at the extreme lower end, the detail still provided approximately .51 inches of virgin ablator over the ventral structure.

2. MA-25s Ablator Layer - The primary ablator layer experienced very little thermal degradation as a result of the Mach 5.0 flight exposure. On the wings and horizontal stabilizers, only the areas immediately adjacent to the molded leading edges were degraded. These areas exhibited the normal random reticulation of the surface, and there was no evidence of delamination, and all material was intact.

This area of the ablator layer is shown in Figure III-2, and actual char depths were less than .020 inches.

Near the outboard end of the left wing lower surface, some superficial blistering of the ablator layer occurred. Their depths varied and their sizes ranged downward from approximately .50 inches in diameter. There was no evidence of a preferential separation plane within the ablator layer, and the apparent blistering was most probably caused by the excessively thick wear layer application. The wear layer base resin apparently degrades more slowly than the ablator base under low thermal exposure. This results in a somewhat impermeable and elastic membrane over the surface of the degrading ablator, thus trapping the pyrolysis products. When fissuring of the ablator surface does occur, the presence of the elastic surface layer changes the reticulation pattern from random to one of least resistance (i.e.: circular).

The other areas of ablator layer degradation included the upper and lower speed brakes and the forward portion of the ventral fin. These areas all exhibited the normal random fissuring of the ablator surface, with the lower speed brakes being most significantly degraded. All charred material was intact, and there was no significant erosion or signs of delamination within the ablator layer. These areas of the aircraft are shown in Figures III-6, -8, and -9.

The only questionable area of ablator performance was the left side of the upper vertical tail movable section. After the flight a number of circular pieces of ablator had been lost. These were approximately 1.5 inches in diameter and are shown in Figure III-8. Examination of the area revealed that all separation had occurred at the spray layer interface, and significant additional delamination had occurred. The heavy wear layer had held most of the material in place and had precipitated the circular shape of the separated pieces.

Similar delamination had been encountered in the early stages of the ablator flight test program of the predecessor contract. The condition had been found to be attributable to improper application techniques, and procedures were modified to avoid the situation.

Separation of the ablator at a spray plane interface is a possibility whenever the later application is not made sufficiently "wet" to prevent excessive amounts of solvent being drawn from the new material into the existing ablator layer. If this occurs, the newly deposited material cures prematurely, without adequate cross linking of the material layers, and results in a sub-strength inter-layer bond.

This situation apparently existed during the second application of ablator to the left side of the movable vertical tail. It is significant to note that the proof test plugs in this area were the only ones to exhibit a preferential plane of separation within the ablator layer (ref Fig. II-7). Ablator failure occurred at the spray plane but the proof load was not sufficiently low to warrant rejection of the ablator application.

Except as specified in the preceeding paragraphs, there was no evidence of thermal damage to the ablator layer.

3. MA-25s-1 Strips - Two experiments had been conducted with the MA-25s-1 ablator strips around the peripheries of the service panels of the aircraft. The strips had been secured to the panel edges by:

1) permanently bonding with DC93-027 adhesive, and 2) securing them with a contact adhesive.

All the strips had performed extremely well during the many handling and servicing operations that preceeded the actual test flight. They had withstood the rigors of repeated panel removal, handling, and replacement, and had protected the vulnerable primary ablator layer from significant damage during this phase of operations.

The majority of the strips had been permanently bonded to the structure with DC93-027 adhesive. Of these, only one piece, approximately 3 inches long, had become dislodged during the flight. The area is shown in Figure III-11, and failure was precipitated by the considerable amount of wear layer that extended into the area of bond. Post flight inspection disclosed that the DC93-027 did not achieve a satisfactory bond to the DC90-090 wear layer material.

Eight (8) panels were arbitrarily chosen near the back of the aircraft, and their peripheral strips were secured with contact adhesive. Post flight inspection revealed that four (4) of these panels had experienced loss of complete strips, and the remaining panels evidenced varying degrees of bond failure. From these observations, it was evident that use of the contact adhesive was unacceptable for higher speed flights.

The condition of the various peripheral strips are shown in Figures II-1, -6, -7, -8, -10, and -11.

The ablator buttons used to close the fastener access cutouts were secured with contact adhesive after final panel installation. They performed satisfactorily with only a minimal number having been lost during the flight.

4. Hard Point Inserts, Repairs, and Miscellany - The various ablator bearing pad inserts performed satisfactorily during this flight test. Although the drop tanks had not been used for the actual test flight, they had been mated for the engine runs and the captive flight which preceded the test flight. The ablator inserts in the areas of the tank inboard sway braces had experienced no damage or deformation during these periods of tank installation.

The hard point insert at the forward jacking point had been inadvertently removed by the ground crew after the flight. The material was unaffected by the flight and had exhibited good bond strength at the time of removal.

Local inserts of MA-25s-1 material had been used at the active pressure tap locations and in the areas of sling and alignment fixture attachment. Some of these inserts are visible in Figures III-6 and 9 , and all were unaffected by the flight exposure.

The mechanical eyelid assembly over the left canopy windshield functioned as planned and provided the necessary visibility for the pilot at landing (Fig. III-4). The forward portion of the unprotected right windshield had become clouded during the flight. It is shown in Figure III-3, and an inspection of the upstream areas of the vehicle revealed that a significant amount of tape residue had inadvertently been left on the fixed pitot probe prior to the flight. There was evidence that the adhesive had melted during the heating phase of the flight and flowed back onto the windshield. The later test flight, however, proved the windshield deposit to be primarily from the ablator, and the adhesive had contributed little, if anything, to the window clouding.

5. Wear Layer - Relatively few areas of the wear layer over the ablator were thermally degraded. The majority of the coating was still fully resilient, and showed no signs of thermal exposure. The fuselage nose, leading edges, speed brakes, and forward portions of the ventral fin exhibited varying degrees of wear layer degradation. The condition of the DC90-090 material in these areas ranged from complete erosion, through a residual powdery residue, to small surface blistering of the coating. The various stages of wear layer decomposition can be seen in Figures III-1, -2, -3, -4, -5, -6, -9, -10, and -11.

B. Mach 6.7 Flight

After restoration of the ablation system, the environmental envelope for evaluation of its performance was expanded further in a planned Mach 6.5 flight test. This flight utilized the external drop tanks in addition to the modified ventral, dummy ramjet assembly, and full ablator application. The actual test mission achieved a maximum velocity of 6550 fps at an altitude of 99,000 ft, and achieved a Mach number of 6.7 instead of the target 6.5 value.

The actual flight environment in the area of the modified ventral fin proved to be much more severe than anticipated. The condition was directly attributable to interaction affects of the shock waves generated by the dummy ramjet, the ventral, and the pressure probes. The ablator applications in this area were in dequate to protect the structure under these flow conditions, and the vehicle suffered localized damage in the area. Because of the exceptional conditions in the area, all evaluation of the ablator application for the ventral are presented in a separate section following the descriptions of the normal ablator performance.

1. Molded Leading Edge Details - The ablator details over the leading edges of the wings, horizontal stabilizers, canopy, and upper vertical tail were uniformly charred along their lengths. All the parts had maintained good shape retention and the char layers were tenaciously attached. The wing and stabilizer details showed signs of locallized surface melt flow in the areas of low shock impingement during peak heating. Because of the continually varying velocity during the mission, shock presence in any one area was limited, and the additional amount of degradation in these areas was insignificant. Performance of the joints between leading edge segments was good and very little evidence of burning within the gaps was observed.

The lower surfaces of the wing details were more heavily degraded than the upper surfaces. This condition was reversed for the horizontal stabilizers, with the upper surfaces bearing the brunt of the heating. The wing and stabilizer areas are shown in Figures III-12, -13, -14, and III-19, -20, and -21, respectively.

The lower, fixed, portion of the vertical tail leading edge was somewhat more heavily charred than the detail over the movable section. Some evidence of unsymmetrical heating of the movable leading edge section was evident, with the left side having sustained a higher heat load. This area of the exposed ablator is shown in Figures III-19 and III-20.

The canopy detail had also experienced uniform charring along its length. No erosion or spallation of the ablator was observed, but there was evidence of additional burning at the lower end of the detail where a cutout had been added for the handling sling attachment. The canopy detail is shown in Figures III-15 and -16.

Post flight measurements were taken at representative locations on each of these leading edge details. The values are included in table III-1 and show total, char and residual virgin material thicknesses.

The ablator details on the leading edges of both of the vane antennas were heavily charred and had experienced local erosion or spallation of the char from their surface. Shape retention was poor along these details, but post flight measurements disclosed that more than 0.5 inches of ablator remained on the antennas. The appearance of the details after flight exposure is shown in Figures III-17 and III-18 for the forward and aft antennas respectively. The measured residual ablator thicknesses for these items are presented in Table III-2.

2. MA-25s Ablator Layer - The sprayed ablator layer over the fuselage and side fairings of the vehicle showed varying degrees of thermal effects. Thermal degradation, with the resultant reticulation of the ablator surface occurred only on the forward areas of the vehicle body. Ablator fissuring extended along the fuselage belly to approximately the forward vane antenna (Fig. III-17). Along the sides, degradation was experienced approximately back to the wing (Fig. III-26). Visual effects along the upper portions of the fuselage disappeared before reaching the canopy. Local charring of the ablator was experienced on the sides of the canopy around the windshields and shutter mechanism as shown in Figures III-15 and III-16. The severity of thermal affects varied over these areas and some other isolated degradation of the fuselage ablator was experienced. The ablator layer

on the crown and belly of the fuselage aft of the aforementioned areas, however, showed no evidence of any thermal exposure.

The varying amounts of charring experienced over the fuselage were easily correlated with their location or proximity to the various design features of the aircraft. Figure III-24 shows graphically the different thermal affects of laminar and turbulent flow. The heavily charred regions lie directly behind the pressure orifices in the ball nose. These openings apparently are sufficient to trip the flow causing a rapid transition to turbulent conditions.

The effects of local discontinuities on heating are illustrated in Figure III-25. The non flush BCS apertures greatly increased the heating in their vicinity. Localized stagnation within the recesses apparently permitted burning of the ablator as evidenced in the surface discoloration. The effects on ablator performances were discernable back past the edge of the nose gear door. Measurements of the ablator layer were taken in this area, are shown in Table III-3, and clearly reflect the abrupt increase in material degradation caused by the local discontinuities. Because of the vehicle angle of attack during the heating phase of the mission, the affects of the nozzle aperatures on the sides and top of the nose were nil.

Before leaving the forward nose of the aircraft, it is significant to note the reticulation of the ablator in this area. Replacement of the ball nose assembly before the flight had necessitated re-application of the ablator in this area. An outdated batch of ablator material was employed in the area because other material had been depleted. Although its application characteristics, cure rate and appearance were the same as the "fresh" ablator used over the rest of the vehicle, the thermal exposure revealed a greater shrink rate than the newer material. This is evident in Figures II-24 and II-25 as much more pronounced fissuring of the ablator was experienced in this area. It is suspect that other thermal performance characteristics varied, but insufficient data was available to estimate the amount of change in its overall ablator efficiency.

Locally heavy ablator degradation was also experienced at the front of the canopy eyelid mechanism where the compression shock from its leading edge ramp increased heating conditions. Measurements taken in this area are shown in Table III-3 and reflect the large reduction in char depth behind the expansion shock at the end of the ramp section.

Similar conditions existed elsewhere over the aircraft at discontinuities or protuberances from the skin. The positions of the stagnation shock and trailing wake are clearly apparent in Figures III-17 and III-18 for the vane antennas. Figure III-27 shows a similar phenomenon at the drop tank claw shell door which failed to close during the flight. Ablator degradation changed abruptly in direct agreement with the observable flow conditions.

The various stacks and vents protruding from the vehicle created similar situations. Some of these are visible in Figure III-26, and the severity of their effects varied depending on their size, shape and location on the vehicle. Ablator measurements taken around some of these protuberances are shown in Table III-4.

Flow conditions and resultant ablator layer degradation in the area of the main gear and ventral fin leading edges are recorded in

Table III-5.

The MA-25s ablator layer on the lower wing surfaces experienced varying degrees of charring over the whole area. The degree of ablator surface reticulation was heaviest adjacent to the molded leading edges and diminished chordwise across the wing. Some superficial blistering occurred near the wing tips, and a few areas of impact damage were experienced near the root of the right wing. These ablator performance features are shown in Figure III-12, -13, and -14.

The upper wing surfaces were thermally degraded only near the leading edge details. The remainder of the surface was unaffected. Thickness measurements were taken for the forward areas of the right wing and are presented in Table III-6. Grid locations are those defined in ER 14539 for the wing ablator application, however, additional measurements were made between some of the grid points to better identify the ablator degradation pattern.

The ablator application on the upper surfaces of the horizontal stabilizers was more heavily degraded than that on the lower surfaces. Reticulation of the ablator extended to mid-chord on the upper surfaces while almost no degradation was experienced on the bottoms. Along the inboard edge of the stabilizers, next to the side fairings, sections of ablator were missing from both the top and bottom surfaces, forward of the torque tube. This area is shown in Figures III-21 and III-22. The open cavity of the stabilizers' inboard closing rib and the adjacent fairing forms a channel to trap the air flow during flight. This results in severe heating within the cavity and caused degradation of the ablator from the back face. There was also evidence of ablator burning on the side fairing adjacent to the stabilizer. Surface discoloration of the side fairing ablator layer is clearly apparent in both Figures III-21 and III-22. The location of the burned area reflects a stabilizer nose down attitude during the heating phase. Some areas of the side fairing had been wiped clean of ablator. This was probably due to the thermal distortions caused by the excessive local heating in this area of flow trappage. It was impossible to determine if the ablator had dislodged from along the inboard edges of the stabilizers due to aerodynamic conditions or was pulled loose during movement of the stabilizers. In either event, separation came late in the flight since the exposed edges of the remaining ablator were uncharred.

In addition to the thermal degradation, a significant amount of impact damage was sustained by the stabilizer upper surfaces. This can be seen in III-19 and III-20 and consisted of narrow gouges in the ablator layer. Their depths and dimensions varied as well as their distribution, but the right stabilizer had considerable more damage of this nature. Some of the abrasions had obviously occurred on landing since the exposed ablator was virgin material. Others had occurred early in the flight and the exposed ablator had become charred. Spallation of small pieces of upstream ablator or fluid droplets from the various vents and drains were the likely causes of the early damage. Post flight ablator thicknesses are shown in Table III-7 for a portion of the right stabilizer upper surface. No measurements were taken for the lower surface because of the lack of thermal degradation.

Both sides of the upper vertical tail showed the normal reticulation of the ablator surface. The left side was uniformly charred over the whole surface, and is shown in Figure III-20. Unlike the first test flight, there was no sign of delamination within the ablator layer. The right side had experienced a lesser amount of charring, and thermal affects were apparent only to mid-chord.

The upper speed brakes are shown in Figures III-19 and III-20 and had experienced heavy charring. Despite the degree of thermal degradation, all material was intact, and there was no evidence of bond line failure or delamination within the residual ablative material. Thickness measurements taken over the speed brakes after the flight are presented in Table III-8.

To check the integrity of the twice exposed ablator application, a number of test plugs were bonded to the ablator surface at various locations over the vehicle. Surface preparation entailed removal of all charred material prior to bonding the plugs in place. Proof test loadings were determined for the locations, and the results are shown in Table II-7. At time of test, it became evident that all degraded ablator had not been removed prior to bonding all the plugs. Where adequate plug attachment was obtained, observed results were well above the acceptable limits for an ablator application.

3. MA-25s-1 Strips - The poorly performing contact adhesive fastened strips had been replaced prior to this flight. All peripheral panel strips were permanently bonded with DC93-027 adhesive. Following the Mach 6.7 flight no strip loss or evidence of partial bond failure were experienced. Some of the MA-25s-1 strips had encountered a degree of thermal degradation, but no areas of significant charring were found. The one strip which had been filled with the modified DC90-090 material at time of touch up activity performed satisfactorily. Though somewhat

degraded, the material showed no surface fissures, signs of shrinkage or loss of adhesion. This area is shown in Figure III-26, and is the second vertical strip from the front of the conduit assembly. The post flight conditions of other strips over the vehicle can be seen in Figures III-12, -13, -19, -20, -21, -22, -23, -24, -25, -26, and -27.

4. Hard Point Inserts, Repairs and Miscellany - None of the ablator structural inserts suffered either thermal degradation or bond failure as a result of this flight exposure. There was no indication that any of the repaired areas of the ablator layer performed differently than the original application.

The canopy eyelid again proved satisfactory to prevent clouding of the left windshield. The bare right windshield received the same deposition of ablation products as during the first flight, and was partially clouded at completion of the test. These areas of the aircraft are shown in Figures III-15 and III-16.

5. Wear Layer - The DC90-090 wear layer application was degraded in the same general areas as after the Mach 5.0 flight test. Leading edge areas had experienced erosion of the wear layer while the powdery residue was present in adjacent areas. Local blistering of the coating occurred in areas of low heat input and large portions of the DC90-090 layer were unaffected by the flight.

6. Ventral Fin - The shock wave interactions set up by the dummy ramjet installation made the environmental predictions for this area quite unconservative. The ablator system designs was, therefore, inadequate, and failed to provide sufficient protection for the vehicle structure thoughout the flight. The ablator application, including both

molded leading edge detail and the sprayed MA-25s layer was completely eroded from the forward portion of the fin following the flight. The exposed ventral had sustained damage due to the excessively high heating in the area of shock impingement. The vehicle skin was burned through at the leading edge and on the ventral sides at the torque box assembly. The torque box was also damaged, and the wiring and pressure lines in the forward compartment of the fin were destroyed. This area ofthe aircraft is shown in Figures III-28, -29, and-30, and shows the extent of ablator erosion and resultant structural damage.

The abnormally high temperatures caused premature jettisoning of the dummy ramjet assembly and precluded normal recovery of the component. The assembly is shown in Figure III-31 after free-fall from the aircraft during the final landing maneuver.

Study of the thermocouple responses in the ventral fin area indicated that the ablator had provided protection through the first 140 seconds of the flight. Continual erosion of the ablator surfaces was occurring during this period, and by approximately 160 seconds, degradation was such that all protection broke down. Ablator materials which had been predicted to have zero surface recession were, in fact, being continually eroded away. The particles from the forward sections of ablator, in turn, caused severe impact erosion of the downstream ablator layer. The lower speed brakes were bare of ablator, and the material on the inboard edges of the main gear and the undersides of the side fairings experienced considerable abrasion.

C. Conclusions and Recommendations

The post flight examination of the thermal protection system showed the ablator design to have performed satisfactorily except in the area of the modified ventral fin. Despite the overall satisfactory condition of the ablator application, there were some areas of potential problems as the environmental envelope is expanded for the aircraft. These are delineated in the following paragraphs, and recommended system design changes are presented for their resolution.

1. BCS Nozzle Aperatures - The ablator system design had specified that these openings would be covered with flush plates. This could not be accomplished because three of the nozzles had to remain open for attachment of an aircraft righting sling in the event of an emergency. For the first application, the nozzles were plugged with corks and the spray applied directly over this combination. No attempt was made to fill the plugged cavity with material, and the resultant discontinuities caused locally increased degradation of the ablator.

For future applications, the nozzles can still be plugged with corks, but MA-25s material should be trowelled over the plugs to provide a flush surface to the ablator layer. External identification of the plug locations required for sling attachment is necessary to permit rapid removal of the ablator from the areas in an emergency.

2. Nose Gear Door - Increased charring of the ablator layer was encountered in this area of the aircraft. This condition was attributable both to the non-flushed BCS nozzles, and the transverse gaps at the forward edges of the nose gear and scoop doors. To eliminate the possible chance of inadvertent opening of the doors due to thermal deformation, the ablator application in this area will be increased to provide greater margin of safety.

3. Horizontal Stabilizer Inboard Edge - The inboard closing rib of the horizontal stabilizers is a channel section, facing inboard. This

forms a cavity with the skin of the fuselage and channels the airflow into the area to stagnate against the stabilizer torque tube assembly. Considerable heating within this area was experienced during the test flights and resulted in local loss of ablator due to charring outward from the skin line. This cavity heating is also detrimental to the closing rib, fuselage and stabilizer torque tube structure. On future applications, a closure should be provided for the stabilizer end, and if necessary, an ablator application made over the area for additional protection.

4. Speed Brakes - The ablator degradation on lower speed brakes was attributable primarily to particle impact erosion from the ventral fin area. Redesign of the ablator in this area is dependent upon a re-evaluation of the local environmental conditions.

The upper speed brakes, though heavily charred, had performed satisfactorily. This initial application was made thicker than specified in the design, and post flight evaluation of the area would suggest using the thicker layer for future applications.

5. Canopy Eyelid Mechanism - The ablator layer on the forward end of the eyelid mechanism had experienced heavy charring. The compression shock generated by the front wedge of the eyelid apparently caused the condition. On future ablator applications, the MA-25s layer in this area should be increased, and a local grid network established to monitor the application.

6. Protrusions - The various protrusions from the aircraft caused local increases in ablator degradation in their vicinities. Ablator performance was adequate, but there was some indications of peripheral back face heating due to conduction from the various bare extensions.

In future applications, the ablator layer will be extended partially along the protrusions to minimize the conduction effects at the vehicle skin. Local increases in the ablator thicknesses around the protrusions would provide greater protection against the increased heating caused by their presence.

7. Ventral Fin - It was obvious that the environment utilized in designing the ablator application for the ventral fin was not an accurate representation of actual environmental conditions. When better predictions of the environmental extremes encountered in this area of the aircraft are available, the ablation system will be redesigned to provide the necessary thermal protection.

TABLE III-1

ABLATOR THICKNESS SUMMARY
PERFORMANCE CORRELATION POINTS

NUMBER	AIRCRAFT LOCATION	ORIGINAL THICKNESS	AFTER 2-52 FLIGHT TOTAL REMAINING	AFTER 2-52 FLIGHT CHAR DEPTH	REFURB. TOTAL THICKNESS	AFTER 2-53 FLIGHT TOTAL REMAINING	AFTER 2-53 FLIGHT PYROLYSIS DEPTH	AFTER 2-53 FLIGHT CHAR DEPTH
TF-2T	NOSE PANEL F-2	.136	-	0	-	.223	.050	.050
04017	NOSE GEAR DOOR	.184	-	0	-	.178	.086	.086
05019	CANOPY LEADING EDGE	F .535	-	0	-	F .522	.236	.049
		L .380	-	0	-	L .375	-	-
		R .425	-	0	-	R .381	-	-
TF18M	SIDE FAIRING PANEL F-18	.125	-	0	-	.138	0	0
09001	FUSELAGE BELLY STA 335	.104	-	0	-	.116	0	0
T2022	FUSELAGE CROWN STA 340	.074	-	0	-	.076	0	0
13050	WING LEADING EDGE	F .500	.510	.050	.460	F .514	.269	.175
		T .479	-	-	-	T .381	-	-
		B .431	-	-	-	B .420	-	-
13057	WING TOP SURFACE	.092	-	0	-	.076	0	0
13076	WING BOTTOM SURFACE	.220	-	0	-	.212	.042	.042
15017	HOR. STAB. LEADING EDGE	F .647	.658	.055	.605	F .652	.242	.147
		T .487	-	-	-	T .353	-	-
		B .525	-	-	-	B .424	-	-
15018	HOR. STAB. UPPER SURFACE	.188	-	0	-	.162	.062	.062
15025	HOR, STAB. LOWER SURFACE	.165	-	0	-	.157	0	0
16020	VERT. TAIL LEADING EDGE	F .481	-	.020	.465	F .477	.278	.149
		L .336	-	-	-	L .303	-	-
		R .375	-	-	-	R .322	-	-
16025	VERT. TAIL RIGHT SIDE	.256	-	0	-	.278	.005	.005
16018	UPPER RIGHT SPEED BRAKE	.184	-	.020	.178	.198	.176	.075

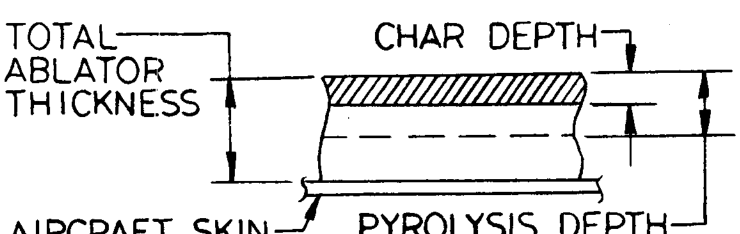

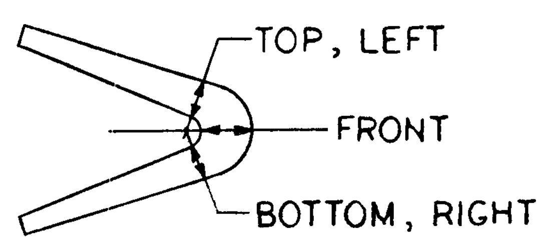

TABLE III-2

ABLATOR THICKNESS RECORD
VANE ANTENNAS
POST 2-53 FLIGHT

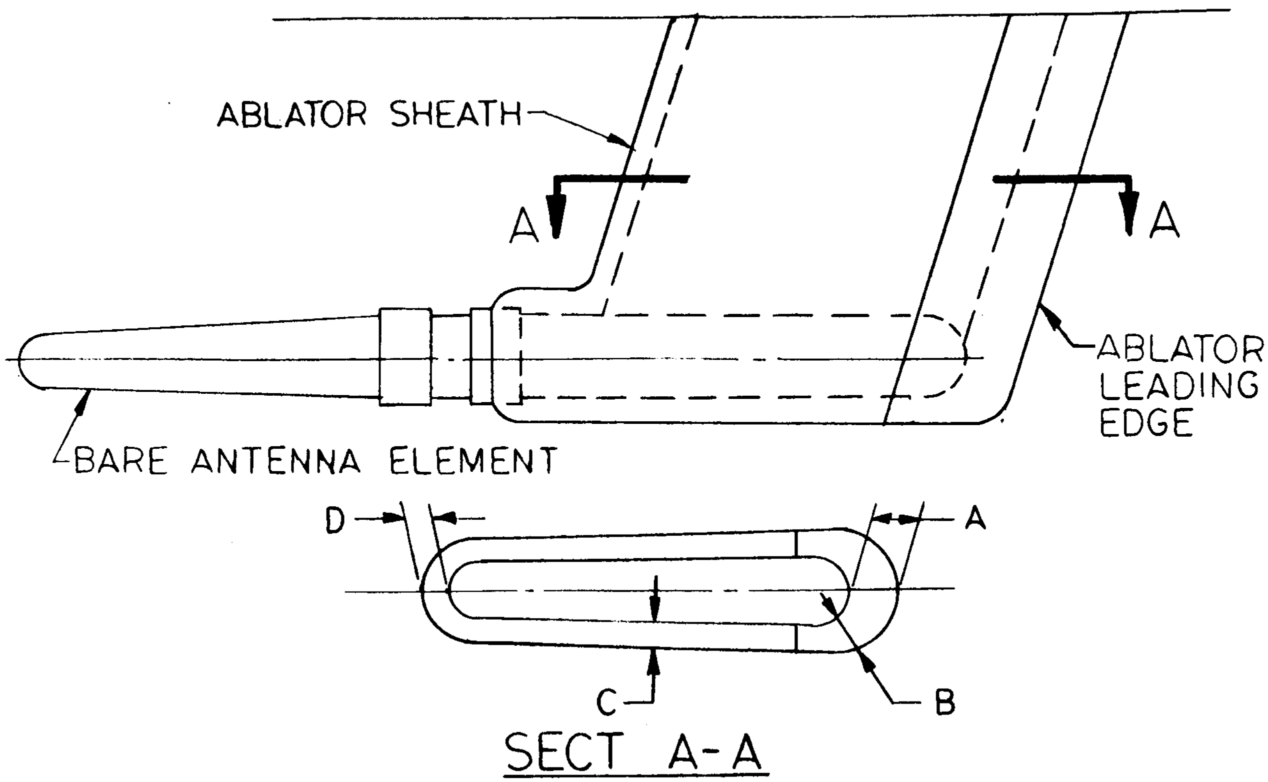

DIM LOC	FWD ANTENNA TOTAL THICKN'S	FWD ANTENNA CHAR DEPTH	FWD ANTENNA VIRGIN MATERIAL	AFT ANTENNA TOTAL THICKN'S	AFT ANTENNA CHAR DEPTH	AFT ANTENNA VIRGIN MATERIAL
A	.547	.323	.224	.607	.193	.414
B	.491	.217	.274	.434	.052	.382
C	.472	.029	.443	.512	.081	.431
D	.479	0	.479	.451	0	.451

TABLE III-3

ABLATOR PERFORMANCE RECORD

CANOPY EYELID & BOTTOM OF FUSELAGE NOSE

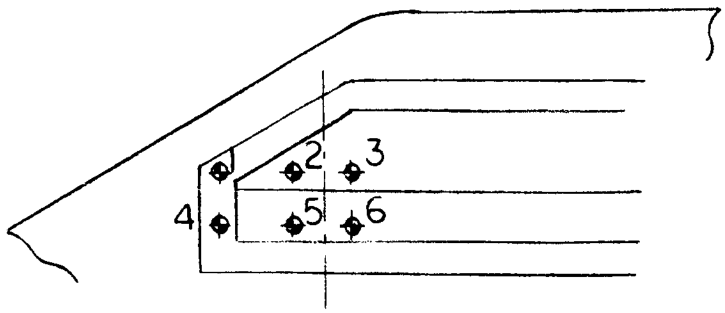

CANOPY EYELID

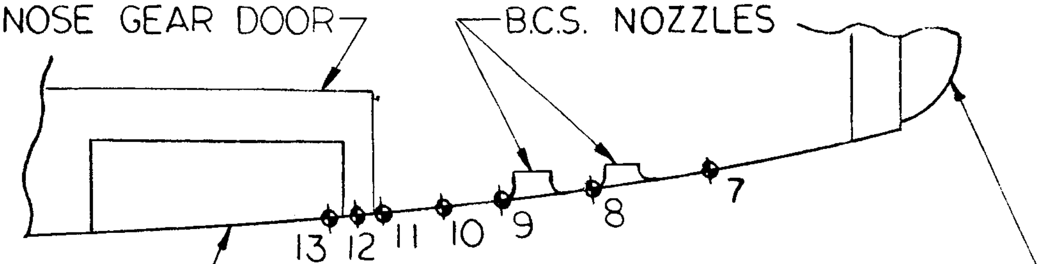

FUSELAGE NOSE

AREA	ABLATOR MEASUREMENT			
	LOC	TOTAL	CHAR	VIRGIN
EYELID	1	.112	.097	.015
	2	.100	.090	.010
	3	.170	.060	.110
	4	.190	.120	.070
	5	.148	.083	.065
	6	.220	.035	.185
FUSELAGE	7	.115	.047	.068
	8	.170	.115	.055
	9	.160	.100	.060
	10	.165	.090	.075
	11	.170	.095	.075
	12	.150	.090	.060
	13	.175	.085	.090

TABLE III-4

ABLATOR THICKNESS RECORD
STACKS AND VENTS
POST 2-53 FLIGHT

PENETRATION	DESCRIPTION & LOCATION	THICKNESS MEASUREM'T	POSITION OF MEASUREMENT FWD	AFT	ABOVE	BELOW	REMARKS
A.P.U. EXHAUST STACK (RIGHT SIDE)	2" DIA SHEET METAL STACK UPPER SIDES OF FUSELAGE	TOTAL	.140	.140	.210	.190	POOR ADHESION OF THE DC93-027 TO THE SKIN AROUND THE STACK.
		CHAR	.005	.000	.010	.025	
		VIRGIN	.135	.140	.200	.165	
A.P.U. EXHAUST STACK (LEFT SIDE)	2" DIA SHEET METAL STACK UPPER SIDES OF FUSELAGE	TOTAL	.108	.140	.194	.180	ONE HEAVILY CHARRED AREA ON LOWER FWD SIDE.
		CHAR	.018	.000	.000	.043	
		VIRGIN	.090	.140	.194	.137	
PEROXIDE COMPARTMENT DRAIN (LEFT SIDE)	1" DIA SHEET METAL STACK LOWER SIDES OF FUSELAGE	TOTAL	.125	.112	.130	.105	
		CHAR	.070	.002	.055	.030	
		VIRGIN	.055	.110	.075	.075	
PEROXIDE COMPARTMENT DRAIN (RIGHT SIDE)	1" DIA SHEET METAL STACK LOWER SIDES OF FUSELAGE	TOTAL	.140	.155	.130	.125	SMALL HOLE THRU ABLATOR AT LOWER FWD AREA.
		CHAR	.085	.005	.094	.070	
		VIRGIN	.055	.150	.046	.055	
HYDRAULIC RESERVOIR VENT (LEFT SIDE)	¾" DIA SOLID METAL STACK LOWER SIDES OF FUSELAGE	TOTAL	.100	.114	.140	.135	ABLATOR CHARRED TO SKIN NEXT TO STACK.
		CHAR	.055	.019	.060	.055	
		VIRGIN	.045	.095	.080	.080	
HYDRAULIC RESERVOIR VENT (RIGHT SIDE)	¾" DIA SOLID METAL STACK LOWER SIDES OF FUSELAGE	TOTAL	.065	.108	.105	.108	
		CHAR	.015	.000	.065	.043	
		VIRGIN	.050	.108	.040	.065	

ABLATOR · PE
VENTRA

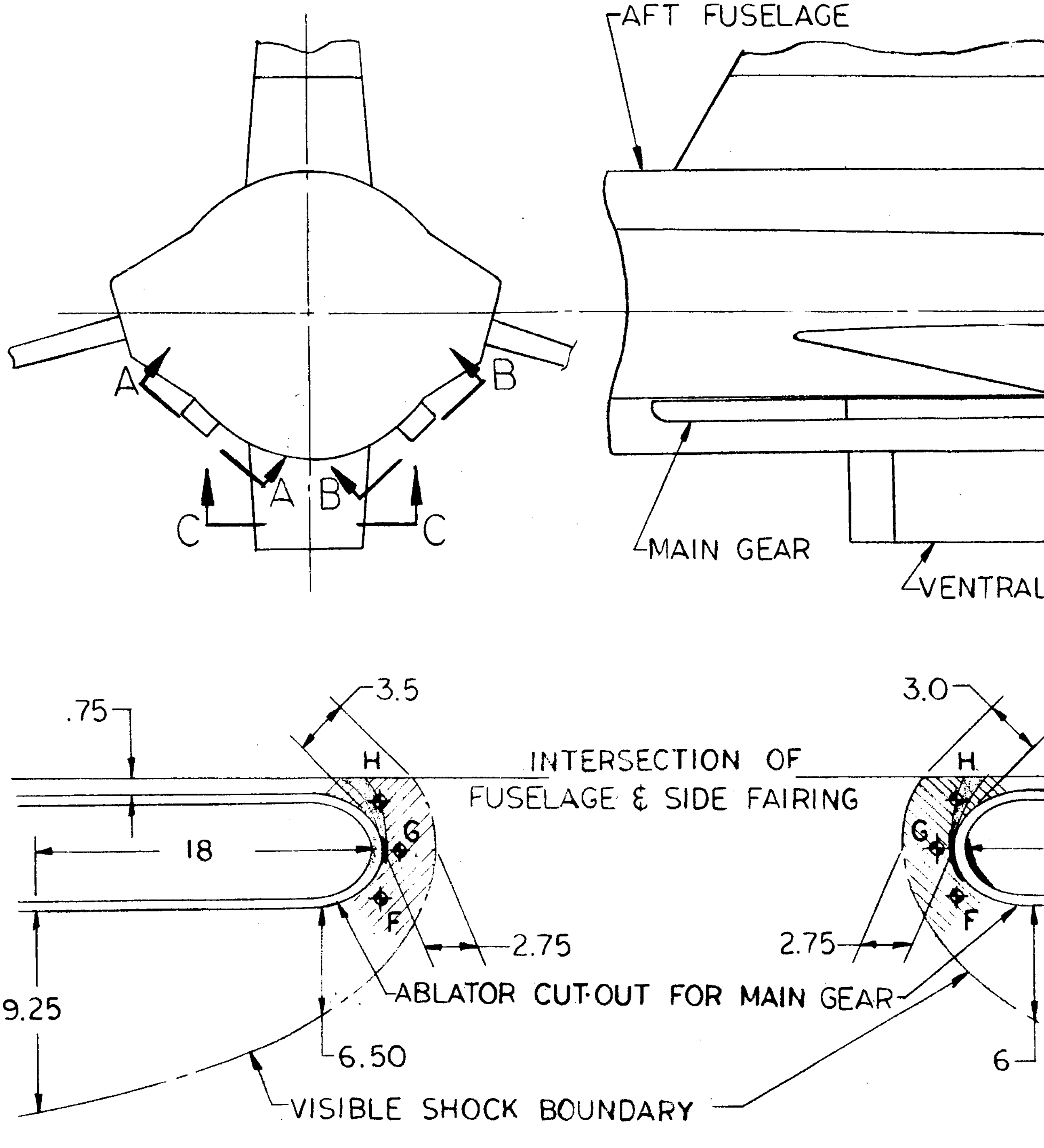

SECT A-A

RIGHT GEAR

SECT

LEFT G

LEGEND

(blank box)	MINOR OR NO DEGRADATION
(hatched box)	DEGRADATION OF WEAR LAYER
(dotted box)	PARTIAL EROSION OF ABL
(solid black box)	SIGNS OF ABLATOR BURNI
(cross-hatched box)	ABLATOR ERODED TO SKIN

RFORMANCE RECORD

_ ₵ MAIN GEAR

ABLE III-5

FOLDOUT FRAME 2

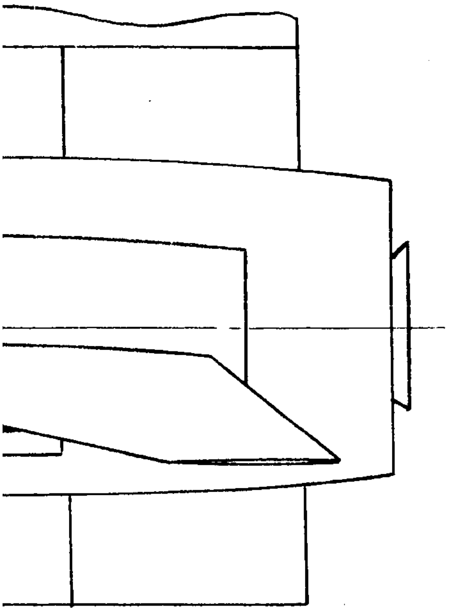

. FIN

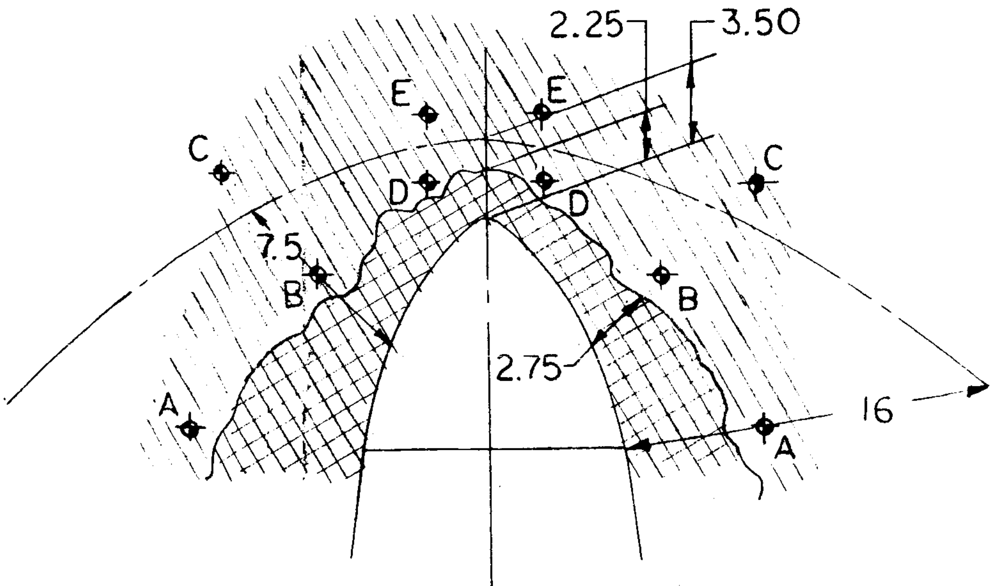

SECT C-C

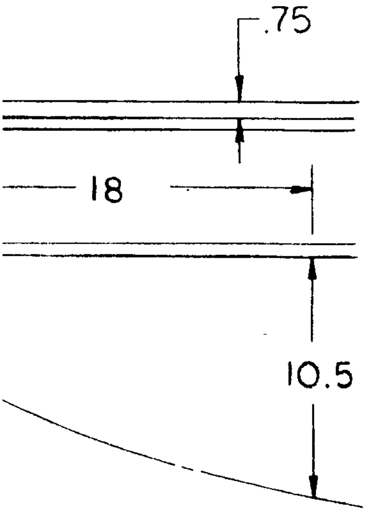

3-B

EAR

ATOR

NG

AREA	ABLATOR MEASUREMENT LOC	TOTAL	CHAR	VIRGIN
VENTRAL RIGHT SIDE	A	.150	.088	.062
	B	.162	.097	.065
	C	.160	.018	.142
	D	.205	.135	.070
	E	.196	.058	.138
VENTRAL LEFT SIDE	A	.143	.070	.073
	B	.145	.105	.040
	C	.160	.008	.152
	D	.168	.118	.050
	E	.180	.050	.130
RIGHT MAIN GEAR	F	.085	0	.085
	G	.108	.013	.095
	H	.050	0	.050
LEFT MAIN GEAR	F	.120	.045	.075
	G	.120	.035	.085
	H	.103	.043	.060

TABLE III-6

POST FLIGHT ABLATOR DATA

RIGHT WING

UPPER SURFACE

Grid Loc.	Orig. Thkns	Post Flt Total	Residual Virgin	Full Char
.5	-	.200	.200	0
1	.140	.128	.128	0
1.5	-	.195	.195	0
2	.156	.145	.145	0
3	.095	.095	.095	0
3.5	-	.248	.248	0
4	.160	.157	.157	0
7.5	-	.246	.228	.018
8	.122	.125	.125	0
12.5	-	.230	.220	.010
13	.120	.120	.120	0
18.5	-	.217	.198	.019
19	.116	.112	.112	0

LOWER SURFACE

Grid Loc.	Orig. Thkns	Post Flt Total	Residual Virgin	Full Char
.5	-	.255	.177	.078
1	.209	.185	.115	.070
1.5	-	.261	.177	.084
2	.190	.179	.142	.036
3	.190	.191	.176	.015
3.5	-	.283	.180	.103
4	.220	.230	.181	.049
5	.186	.181	.158	.023
7.5	-	.343	.263	.080
8	.228	.223	.172	.051
9	.194	.191	.168	.023
12.5	-	.339	.239	.100
13	.240	.229	.162	.067
14	.210	.196	.156	.040
18.5	-	.323	.244	.079
19	.232	.217	.150	.067
20	.200	.230	.180	.050

TABLE III-7

POST FLIGHT ABLATOR DATA

RIGHT HORIZONTAL STABILIZER

UPPER SURFACE

Gric Location	Original Thickness	Post Flight Thickness	Residual Virgin	Char Thickness
1	.205	.183	.130	.053
2	.210	.207	.140	.067
3	.166	.165	.092	.073
4	.216	.220	.142	.078
5	.163	.142	.122	.020
6	.137	.140	.140	0
7	.202	.195	.132	.063
8	.160	.140	.132	.008
12	.135	.125	.112	.013
16	.175	.162	.095	.067
25	.152	.145	.087	.058
28	.157	.155	.095	.060

TABLE III-8

ABLATOR PERFORMANCE RECORD

UPPER SPEED BRAKES

POST MACH 6.7 FLIGHT

Grid Point	ABLATOR THICKNESS MEASUREMENTS								
		LEFT SIDE				RIGHT SIDE			
			POST FLIGHT				POST FLIGHT		
	Required	Actual	Total	Char	Virgin	Actual	Total	Char	Virgin
7	.200	.214	.210	.059	.151	.197	.190	.007	.183
8		.201	.184	.074	.110	.175	.155	.035	.120
9		.207	.175	.085	.090	.180	.166	.095	.071
10		.217	.187	.110	.077	.196	.180	.134	.046
17		.199	.181	.107	.074	.187	.181	.126	.055
18		.214	.167	.067	.100	.195	.203	.107	.096
19	.200	.217	.155	.065	.090	.206	.179	.128	.051

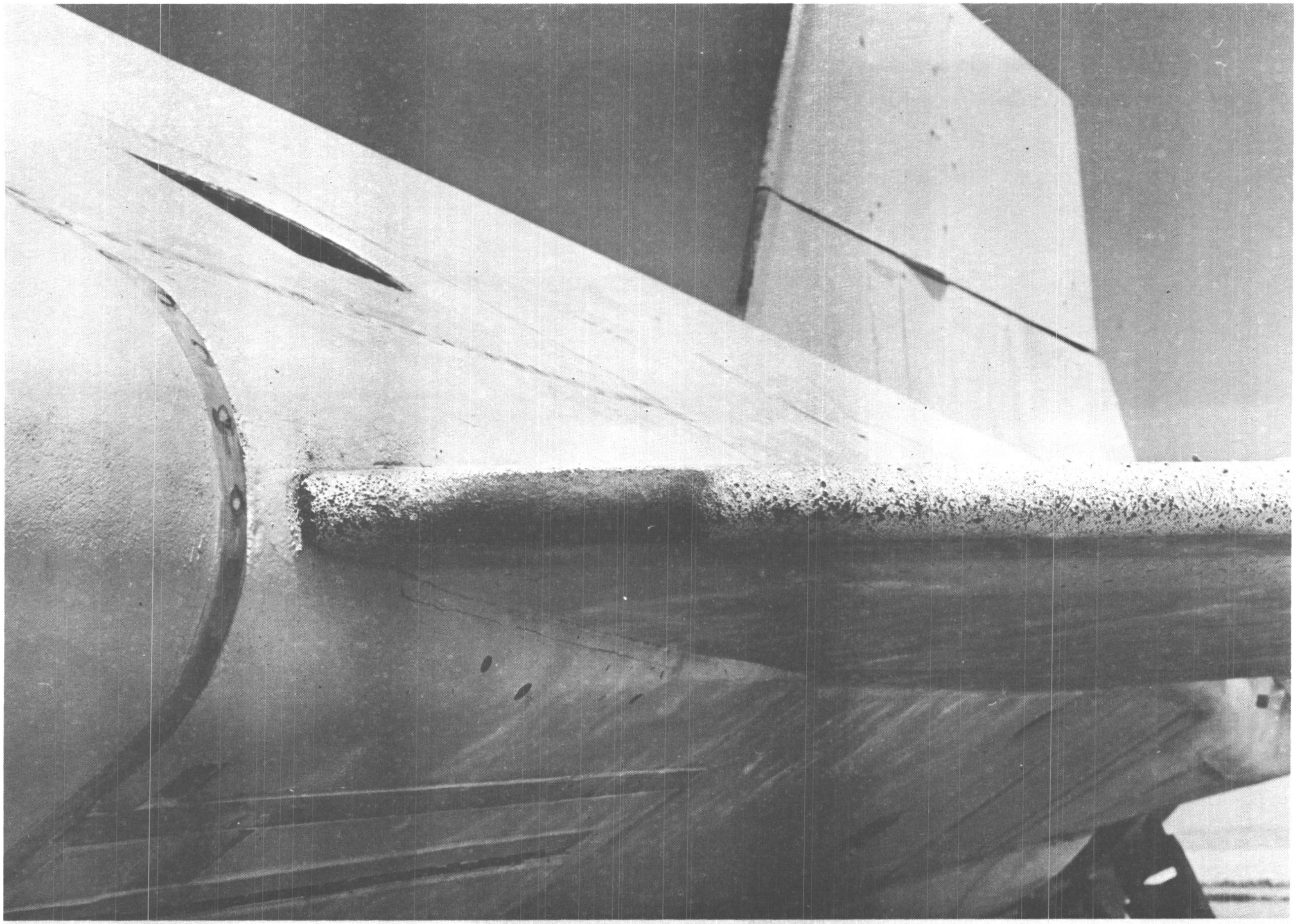

Figure III-1 Wing Leading Edge, Post Mach 5.0 Flight

Flight Research Center
Edwards, California

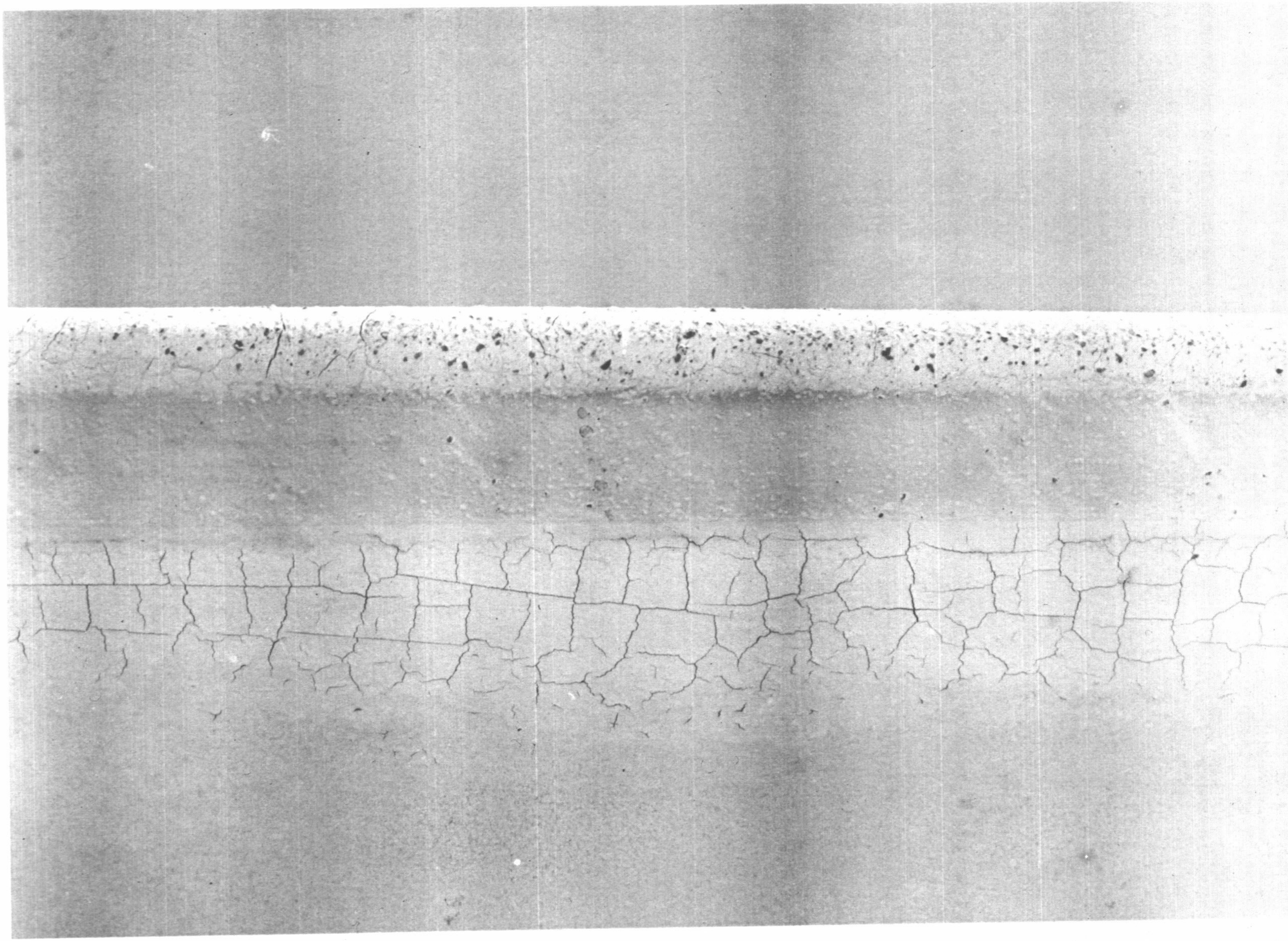

Figure III-2 Wing Leading Edge Lower Surface, Post Mach 5.0 Flight

Flight Research Center
Edwards, California

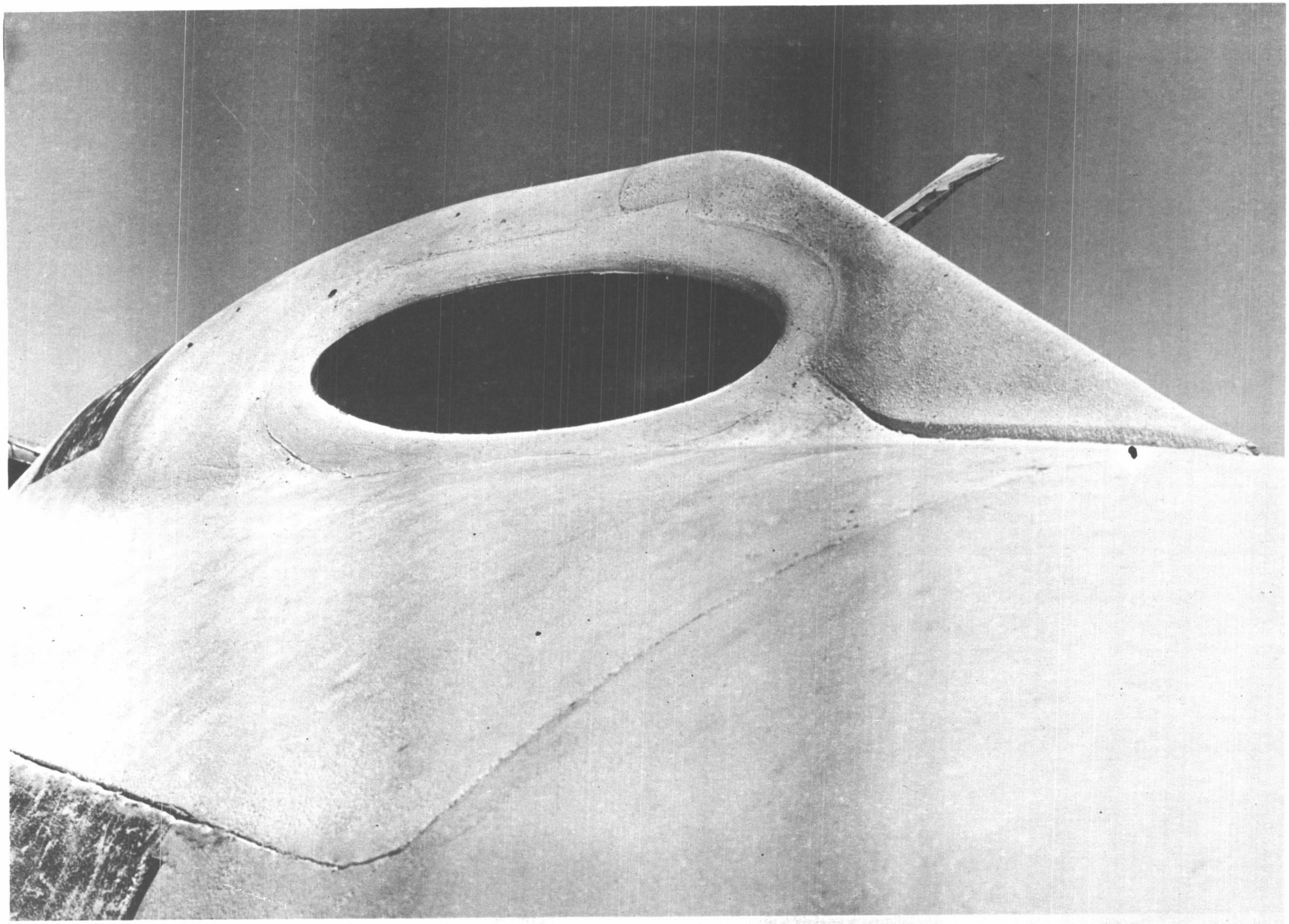

Figure III-3 Canopy Right Windshield, Post Mach 5.0 Flight

NASA Flight Research Center
Edwards, California

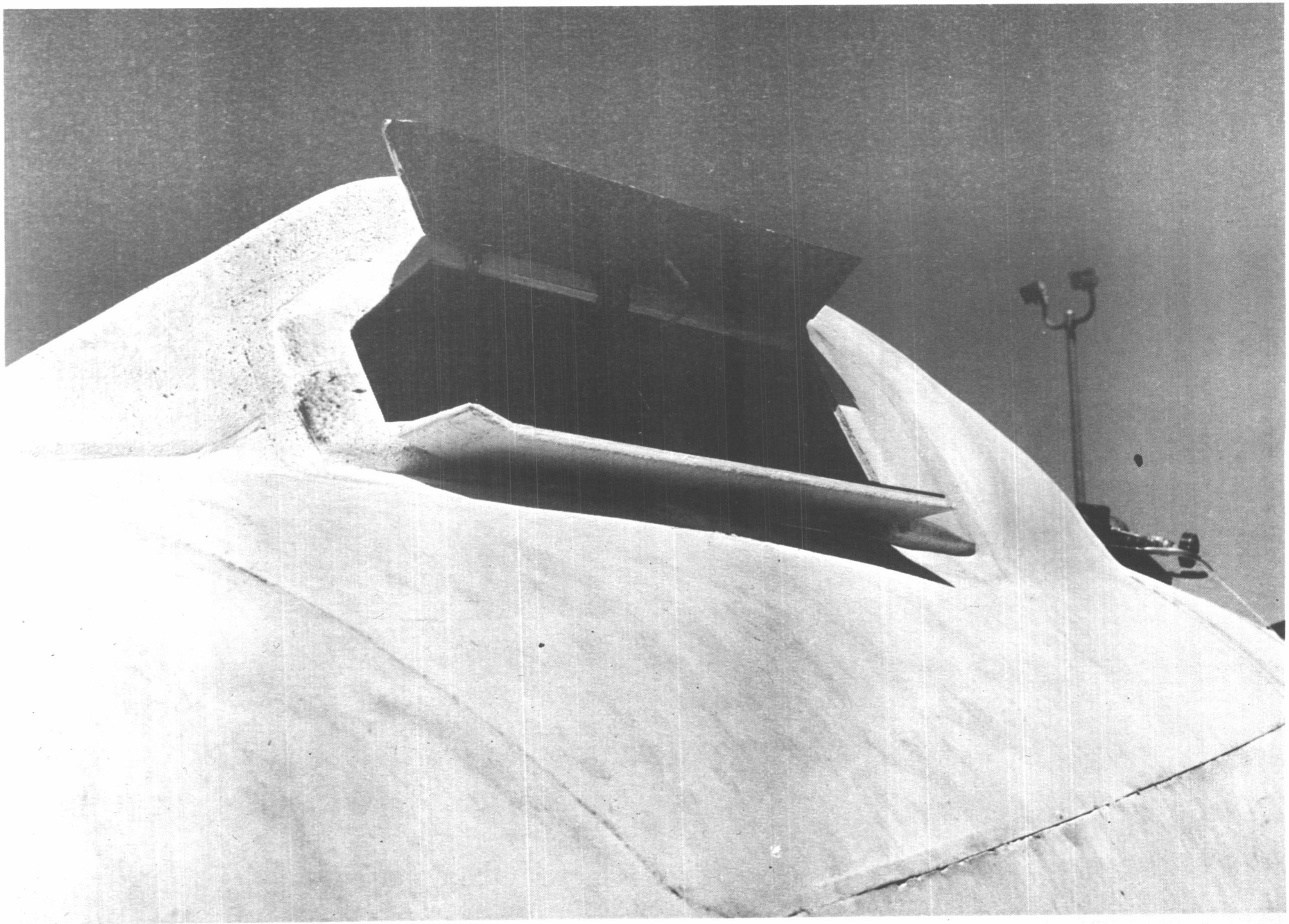

Figure III-4 Canopy Left Windshield Shutter Mechanism, Post Mach 5.0 Flight

Flight Research Center
Edwards, California

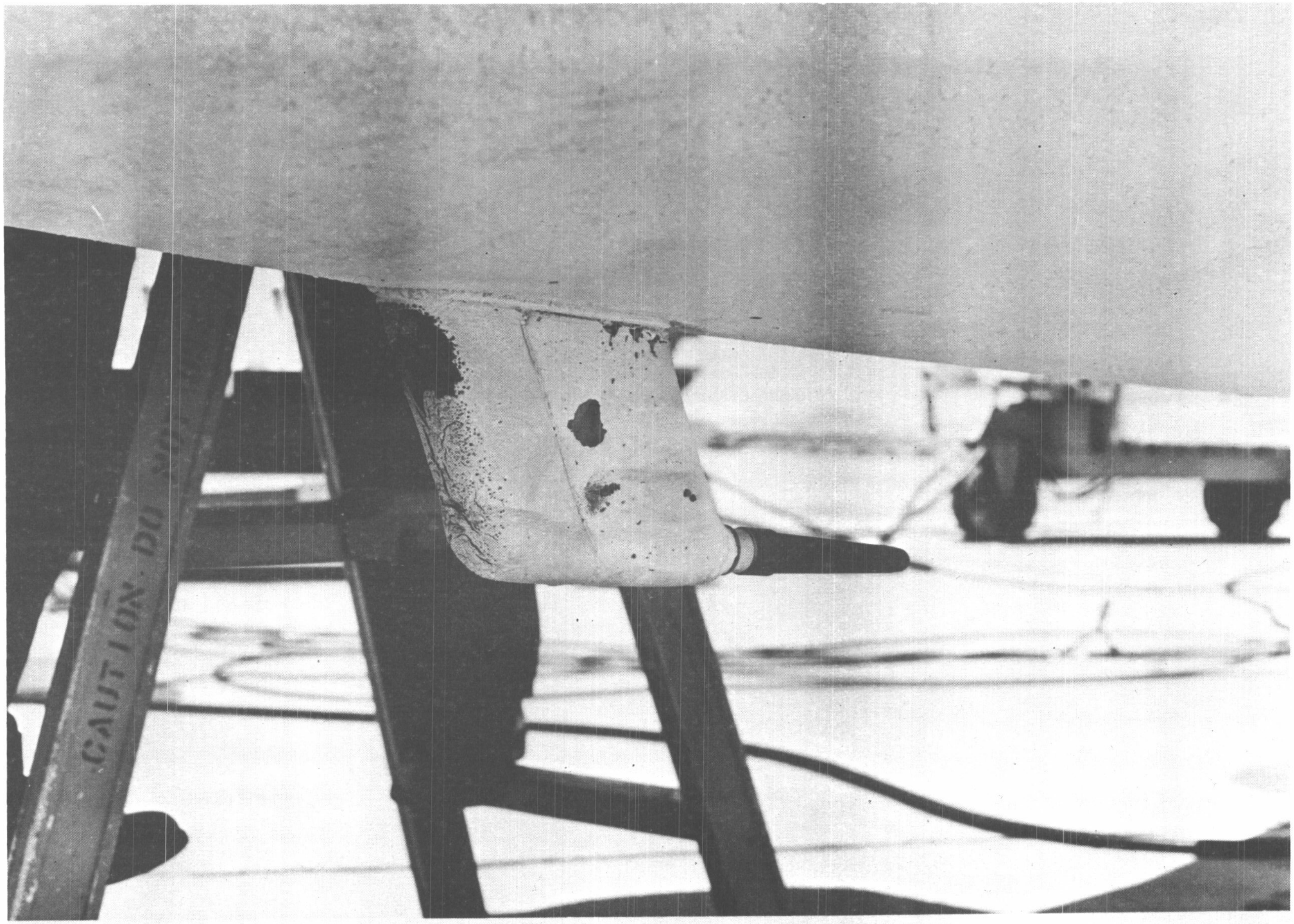

Figure III-5 Forward Vane Antenna, Post Mach 5.0 Flight

NASA Flight Research Center
Edwards, California

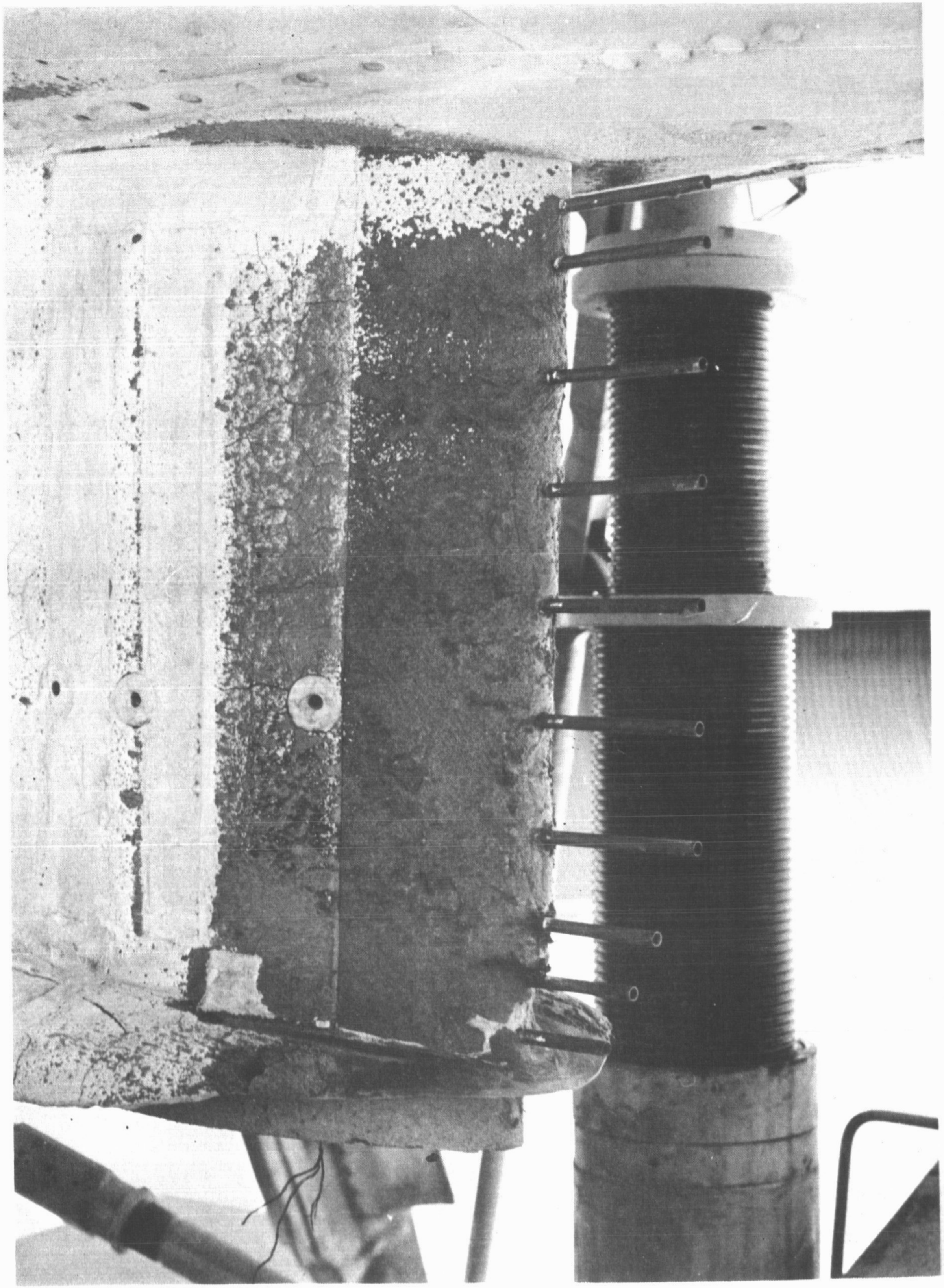

Figure III-6 Ventral Fin Leading Edge, Post Mach 5.0 Fligh

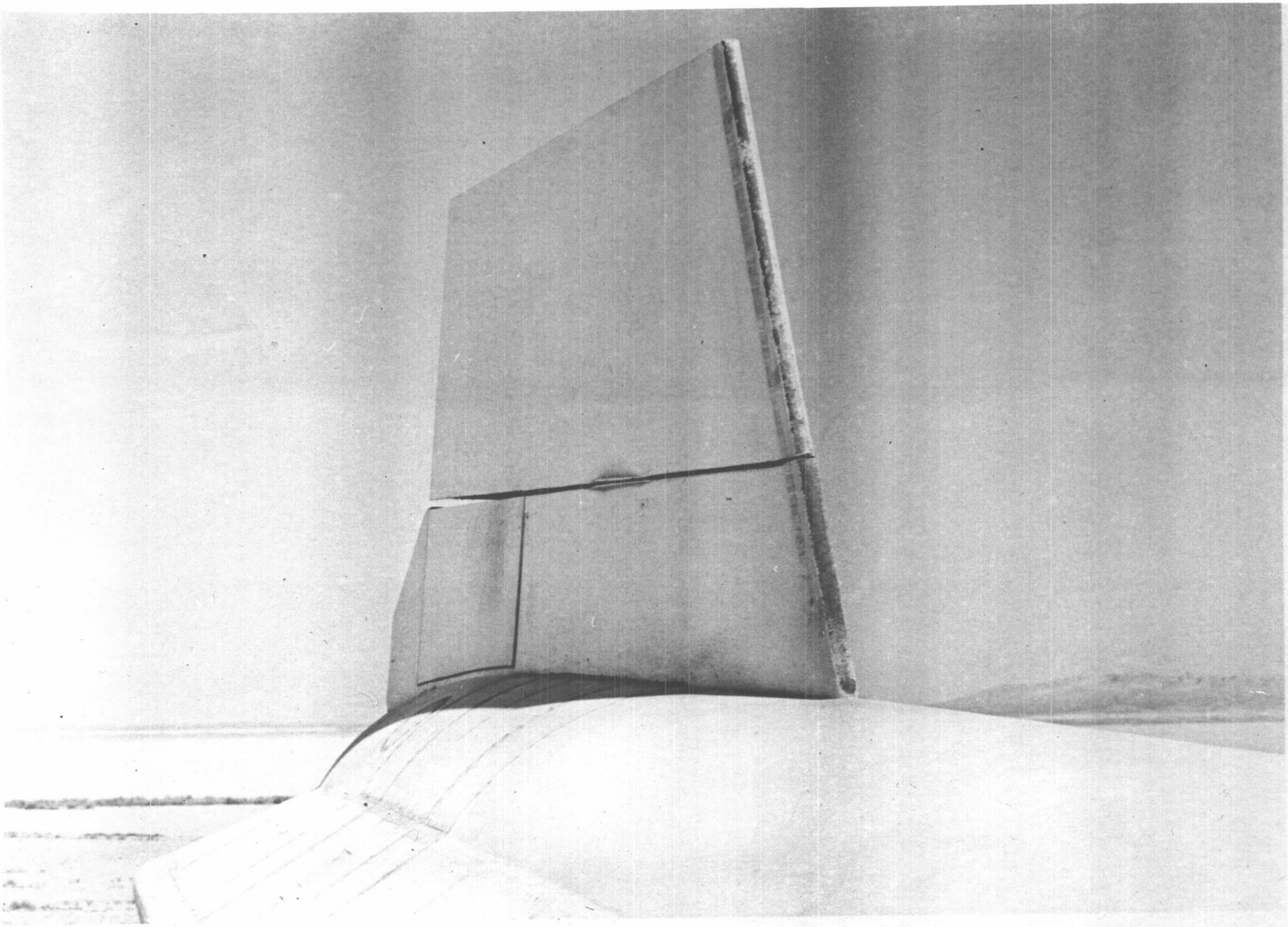

Figure III-7 Upper Vertical Tail Right Side, Post Mach 5.0 Flight

NASA Flight Research Center
Edwards, California

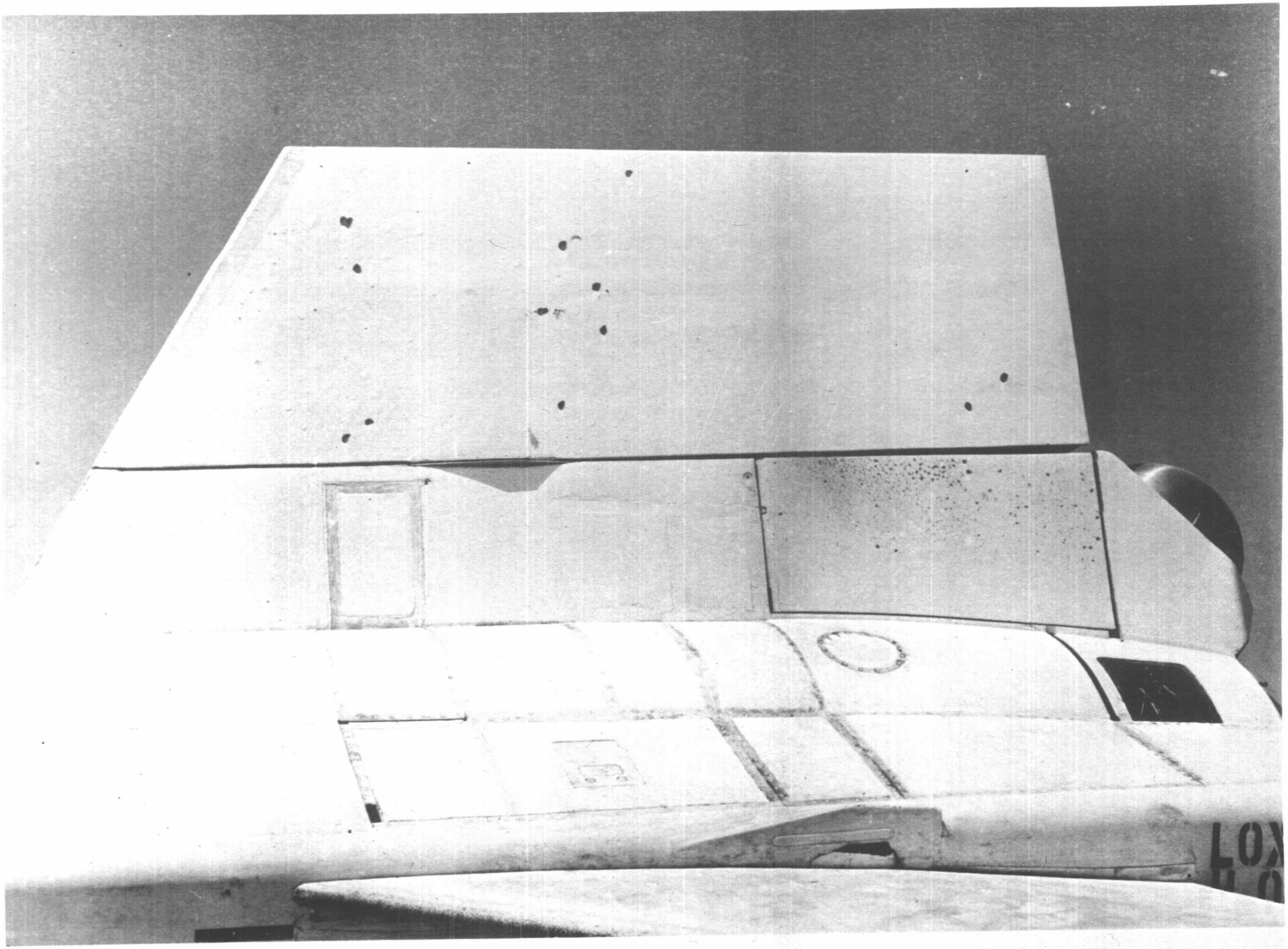

Figure III-8 Upper Vertical Tail Left Side, Post Mach 5.0 Flight

NASA Flight Research Center
Edwards, California

Figure III-9 Right Lower Speed Brake, Post Mach 5.0 Flight

Flight Research Center
Edwards, California

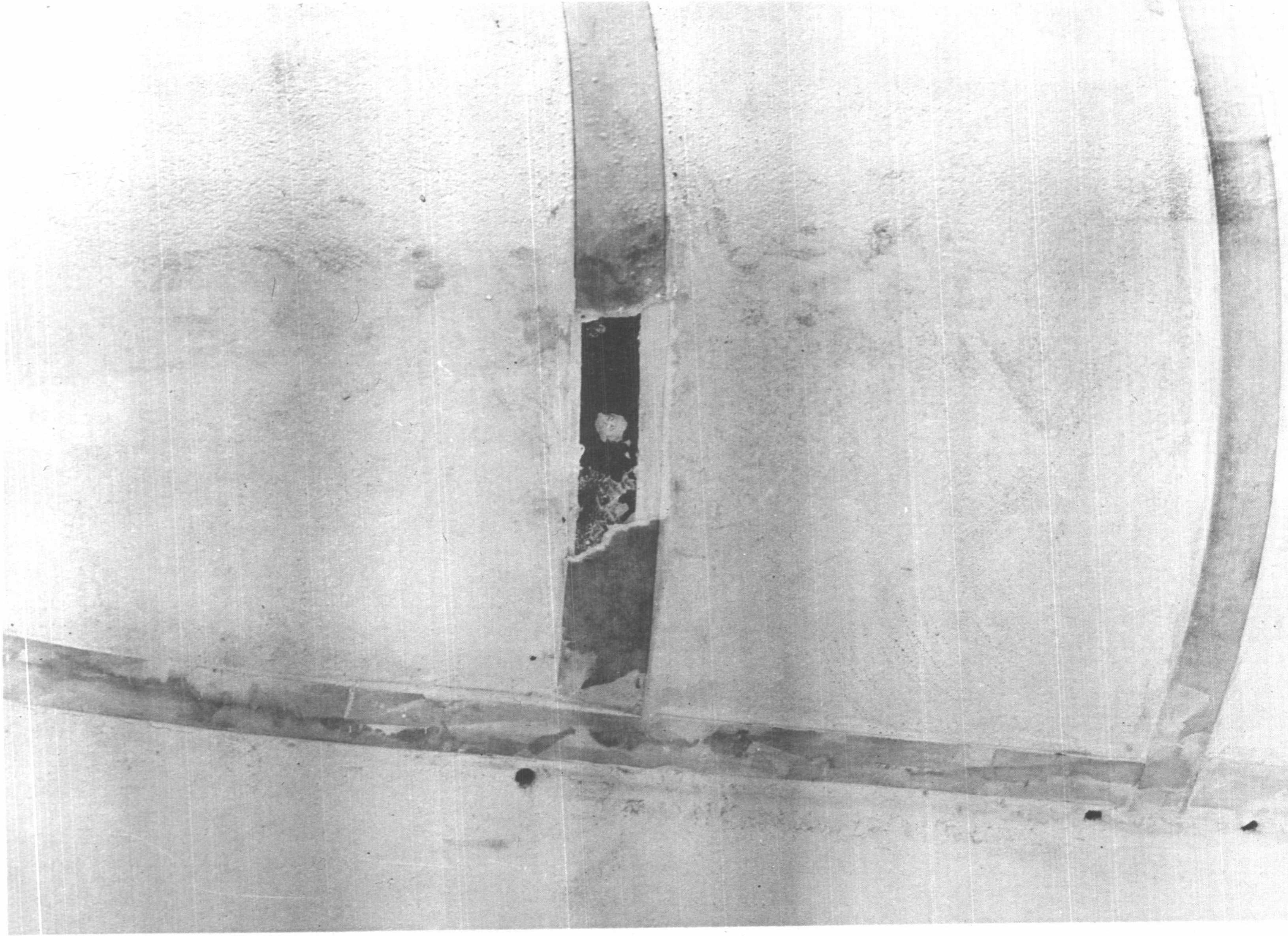

Figure III-10 Bonded Strip Failure, Left Conduit Assy.,
Post Mach 5.0 Flight

NASA Flight Research Center
Edwards, California

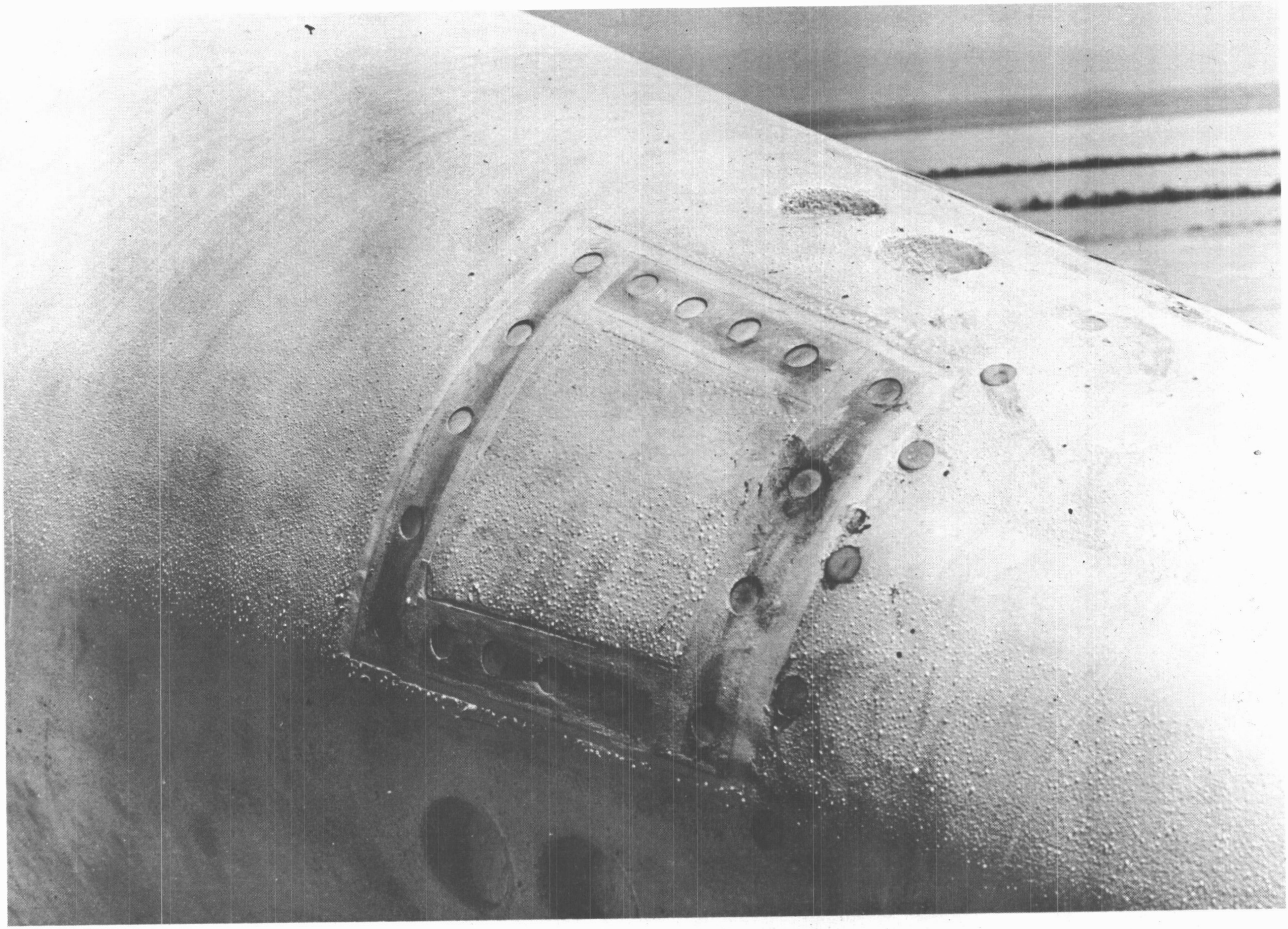

Figure III-11 Fuselage Nose, Post Mach 5.0 Flight

NASA Flight Research Center
Edwards, California

Figure III-12 Right Wing Lower Surface, Post Mach 6.7 Flight

Flight Research Center
Edwards, California

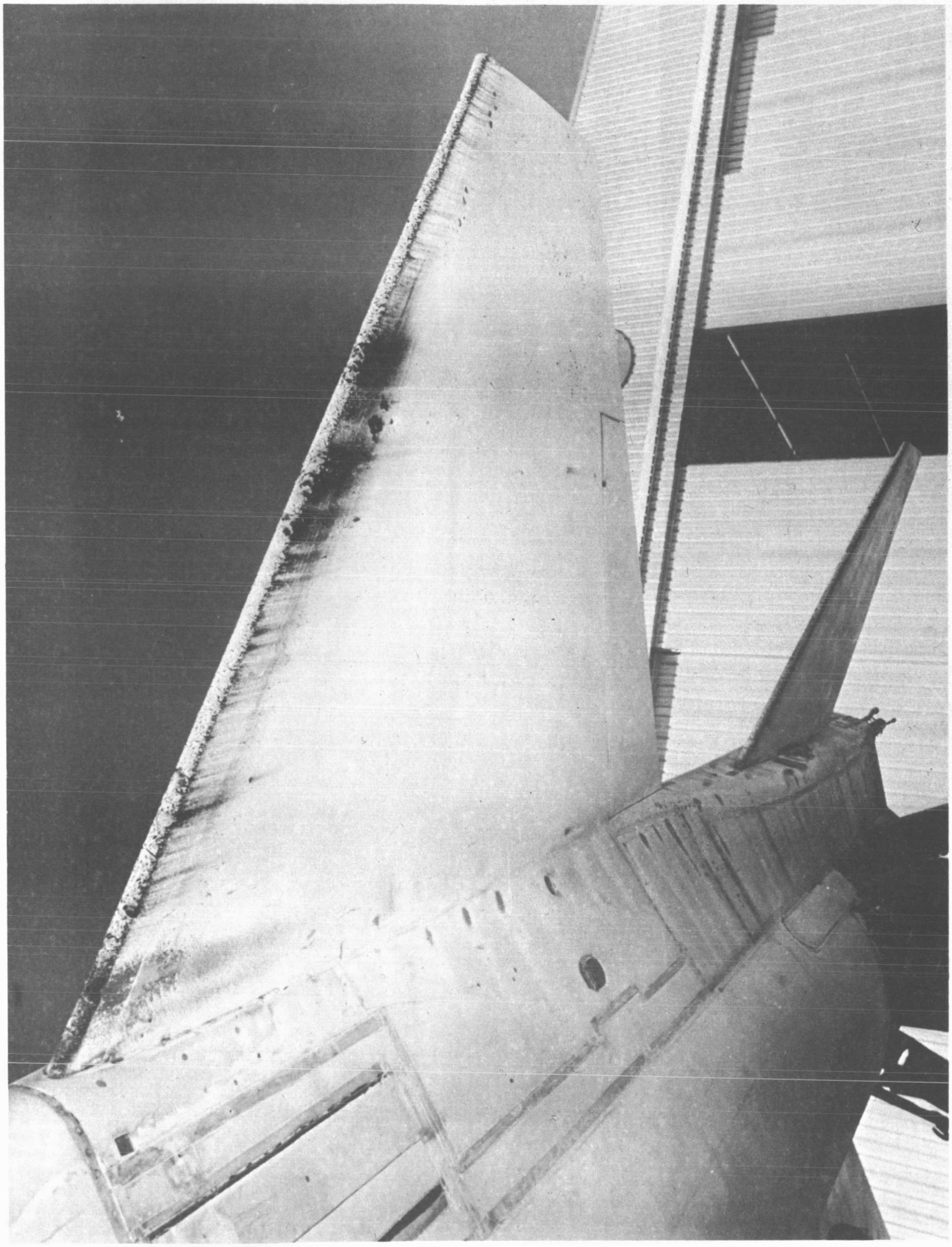

Figure III-13 Left Wing Lower Surface, Post Mach 6.7 Flight

NASA Flight Research Center Edwards, California

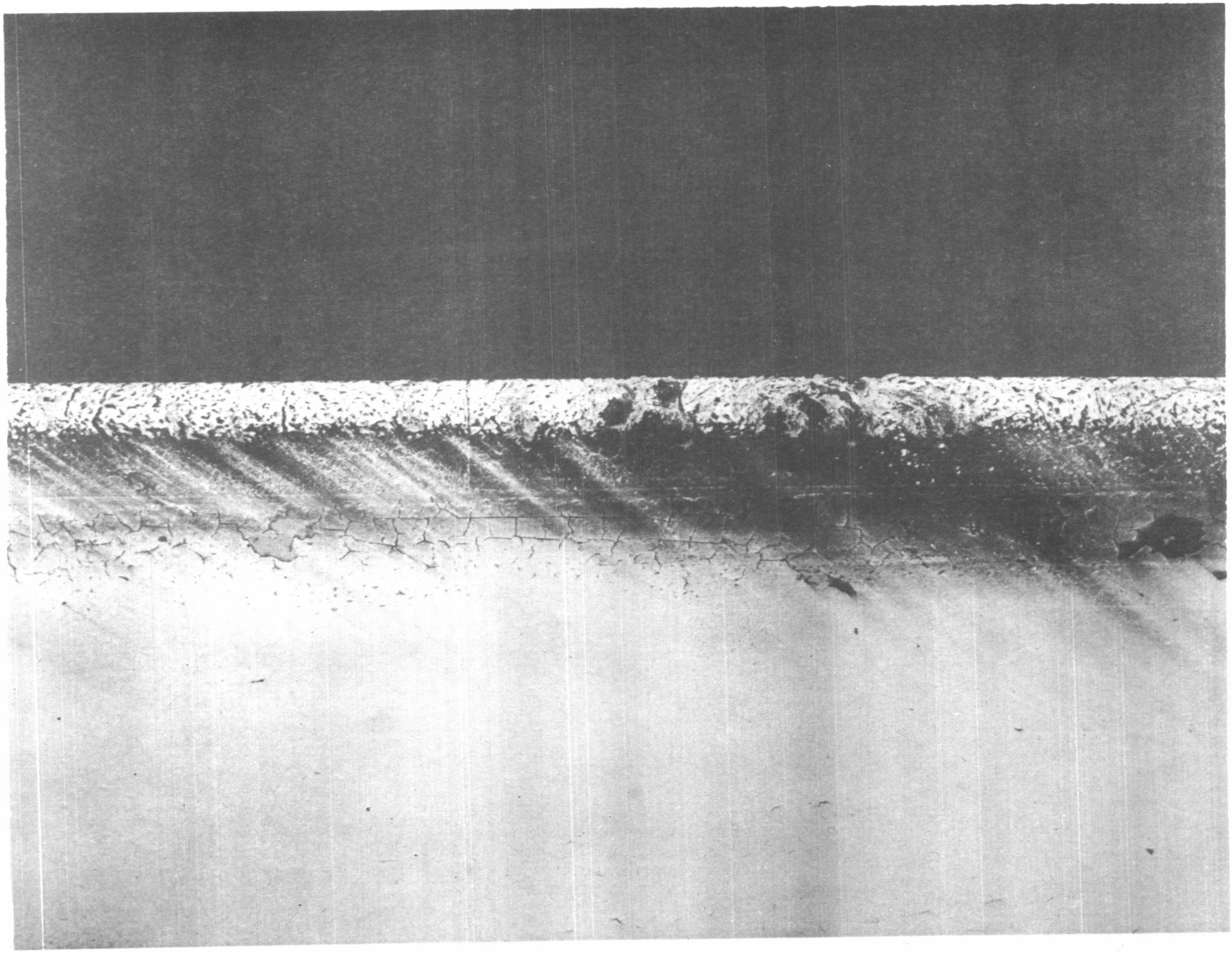

Figure III-14 Left Wing Leading Edge, Post Mach 6.7 Flight

Flight Research Center
Edwards, California

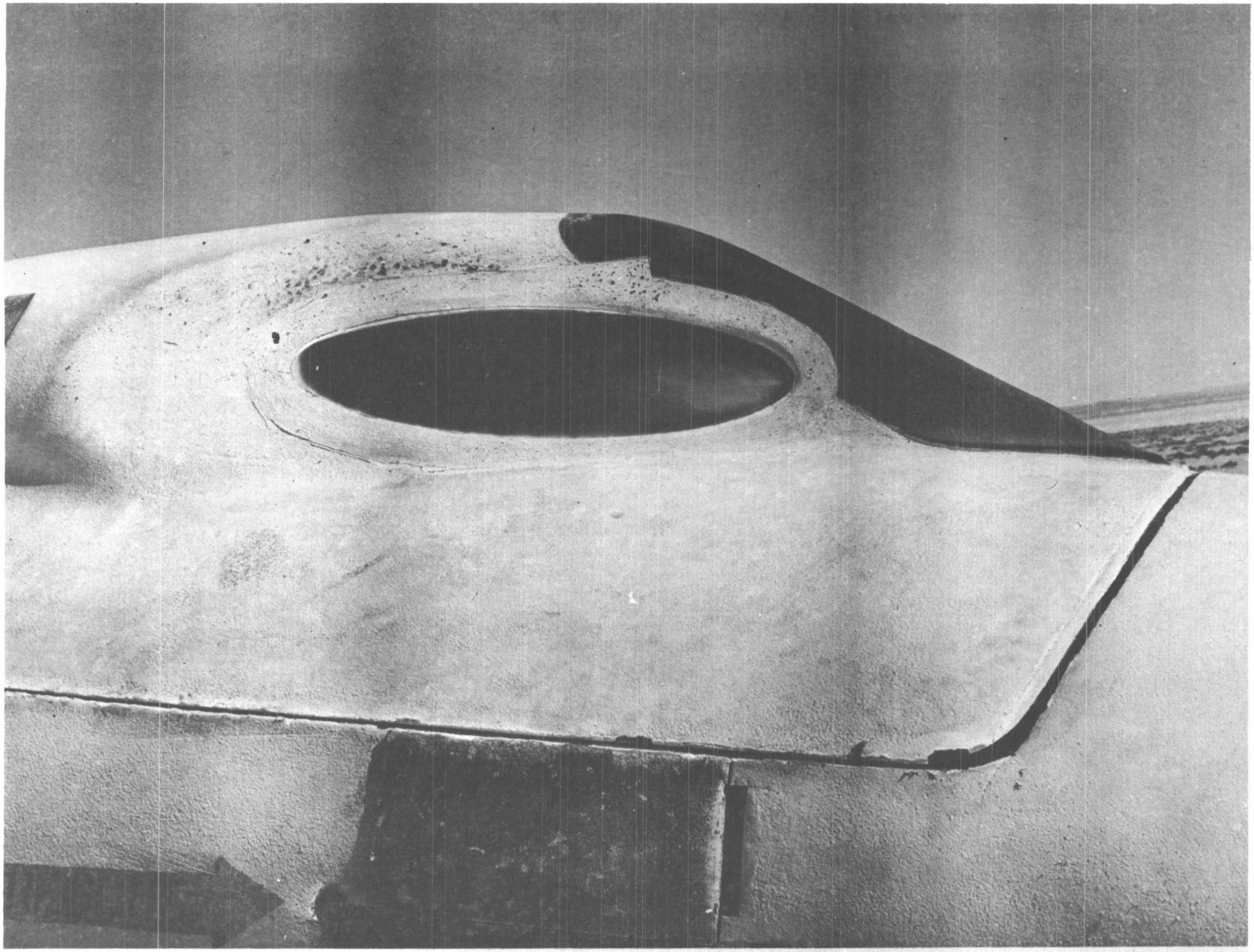

Figure III-15 Canopy Right Windshield, Post Mach 6.7 Flight

Flight Research Center
Edwards, California

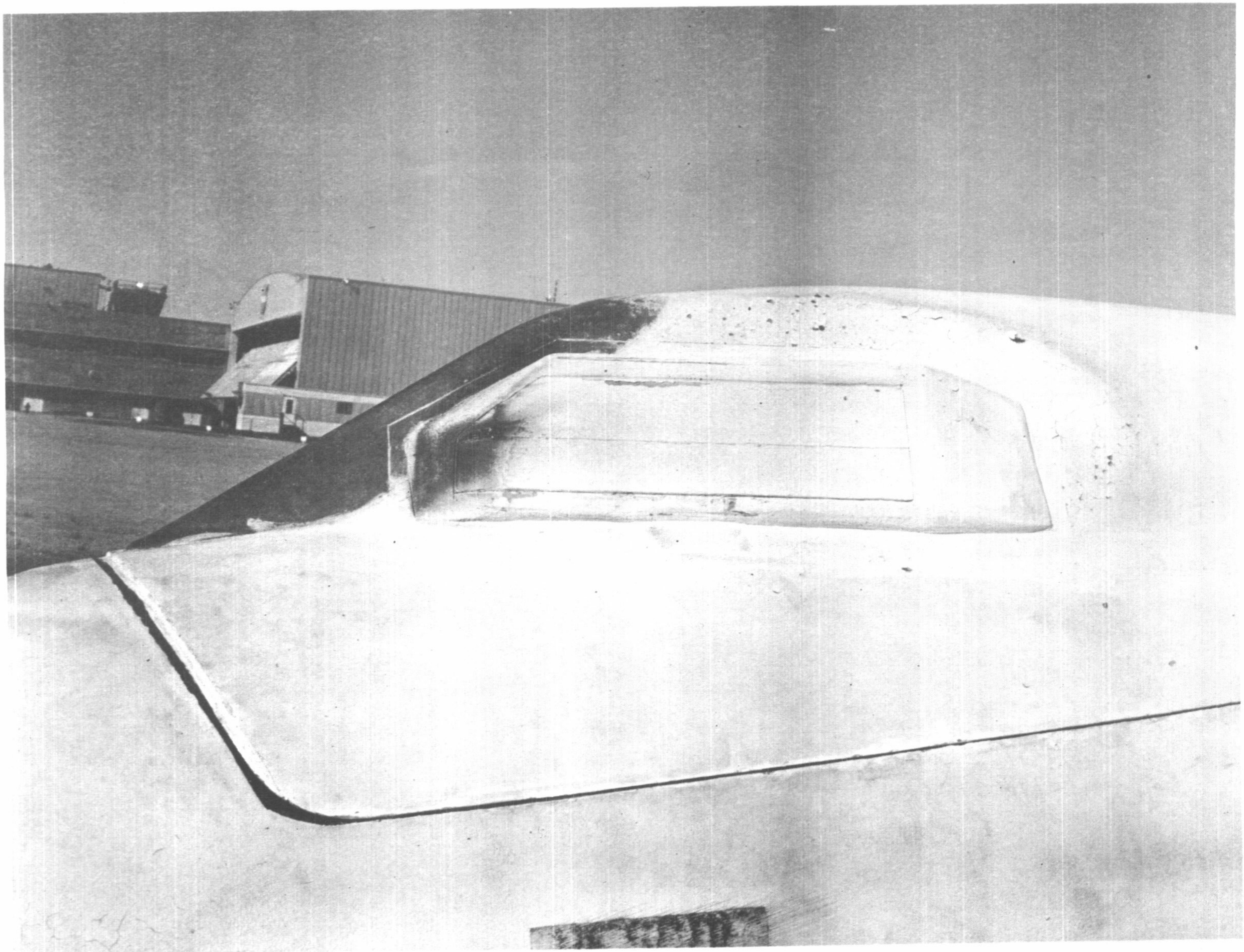

Figure III-16 Canopy Left Windshield Shutter Mechanism, Post Mach 6.7 Flight

Flight Research Center
Edwards, California

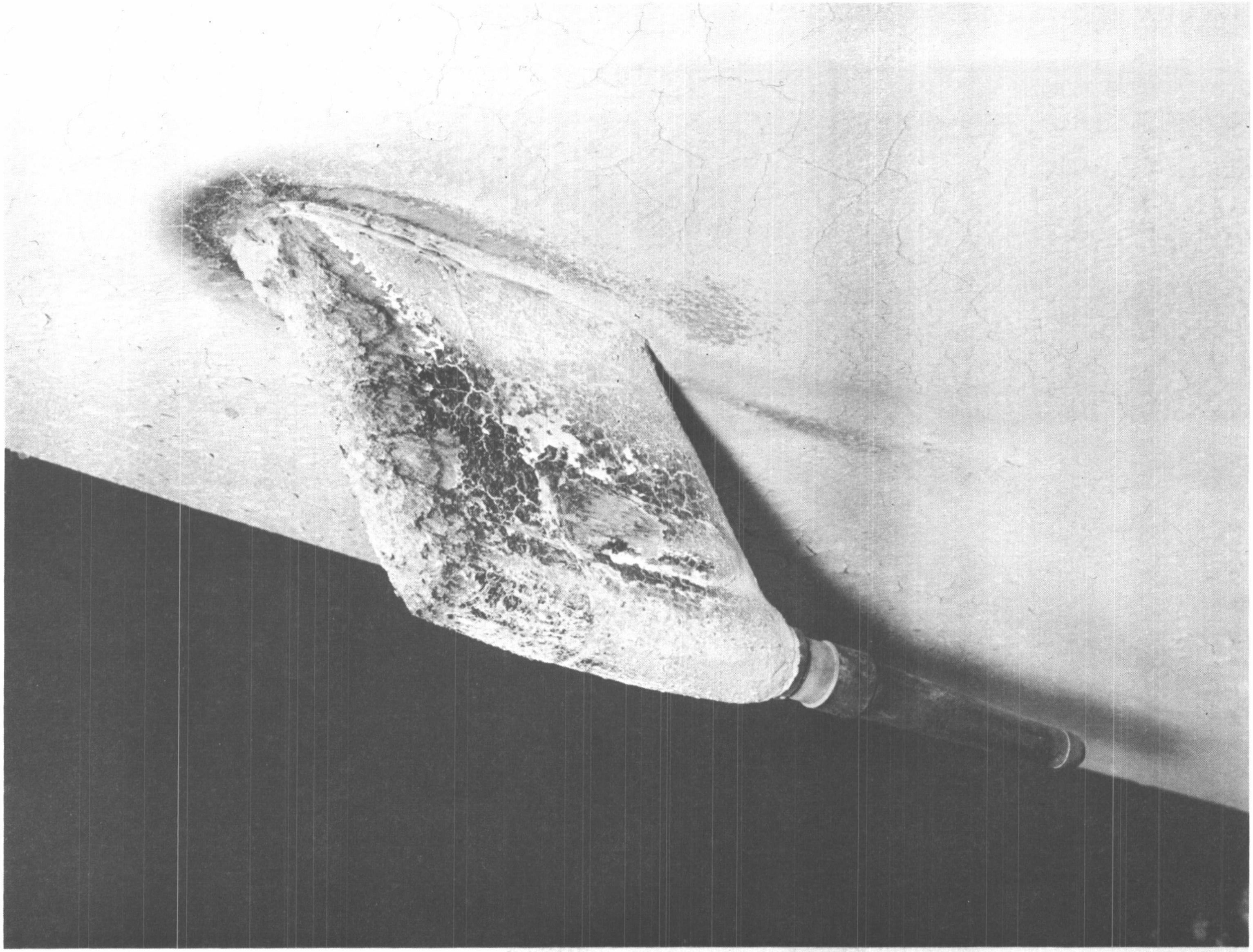

Figure III-17 Forward Vane Antenna, Post Mach 6.7 Flight

Flight Research Center
Edwards, California

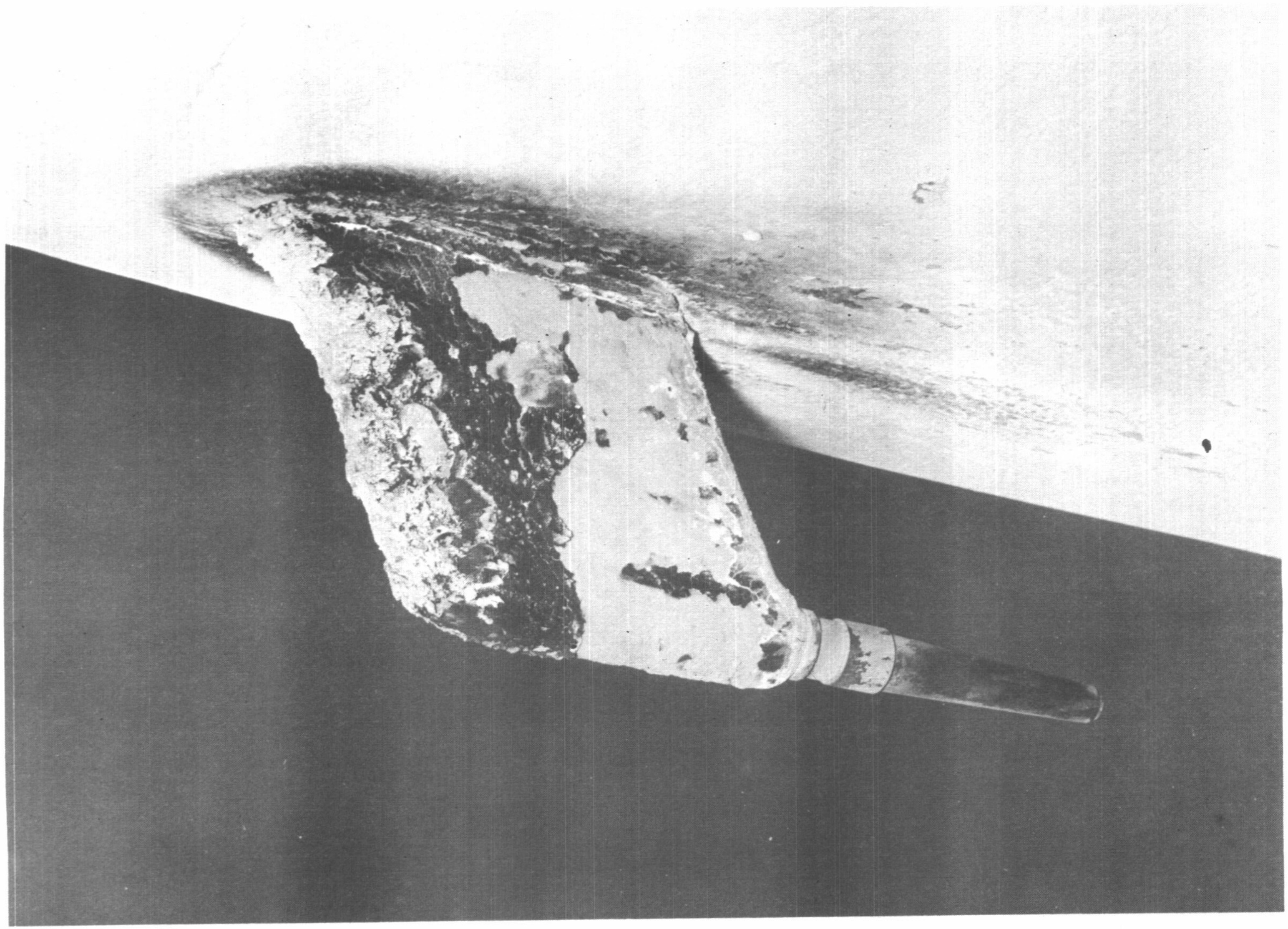

Figure III-18 Aft Vane Antenna, Post Mach 6.7 Flight

Flight Research Center
Edwards, California

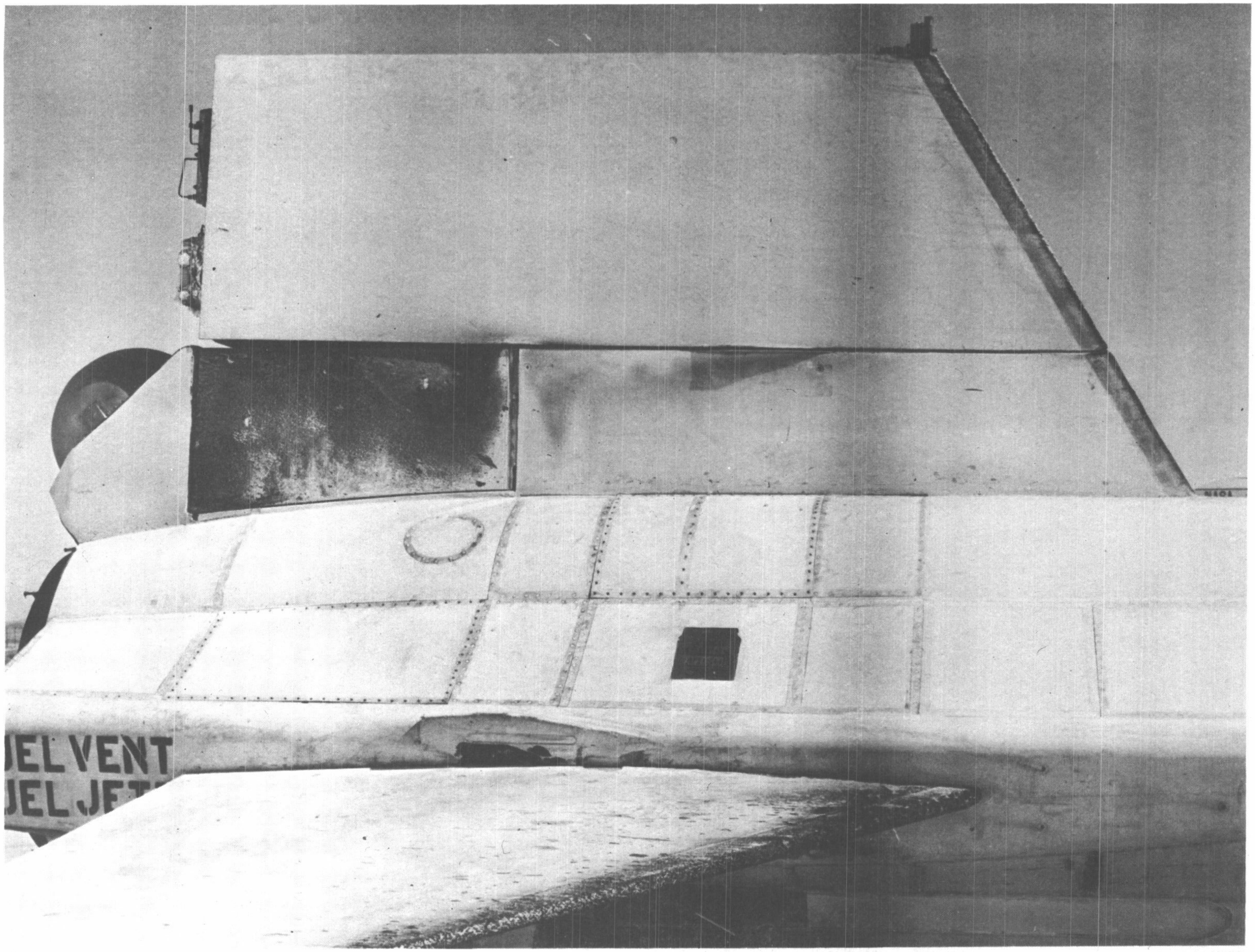

Figure III-19 Aft Fuselage and Vertical Tail, Right Side,
Post Mach 6.7 Flight

Flight Research Center
Edwards, California

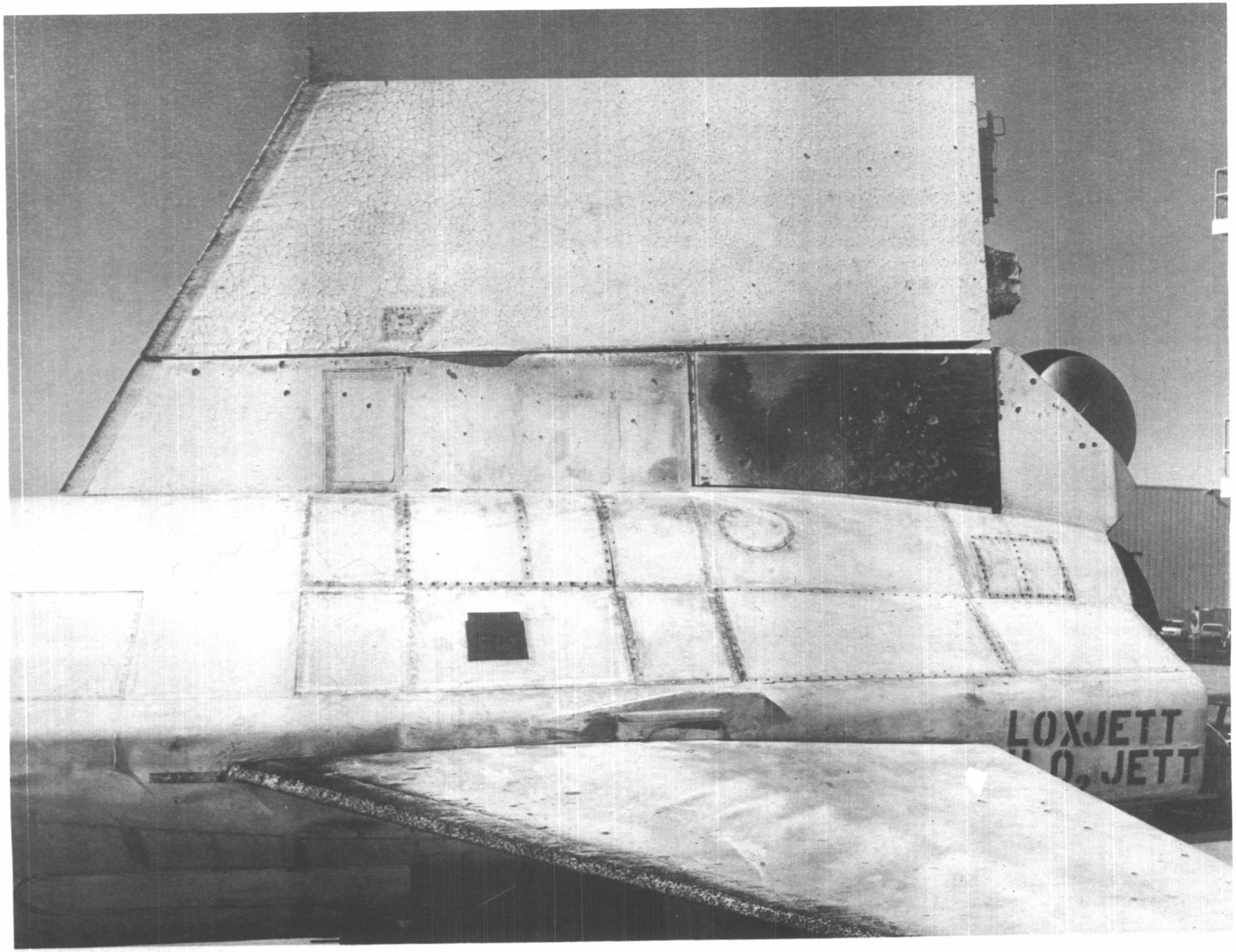

Figure III-20 Aft Fuselage and Vertical Tail, Left Side, Post Mach 6.7 Flight

NASA Flight Research Center Edwards, California

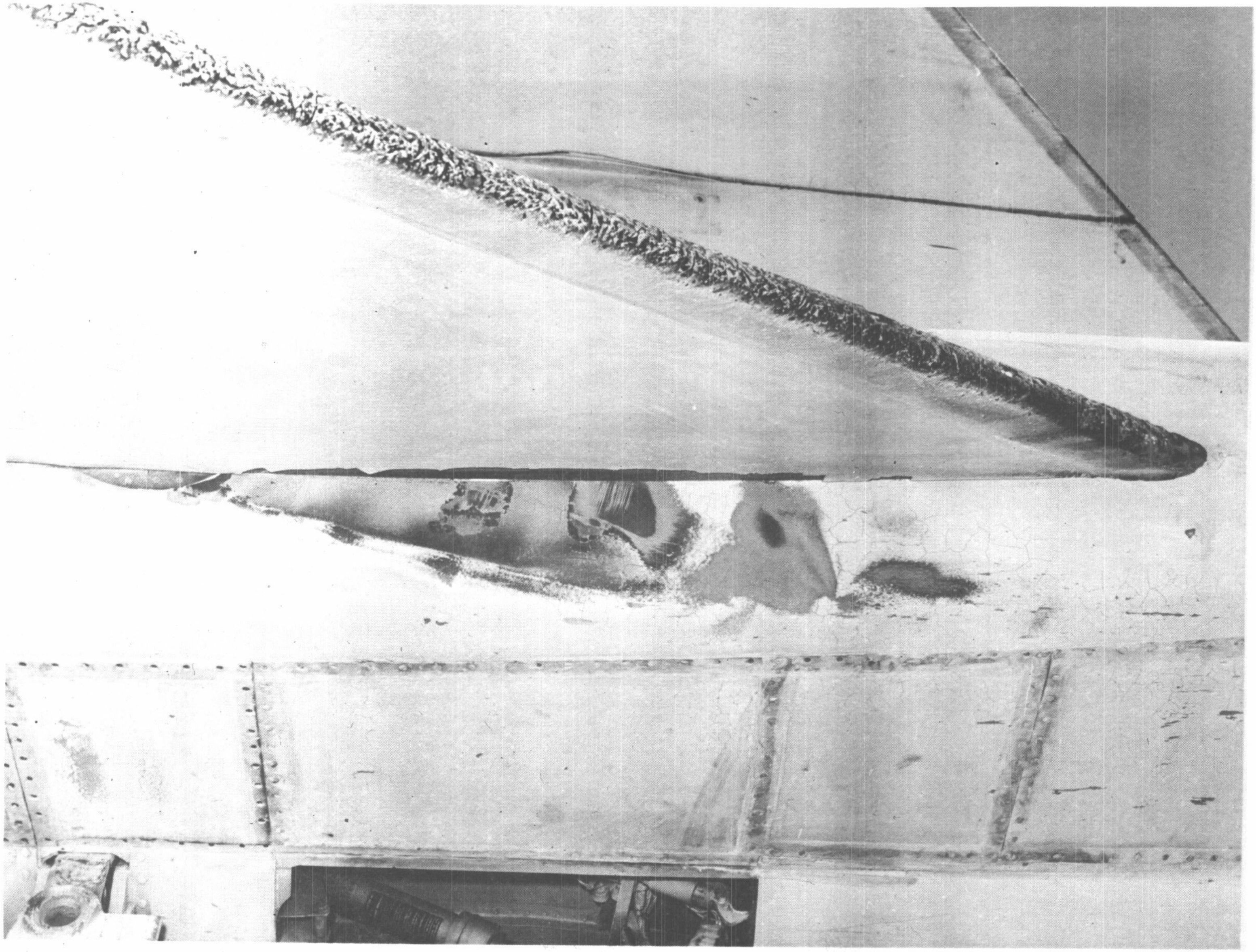

Figure III-21 Right Horizontal Stabilizer and Side Fairing, Post Mach 6.7 Flight

Flight Research Center
Edwards, California

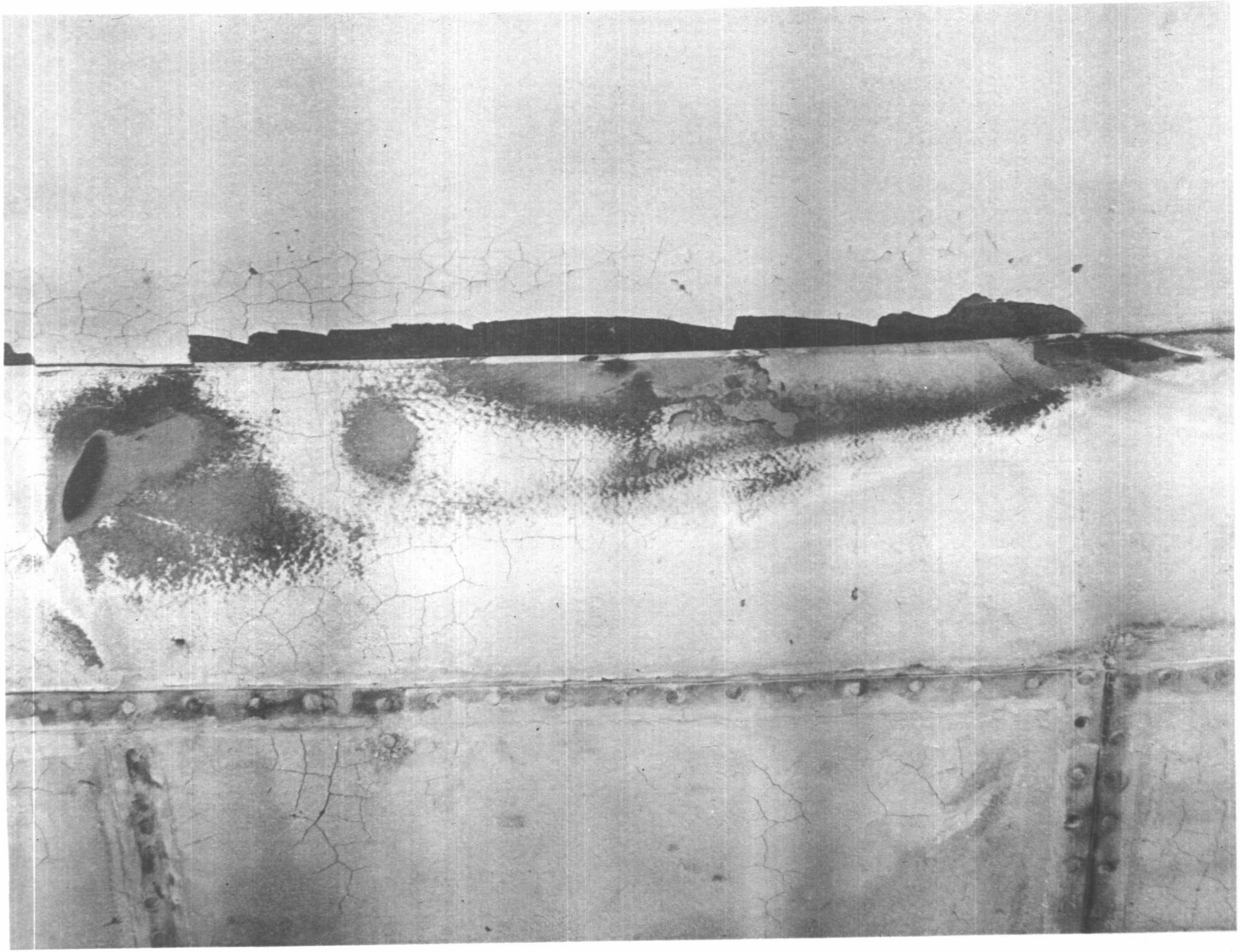

Figure III-22 Inboard End of Left Horizontal Stabilizer and Side Fairing, Post Mach 6.7 Flight

Flight Research Center
Edwards, California

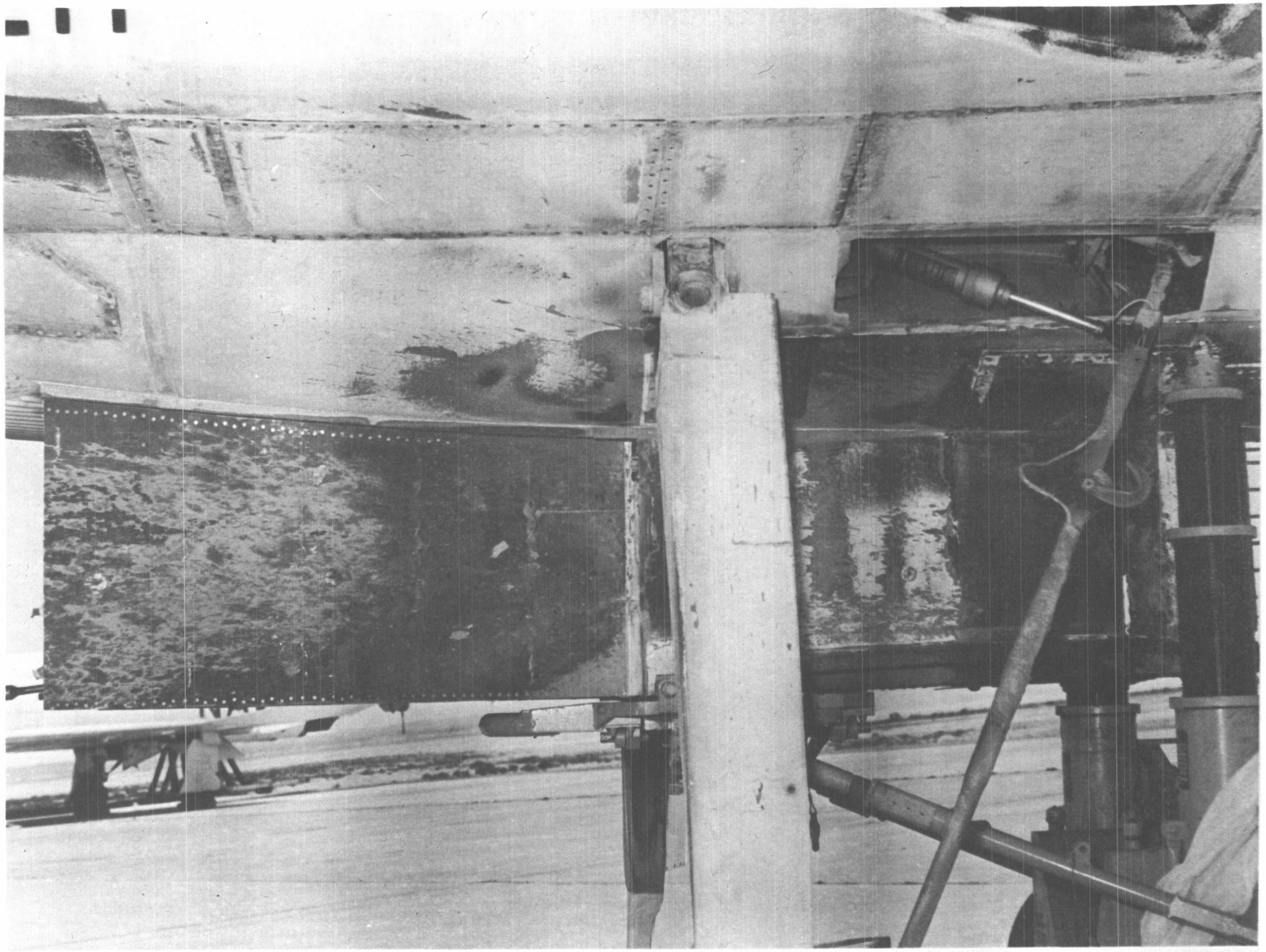

Figure III-23 Right Speed Brake and Ventral Fin, Post Mach 6.7 Flight

Flight Research Center
Edwards, California

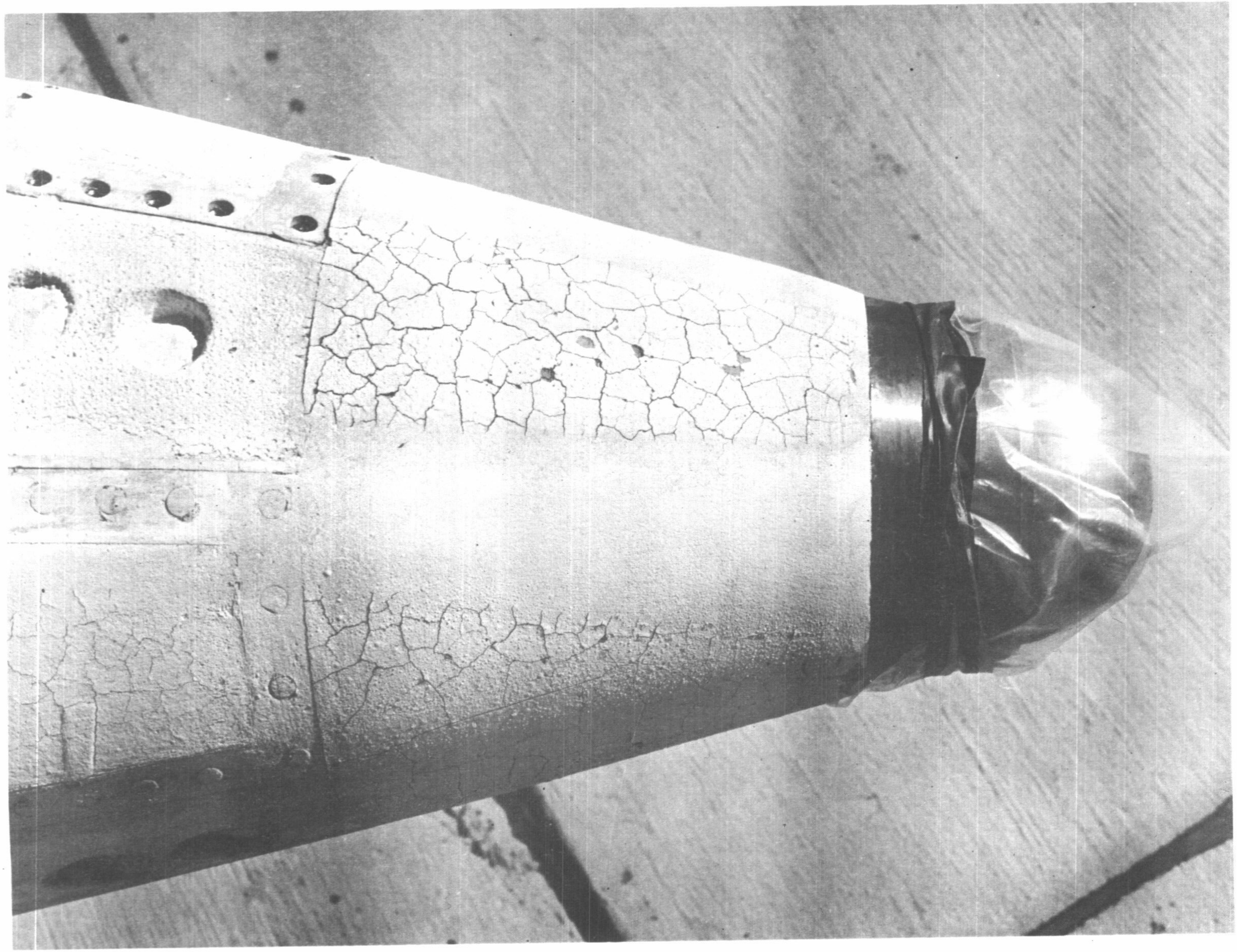

Figure III-24 Top of Fuselage Nose, Post Mach 6.7 Flight

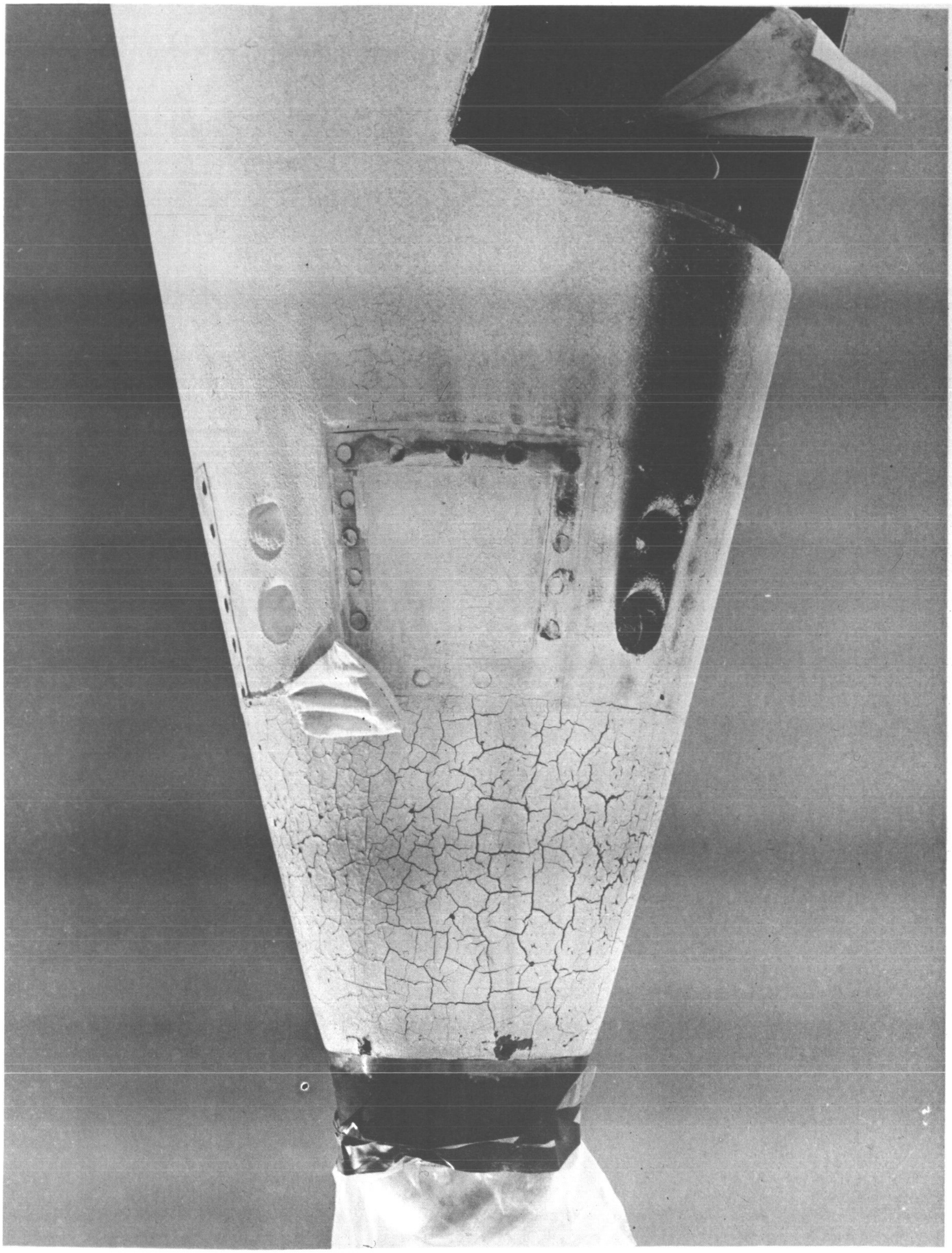

Figure III-25 Bottom of Fuselage Nose, Post Mach 6.7 Flight

NASA Flight Research Center
Edwards, California

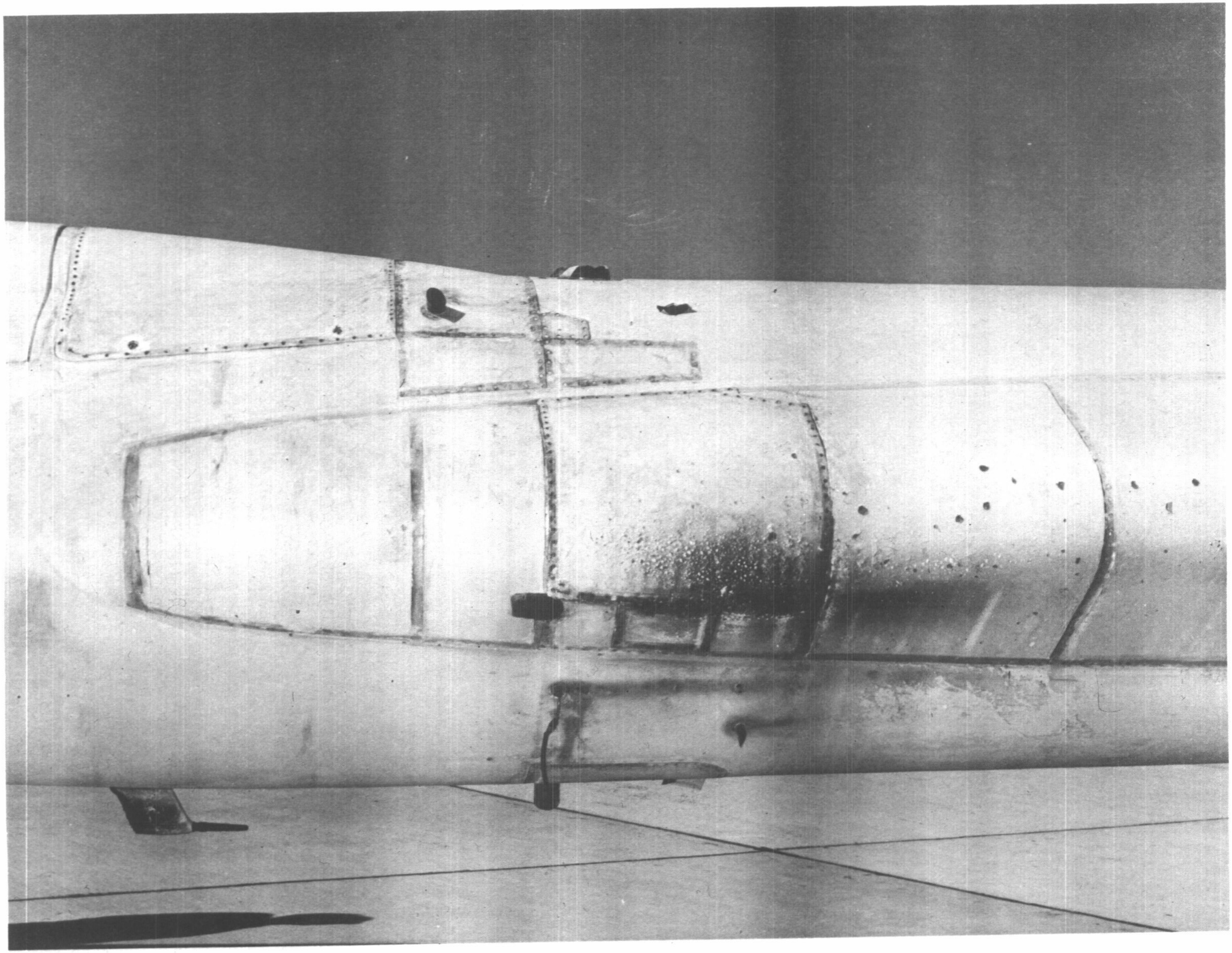

Figure III-26 Left Side Fuselage Forward Side Fairing,
Post Mach 6.7 Flight

Flight Research Center
Edwards, California

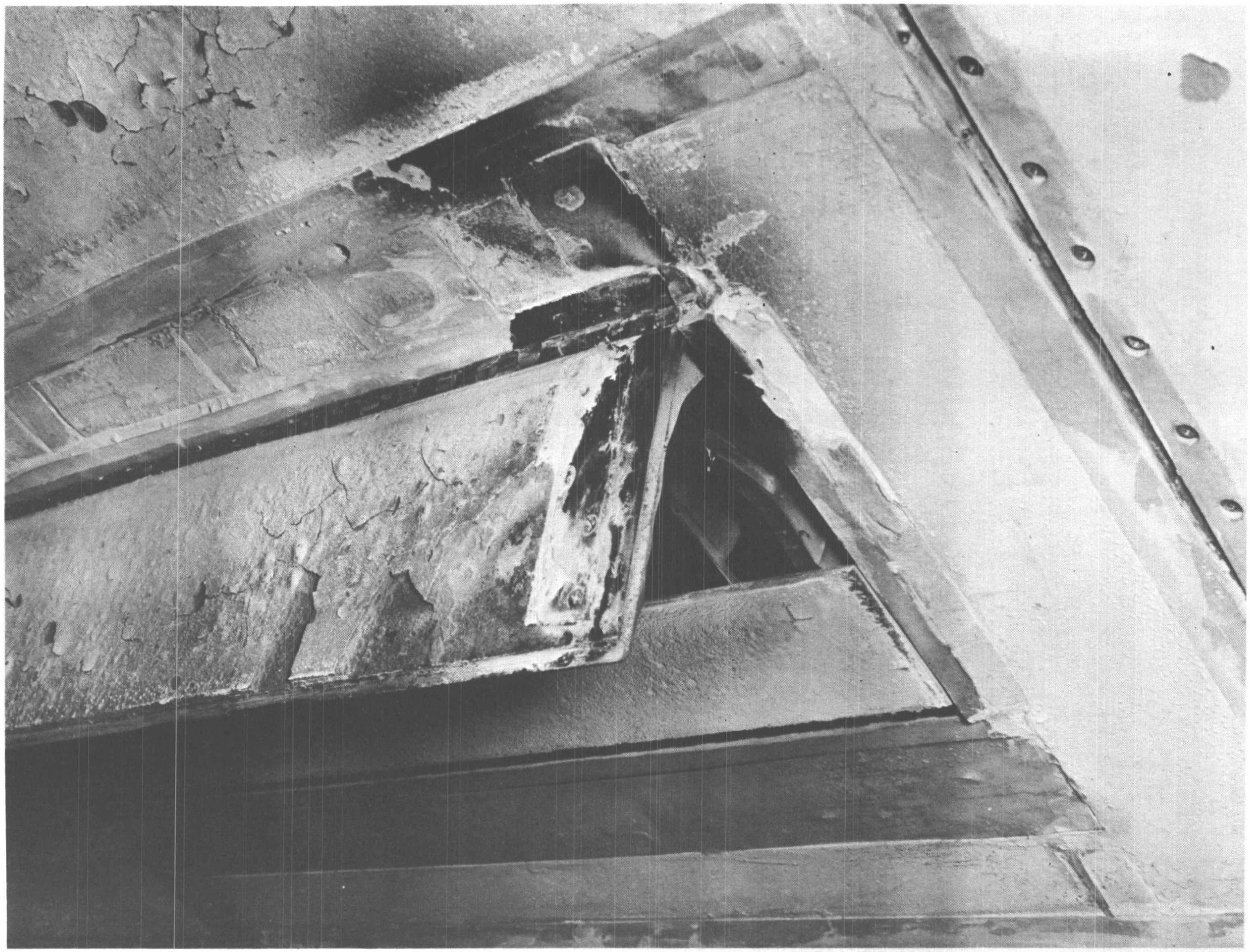

Figure III-27 Right Drop Tank Clam Shell Door Forward End, Post Mach 6.7 Flight

Flight Research Center
Edwards, California

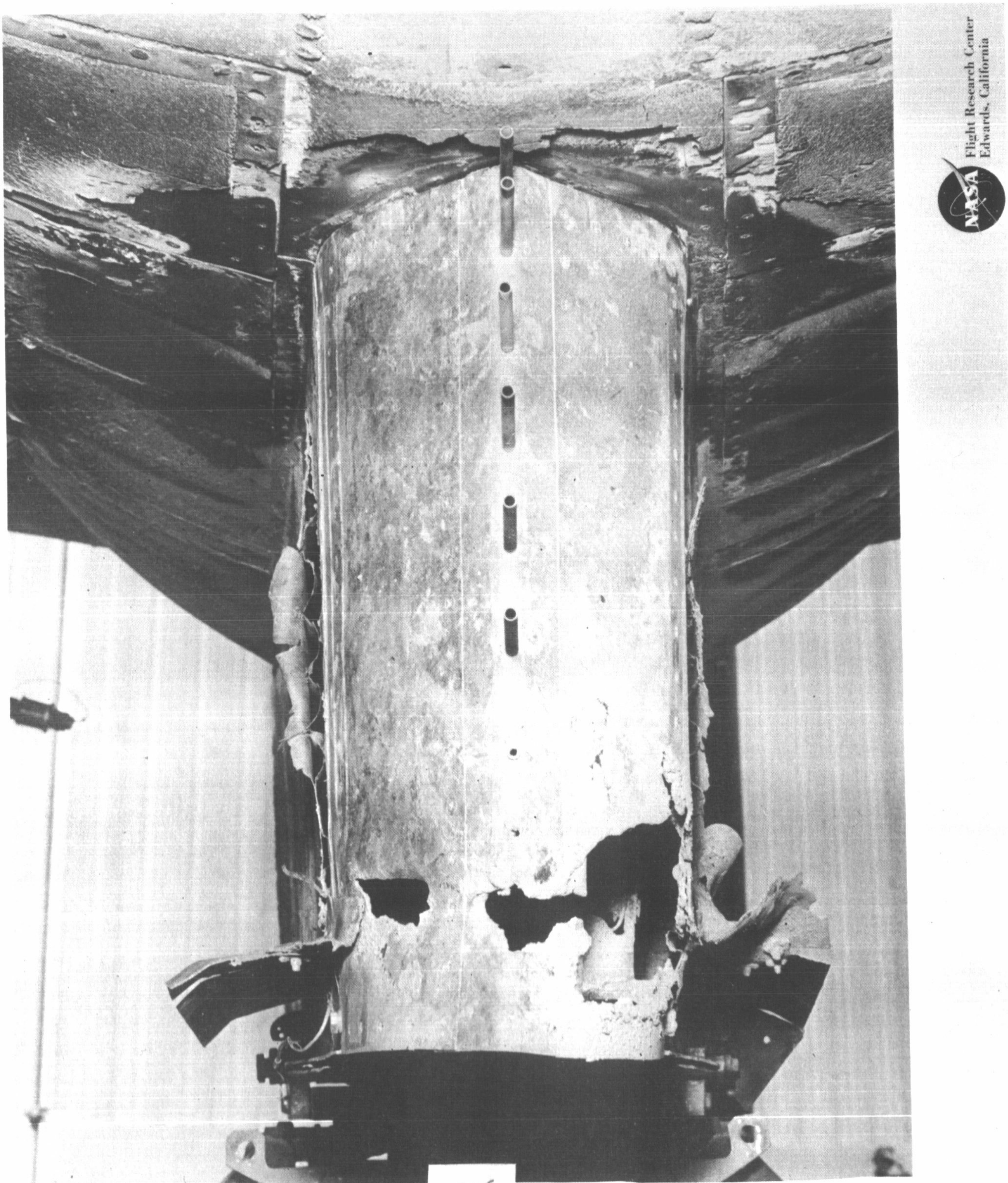

Figure III-28 Modified Ventral Fin Leading Edge, Post Mach 6.7 Flight

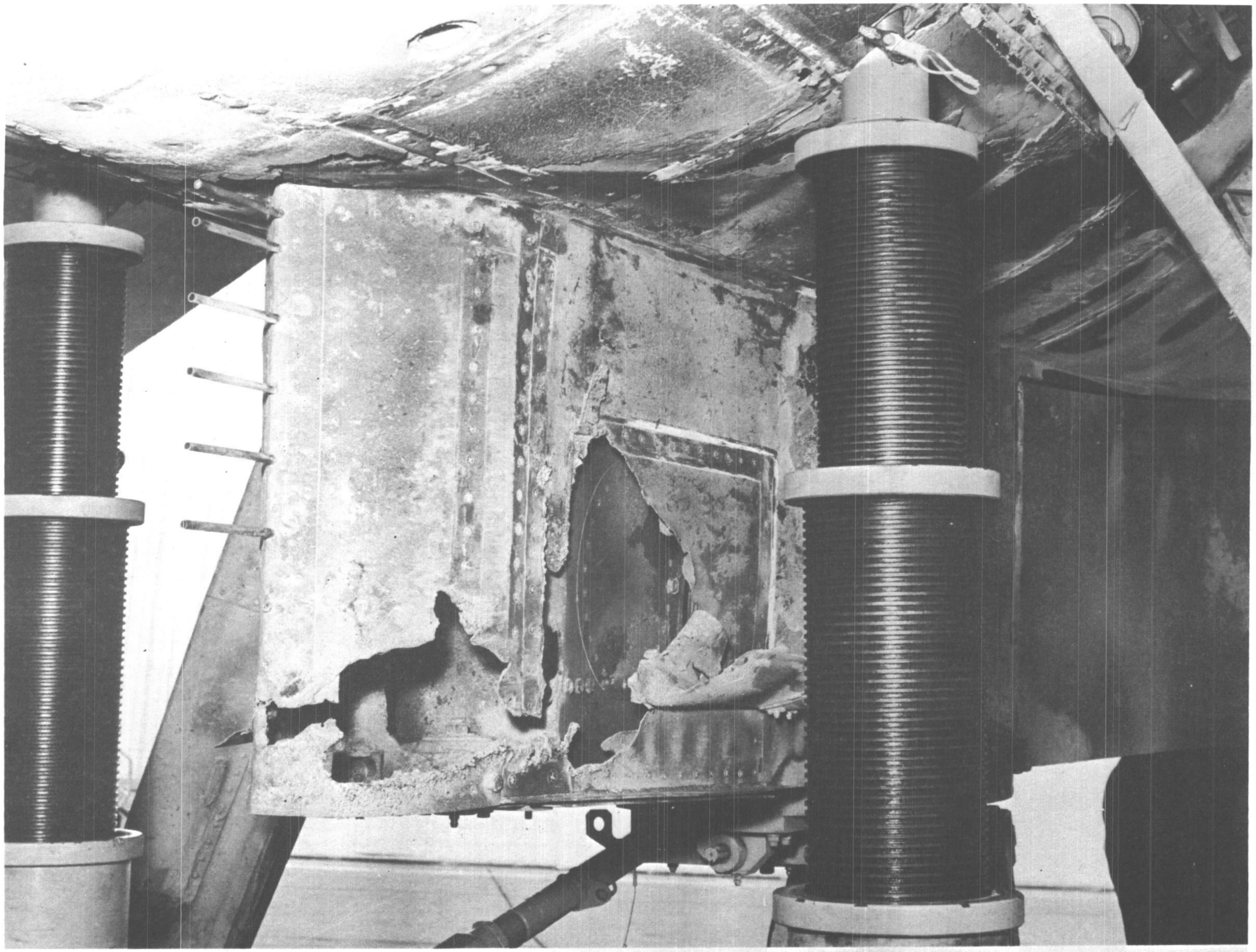

Figure III-29 Modified Ventral Fin Left Side, Post Mach 6.7 Flight

Flight Research Center
Edwards, California

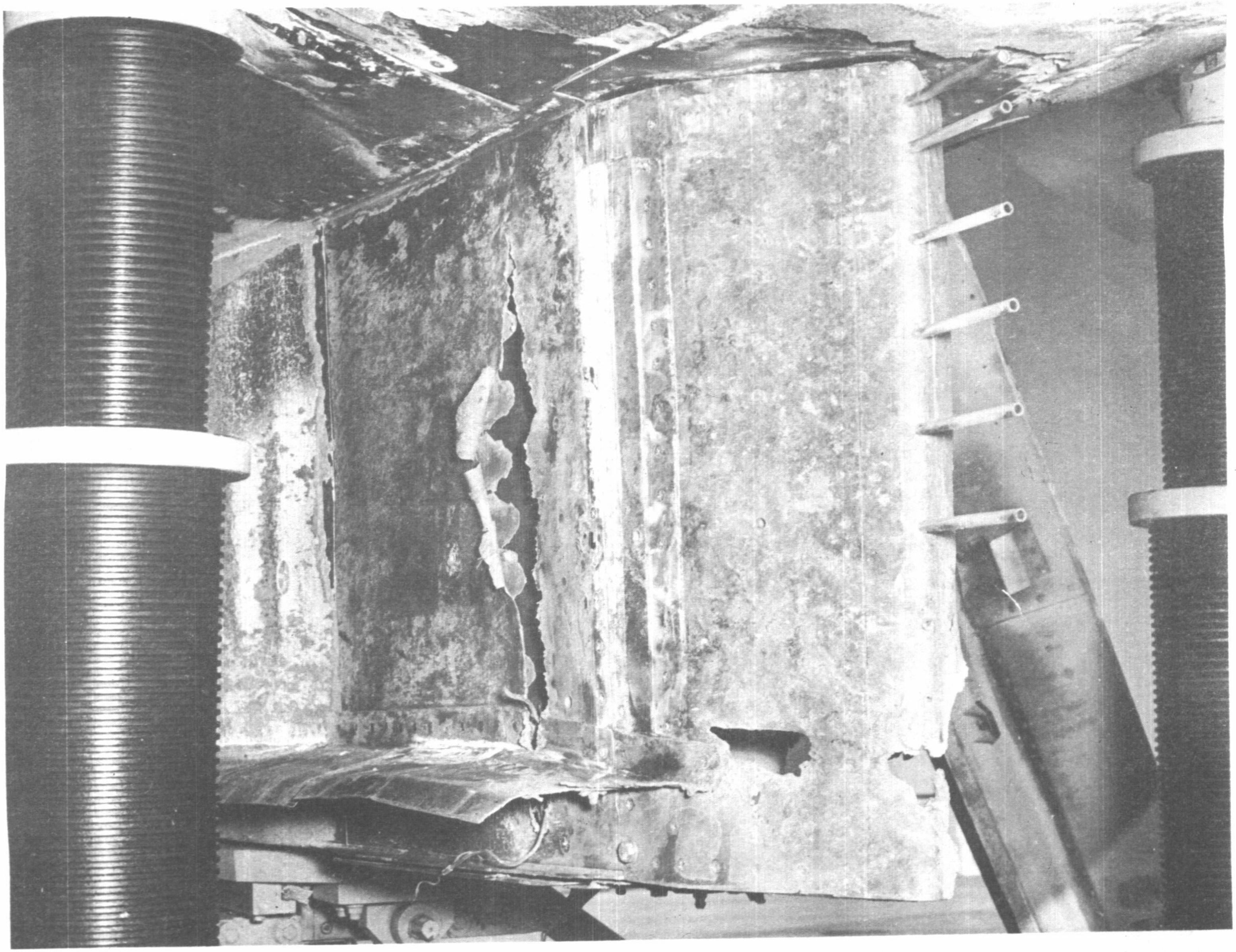

Figure III-30 Modified Ventral Fin Right Side, Post Mach 6.7 Flight

Flight Research Center
Edwards, California

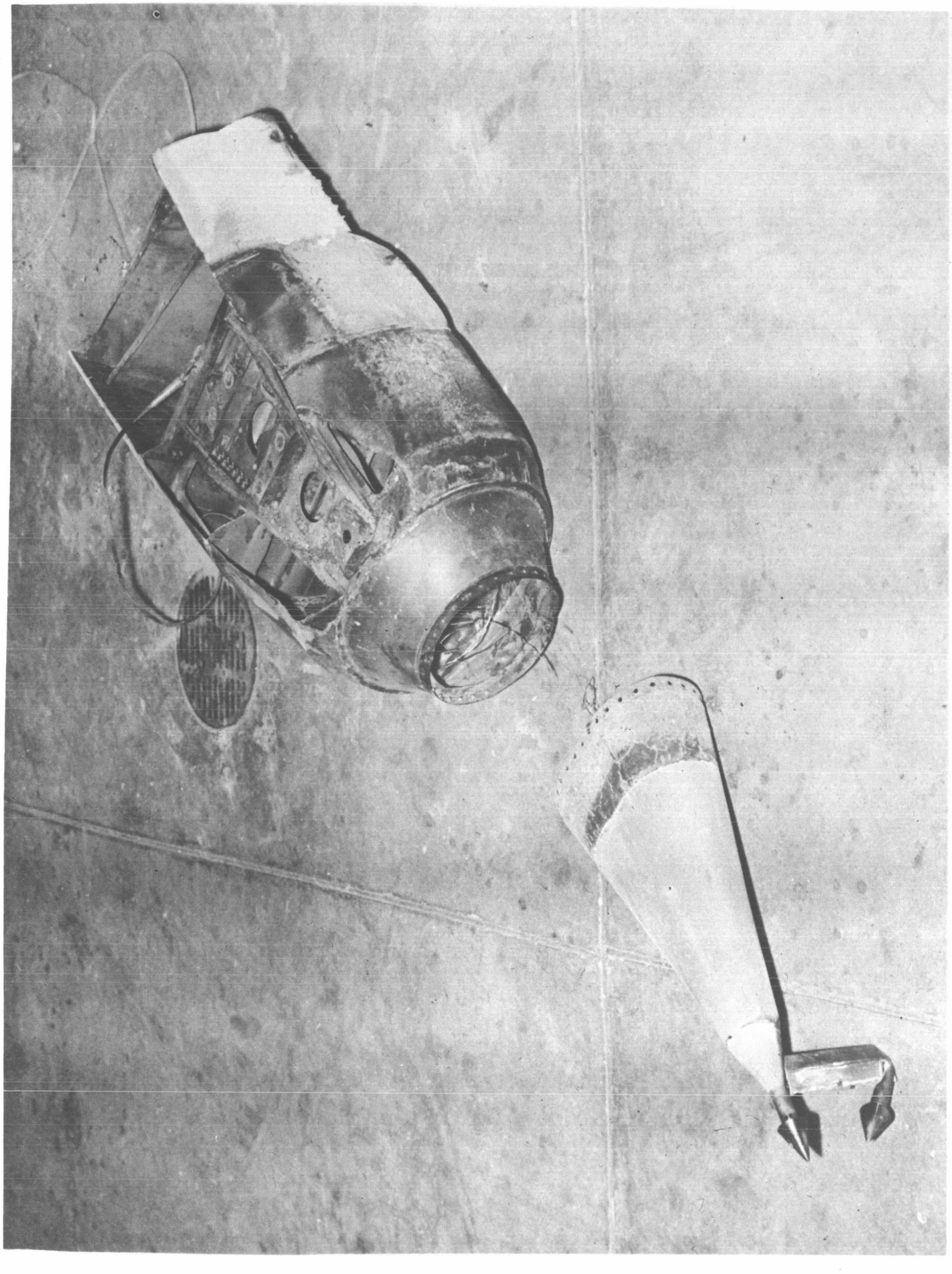

Flight Research Center
Edwards, California

Figure III-31 Dummy Ramjet Assembly, Post Mach 6.7 Flight

IV. FLIGHT TEST DATA ANALYSIS

The availability of airborne instrumentation data from the two test flights permitted the visual and physical evaluation of ablator performance to be supplemented by analytical correlation of thermal response. This report section documents the available data and defines the methods employed to validate the predictability of the thermal protection system performance.

A. Data Analysis

Fifteen (15) representative vehicle locations were chosen for analytical correlation of ablator performance. NASA provided the pertinent trajectory parameters for the flights and measured skin temperature histories and calculated heating rate data for as many of these locations as possible and numerous other areas of the aircraft. The locations for the points and the available flight test data are given in Table IV-1.

1. Preparation - The as received heating profiles were "cold wall" values at a 0°Fahrenheit base temperature. The computational programs available at Martin Marietta for ablator performance analysis require input of "cold wall" heating rates to a 0°Rankine base temperature. The information received for the correlation locations was, therefore, converted to the new base temperature by the relationship

$$\dot{q}_R = \frac{H_R}{H_R - H_{0^{\circ}F}} \times \dot{q}_F$$

and new total inputs were determined.

Another conversion operation was required for the received heating data in the area of the vehicle leading edges. The original information had been calculated to the skin line contour of the aircraft. Addition of the molded ablator details increased the effective leading edge radius so that NASA data was adjusted by the relationship

$$\dot{q}_A = \sqrt{\frac{R_M}{R_A}}\ \dot{q}_M$$

and the total heat load reduced accordingly.

Table IV-1 shows the designation and location for the fifteen points chosen for performance analysis. As seen in the table, flight data was not available for all of the locations. Where possible, adjacent thermocouple information was employed for the analytical correlation.

Ablator measurements were taken at the chosen vehicle locations after the mach 6.7 flight. These are presented in Table III-1 and provide total, char and virgin thickness at each location. In some instances, thickness information was available for the ablator prior to flight.

2. Analysis Methods - Thermal analysis of the ablator performance was accomplished by the use of the T-CAP-III and T-CAP-IV transient, charring ablator, digital computer programs. Both employ the

analytical model described below; however, T-CAP-III performs a one dimensional analysis in the ablator layer while the T-CAP-IV program has three dimensional capability.

The analytical model used by these programs consists of a virgin plastic layer, a pyrolysis zone, a char layer and where applicable, a melt layer of ablator over a nonablative substrate. For purposes of this performance correlation, in the sake of economy and speed, only one dimensional analyses were conducted except for one leading edge location where a two dimensional analysis was conducted. The models utilized in the correlation runs are shown in Figure IV-1.

Structural element thicknesses were the local skin gages, and no equivalent thermal mass was utilized to approximate the non-symmetrical substructure. The ablator thicknesses in Table III-1 were used for sizing the ablator element. In leading edge areas, preflight measurements were used where possible since the ablator tends to swell somewhat on heating. No such dimensions were available for the surface locations, but the thin ablator layers tended to minimize the affects of material growth.

B. Performance Correlations

Analysis of the ablator models for the test points of the vehicle yielded two types of performance data. Temperature histories of the substrate elements were available and the final degradation distributions through the ablator elements were determined. Calculated temperature responses were plotted along with the measured profiles for each point. These are shown in Figures II-2, 4, 5, 7, 8, 10, 11 and 13 for the Mach 5.0 flight, and in Figures IV-14, 16, 17, 19, 20, 22, 23, 24 and 26 for the Mach 6.7 mission.

The calculated degradation dimensions are tabulated with similar measurements obtained from the vehicle after the flight. This comparison is shown in Table IV-2.

C. Interpretation of Results

Comparisons of the calculated and observed temperature responses over the vehicle reflect less than perfect predictability. The factors which influence analytical results and reduce the degree of correlation obtainable are presented in the following sections along with the interpretations of the actual results.

1. Surface Areas - Peak temperature predictions were, in all cases higher than the measured results. This conservatism in the analysis is attributable to a number of factors.

The three dimensional affects are probably the most significant. The simplified model does not account for the additional presence of internal or back-up structure to the skin and its orientation with respect to the thermocouple location. This additional thermal mass becomes increasingly important as the flight progresses and lateral heat transfer within the actual unsymmetrical structure increases.

The adiabatic back wall constraint imposed on the model's structure element also contributes to peak temperature overestimation. Good simulation of the actual structural cooling by radiation or local convection is difficult to achieve for a number of reasons. Actual total emissivities and view factors for the structure are complicated relationships and vary for each area of the vehicle. The conditions of internal radiation range from approximate parallel plate interchange in the wing, stabilizer and tail areas to near radiation to infinity conditions in locations visible to the cryogenic tankage.

To obtain some estimation of the order of magnitude of these effects, the data for T/C 09001 were rerun with an artificial emissivity of .5 assigned to the structure element. The resultant element temperature prediction is shown in Figure IV-16. It is not intended to be representative of the actual conditions at the point, but only serves to indicate the influence of the analytical simulation simplification.

Disparity of calculated and observed results was also attributable to such other factors as: 1) error in measuring the ablator thickness, 2) accuracy of the calculated heating, and 3) selection of a surface emissivity for the ablator element.

Uncertainty associated with the last item is attributable to the presence of the wear layer over the ablator. The analyses were run using the MA-25s emissivity values, but for many of the locations the wear layer was intact or only partially degraded following the flight. Although some data is available for the emissivity of the DC90-090 material over ablator, and it is considerably higher than the bare MA-25s, no information exists on its variance as the material degrades. Two locations of the vehicle were selected where the wear layer was apparently unaffected during the flight. These were re-analyzed using the emissivity of the DC90-090 on the surface of the ablator element. The results are shown in Figures II-16 and 17 and reflect a cooling of the structure element.

Examination of the figures reveals a reasonably good agreement of the temperature gradients during the early and late stages of the mission. These are the areas in which actual ablator performance is the dominant factor. In the mid-portion of the analysis, the various uncertainties noted previously become more influential, and decrease the accuracy of the predictions. As can be expected, the influence of these factors is noticeable earlier in the higher heating Mach 6.7 mission.

The analysis of the Mach 5.0 data was performed primarily to determine if pre-charring affects of the ablator should be considered when making the Mach 6.7 analytical studies. The amount of thermal degradation from the first exposure was not significant, and all analysis of the Mach 6.7 flight data assumed a completely virgin ablator layer.

2. Leading Edge Areas - The flight data analyses for the leading edge areas were conducted using the one dimensional wedge model of Figure IV-1 to approximate the actual two dimensional case. The stagnation heating was applied to the whole surface of the ablator element which does not account for the variation in heating around the leading edge radius. This model should predict lower than actual structure temperatures because of the conservative stagnation area and heat sink mass utilized. The results of these calculations are shown in Figures IV-3, 6, 9, 12, 15, 18, 21 and 25.

The degree of temperature correlation achieved varied with the location, but reasonably good predictability was obtained except for the wing leading edge. This section of the aircraft employs an extruded leading edge piece rather than the formed sheet metal used at the other locations. The simplified thermal model was, therefore, less representative of actual conditions.

A two dimensional analysis using the model shown in Figure IV-1 more closely approximates the actual thermal arrangement. In addition to more accurately accounting for the variations of ablator thickness and substrate thermal mass, the multiple element arrangement allows the use of the local heating input for each segment to simulate the heating variation over the leading edge area. The results of both the one dimensional and two dimensional analyses for the wing leading edge are shown in Figure IV-18.

The same sources of error, defined in the previous section, exist in the leading edge analyses.

D. Skin Temperature Distributions

The availability of measured temperature data in excess of that specified for ablator performance correlation permitted additional evaluation of the ablator system design. The peak temperatures observed for the various aircraft areas were plotted for each of the flights. These data are shown in Figures IV-27 through IV-30 for the upper and lower surfaces of the right wing, the upper surface of the right horizontal stabilizer, and the sides of the movable vertical tail. The peak temperatures and maximum delta T are tabulated in Table IV-3 .

The ablation system was designed to limit all areas of the aircraft to 600°F maximum temperature with the conservative assumptions of one dimensional heat flow and an adiabatic back face. Examination of these measured temperature distributions gives an indication of the gross effects of internal heat sinks, heat input variations and ablator thickness variations. For a perfect design the curves for each station should be smooth, less than 600°F (because these flights were less severe than the design case), and slope upward (increase in temperature for aft locations). To fully evaluate the measured temperature distributions as to conservatism or unconservatism, and cause of the perturbations from a smooth curve, it would be necessary to calculate the theoretical distributions. Of the selected fifteen (15) points for which analyses have been performed, three locations are applicable to these curves. Of these the upper wing surface appears to be unconservative based on the calculated peak temperature of 425°F at 27 percent chord and station 84 compared to the surrounding measured temperatures. The fact that the measured temperature at this particular location is less than the calculation shows the need for a more thorough evaluation of the data than that of making a limited number of isolated comparisons. The greater degree of perturbation from a smooth curve for the upper wing data could be caused by small variations in the thickness of the thin ablator coating (.015 inches) in this area. Density of the ablator is probably also a contributing factor since difficulty was encountered in applying a smooth coating in this region because of the limitations of available scaffolding. In any event additional thickness of ablative material should be applied in this region and more thorough analyses would most likely show that the ablator thickness could be reduced in most other areas.

TABLE IV-1

PERFORMANCE CORRELATION POINTS

X-15A-2 ABLATOR APPLICATION

POINT NO.	T/C DESIGNATION	AIRCRAFT AREA	LOCATING DIMENSIONS			HEATING DATA AVAILABLE FOR 2-52	HEATING DATA AVAILABLE FOR 2-53	TEMP. DATA AVAILABLE FOR 2-52	TEMP. DATA AVAILABLE FOR 2-53
1	04017	FUSELAGE	STA. 72.5	X = 6.0 FT.	$\phi = 0°$	YES	YES	YES	YES
2	05019	↕	STA. 87.5	X = 7.6 FT.	$\phi = 180°$	YES	YES	YES	YES
3	09001	↕	STA. 335	X = 28.3 FT.	$\phi = 30°$	YES	YES	YES	YES
4	T20-22	↕	STA. 340+	X = 29.9 FT.	$\phi = 225°$	①	①	①	①
5	TF2T	↕	STA. 20	X = 1.6 FT.	$\phi = 135°$	NO	NO	NO	NO
6	TF18M	FUSELAGE	STA. 240	X = 20.4 FT.	$\phi = 90°$	NO	NO	YES	YES
7	13050	WING	STA. 84	L.E.	-	YES	YES	YES	YES
8	13057	WING ②	STA. 84	X = 2.0 FT.	27% CHORD	YES	YES	YES	YES
9	13076	WING ③	STA. 84	X = 2.0 FT.	27% CHORD	YES	YES	YES	YES
10	15017	HOR. STAB.	BUTT 75.5	L.E.	-	YES	YES	YES	YES
11	15018	HOR. STAB. ②	BUTT 75.5	X = 0.8 FT.	19% CHORD	YES	YES	NO	NO
12	15025	HOR. STAB. ③	BUTT 75.5	X = 0.8 FT.	19% CHORD	YES	YES	YES	NO
13	16018	VERT. TAIL	WL 35.5	X = 8.9 FT	90% CHORD	NO	YES	YES	YES
14	16020	VERT. TAIL	WL 62	L.E.	-	YES	YES	YES	YES
15	16025	VERT. TAIL	WL 62	X = 2.1 FT	25% CHORD	YES	YES	YES	YES

① DATA FOR T/C 09005 USED
② UPPER SURFACE
③ LOWER SURFACE

TABLE IV- 2

ABLATOR DEGRADATION COMPARISONS

Loc.	MACH 5.0 FLIGHT						MACH 6.7 FLIGHT					
	Calculated Dimensions			Measured Dimensions			Calculated Dimensions			Measured Dimensions		
	Char	Pyrolysis	Total	Char	Pyrolysis	Total	Char	Pyrolysis	Total	Char	Pyrolysis	Total
TF2T	-	-	-	0	-	-	-	-	-	.050	-	.050
04017	0	0	0	0	-	-	.012	.073	.085	.086	-	.086
05019	.026	.044	.070	0	-	-	.102	.067	.169	.049	.187	.236
TF18M	-	-	-	0	-	-	-	-	-	0	0	0
09001	0	0	0	0	-	-	0	0	0	0	0	0
T20-22	0	0	0	0	-	-	0	0	0	0	0	0
13050	.080	.055	.135	.050	-	-	.217	.060	.277	.175	.094	.269
13057	0	0	0	0	-	-	0	0	0	0	0	0
13076	0	0	0	0	-	-	0	.076	.076	.042	-	.042
15017	.063	.053	.116	.055	-	-	.191	.066	.257	.147	.095	.242
15018	0	0	0	0	-	-	0	.039	.039	.062	-	.062
15025	0	0	0	0	-	-	0	.039	.039	0	0	0
16020	.077	.053	.130	.020	-	-	.219	.060	.279	.149	.129	.278
16025	0	0	0	0	-	-	0	.055	.055	.005	-	.005
16018	-	-	-	.020	-	-	.038	.067	.105	.075	.101	.176

TABLE IV-3

PEAK TEMPERATURE DATA

MACH 5.0 AND MACH 6.7 FLIGHTS

Aircraft Area	Flight	Ave. Max. Temp $\bar{T}$ (°R)	Temperature Increase
Lower Wing Surf.	M 5.0 M 6.7	667 768	101
Upper Wing Surf.	M 5.0 M 6.7	719 807	88
Upper Hor. Stab. Surf.	M 5.0 M 6.7	757 No data available	
WL 60, Vert. Tail	M 5.0 M 6.7	660 757	96
WL 80, Vert. Tail	M 5.0 M 6.7	720 No data available	

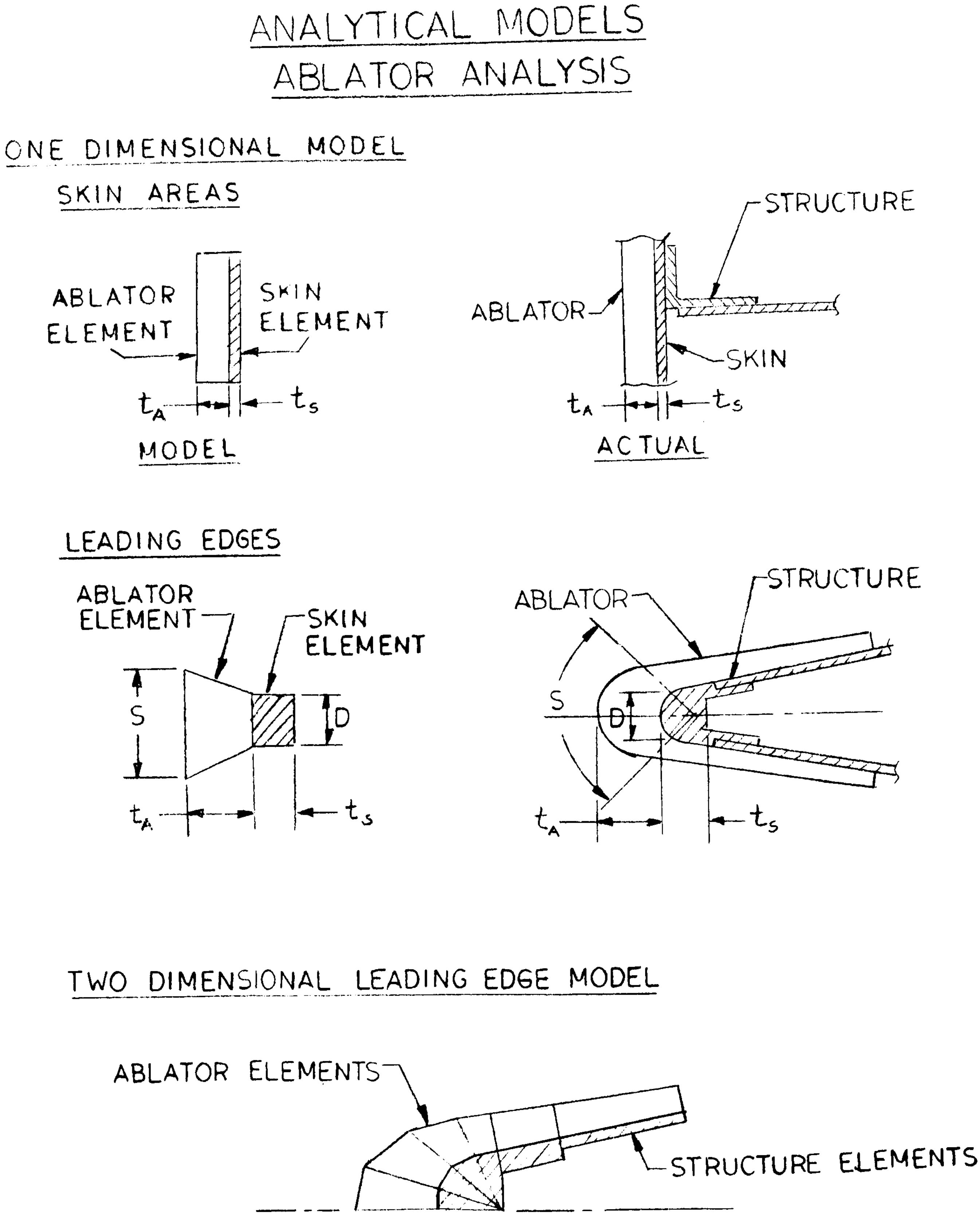
ANALYTICAL MODELS
ABLATOR ANALYSIS
ONE DIMENSIONAL MODEL
SKIN AREAS
ABLATOR ELEMENT
SKIN ELEMENT
t_A
t_s
MODEL
STRUCTURE
ABLATOR
SKIN
t_A
t_s
ACTUAL
LEADING EDGES
ABLATOR ELEMENT
SKIN ELEMENT
S
D
t_A
t_s
STRUCTURE
ABLATOR
S
D
t_A
t_s
TWO DIMENSIONAL LEADING EDGE MODEL
ABLATOR ELEMENTS
STRUCTURE ELEMENTS

Figure IV-1

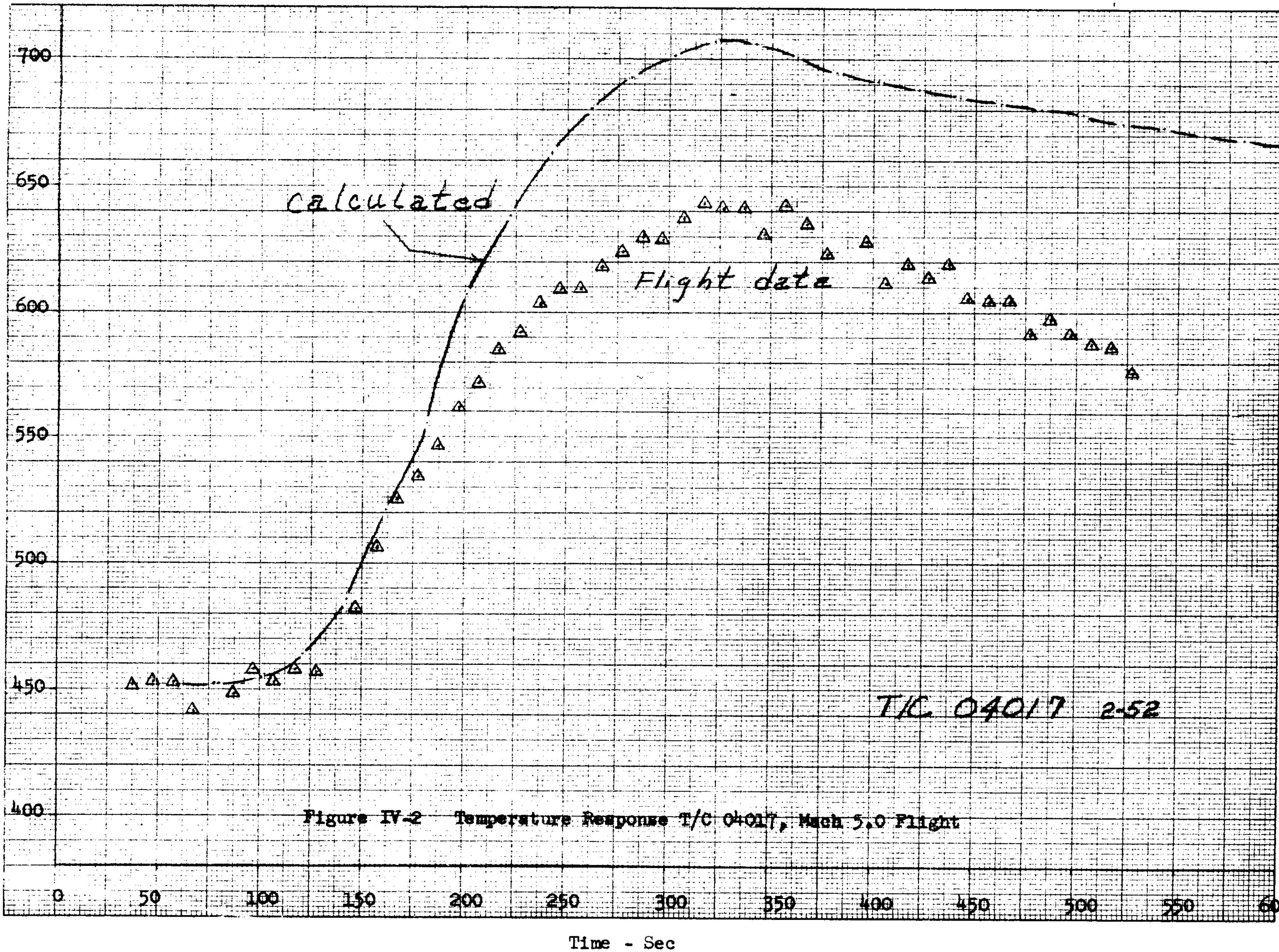

Figure IV-2 Temperature Response T/C 04017, Mach 5.0 Flight

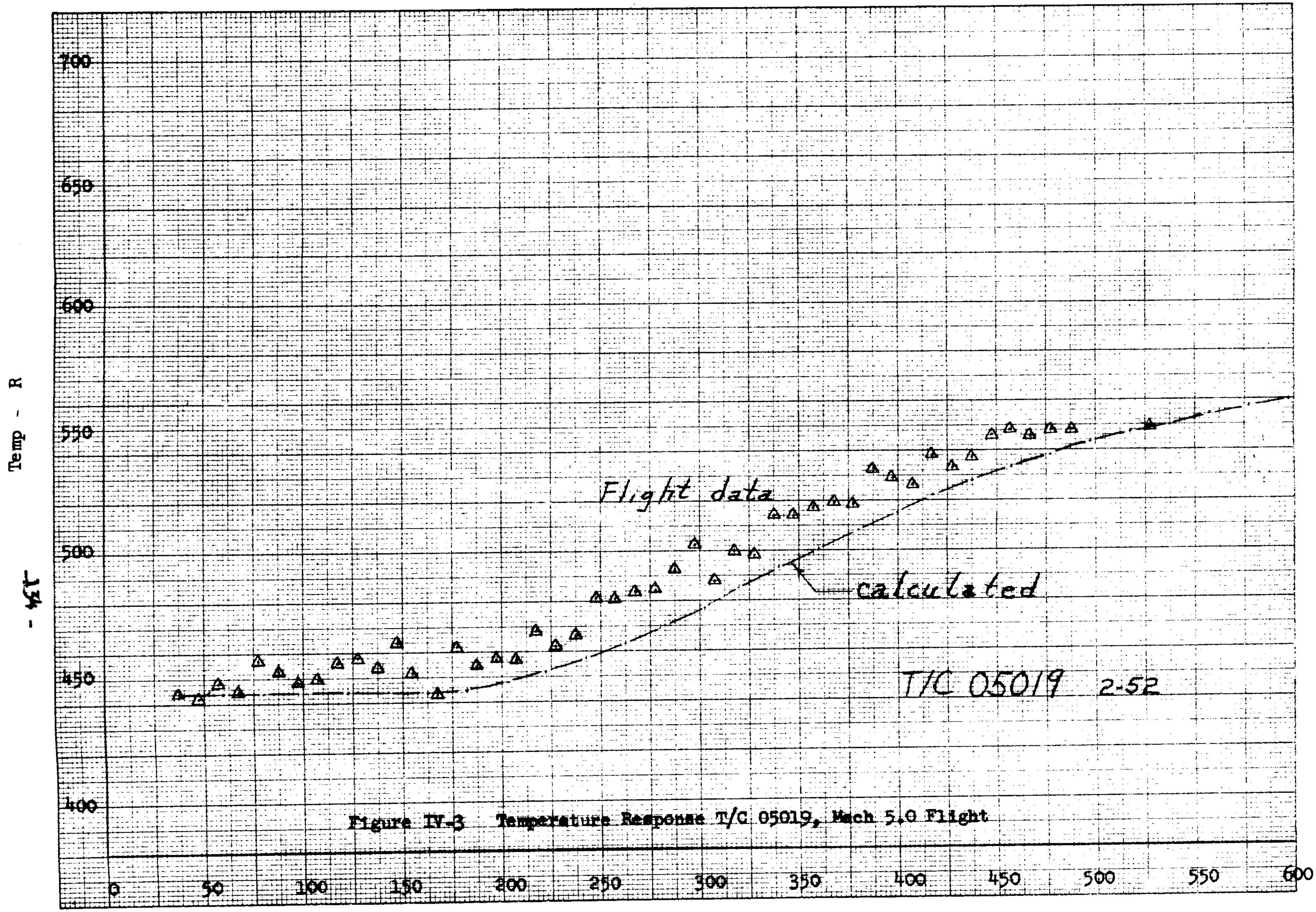

Figure IV-3 Temperature Response T/C 05019, Mach 5.0 Flight

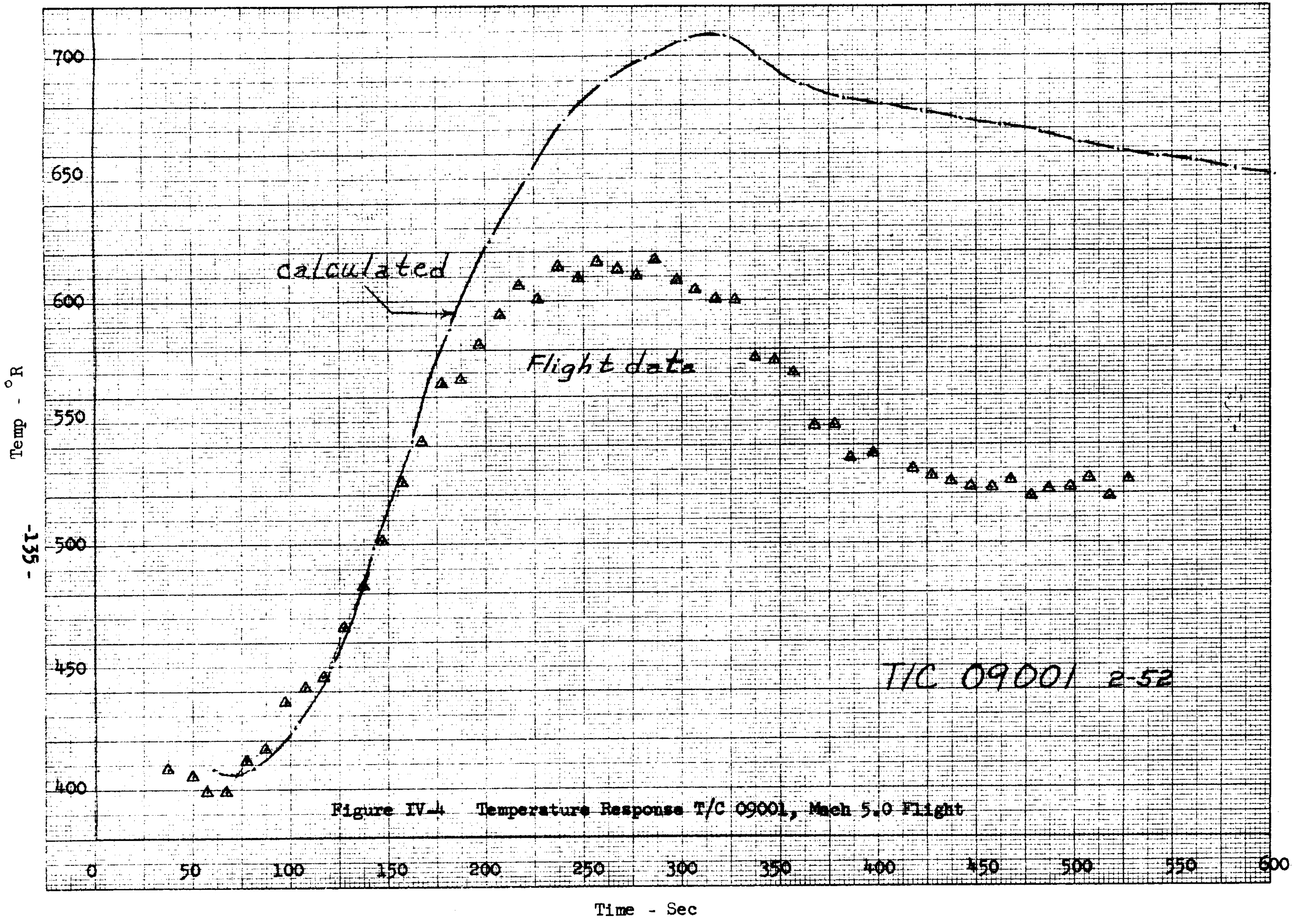

Figure IV-4 Temperature Response T/C 09001, Mach 5.0 Flight

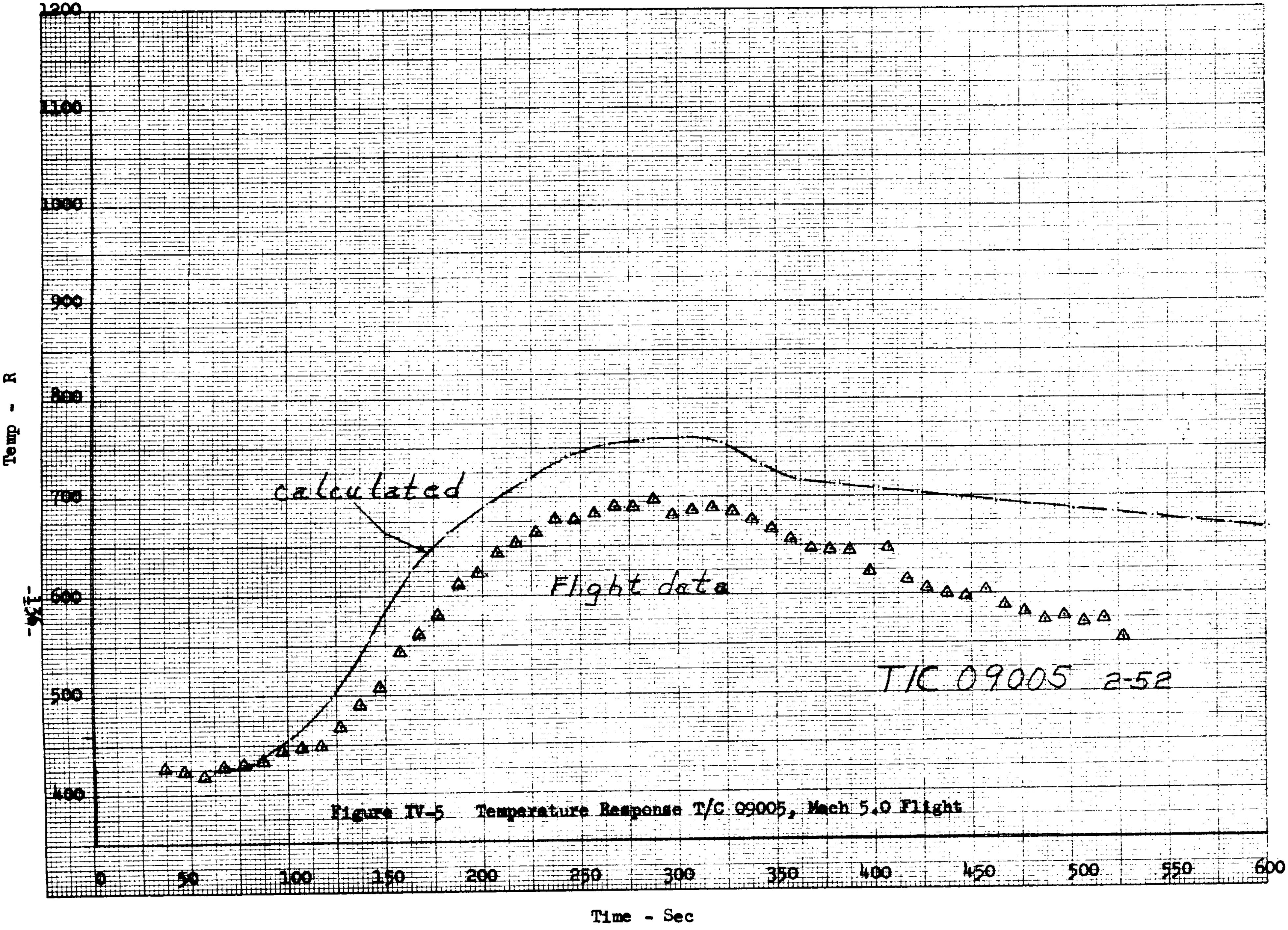

Figure IV-5 Temperature Response T/C 09005, Mach 5.0 Flight

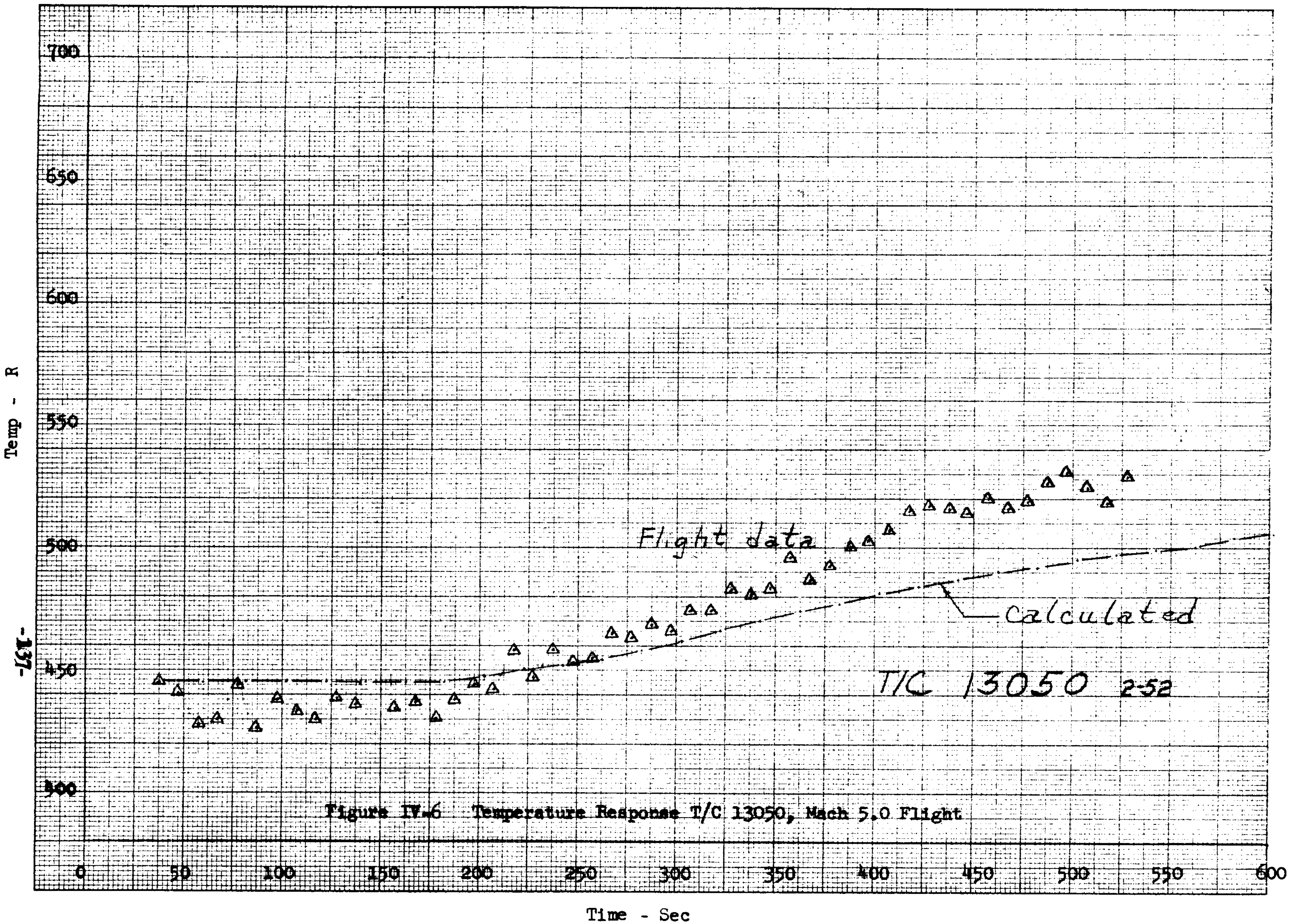

Figure IV-6 Temperature Response T/C 13050, Mach 5.0 Flight

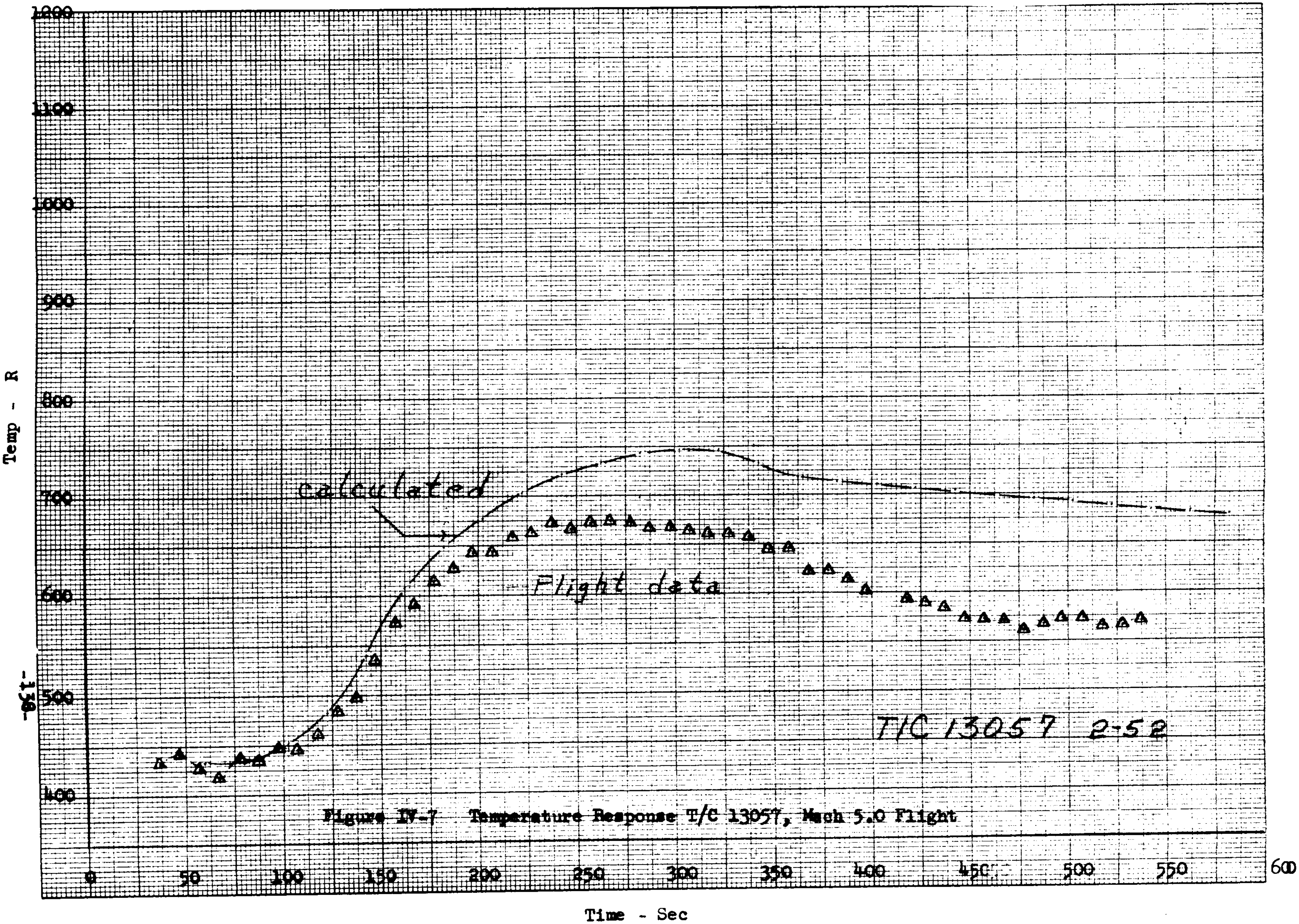

Figure IV-7 Temperature Response T/C 13057, Mach 5.0 Flight

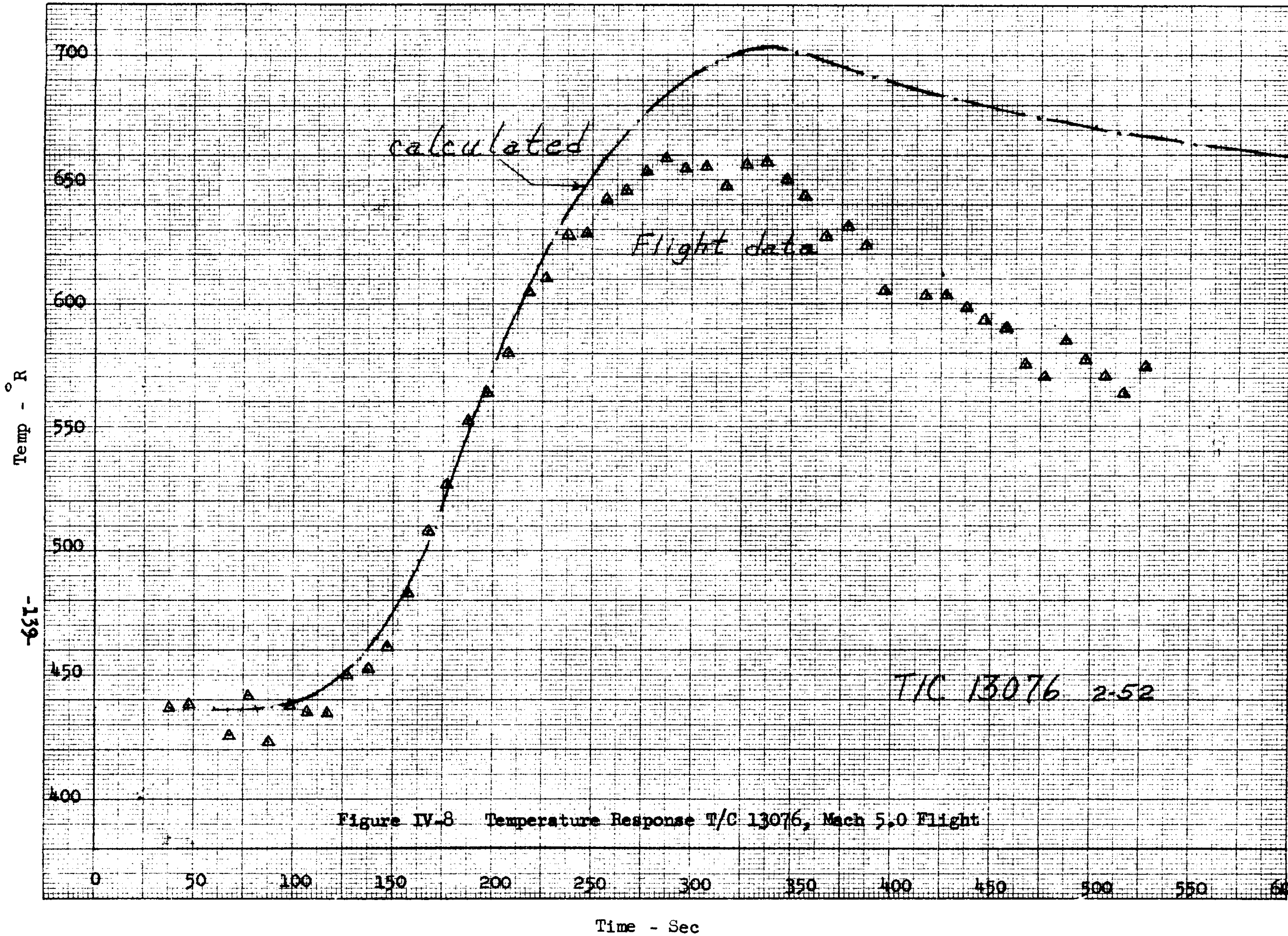

Figure IV-8 Temperature Response T/C 13076, Mach 5.0 Flight

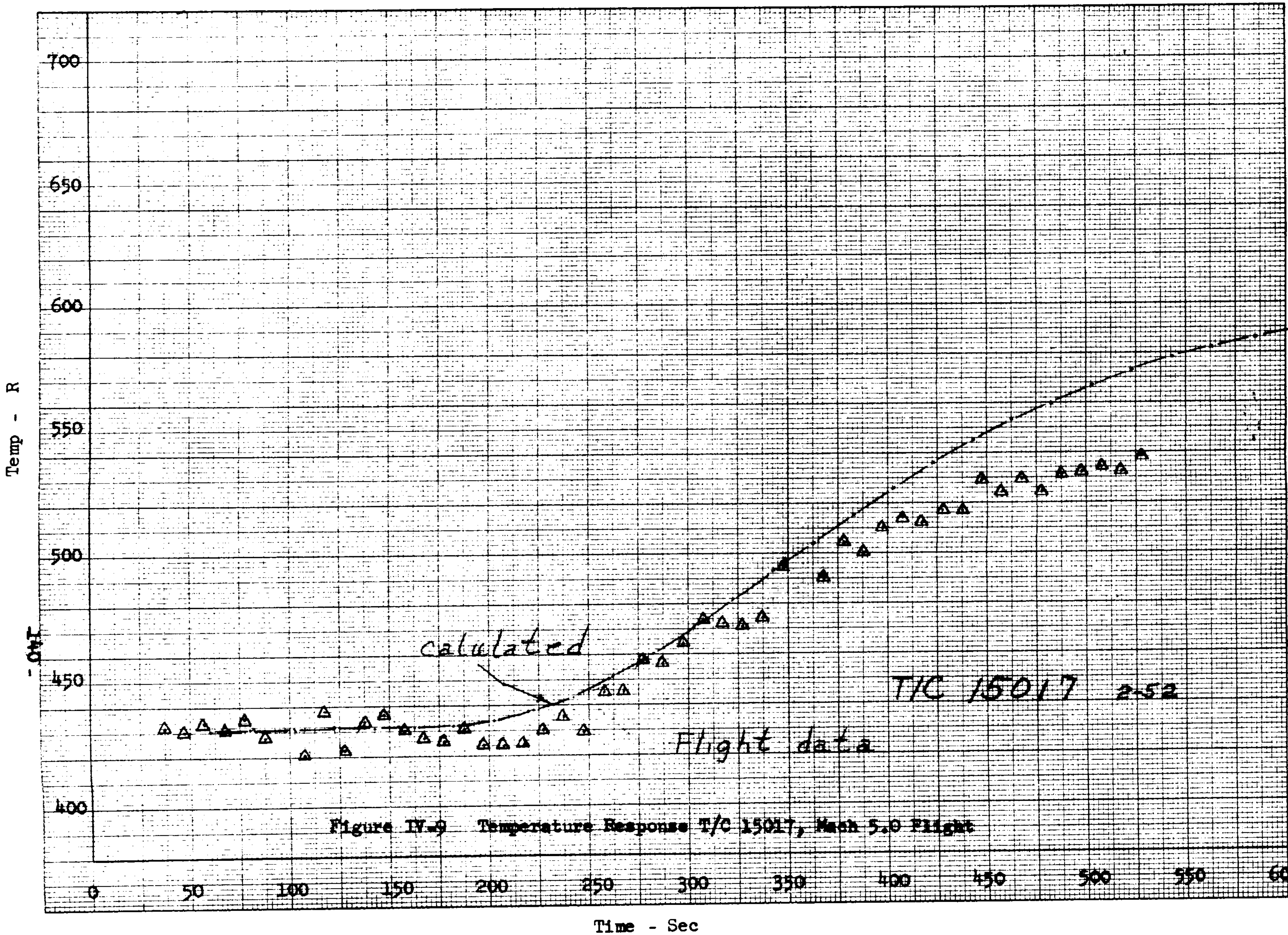

Figure IV-9 Temperature Response T/C 15017, Mach 5.0 Flight

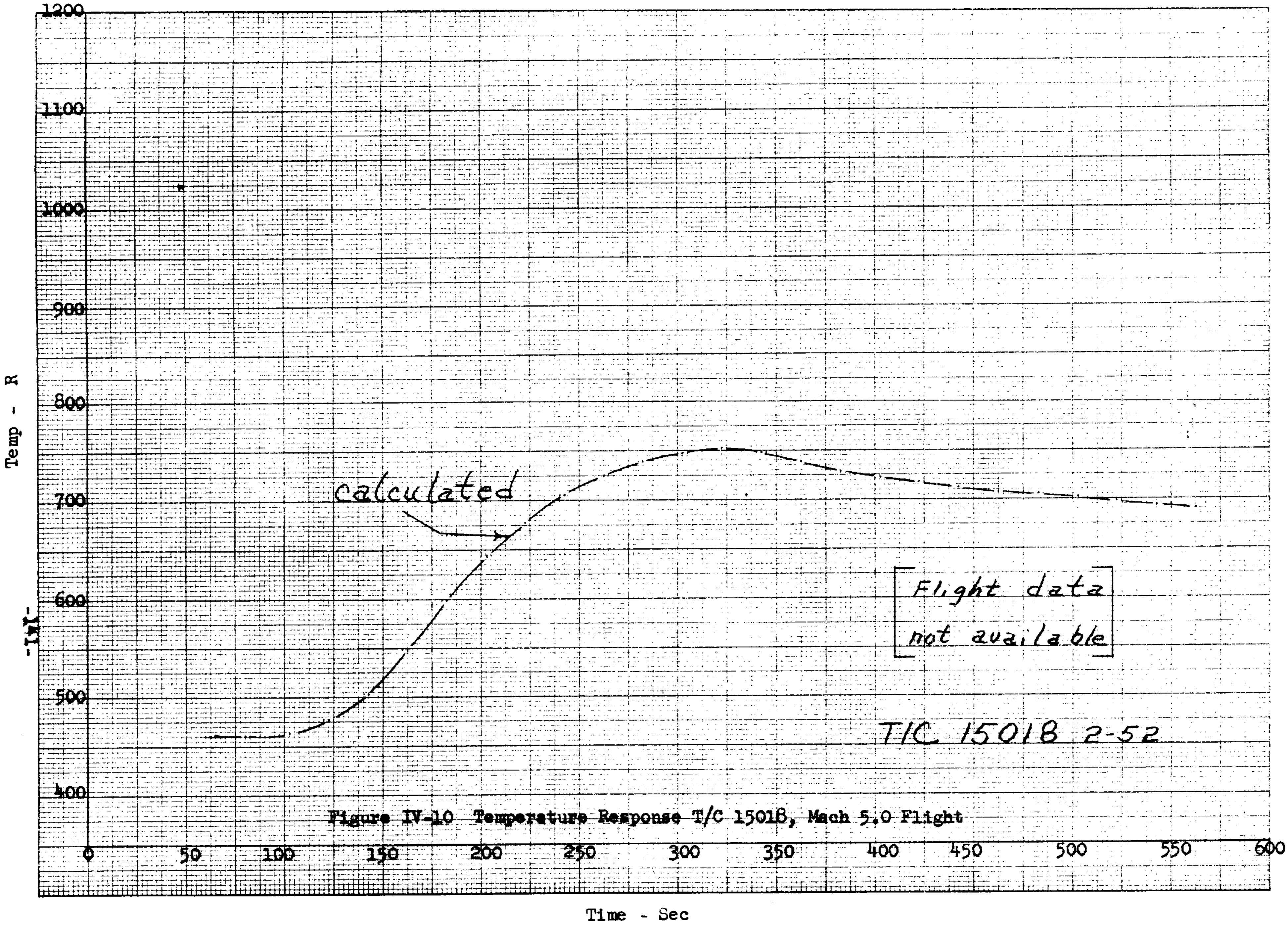

Figure IV-10 Temperature Response T/C 15018, Mach 5.0 Flight

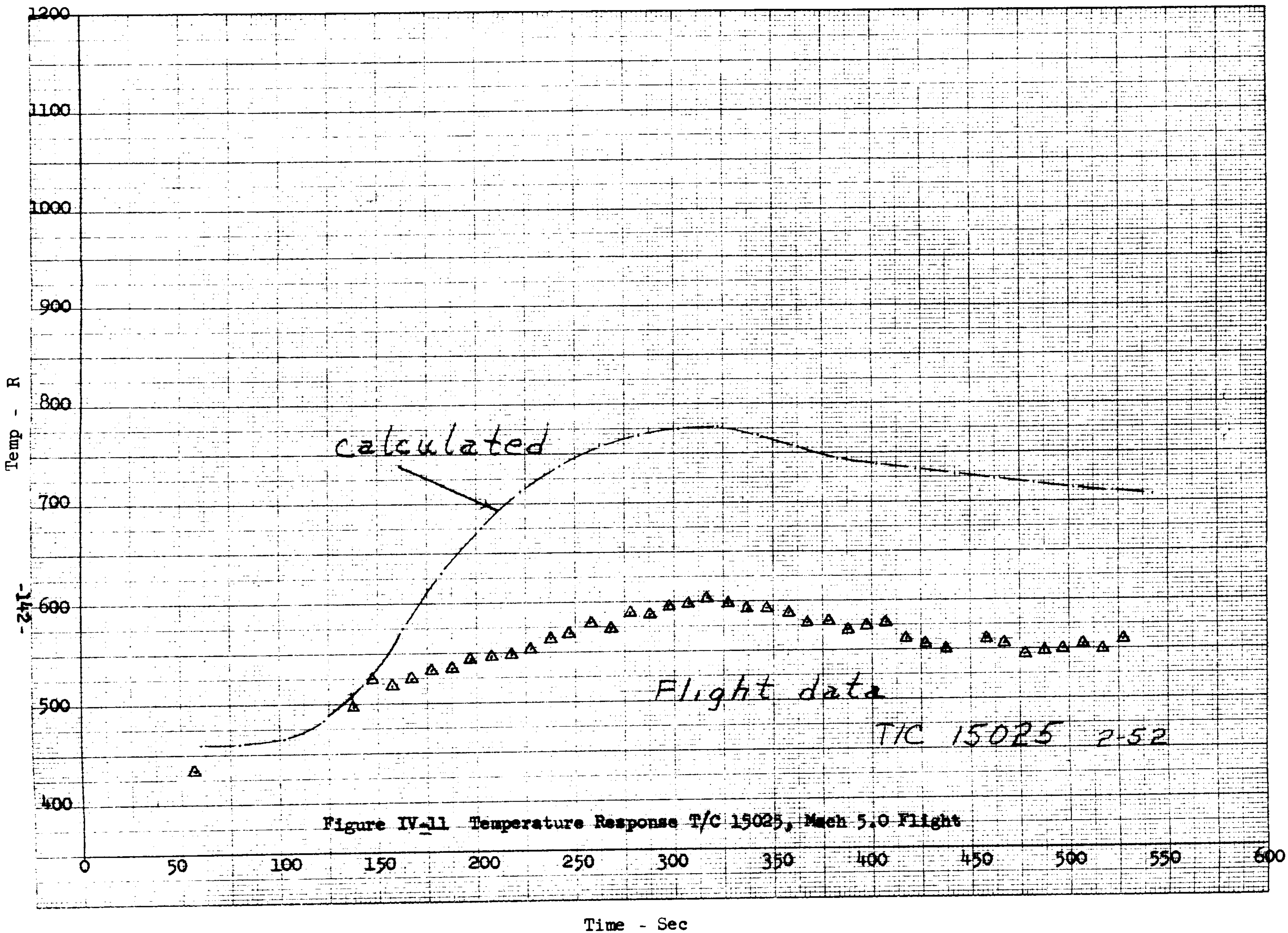

Figure IV-11 Temperature Response T/C 15025, Mach 5.0 Flight

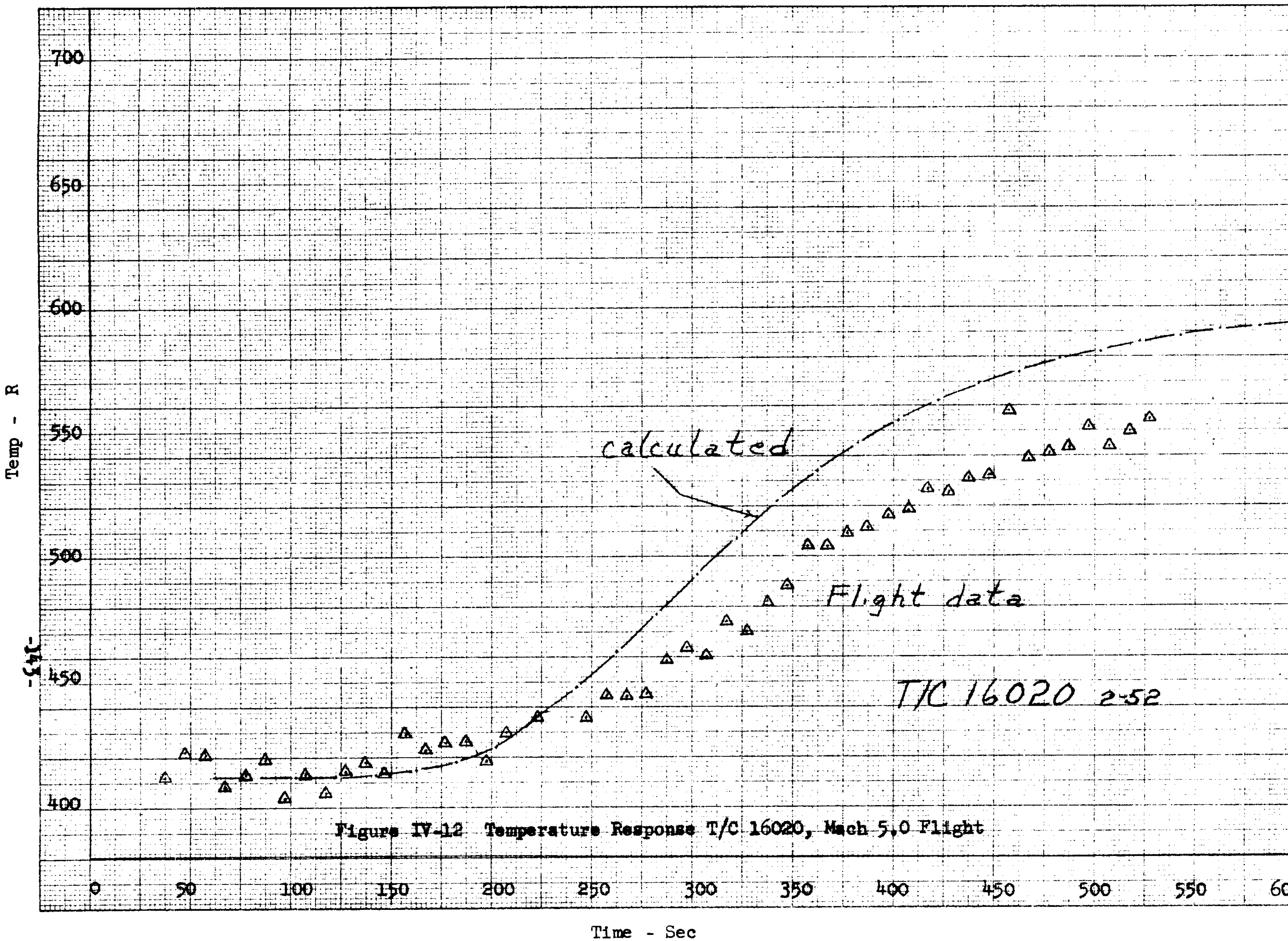

Figure IV-12 Temperature Response T/C 16020, Mach 5.0 Flight

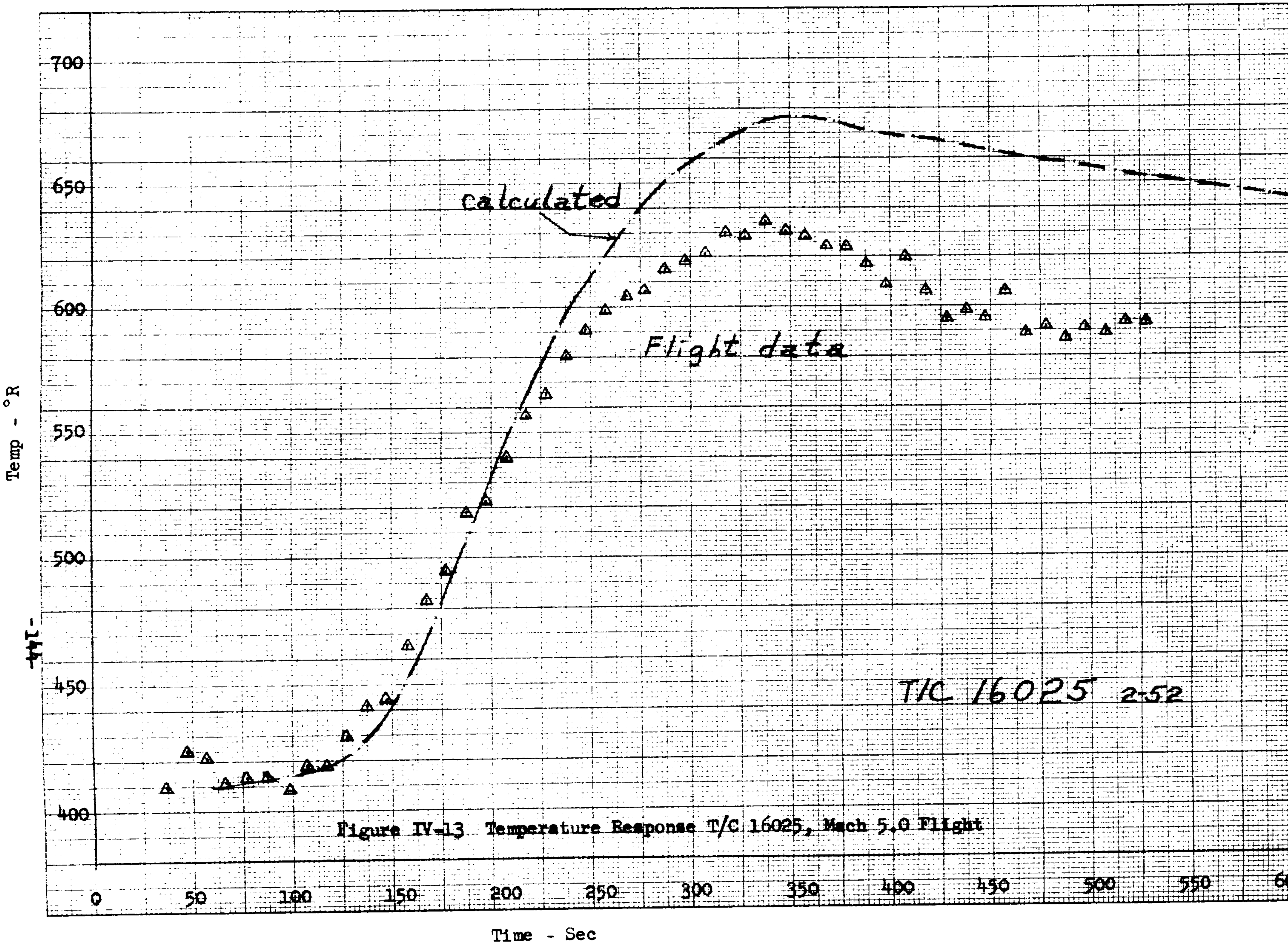

Figure IV-13 Temperature Response T/C 16025, Mach 5.0 Flight

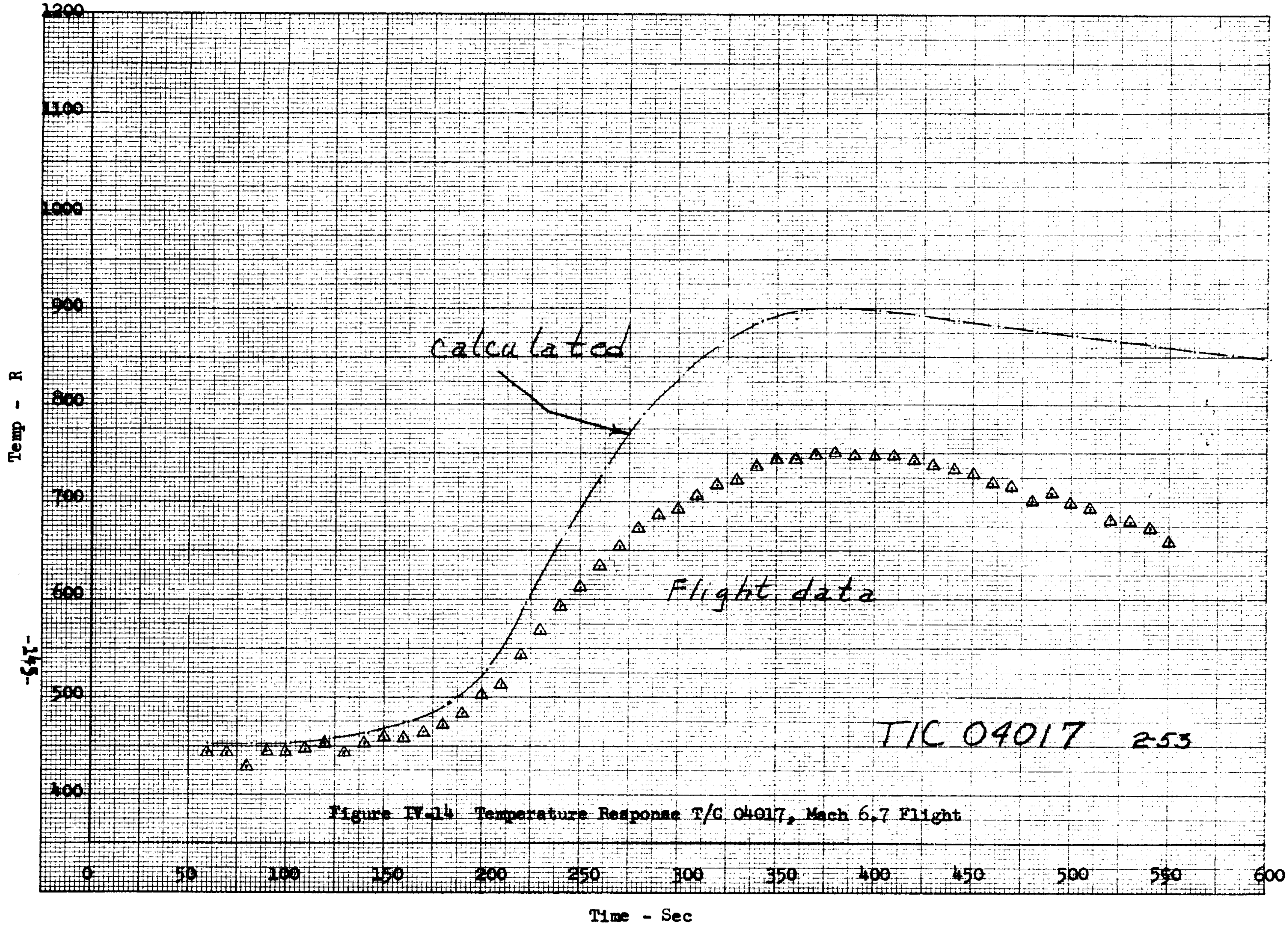

Figure IV-14 Temperature Response T/C 04017, Mach 6.7 Flight

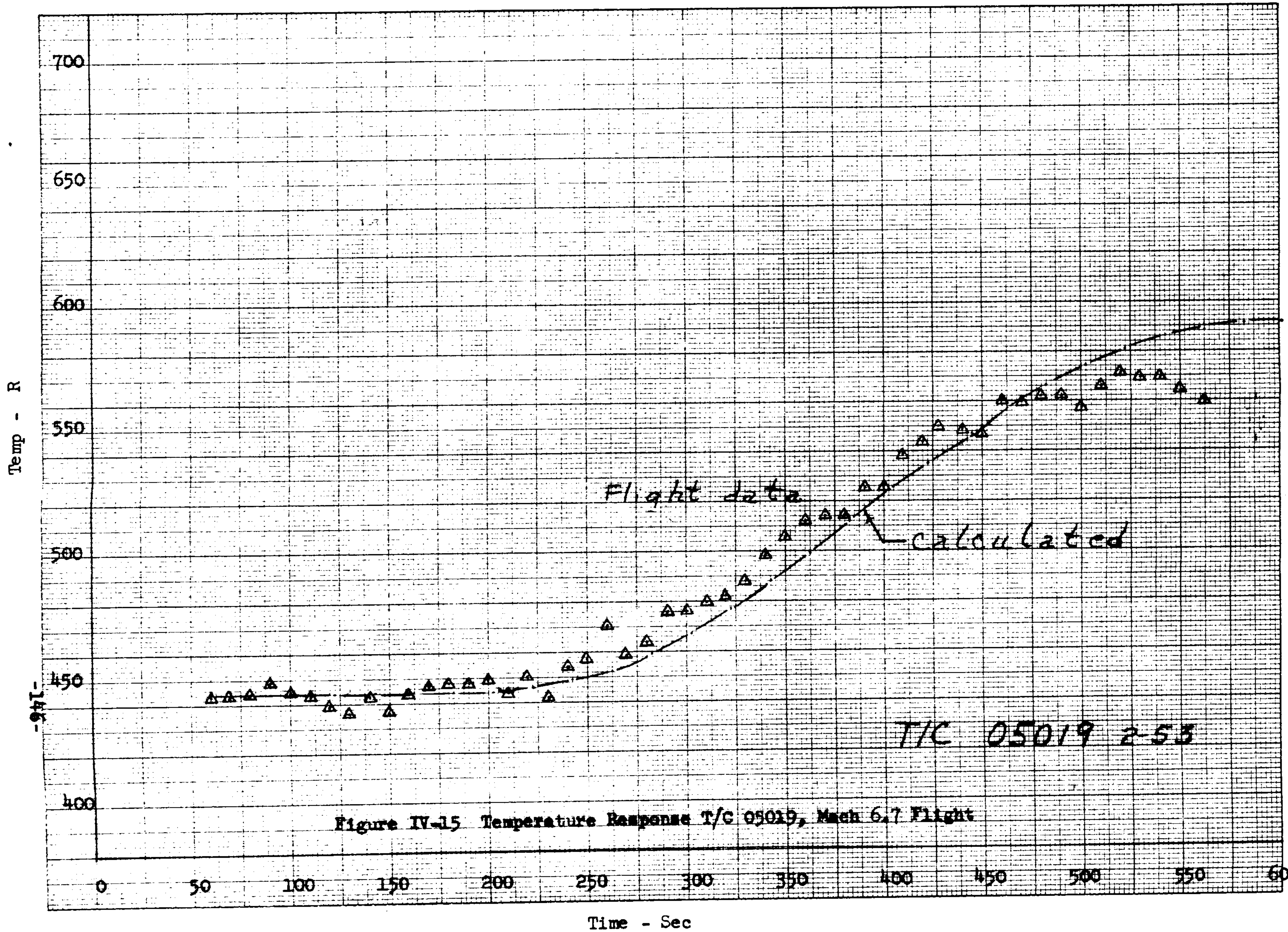

Figure IV-15 Temperature Response T/C 05019, Mach 6.7 Flight

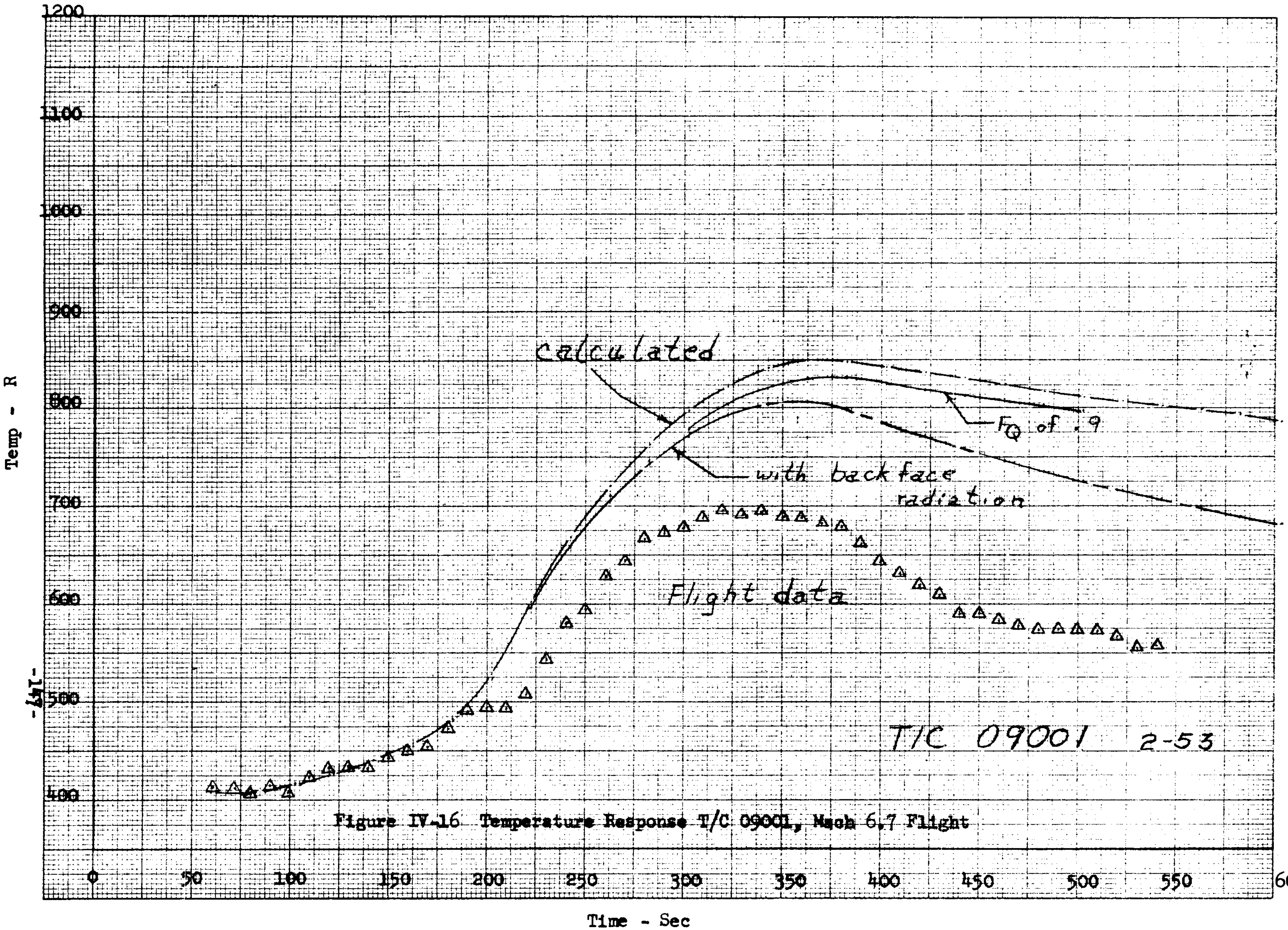

Figure IV-16 Temperature Response T/C 09001, Mach 6.7 Flight

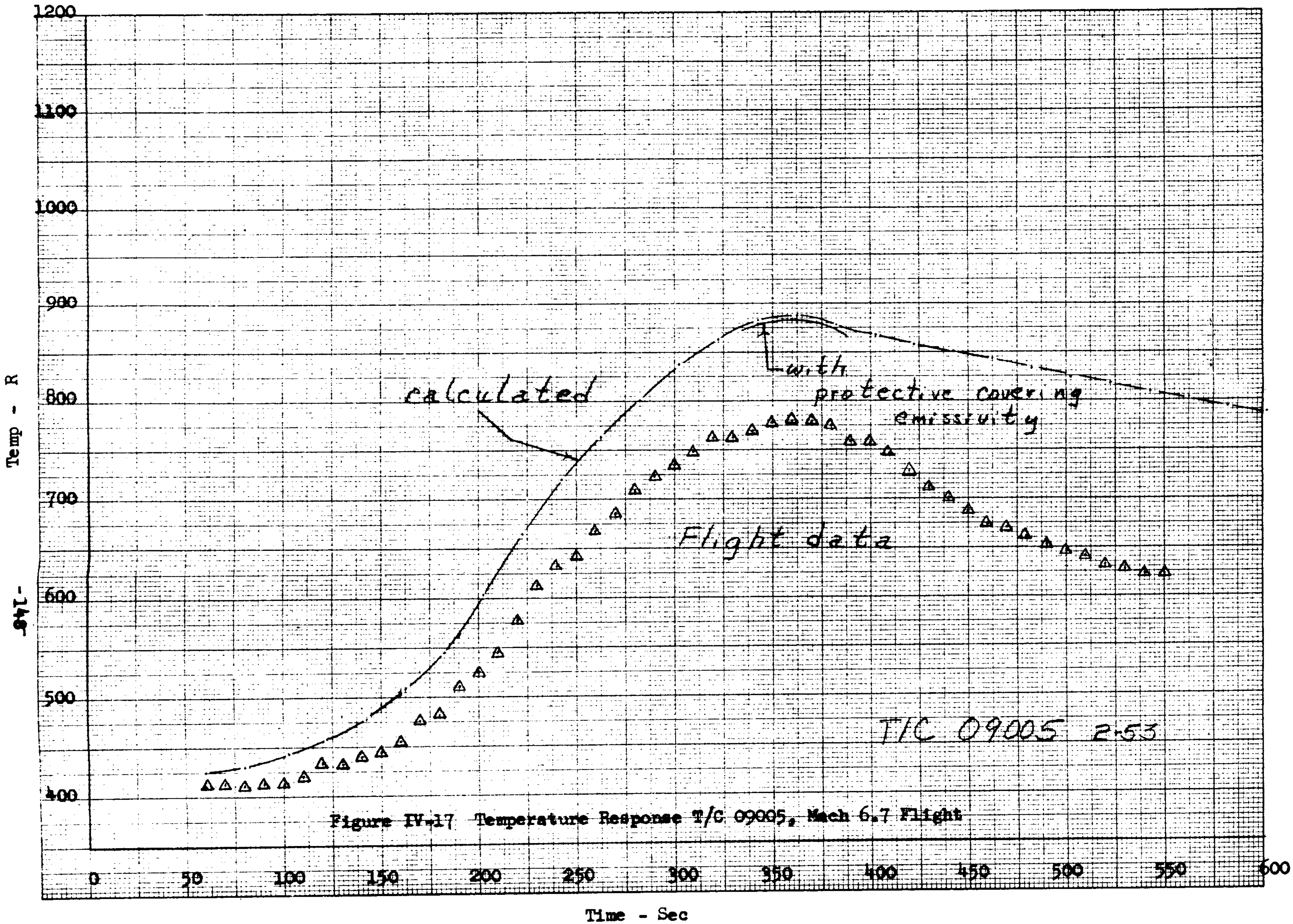

Figure IV-17 Temperature Response T/C 09005, Mach 6.7 Flight

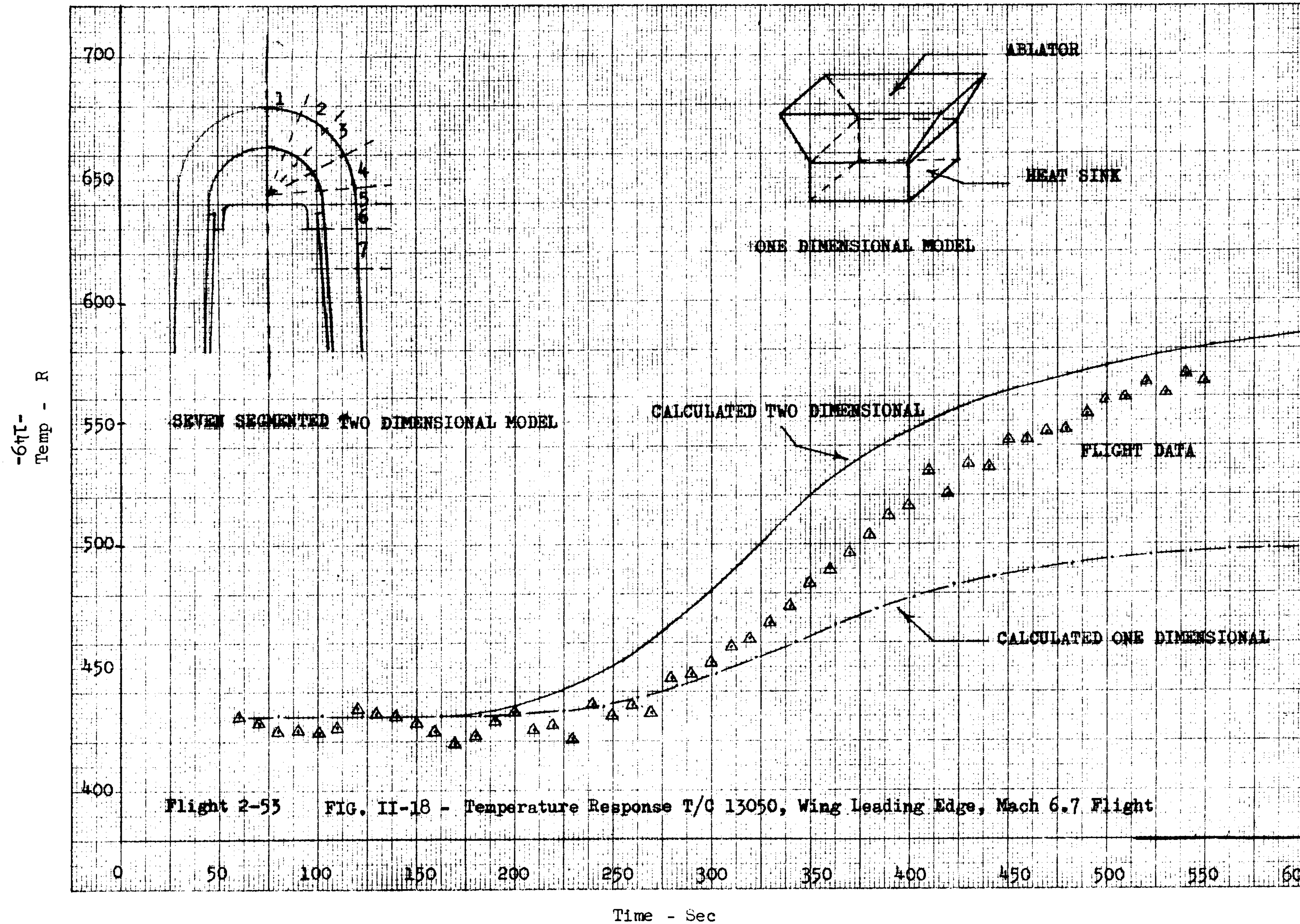

Flight 2-53 FIG. II-18 - Temperature Response T/C 13050, Wing Leading Edge, Mach 6.7 Flight

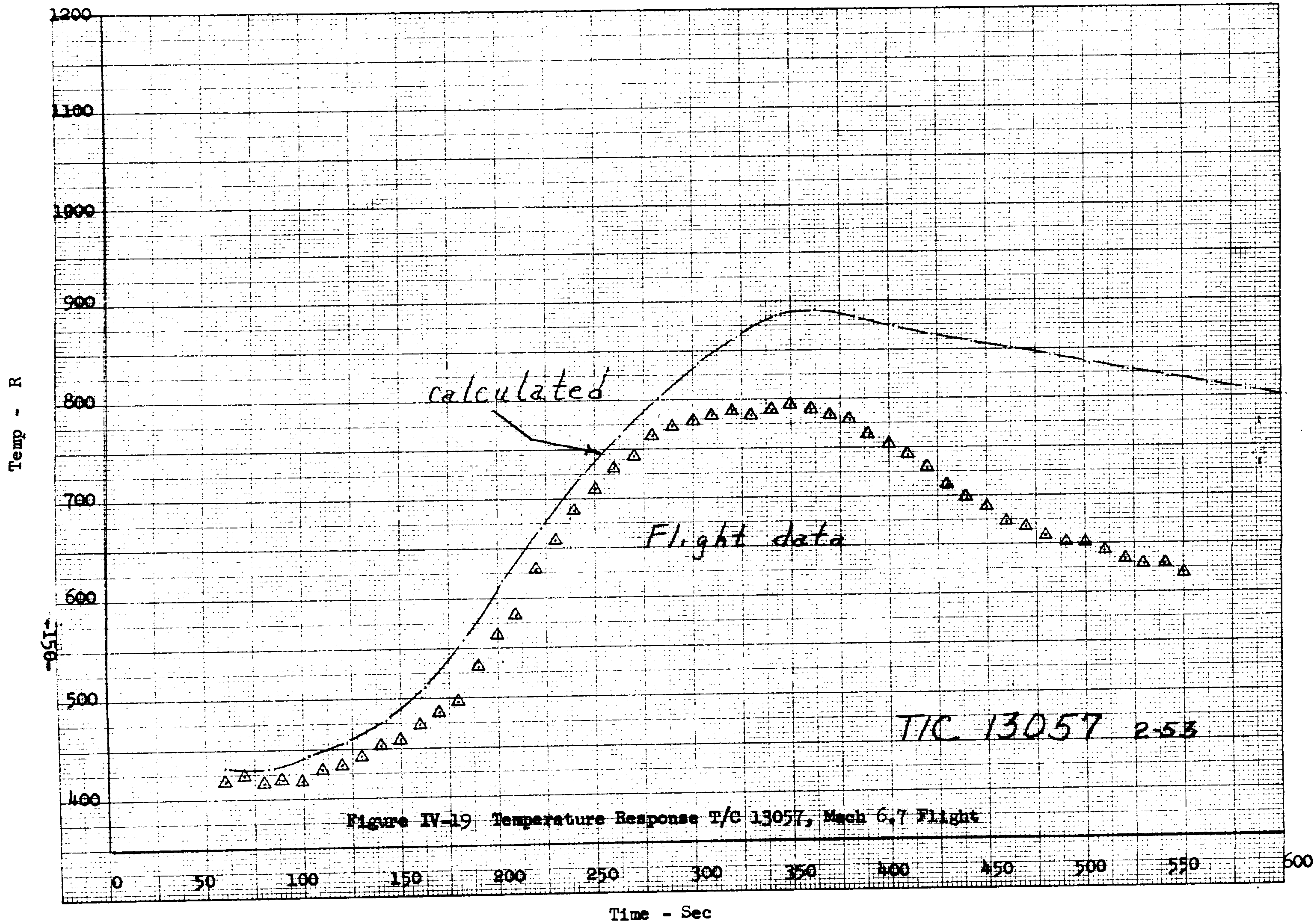

Figure IV-19 Temperature Response T/C 13057, Mach 6.7 Flight

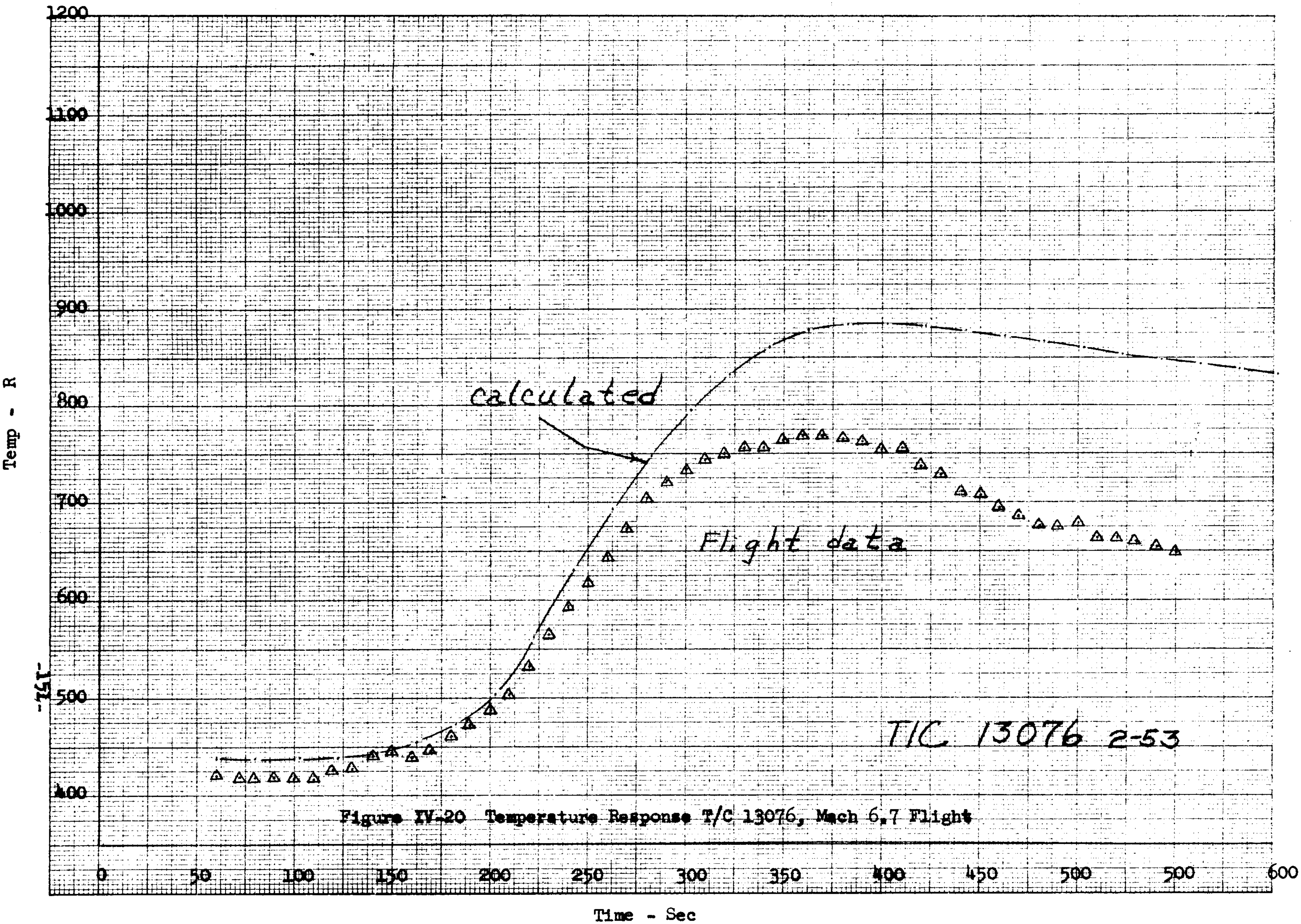

Figure IV-20 Temperature Response T/C 13076, Mach 6.7 Flight

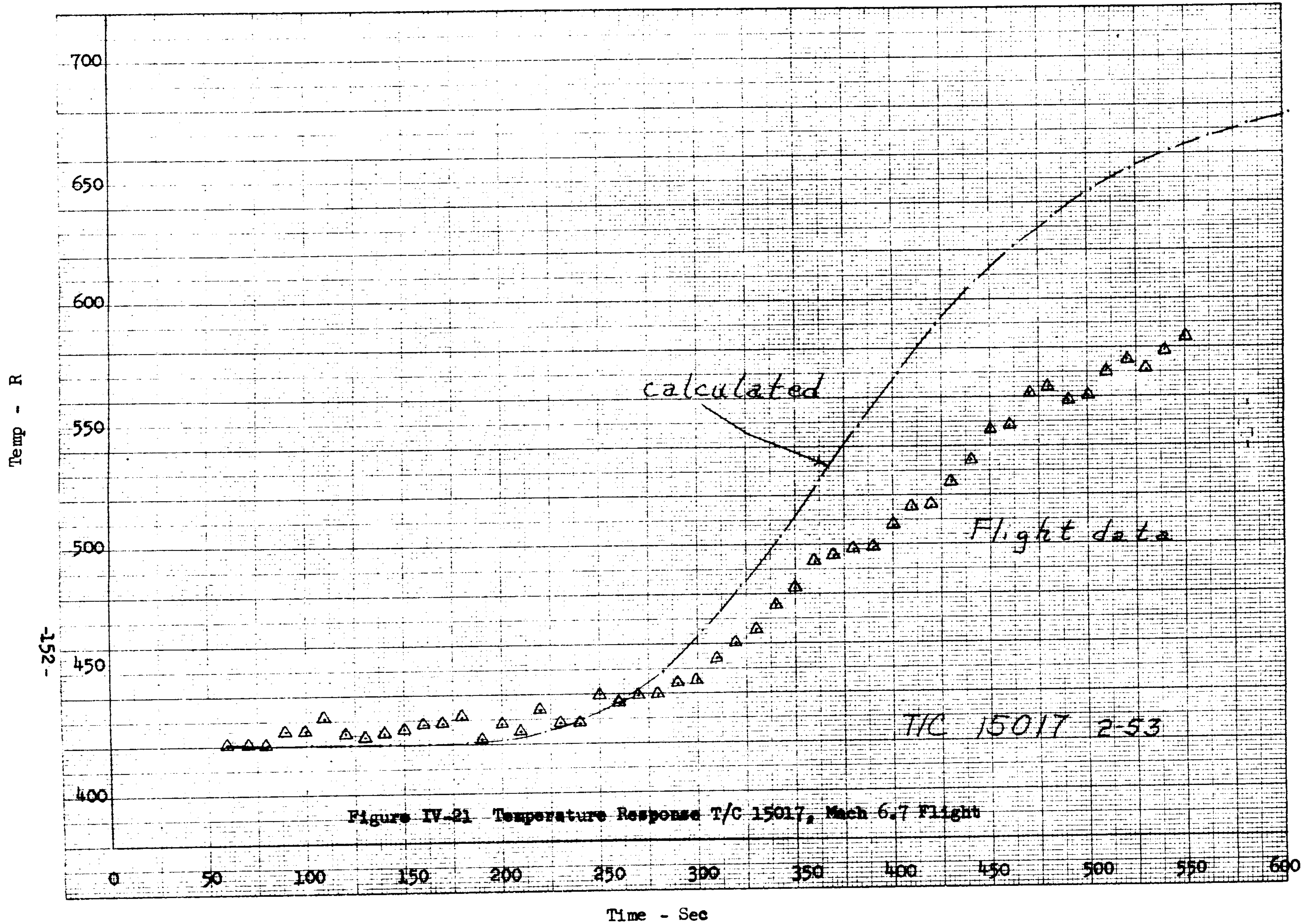

Figure IV-21 Temperature Response T/C 15017, Mach 6.7 Flight

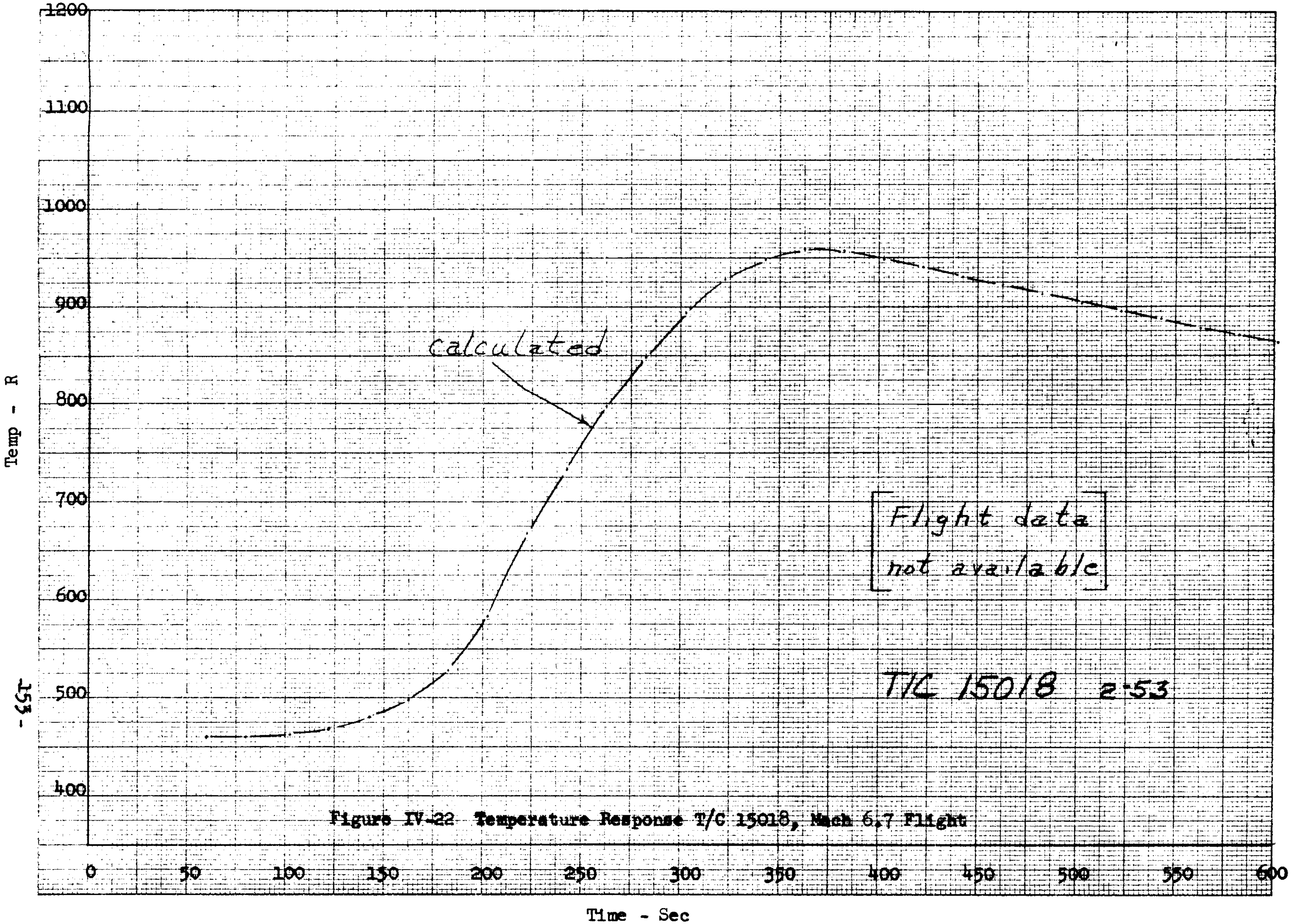

Figure IV-22 Temperature Response T/C 15018, Mach 6.7 Flight

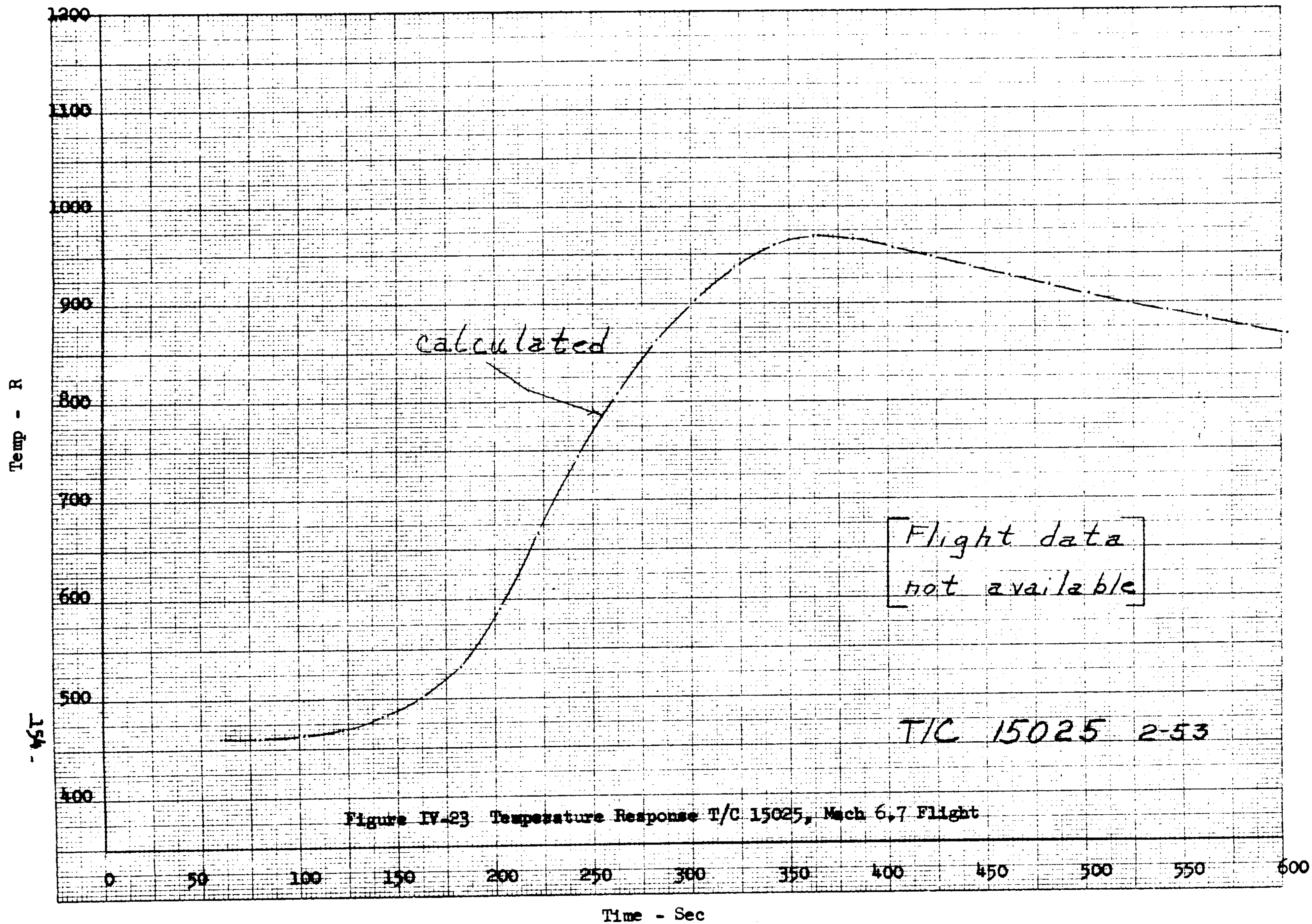

Figure IV-23 Temperature Response T/C 15025, Mach 6.7 Flight

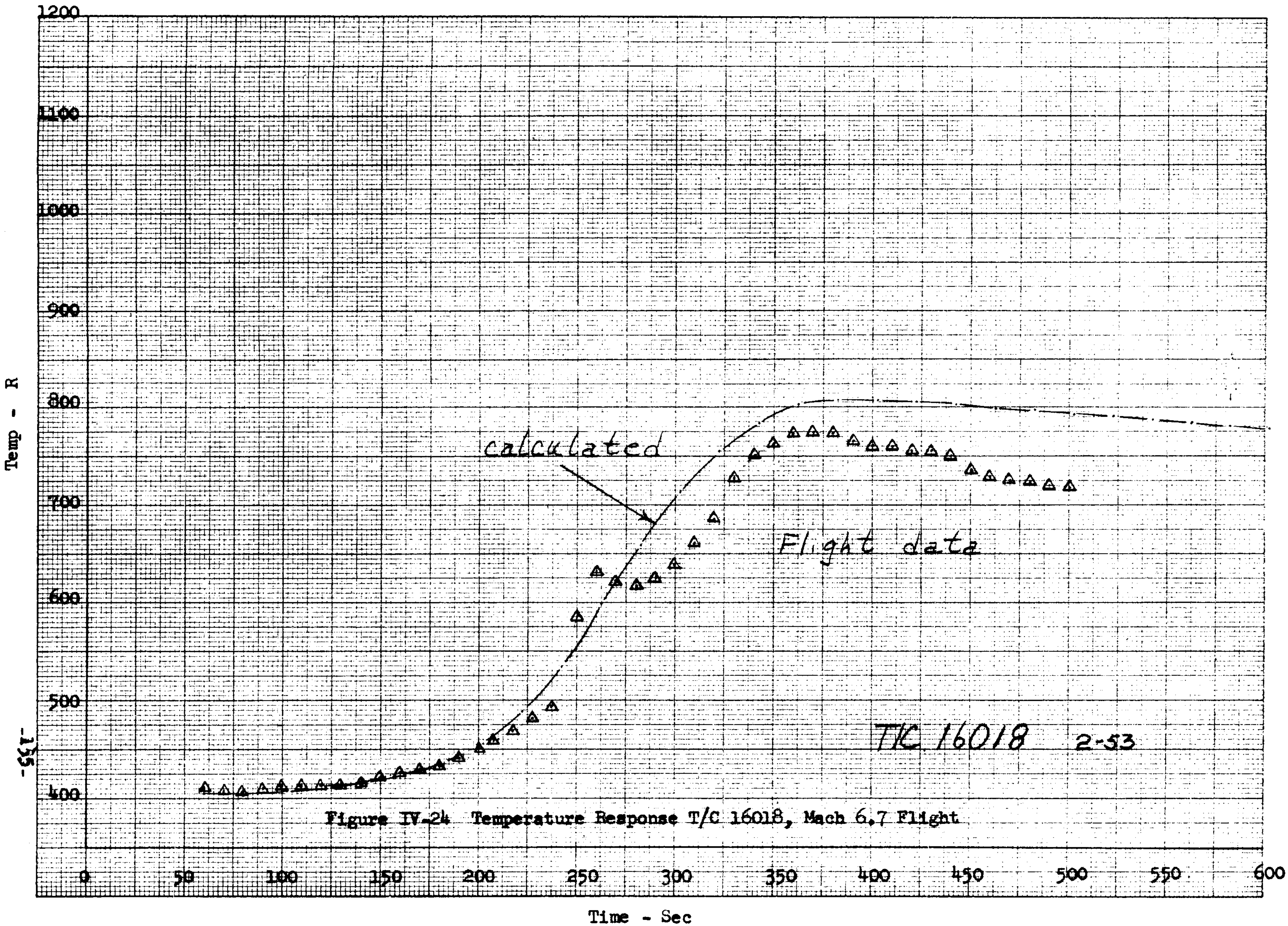

Figure IV-24 Temperature Response T/C 16018, Mach 6.7 Flight

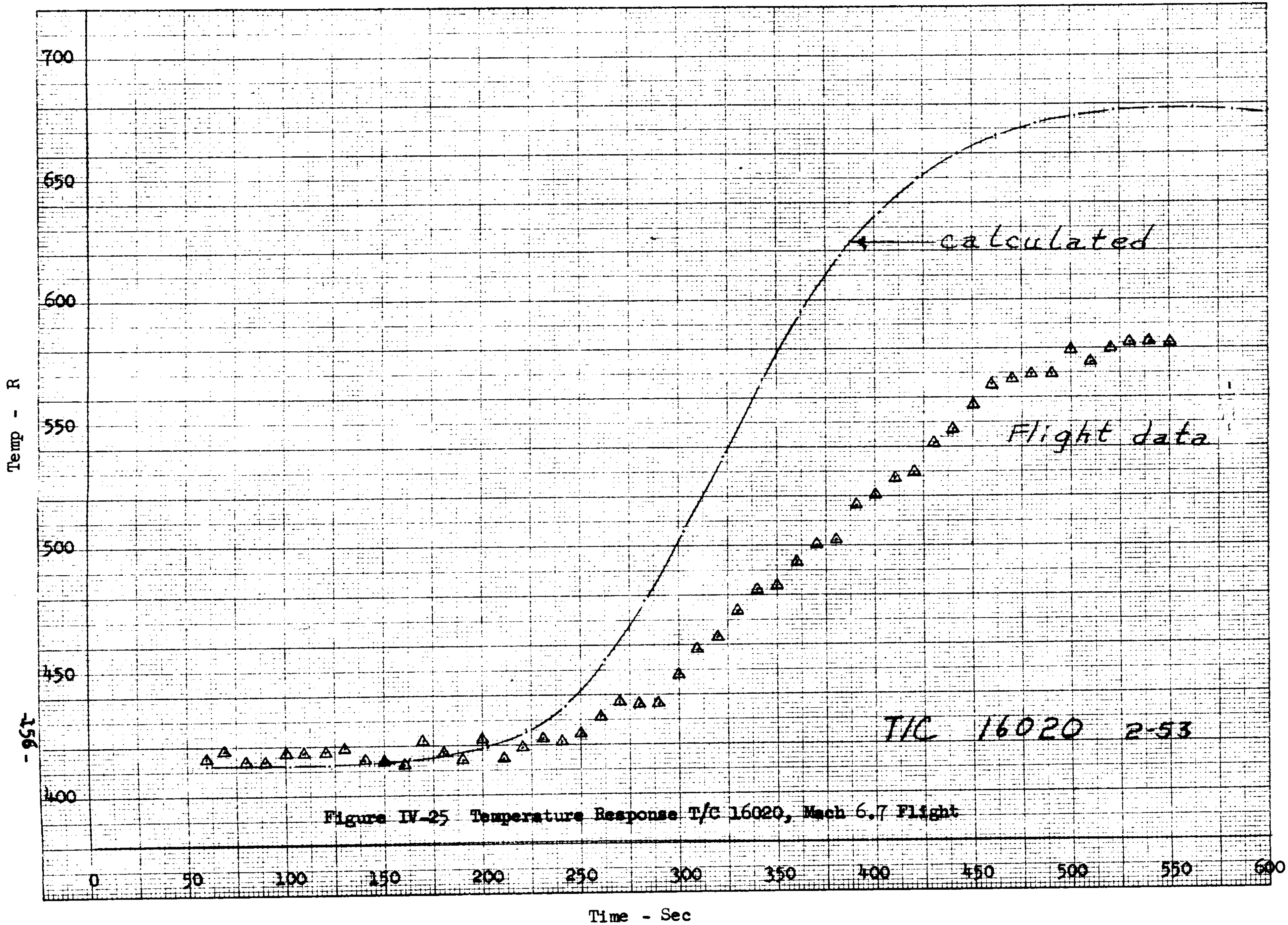

Figure IV-25 Temperature Response T/C 16020, Mach 6.7 Flight

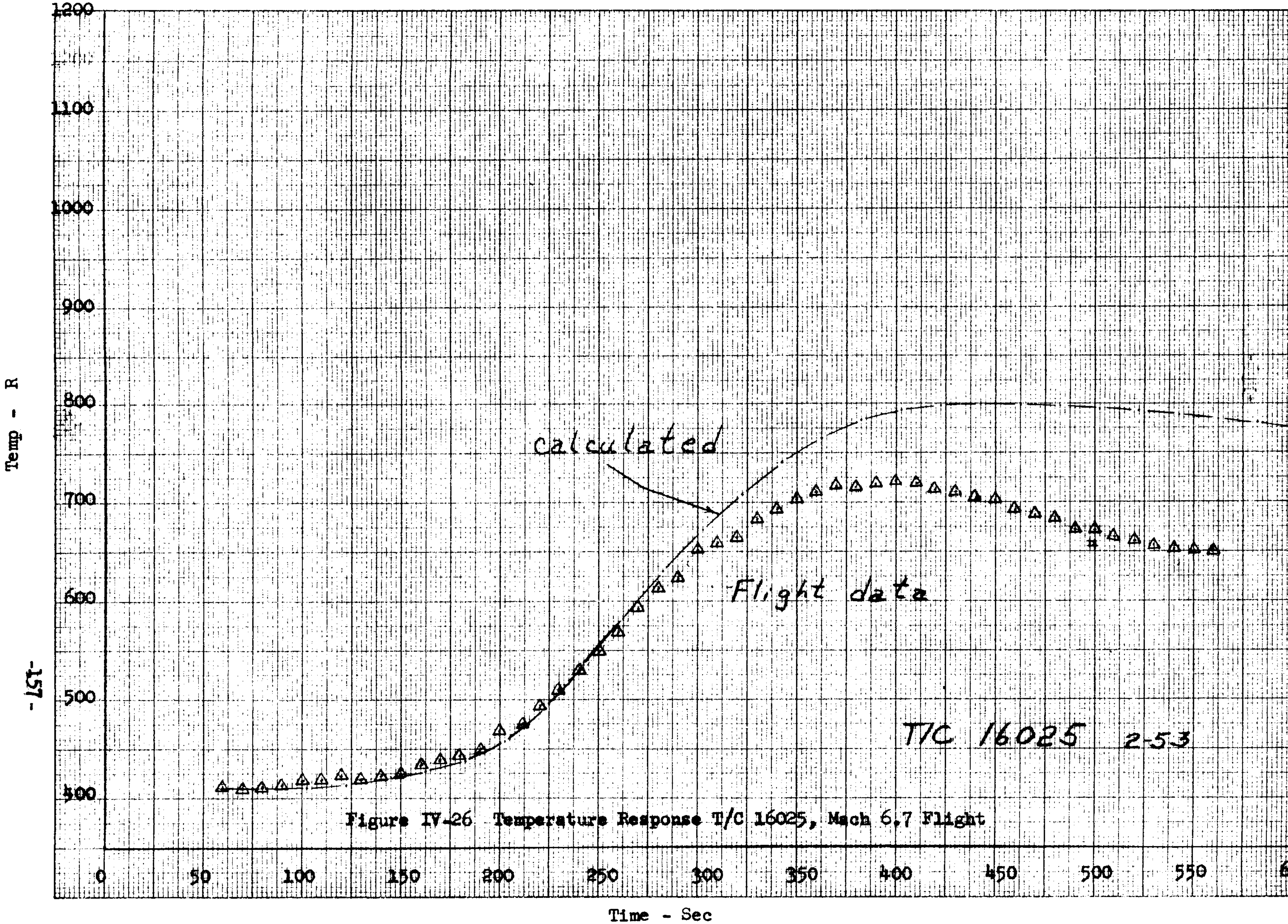

Figure IV-26 Temperature Response T/C 16025, Mach 6.7 Flight

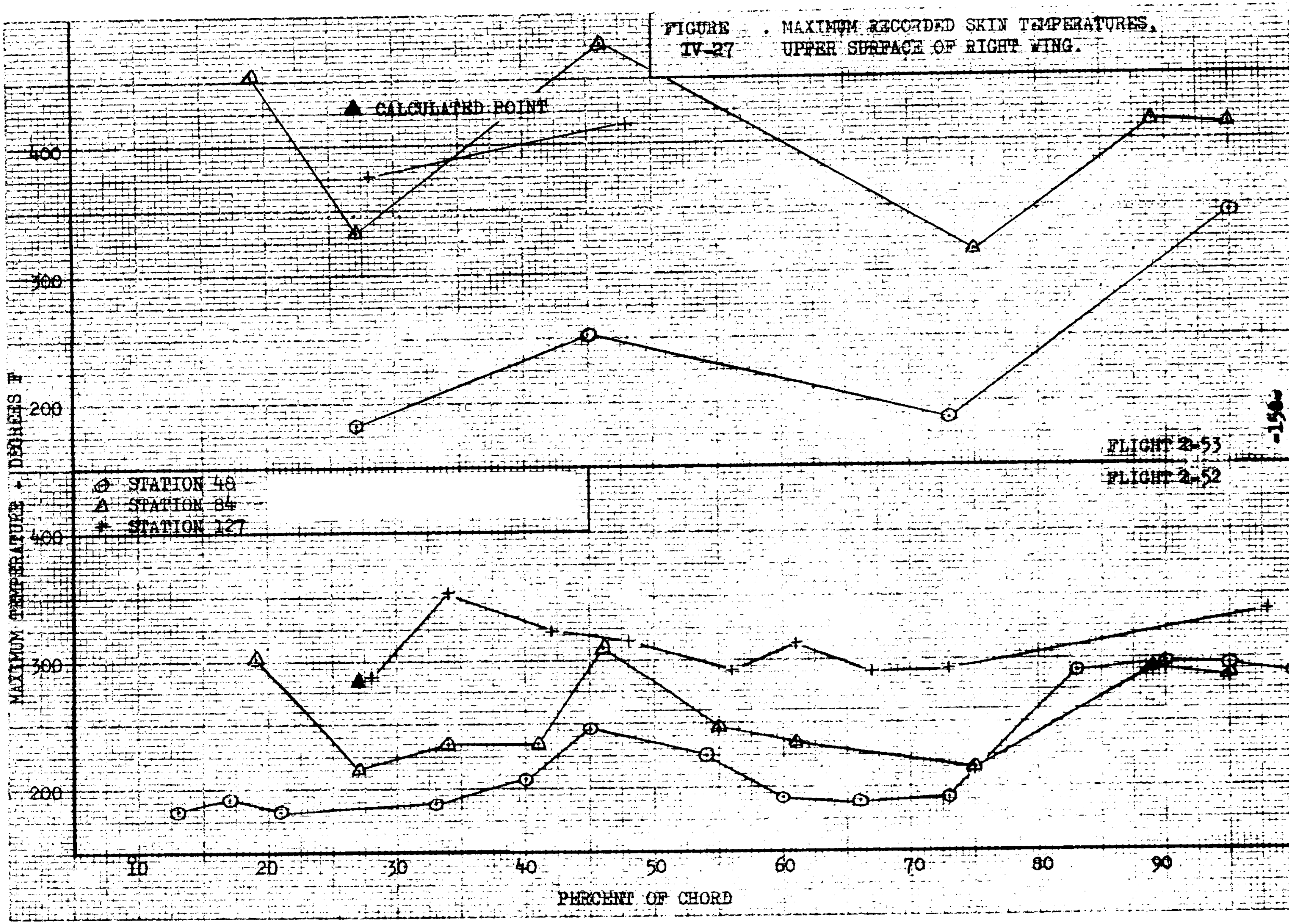
FIGURE IV-27. MAXIMUM RECORDED SKIN TEMPERATURES, UPPER SURFACE OF RIGHT WING.
▲ CALCULATED POINT
FLIGHT 2-53
FLIGHT 2-52
⊖ STATION 48
△ STATION 84
+ STATION 127
MAXIMUM TEMPERATURE - DEGREES F
400
300
200
400
300
200
10
20
30
40
50
60
70
80
90
PERCENT OF CHORD

FIGURE IV-28 . MAXIMUM RECORDED SKIN TEMPERATURES, LOWER SURFACE OF RIGHT WING.

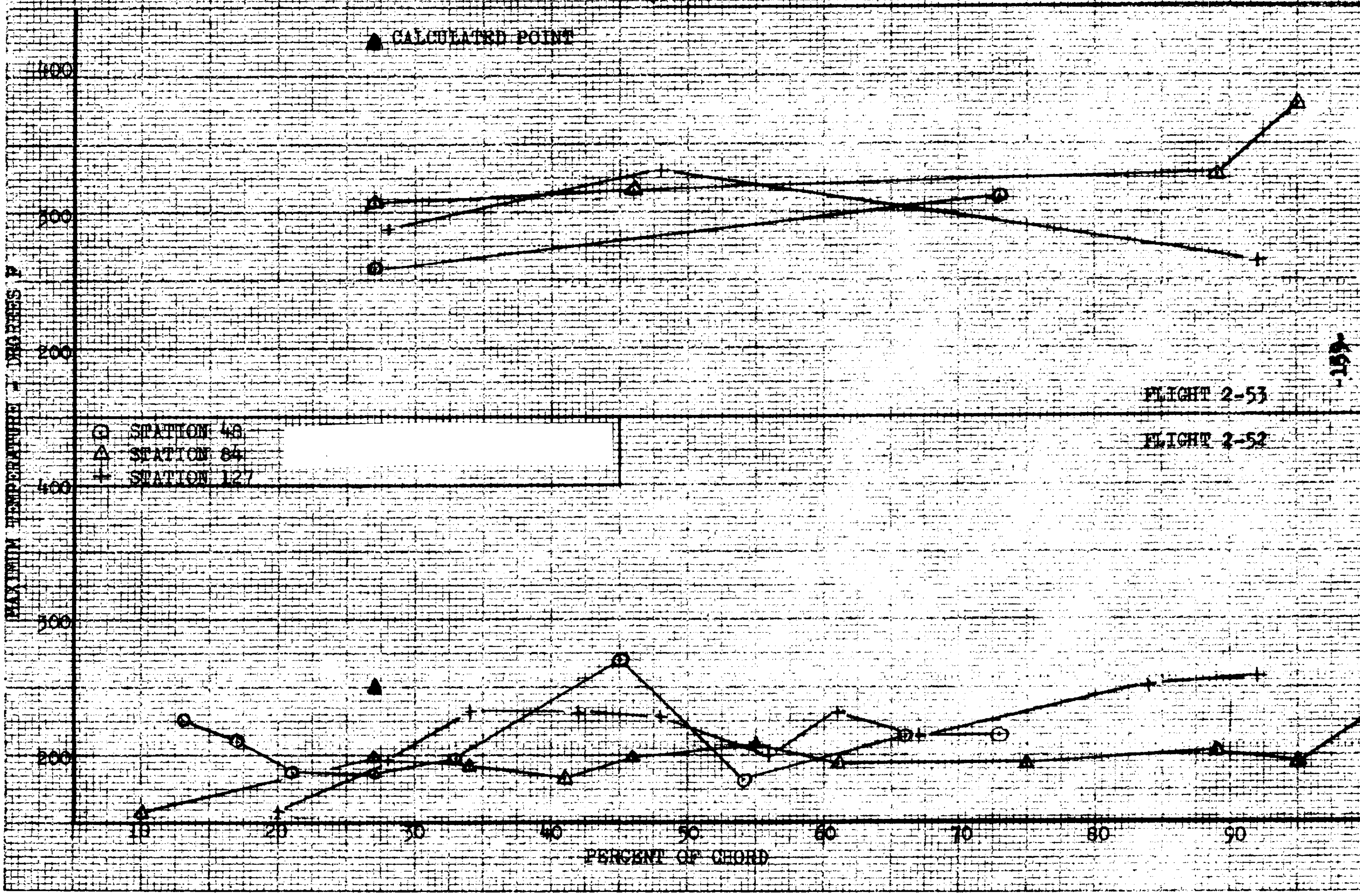

FIGURE IV-29. MAXIMUM RECORDED SKIN TEMPERATURES, UPPER SURFACE OF RIGHT HORIZONTAL TAIL.

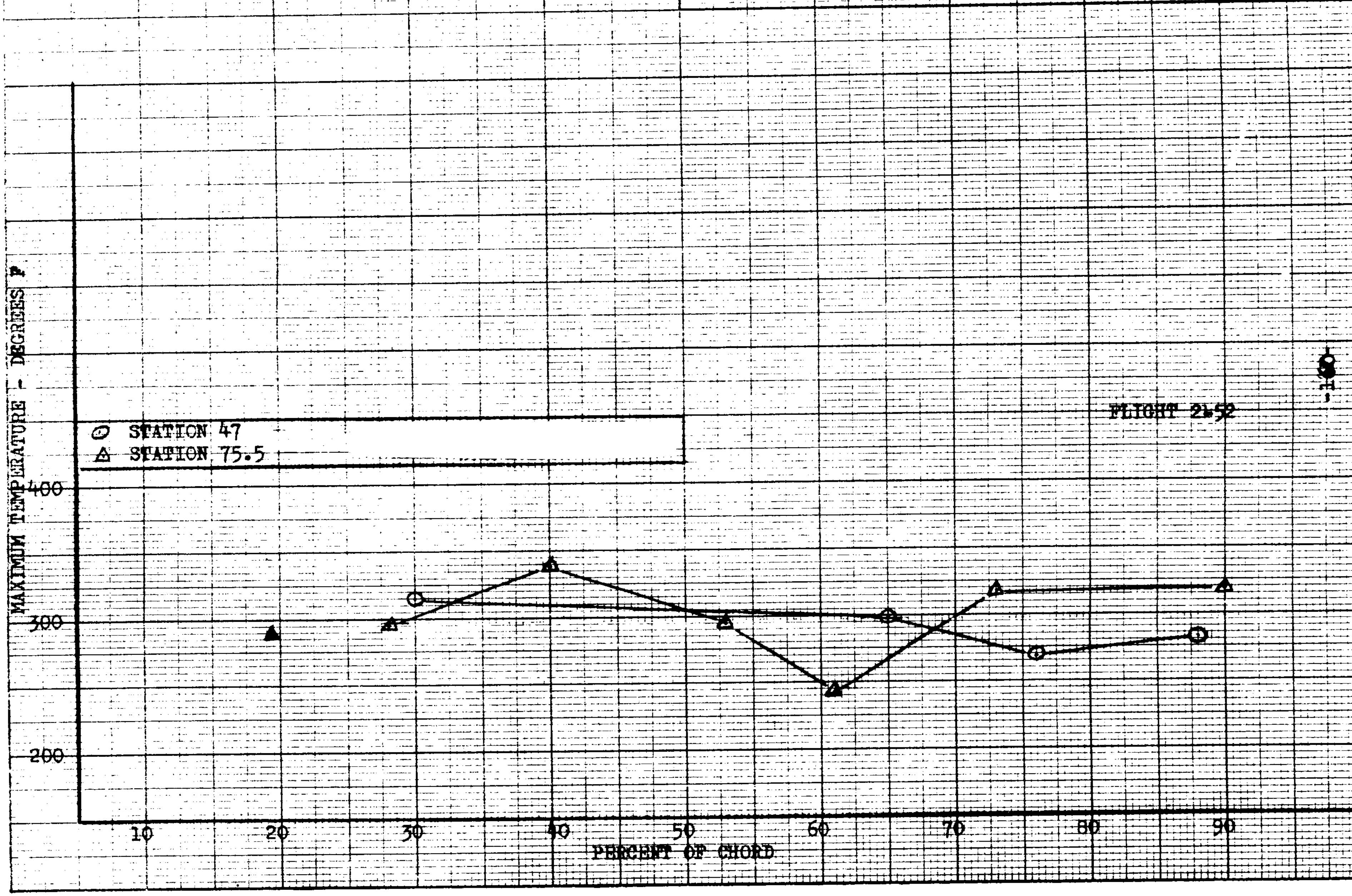

FIGURE IV-30 . MAXIMUM RECORDED SKIN TEMPERATURES, VERTICAL TAIL.

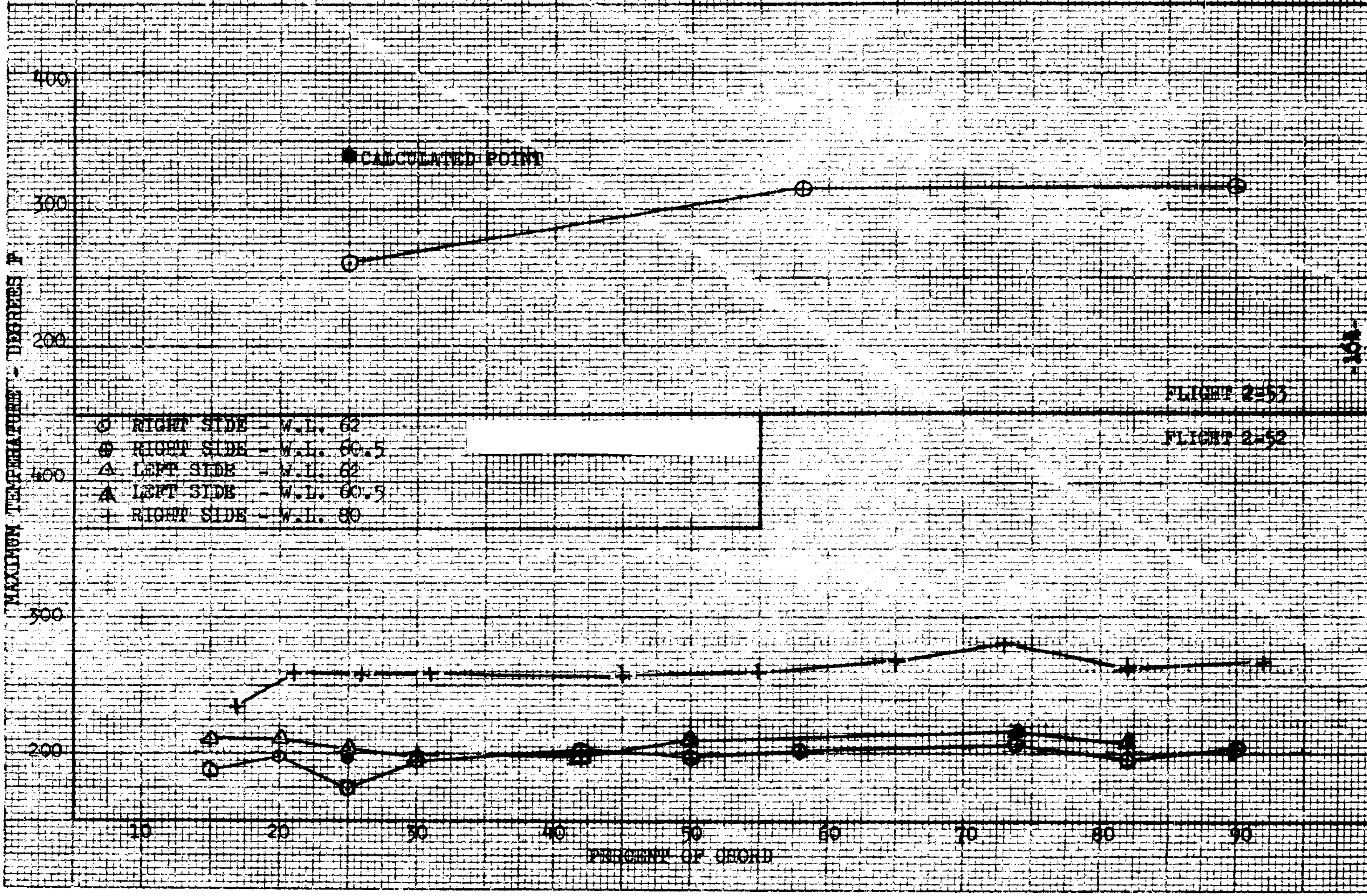

V. ABLATION SYSTEM QUALIFICATION SUMMARY

The ablative thermal protection system for the X-15A-2 aircraft was flight tested to Mach 5.0 and Mach 6.7. Post flight examination revealed satisfactory performance except in the area of the ventral fin. Better definition of the flight environment is required in this area before an adequate ablator protection system can be designed.

The remainder of the system protected the aircraft structure from the aerodynamic heating, and possessed the additional capability for flight envelope expansion.

Operational procedures were validated and the various design features of the ablator system were proven acceptable both from an operational and thermal performance viewpoint. Some minor changes in procedures and the system design were recommended to simplify ablator operations and increase the safety margin of the protection system.

Analytical correlation of the observed ablator performance was achieved and verified the predictability of the ablator materials.